Cover Page

Universiteit Leiden

The handle http://hdl.handle.net/1887/20863 holds various files of this Leiden University dissertation.

Author: Maczuga, Piotr
Title: Towards RNAi based therapy of liver diseases : diversity and complexity of shRNA and miRNA processing and functions
Issue Date: 2013-05-07

Towards RNAi-based therapy of liver diseases

Piotr Maczuga

Towards RNAi-based therapy of liver diseases

Diversity and complexity of shRNA and miRNA processing and functions

Piotr Maczuga

Towards RNAi based therapy of liver diseases
Diversity and complexity of shRNA and miRNA processing and functions

Piotr Maczuga

PhD Thesis, Ledien University, May 2013

Towards RNAi-based therapy of liver diseases Diversity and complexity of shRNA and miRNA processing and functions

ISBN: 978-94-6182-249-9

Layout & printing: Off Page, www.offpage.nl

Cover: Piotr Maczuga & Off Page

Copyright © 2013, Piotr Maczuga. All rights reserved. No part of this thesis may be reproduced or transmitted in any form or by any means, without the prior permission in writing of the author.

A digital version of this thesis can be downloaded from Leiden University Repository: https://openaccess.leidenuniv.nl/handle/1887/9744

The printing of this thesis was financially supported by:
uniQure Biopharma
Macrogen
Leiden University

The research described in this thesis was performed and financially supported by Amsterdam Molecular Therapeutics (now uniQure Biopharma), Amsterdam, The Netherlands.

Towards RNAi based therapy of liver diseases Diversity and complexity of shRNA and miRNA processing and functions

Proefschrift

ter verkrijging van
de graad van Doctor aan de Universiteit Leiden,
op gezag van de Rector Magnificus Prof. Mr. C.J.J.M. Stolker,
volgens besluit van het College voor Promoties
te verdedigen op dinsdag 7 mei 2013 klokke 10.00 uur

door

Piotr Maczuga
geboren te Leżajsk (Polen)
in 1983

PROMOTIECOMMISSIE

Promotor	prof. dr. Sander J.H. van Deventer
Co-promotor	dr. Pavlina Konstantinova
Overige leden	
	prof. dr. Theo van Berkel
	prof. dr. Pieter H. Reitsma
	dr. Hein W. Verspaget
	prof. dr. Bart van Hoek
	prof. dr. John J.P. Kastelein (Universiteit van Amsterdam)
	prof. dr. Ben Berkhout (Universiteit van Amsterdam)

Faculteit der Geneeskunde

CONTENTS

Chapter 1	Introduction	9
Chapter 2	Apolipoprotein B knockdown by AAV-delivered shRNA lowers plasma cholesterol in mice	39
Chapter 3	Optimization and comparison of knockdown efficacy between polymerase II expressed shRNA and artificial miRNA targeting luciferase and Apolipoprotein B100	69
Chapter 4	Embedding siRNA sequences targeting Apolipoprotein B100 in shRNA and miRNA scaffolds results in differential processing and *in vivo* efficacy	95
Chapter 5	Therapeutic expression of hairpins targeting Apolipoprotein B100 induces differential changes in murine liver	125
Chapter 6	Regulated knockdown of Apolipoprotein B100 and Huntingtin by the GeneSwitch mifiprestone-inducible system	175
Chapter 7	Discussion	197
Addendum	Summary	221
	Nederlandse samenvatting	223
	Streszczenie	225
	Curriculum Vitae	227
	Publications	229
	Acknowledgments	231

3'UTR	3' utranslated region
A1AT	Alpha-1-antitrypsin
A1AD	Alpha-1-antitrypsin deficiency
AAV	Adeno-associated virus
Ago	Argonaute protein
ALP	Alkaline phosphatase
ALT	Alanine aminotransferase
APC	Antigen presenting cell
ApoB	Apolipoprotein B
APOBEC2	Apolipoprotein B mRNA editing enzyme, catalytic polypeptide-like 2
AST	Aspartate aminotransferase
bp	basepairs
BGN	Biglycan
CMV	Cytomegalovirus
CTL	Cytotoxic T lymphocyte
dsRNA	double-stranded RNA
DGAT2	Diglyceride acyltransferase 2
F.IX	Factor IX
FH	Familial hypercholesterolemia
GS	Gene Switch system
GFP	Green fluorescent protein
hAAT	human Alpha-1-antitrypsin
HBsAg	Hepatitis B surface antigen
HBV	Hepatitis B virus
HCC	Hepatocellular carcinoma
HCV	Hepatitis C virus
HMG-CoA	3-hydroxy-3-methyl-glutaryl-CoA reductase
IFN	Interferon
INR	Initiator sequence
ITR	Inverted terminal repeat
JNK	c-Jun N-terminal kinase
LDL-C	Low density lipoprotein cholesterol
LDL-R	Low density lipoprotein receptor
LDLRAP1	Low density lipoprotein receptor adaptor protein 1
lhRNA	long-hairpin RNA
LNA	Locked nucleic acid
LPL	Lipoprotein lipase
MDR	Multi drug resistance
MFP	Mifiprestone
MHC	Major histocompatibility complex
mRNA	messenger RNA

miRNA	micro RNA
MTP	Microsomal triglyceride transfer protein
NHP	Non-human primate
NGS	Next generation sequencing
nt	nucleotide
ORF	Open reading frame
OVA	Ovalbumin
pA	polyadenylation signal
PAMP	Pathogen-associated molecular pattern
PKR	Protein kinase R
PCSK9	Proprotein convertase subtilisin/kexin type 9
p.i.	post injection
pre-miRNA	precursor micro RNA
pri-miRNA	primary micro RNA
RISC	RNA induced silencing complex
RNA	Ribonucleic acid
RNAi	RNA interference
shRNA	short-hairpin RNA
siRNA	small interfering RNA
SNALP	Stable nucleic acid lipid particle
ssRNA	single-stranded RNA
ss-siRNA	single-stranded siRNA
TA	Gene Switch transactivator
TATA	TATA box
TLR	Toll-like receptor
tRNA	transfer RNA
TSS	Transcription start site
TTS	Transcription termination signal
VLDL-C	Very low density lipoprotein cholesterol
wk	weeks

CHAPTER 1

Introduction

Introduction

Since its discovery RNA interference (RNAi) mechanism has become a valuable research tool for functional analysis of gene expression and a promising approach for treatment of many disorders including viral infections, hereditary disorders, and cancer. By introducing molecules that constitute substrates for the endogenous RNAi pathway, disease-related messenger RNA (mRNA) and thus production of related proteins can be inhibited. Liver plays a major role in the metabolism and has a number of functions in the body, including glycogen storage, decomposition of red blood cells, plasma protein synthesis, hormone production, and detoxification. Many liver diseases that currently cannot be adequately treated are good candidates for RNAi gene therapy. RNAi-based strategies have recently been explored for treating hepatocellular carcinoma (HCC), hepatitis B (HBV) and hepatitis C (HCV) virus, infections and genetic disorders such as familial hypercholesterolemia (FH) or alpha-1-antitrypsin deficiency (A1AD). The RNAi machinery can directly inhibit RNA, which plays important role in the etiology of these diseases i.e. target transcripts encoding for multidrug resistance proteins in HCC, viral genome of HBV, replication intermediates of HBV, HCV or mutated mRNAs which lead to production of amended proteins in FH and A1AD. Additionally, the RNAi machinery, in particular endogenous miRNAs can be exploited to regulate transgene expression. This approach was successfully applied to reduce immune response to Factor IX (F.IX) used for treatment of Hemophilia B by inhibiting F.IX expression in antigen presenting cells (APC) using hematopoietic cell-specific miRNA binding sites in 3' untranslated region (3'UTR) of the transgene.

However, serious concerns have been raised about safety of the RNAi-based therapeutic approach when toxicity was described in rodents and non-human primates (NHP). This thesis addresses important questions about the long-term efficacy and safety of RNAi for treatment of liver diseases, which also involves aspects of processing of RNAi molecules *in vivo*, transcriptome analysis and liver functioning after injection with adeno-associated viruses (AAV) encoding RNAi-inducing molecules.

The natural RNAi pathway

RNAi is an evolutionary conserved mechanism for regulating gene expression. It plays an important role in defense against viruses but also in development and in normal functioning of the cell [1-3]. RNAi was initially discovered in plants where delivering DNA encoding the rate limiting enzyme in anthocyanin biosynthesis in order to generate petunias (*Petunia hybryda*) with darker color, unexpectedly induced the opposite effect of less pigmented or white flowers [4,5]. This "co-suppression" of endogenous gene phenomenon was suggested to function via hybridization with endogenous mRNA resulting in double stranded RNA, which was targeted for

destruction or led to translational repression. The same mechanism was later found to be conserved in other species i.e. fungi *Neurospora Crassa* [6] and *Caenorhabditis elgans* worm [7]. In 1998 a breakthrough discovery was made by A. Fire and C. Mello which provided the explanation for these previously described phenomenons [8]. They identified molecules which were responsible for inducing target degradation of mRNA and showed that a double-stranded RNA (dsRNA) contamination in mRNA preparations rather than single stranded RNA was inhibiting a gene with complementary sequences [8]. Their discovery was a milestone which was just beginning of identification of novel mechanism of gene regulation. In 2006, A. Fire and C. Mello were awarded the Noble prize for their discovery of RNA interference-gene silencing by double-stranded RNA.

The RNAi mechanism is initiated by dsRNA molecules (Fig. 1). The natural RNAi mechanism in mammalian cells functions by endogenous miRNA molecules, which are synthesized in cells as longer primary RNA transcripts (pri-miRNAs). Most miRNA are usually transcribed by RNA polymerase II; however RNA polymerase III (Pol III) transcribes some miRNAs, especially those with upstream Alu sequences and transfer RNAs (tRNAs) [9]. Pri-miRNAs are cleaved by the nuclear Microprocessor complex (Drosha-DGCR8 complex) to produce miRNA precursors (pre-miRNAs) of 70 nucleotides (nt) [10], which are then transported by Exportin 5 to the cytoplasm and processed by the RNAse III endonuclease family enzyme Dicer to produce a mature miRNA duplex of ~21-25 basepairs (bp) [11]. The guide strand of the miRNA enters a multiprotein RNA-induced silencing complex (RISC) enabling it to bind to the 3′ untranslated region (3′UTR) of its target mRNA. Although either strand of the duplex may potentially act as a functional miRNA, one strand called "guide strand" or "antisense strand" is preferentially incorporated into the RISC complex. The selection of guide strand is highly influenced by the thermodynamic stability of 5′ and 3′ ends of Dicer products [12]. Generally, the strand with the lower 5′ stability will be preferentially loaded into RISC, while the other strand is degraded. The active components of the RISC complex are endonucleases called Argonaute proteins (Ago) and in human cells the Ago family consists of four Argonaute proteins (Ago1-4) [13]. It is known that only RISC association with Ago2 has the capability to cleave target mRNA, whereas Ago1 association can mediate translational repression [12]. The process of loading Dicer substrates on different mammalian Agos *in vivo* is not well established and it is known that miRNA are not loaded into specific RISC-Ago complexes but can interact with any of them [12]. The RISC-Ago complex recognizes mRNA with the complementary target sequence and consequently induces cleavage or translational repression [14].

The specificity of miRNA target recognition is primarily determined by the sequence from 2 to 8 nt from the 5′ end of the miRNA guide strand which is called the "seed sequence" [15,16]. As a result target binding can be remarkably imperfect and

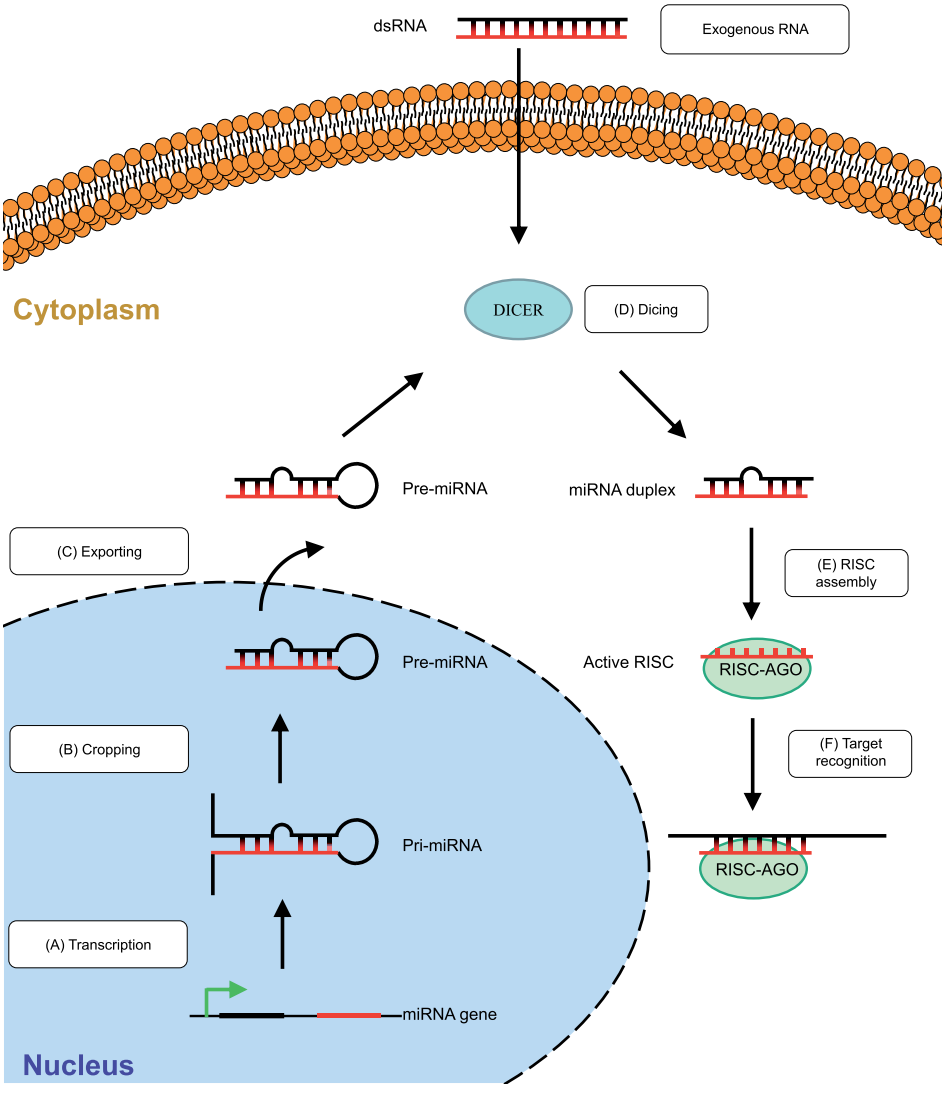

Figure 1. Endogenous RNAi pathway. (A) RNA Pol II or III transcribe the primary transcript of miRNA (pri-miRNA) (B) Microprocessor complex (Drosha-DGCR8) cleaves the single-stranded sequences flanking of pri-miRNA to produce pre-miRNA (C) pre-miRNA is exported with Exportin-5 from the nucleus to the cytoplasm (D) Dicer cleavage produces mature miRNA complex of ~21 bp. Dicer also processes exogenous dsRNA (E) miRNA guide strand (red) is incorporated into RISC, while the passenger strand (black) is degraded (F) Active RISC recognize target mRNA which in consequence leads to target degradation or translational repression.

therefore single miRNA is capable of regulating multiple cellular targets. Conversely, each gene can be controlled by several miRNAs [15].

RNA entering RNAi pathway can also originate from an exogenous source, for example during a viral infection [17,18], which -when processed- can also generate mature miRNA. By targeting viral mRNA this can inhibit the expression of crucial viral proteins and prevent the spread of the infections. In fact, RNAi does work effectively as an antiviral agent in plants and mammalian cells [19-21].

RNAi therapeutics

Identification of the RNAi pathway structural components and intermediates initiated studies on the application of RNAi as therapeutics. The general idea is that by introduction of molecules that constitute substrates for the endogenous pathway, specific inhibition of disease-related mRNA can be induced and as a consequence reduction of disease-related proteins can be achieved. Therapeutic RNAi can be induced in different ways (Fig. 2).

Therapeutic RNAi is generally induced by delivery of 20-25 nt-long small interfering RNAs (siRNAs) [22] which serve as substrates for the RISC complex (Fig. 2a). siRNA are chemically synthesized and can be delivered directly or by using chemical carriers: cationic lipids, cationic polymers or peptides to facilitate their penetration [23]. However siRNAs are rapidly cleared from the body and have to be re-administered weekly or bi-monthly in order to induce long-term efficacy [24]. Poor uptake of exogenous nucleic acids by cells represents the major barrier to the development of siRNA-based drugs. To enhance intracellular uptake of nucleic acids for systemic administration, siRNA can be encapsulated within liposomes termed stable nucleic acid lipid particles (SNALP). Alternatively, siRNAs can be generated by embedding in a stem loop structure of short hairpin RNA (shRNA, Fig. 2b) [25], long hairpin RNA (lhRNA, Fig. 2c) [26-28] or artificial microRNA (miRNA, Fig. 2d) [29] and expressing from viral [30] or plasmid [31] vector for sustained gene silencing. After transcription all these have certain specific RNA structures: a central stem of variable length, a terminal loop region, and a single stranded RNA (ssRNA) region, being the characteristic features of endogenous substrates of RNAi machinery. These structures are recognized by Drosha and Dicer and serve as reference points for endonuclease digestions and processing into mature siRNA/miRNA. The guide strand of siRNA/miRNA that is embedded into RISC determines target recognition. Similar to endogenous miRNAs, siRNA, and shRNAs are not sorted into Ago-specific RISCs [12] yet, in contrast to cellular miRNA, siRNA and shRNA induce target mRNA cleavage rather than translational repression. The crucial difference between shRNAs, lhRNAs, and artificial miRNAs is in their tertiary structure, which determines the entry point, processing and finally functioning in the RNAi pathway (Fig. 2 and 3). The majority of mammalian miRNAs contain an extensive

bulge structure in their stem that at least partially can explain differences in their functioning. siRNA, shRNA and lhRNA are perfectly complementary to their targets, which induce degradation rather than translational repression.

Another important difference is the mechanism of transcription. shRNAs are generally expressed from constitutive polymerase III (pol III) promoters and directly generate a mature stem-loop product, which is exported and processed by Dicer [32]. Although shRNA can be expressed from pol II promoters [12,34-35], this has not been very successful due to inefficient processing of the hairpins by the RNAi machinery and the lack of detailed knowledge of the transcription start site (TSS), transcription termination signal (TTS), and hairpin location. Alternatively, siRNA can be expressed as a long hairpin RNA (lhRNA) in which the stem can be extended up to 300 bp and can incorporate multiple ~21 bp siRNA sequences. lhRNAs can be expressed with pol III or pol II promoters and undergo processing by Dicer [26,28,36]. In contrast to shRNA, miRNAs transcripts are generally expressed from pol II promoters that allow for the use of tissue-specific or regulated expression systems. They have additional flanking sequences adjacent to hairpin structure therefore miRNA processing requires an additional step of excision from the longer pre-miRNA sequence by the Drosha-DGCR8 complex [10,37]. miRNA can be expressed in clusters allowing expression of different siRNA, which can be used for viral infections or cancer, where multiple sequences have to be targeted [38].

There are advantages and disadvantages inherent to the various ways of inducing RNAi in cells and the choice greatly depends of the desired effect. Characteristic features of different RNAi systems are summarized in Table 1.

In addition to gene silencing, the intracellular RNAi machinery and miRNA expression profile can be used in other, more refined, therapeutic approaches. The genetic regulation by miRNA is important in the fundamental processes of cell growth and differentiation. Emerging studies showed evidence of quantitative and mutational changes in miRNA expression and their target binding sites, which promote the development and progression of many diseases [39,40], Correction of the endogenous miRNA profile,

Table 1. Comparison of different approaches for inducing RNAi in cells

	siRNA	shRNA	artificial miRNA	lhRNA
Structure	dsRNA 21-25bp	~21 bp stem loop structure with 2 nt 5′ and 3′ overhangs	~21-25 bp stem loop structure with bulges and 5′ and 3′ flanking sequences	40-300 bp perfect stem loop structure
Expression	-	pol III, limited pol II	pol III and pol II	pol III and pol II
Processing	-	Dicer, Ago2	Drosha, Dicer	Dicer
Delivery	Direct injections	Expression from vector	Expression from vector	Expression from vector
Mechanism	mRNA degradation	mRNA degradation	mRNA degradation or translational repression	mRNA degradation

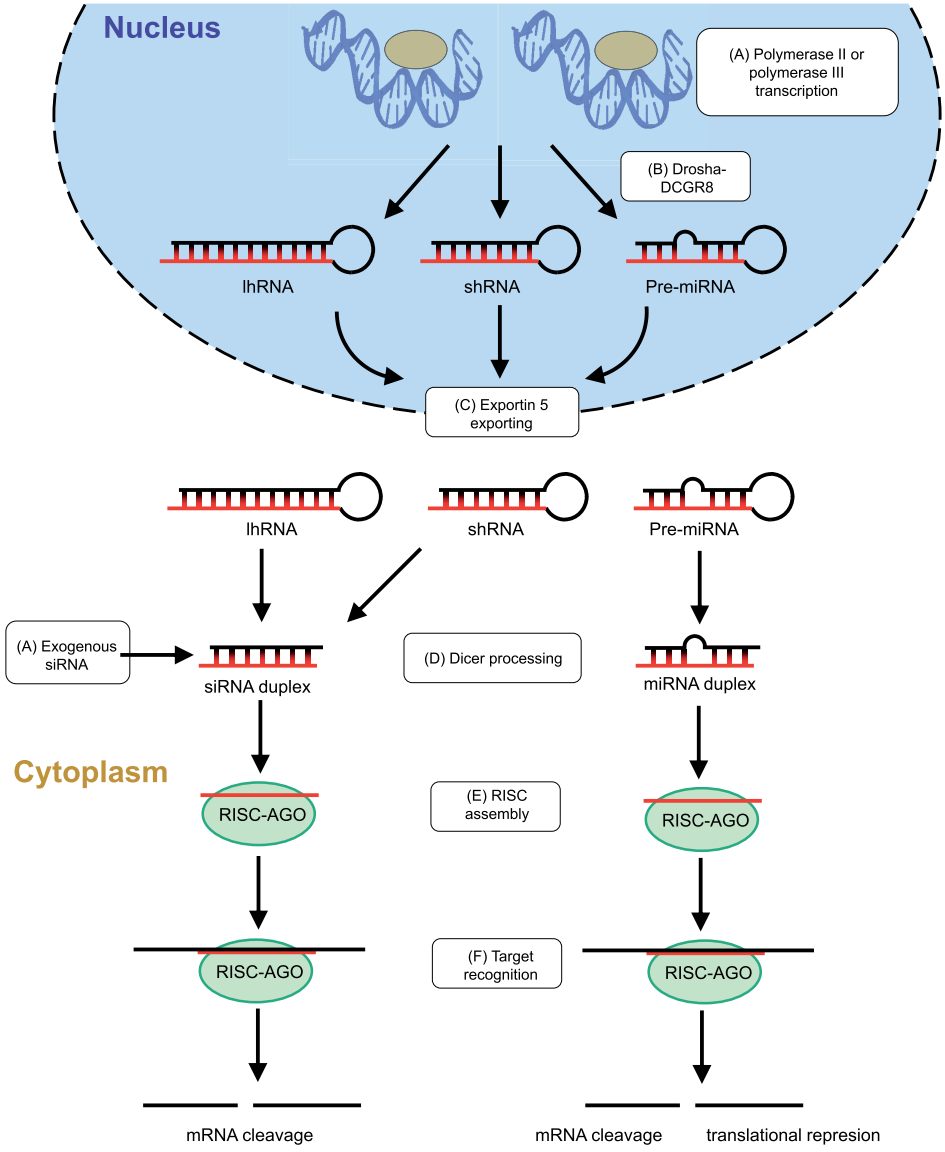

Figure 2. Induction of RNAi therapeutics in cells. RNAi induction in cells include resembles endogenous pathway. (A) RNA Pol II or III transcribe the primary transcript of shRNA, lhRNA and pri-miRNA siRNA can be delivered exogenously without transcription in nucleus (B) Microprocessor complex cleaves ssRNA flanking sequences of pri-miRNA to produce pre-miRNA (C) pre-miRNA, shRNA and lhRNA are exported via Exportin-5 from the nucleus to the cytoplasm (D) Dicer cleavage produce mature siRNA/miRNA complex of ~21 bp (E) siRNA/miRNA guide strand (red) is incorporated into RISC, while the passenger strand (black) is degraded. (F) Active RISC recognizes target mRNA which in consequence leads to target degradation (shRNA, lhRNA, miRNA) or additionally can lead to translational repression (miRNA).

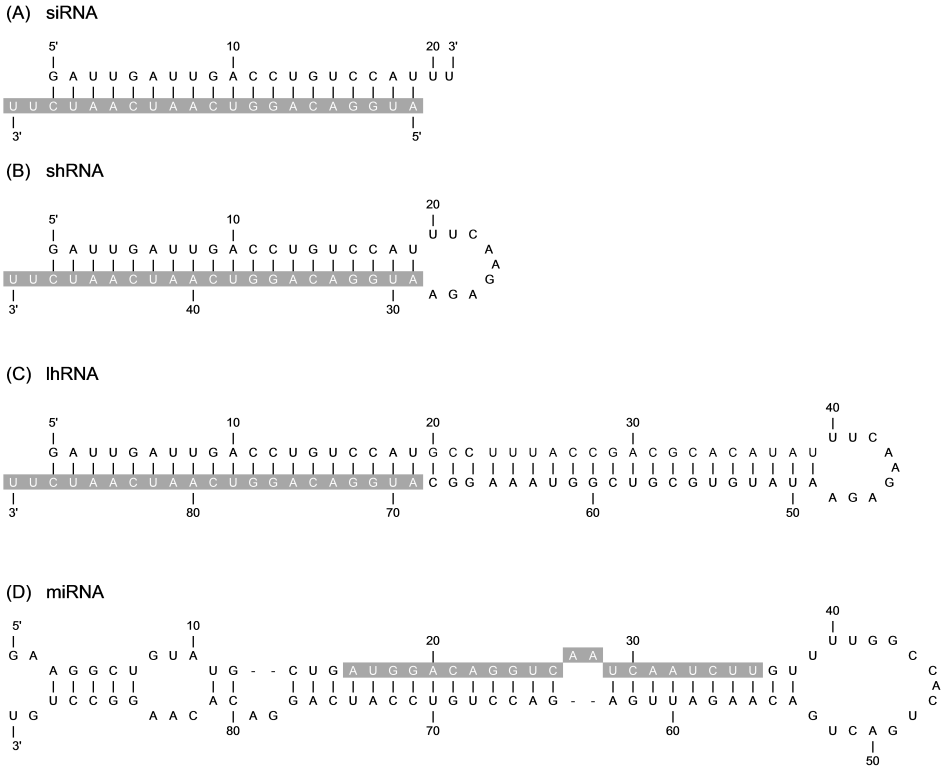

Figure 3. Structure of (A) siRNA, (B) shRNA, (C) lhRNA and (D) miRNA targeting ApoB. Sequence and predicted structure for siApoB, shApoB, lhApoB and miApoB with the guide strand indicated in grey.

can restore normal functioning of cells [41,42]. This approach is intensively investigated to prevent or treat metastasis of cancer cells. Inhibition of particular miRNA's resulting in inhibition of its target mRNA is a promising treatment for viral infections [40]. Additionally by incorporation in the 3′ UTR region of transgenes, an intracellular RNAi mechanism can be employed to regulate their expression in different cells [43,44]. In particular this approach is interesting for inhibition of transgene expression in non-target cells because cells which are not expressing the particular miRNA will not inhibit expression. Hence, genetic regulation by endogenous miRNA is a promising strategy of avoiding immune responses to transgene (i.e. F.IX for hemophilia B) that are seen as "foreign" by the immune system of the patient lacking F.IX expression [45].

RNAi therapeutics in the liver

Despite the progress in understanding causes of many diseases, current therapies involving pharmacological and biological drugs only alleviate disease symptoms.

Inappropriate gene activity is being linked to a number of liver diseases and because RNAi controls gene expression at the level of RNA, a unique opportunity is being offered to stop the actual cause of diseases. Therefore, gene silencing in cells creates an entirely new horizon in the therapy of liver diseases allowing new treatment strategies to be developed. Proof of concept for the therapeutic efficacy of RNAi has already been convincingly demonstrated in a number of preclinical models of FH, hepatitis, cancer and others. The key of RNAi approach success is mainly dependent on careful target selection, the RNA inducer used and a convenient delivery system. In this paragraph, a short description of disease etiology, conventional treatments and possible RNAi targets is given.

Familial hypercholesterolemia (FH)

FH is a genetic disorder characterized by high cholesterol levels in the blood, specifically very high levels of low density lipoprotein cholesterol (LDL-C) and early onset of cardiovascular disease [46]. The most common genetic defects in FH are mutations in genes that regulate for cholesterol homeostasis such as the LDL-C receptor (LDL-R) [47] and apolipoprotein B (ApoB), which is the part of LDL-C that binds with the receptor. Mutations in other genes including Proprotein convertase subtilisin/kexin type 9 (Pcsk9) or low density lipoprotein receptor adaptor protein 1 (Ldlrap1) in FH patients are rare [49-50], however they are also used as therapeutic targets in FH. Patients who have one abnormal copy of the mutated gene (heterozygous FH) have increased risk of cardiovascular disease, which can develop at age 30-40 [50]. Having two abnormal copies may cause severe cardiovascular disease onset early in the childhood [51]. Heterozygous FH is a common genetic disorder, occurring in 1:500 people in most countries; homozygous FH is much rarer, occurring in 1 in a million births [52]. LDL-C normally circulates in the body for 2.5 days and subsequently binds to the LDL-R on the liver cells, undergoes endocytosis and is digested. As a consequence LDL-C is removed and de novo synthesis of cholesterol by the liver is suppressed in the 3-hydroxy-3-methyl-glutaryl-CoA reductase (HMG-CoA) pathway [53]. When LDL-R function is reduced or absent, LDL-C circulates for an average duration of 4.5 days, resulting in significantly increased level of LDL-C in the blood with normal levels of other lipoproteins. The same effect is caused by mutations in the ApoB protein, where reduced binding of LDL-C particles to the receptor causes the increased level of LDL-C in plasma. Increased LDL-C circulation in blood increases the probability that it will be taken up by endothelial cells of vascular walls and through modifications such as oxidation will induce damage. This initiates immune system activation and a inflammatory cascade of events leading to arteriosclerosis plaque formation. Generally the type of FH determines the treatment that can be applied to a patient. Whereas the heterozygous form can be successfully treated with statins, which are HMG-CoA inhibitors, homozygous FH is difficult to treat and conventional

treatment often fails to reduce LDL-C levels. Therefore homozygous FH was among the first monogenic diseases targets for treatments with RNAi and conventional gene substitution therapies. Recently, a single intravenous injection of an AAV8 vector containing the mouse LDL-R gene to a humanized mouse model of FH, the LDL-R-/-APOBEC-/- mouse, was found to significantly reduce plasma cholesterol levels in chow-fed animals [54]. In addition to the LDL-R gene augmentation approach, the successful use of the VLDL-R for the complementation of mutated LDL-R function in homozygote FH has also been shown [55]. As alternative strategy, inhibition of Pcsk9 with siRNA has been shown to increase LDL-R levels in liver and in consequence reduce LDL-C levels [56]. However conventional gene therapy (resulting in LDL-R expression) and Pcsk9 inhibition is not suitable for FH patients that have ApoB mutations. In those cases RNAi can be used to target ApoB. In 2004, Soutschek *et al*. [57] showed silencing of ApoB in mice with systemically delivered modified siRNA, which was associated with reduction in plasma cholesterol. Later, Zimmermann *et al*. showed siRNA mediated ApoB silencing in human primates [58], however the effect was stable only for up to 11 days. Albeit ApoB reduction by siRNAs was successful in lowering LDL-C levels in plasma, the effect was transient and treatment caused liver steatosis [57,58]. In order to achieve stable reduction of ApoB and in consequence LDL-C without the need to re-administration, siRNA has to be embedded in shRNA or miRNA scaffolds, expressed from a pol II or pol III promoters and delivered to the target cells by using an appropriate vector system.

Alpha-1-antitrypsin deficiency (A1AD)

A1AD is a genetic disorder caused by defective production and secretion of alpha-1-antitrypsin (A1AT) from liver cells [59]. One of the A1AT functions is to protect the lungs from neutrophils' elastase and consequently patients suffering from the disease develop emphysema. Because A1AT is not secreted properly from the liver, patients often also develop liver cirrhosis [60]. Circulating A1AT levels depend on the genotype and the most severe disease phenotype characterizes patients with PiZ mutation where only 10-15% of normal A1AT levels are present in blood [60,61]. Current treatment alleviates symptoms by infusions of isolated or recombinant A1AT protein; however some patients can be treated by simultaneous liver and lung transplantation. Since A1AD not only affects lung where levels are insufficient but also liver where mutated AAT accumulation leads to liver cirrhosis [62,63], gene therapy approaches should aim to both decrease levels of mutant A1AT and increase wild-type A1AT levels by expressing the correct version of the gene. Such an approach was implemented by Li *et al.,* by delivering rAAV simultaneously expressing an shRNA, targeting mutated A1AT and an optimized A1AT cassette in mice expressing the human PiZ allele [64]. This resulted in inhibition of mutated A1AT and correction of wild type A1AT levels and interestingly, liver histology was also significantly improved. Similarly, transgenic

mice treated with rAAV vectors simultaneously expressing artificial miRNA targeting PiZ and codon optimized A1AT gene showed that serum PiZ level was stably reduced by an average of 80% [65]. In addition, decreased globular accumulation of misfolded Z-A1AT in hepatocytes and a reduction in inflammatory infiltrates in the liver were observed. Finally endogenous miRNAs were minimally affected by this treatment suggesting that miRNA mediated knockdown did not saturate the miRNA pathway.

Hepatocellular carcinoma (HCC)

HCC is the most common type of liver cancer. Most cases of HCC are secondary to viral infections or cirrhosis [66]. Prognosis and treatment depends on the stage of the disease, however ~70% of patients are diagnosed at intermediate and late stages when no curative treatment is available. These patients often develop multidrug resistance to chemotherapeutics due to overexpression of ABC family transporter proteins. Among them ABBC1 and ABBC2 are characterized for the liver and their implication in chemotherapy resistance is suggested [67]. Borel *et al.* showed successful inhibition of ABCC2 transporter *in vivo* by AAV delivered shRNA and artificial miRNA [68]. Despite effectiveness mice exhibited serious side effects due to oversaturation of endogenous RNAi machinery. Additionally, Borel *et al.* investigated panel of endogenous miRNA whose expression pattern change in hepatocellular cancerogenesis [69]. These miRNAs not only can be used as marker for disease's prognosis but also by overexpression of miRNA which are downregulated, normal functioning of the cell may be restored i.e. restoration of mir-122 expression in liver cancer correlates with suppression of both the malignant phenotype and metastatic properties [70]. Restoring endogenous miRNA pathway can also improve response to chemotherapy as many of MDR transporter transcripts have been identified as miRNA targets [69,71,72].

Hepatitis B virus (HBV) infections

HBV infection is still a major health problem. Even though effective vaccines have been available for the last 20 years, worldwide, over 350 million people are infected with this virus [73]. Chronic HBV infections may have serious consequences, including liver cirrhosis and HCC; prevention of this infection is a key to then prevent the HCC [74]. HBV, which belongs to *Hepadnaviruses*, have small genome of 3,2 kb - partially double-stranded, partially single stranded circular DNA [75]. It contains four open reading frames (ORFs) that encode structural proteins of core, polymerase, surface and viral X protein. The core gene encodes the viral capsid protein, known as hepatitis B virus core antigen (HBsAg). Upon infection viral DNA is transported to the nucleus where is made completely double stranded and circular and serves as a template for transcription of four viral mRNAs. HBV is an excellent candidate for therapeutic RNAi, as its compact and overlapping transcripts can be simultaneously targeted with a single shRNA. Additionally, the compact genome prevents from evading RNAi by

mutations. McCaffrey *et al.* showed 85% reduction in secreted HBsAg in mice plasma when HBV genome plasmid was delivered with a plasmid encoding shRNA targeting the HBV sAg [76]. Importantly, viral inhibition occurred in absence of active viral replication suggesting that this strategy is independent from viral replication thus can be used for treatment of chronic HBV infections. An alternative to anti-HBV shRNA cassettes involves utilization of pri-miRNA scaffold sequences [77]. This is an appealing strategy as multiple miRNA can be expressed from single transcripts and this approach has been already validated *in vivo* [78]. Another approach was used by Weinberg *et al.*, who assessed the efficacy of lhRNAs targeting the conserved hepatitis B protein X (HBx) open reading frame of HBV [28]. After hydrodynamic injection in mice one of the lhRNA vectors decreased viral replication by 70–90% with no evidence of induction of an interferon response induction. RNAi therapy has a major disadvantage, being the inability to completely eliminate DNA genome, but it can complement conventional anti-HBV therapies by affecting multiple steps in the viral life cycle.

Hepatitis C virus (HCV) infections

Like HBV, HCV is one of the major causes of liver morbidity and also a leading cause of liver transplantation, with around 170 million people infected [79]. HCV is small, enveloped member of family *Flavividae* [80]. Its genome consists of about 9,6kb single stranded positive sense RNA, which is translated into large multiprotein complex and translationaly processed into the structural components of the virus. HCV is particularly attractive target for RNAi, which in theory can target not only the replicative forms but also genomic RNA templates and eventually lead to viral clearance. However due to the high mutation rate only highly conserved regions of the virus can be targeted to prevent escaping from RNAi activity [81]. As with HBV, HCV has been the target of both synthetic and expressed activators of the RNAi pathway and effective inhibition of markers of virus replication has been described in several studies. Yokota *et al.* used both synthetic siRNA and expressed shRNA effectors against the 5'-NTR (5' Non translated region) and approximately 80% suppression was observed in a replicon model of the HCV [82]. Other studies also show that targeting HCV with RNAi can be promising strategy [83,84] and reviewed in [85]; however a major concern was raised about the ability of the virus to accumulate evading nucleotide sequence mutations [85]. A recent report showed emergence of resistant HCV RNAs after several treatments of replicon-expressing cultured cells with siRNA targeted against the NS5B coding region [86]. Resistant replicons remained sensitive to a siRNA that targets another part of the genome, suggesting that use of siRNA combinations limits evolution of escape. Recent studies also showed that modified lhRNAs comprising 50–100 bp were capable of silencing hepatitis C virus targets in cell culture [87-88]. Recently, an alternative strategy for inhibition of HCV replication has been employed. Replication of HCV is dependent on the liver specific

mir-122 expression, which regulates HCV by binding directly to two adjacent sites close to the 5' end of HCV RNA [89], Although the precise mechanism of regulation is not yet clear, inhibition of endogenous mir-122 function is a promising therapeutic approach. This can be accomplished by delivering single-stranded, modified RNA oligonucleotides complementary to miRNA guide strand, resulting in tight binding and efficient inhibition [90,91]. Santaris Pharma have developed drug- Miravirsen, which is a locked nucleic acid-based (LNA) antisense oligonucleotide to mir-122 that is delivered to the liver with intravenous injection. This molecule reduced HCV replication in a small-scale trial in chimpanzees without inducing liver toxicity [90].

Hemophilia B

Hemophilia is caused by hereditary genetic disorders that impair the body's ability to establish blood coagulation. The defect in blood clotting in hemophilia B is caused by the lack of functional clotting Factor IX (F.IX) as a result of mutations in the gene encoding this protein. As an X-linked recessive chromosomal disorder, almost all people living with haemophilia are male, while females are generally asymptomatic carriers of the mutated allele [92]. It occurs in around 1 in about 30,000 male births. F.IX deficiency leads to an increased risk for bleeding in response to mild trauma or even spontaneously, such as in joints (haemarthrosis) or muscles. Patients are grouped according to circulating levels of F.IX, which correlate closely with clinical severity. Plasma concentrations of F.IX of 5–25%, 1–5%, and <1% of normal levels refer to mild, moderate and severe hemophilia respectively. Protein replacement is the current standard of care. Frequent intravenous administrations (two to three times a week) of recombinant F.IX are required to stop or prevent bleeding. A goal for the treatment of hemophilia B is the development of a gene transfer strategy that can maintain sustained production of clotting F.IX in the liver, where it is normally produced. At present, gene transfer mediated by viral vectors delivering F.IX expressing cassette shows the greatest promise for long-term correction of hemophilia B in the preclinical setting [93-96]. Improvement of levels to above 1% is sufficient to prevent most spontaneous and nearly all life-threatening bleeding episodes [95]. Unfortunately, initial evaluation of viral vectors expressing F.IX failed to achieve sustained F.IX expression in hemophilia B mice due to the recognition of F.IX as foreign antigen which resulted in anti-F.IX cellular immune response [97,98]. Further analysis suggested that this may be a result of off-target transgene expression in hematopoietic-lineage cells of the spleen which resulted in antigen presenting cells (APCs) maturation and activation of cytotoxic T lymphocytes (CTLs) [99,100]. As a consequence transduced hepatocytes were eliminated and expression diminished.

To overcome this problem, a novel strategy that exploits endogenous miRNA activity to prevent vector expression in non-target cells has been developed [43,44]. The vector can be modified to contain a target sequence for the hematopoietic-

specific microRNA, mir-142-3p in its 3' UTR [45,101]. This allows expression in hepatocytes, while preventing F.IX production in hematopoietic cells- including APCs. By restricting transgene expression exclusively to the liver, while preventing F.IX production in hematopoietic cells including APCs, immunologic tolerance was induced. Importantly, analysis of miRNA revealed that the mir-142-3p–regulated vector did not affect the natural levels of expression of mir-142-3p or other miRNAs in either the liver or spleen. However these results are in opposite to F.IX gene transfer mediated by AAV vectors, which showed expression of clotting factor without inducing cellular response to transgene [96]. Interestingly expression of F.IX was limited by presence of anti-AAV immune response which probably eliminates transduced hepatocytes [102] while no anti-F.IX immune response was detected. Still this possibility has to be considered especially when strategies to overcome existing immune response to AAV will be applied (immune response to AAV is discussed in details in paragraph 7). Incorporation of mir-142-3p sites for transgenes expressed with AAV can be used as additional safety measure to prevent immune reaction and allowing long-term expression of transgenes.

RNAi toxicity

RNAi can interfere with normal functioning of cells and therefore safety is an important aspect of the implementation of RNAi based therapies. Non-specific effects resulting from the RNAi induction appear to have three separate mechanisms: innate immune response, off-target effects and oversaturation of the RNAi pathway. In addition, immune response to the delivery method can negatively contribute to the efficacy and safety of RNAi therapeutics. These side effects are often associated with severe toxicity that in some cases can be even fatal. In this chapter only RNAi toxicity and strategies to avoid them will be considered. Several toxicity issues involving response to the transgene or the RNAi inducer and the delivery vector will be described in paragraph 7.

The first source of RNAi toxicity is related to activation of innate immune responses. It is now well established that RNAi therapeutics, in particular siRNAs can be potent inducers of interferon (IFN) and inflammatory cytokines both *in vivo* and *in vitro* [103]. Most often, the IFN response is caused by the activation of the dsRNA-dependent protein kinase R (PKR) leading to a global inhibition of protein synthesis [104]. However siRNAs with stem shorter than 30 bp were shown to evade PKR activation [105]. Another mechanism which leads to activation of inflammatory cytokines goes via Toll-like receptor (TLR) activation [106,107]. TLRs are activated by molecules referred to as pathogen-associated molecular patterns (PAMPs). PAMPs are normally not present in cells but commonly shared by pathogens. TLR3 recognizes dsRNA and poly I:C [108], whereas TLR7 and 8 can recognize small ssRNA [109,110]. Upon ligand binding TLRs activate NF-kB and MAP kinases which subsequently

activate early response genes and genes encoding cytokines [107]. TLR activation by RNAi therapeutics leads in consequence to activation of immune response. Activation of the immune system by siRNAs is sequence-dependent as U and GU rich regions seem to be preferentially recognized by TLR [110]. Therefore, chemical modification of siRNA can prevent the recognition by the immune system [111]. It has been shown that modification of 2′ ribose with 2′-O-methyl, 2′fluoro-, 2′deoxy- or locked nucleic acid can reduce immune stimulation [110]. Although immunostimulatory side effects must be taken in account when inducing RNAi, for certain applications i.e. cancer or viral infections, activation of the immune system can be beneficial.

A second source of RNAi toxicity is off-targeting, when non-targeted transcripts are down-regulated based on sequence complementarity to sh/miRNA seed sequences [112]. Because of the complexity of sh/miRNA processing and RISC loading these unanticipated interactions are difficult to evaluate. However off-targeting can be minimized by adopting a stringent design filter both for sense and antisense strands of the RNAi efector molecules. Most off-target effects appear to be due to miRNA-like targeting, which is not detected by BLAST and therefore algorithms with high sensitivity such as Smith-Waterman should be included in this design [113,114]. This includes computing the distribution of unique shRNAs/miRNA targets in the transcriptome to avoid three or fewer matches with other than target genes. Seed sequence complementary to other genes should also be avoided and, as mentioned before, the selection criteria should include both sense and antisense strands. This is particularly important when miRNA are used because sense and antisense strands are not always identical and may contain bulges and G:U wobbles (Fig. 2 and 3). Hence, consequence off-targets for both stands can be different. The use of siRNA from hairpin constructs (shRNA, lhRNA, miRNA) provides additional complexity and imposes additional risk factors as the cleavage sites of sense and antisense strands slightly differ, resulting in production of a family of siRNAs with different 5′ and 3′ ends. Another serious consideration during sh/miRNA design is strand selection which should lead to preferential loading of the guide strand into the RISC. Although both strands of the siRNA can be incorporated into RISC, strand selection seems to follow the thermodynamic asymmetry rule in which the strand with the less stable 5′ end is incorporated into RISC [115,116]. The unwanted passenger strand functionality can be decreased by introduction mismatches at certain positions of the passenger strand [117]. There are other approaches to minimize off-targeting for example by reducing the concentration of the RNAi inducing agent. This strategy originated from observations that off-target effects are concentration dependent [118]. Dose reduction may cause a loss of RNAi efficacy and this can be solved by using siRNA pool against different sequences of the same target [111]. Chemical modification of nucleotides of siRNA with 2′-O-methyl, not only reduces immune responses but also may minimize

off target effects [115,116]. Modifications should include both strands of the siRNA: sense being loaded into RISC and antisense binding to off-targets. Similarly for shRNA and miRNA passenger strand's interaction with endogenous transcripts can be minimized by expressing the so called "sponge" transcript containing complementary binding sites for the passenger strand. When the passenger strand is loaded into RISC, the complex will bind to sponge transcript instead of endogenous target [119].

A third toxicity aspect is oversaturation of the natural RNAi pathway. Introducing RNAi agents which make use the endogenous RNAi pathway and substitute intermediate products can create competition with the endogenous miRNA processing [68,120,121]. High expression levels of therapeutic shRNA or artificial miRNA can saturate the endogenous RNAi machinery and in consequence lead to deregulation of the complex miRNA network. As referred in paragraph 3, shRNAs are generally expressed from pol III promoters, which provide constitutive high expression levels necessary for potent knockdown of target mRNA. Although these features are valuable for research purposes, they can be disadvantages for therapeutic applications. It has been reported that pol III-expressed shRNA can lead to severe toxicity when high doses are used [68,121,122]. Grimm *et al.* observed liver failure and mortality in mice injected with different AAV-expressed shRNAs irrespective of hairpin length, sequence and target [121]. Toxic side effects were associated with saturation of the cellular RNAi machinery and changes in endogenous miRNA expression. Using lower doses of vectors encoding shRNA may circumvent toxicity but this may result in loss of RNAi silencing and therapeutic efficacy [123]. Alternatively, toxicity resulting from shRNA overexpression can be resolved by embedding the siRNA sequence into an artificial miRNA scaffold and expressing it from weaker pol II promoters [124,125]. Incorporation of a siRNA sequence in an artificial miRNA scaffold has been shown to abolish shRNA-induced neuronal cell death and to avoid disruption of the endogenous RNAi pathway [29,123]. However, in some cases miRNA were found to be less potent compared to shRNA [126]. Another disadvantage of pol III-expressed shRNAs is their constitutive expression in all cell types and organs. In order to limit their expression to target organs, the use of tissue-specific promoters has been applied for shRNA [34,35]. Unfortunately, this has been achieved with limited success as the rules for efficient transcription of shRNA from poll II promoters are poorly understood and these constructs show only mild knockdown efficacy. Others have used inducible systems regulated by tetracycline or by ecdysone for expression of shRNA or artificial miRNA, which allows time- and dose-dependent expression when the inducer is administered and no expression in its absence [127-130]. Proof of concept has been established in transgenic mice enabling inducible and reversible suppression of gene expression by a tetracycline-regulated shRNA which also resulted in phenotypic changes [128]. The applicability of such systems in preclinical and clinical studies is limited because they include two additional components; elements encoding

regulatory proteins that are potentially immunogenic and inducer molecules that need to be safe for long-term applications.

Adeno-associated virus (AAV) delivery

Among the different options of vehicles for delivery of genetic material to living organisms, viruses seem to be a vector of choice because of their natural ability to infect cells. The majority of vectors used in clinical trials are engineered human or animal viruses including adenoviruses, AAV, herpes simplex virus, lentiviruses and retroviruses [131]. Adeno-associated viruses with their unique properties have been shown to be a very promising gene-therapy vector for many genetic diseases [132].

AAV is member of the *Parvoviridae* family with a small single stranded genome of around 4,7kb [133]. The genome encodes structural proteins of capsid (CAP) and replication machinery (REP) flanked by 145 bp inverted terminal repeats (ITRs). After cell infection AAV escapes endosomes or lysosomes and the genetic material translocates to the nucleus. After entry into the host cell nucleus, AAV can follow either one of the two distinct and interchangeable pathways of its life cycle: the lytic and the lysogenic. The lytic cycle develops in cells infected with a helper virus such as adenovirus or in response to DNA damage. When only AAV infects a human cell the lysogenic program is executed and the virus integrates preferentially into the long arm of chromosome 19 (referred as AAVS1) and less frequently into chromosome 5 or chromosome 3 [134,135]. This process is mediated by the REP proteins. During the latency, virus gene expression program is repressed [136]. When a latently infected cell is super-infected with a helper virus or DNA repair machinery is activated, the AAV gene expression program is activated leading to the excision of the provirus DNA from the host cell chromosome, followed by replication and packaging of the viral genome [137,138]. Finally infected cells are lysed and viruses are released. By replacing endogenous AAV genome with gene of interest flanked by ITRs and delivering in trans components for REP and CAP production, recombinant AAVs (rAAV) can be produced. Removal of CAP and REP genes alters AAV ability to specifically integrate in genome; instead the AAV genome forms concatamers which remain episomal [139]. However, recent research shows that integration of rAAV may occur at a very low level [140]. AAV has several advantages over other viral vectors [141]. AAV naturally infects humans and primates - up to 80% are thought to be seropositive for AAV2 [142] but importantly, AAV is not known to cause any disease. AAV vectors induce mild (cellular as well as humoral) immune responses, which are an important aspect of AAV-based gene therapy which will be discussed in more detail later. Based on cross-reactivity of neutralizing antibodies, different AAV serotypes can be distinguished [143]. A new AAV serotype is described when neutralizing antibodies for other virus types cannot cross-react with new virus type. There are 11 serotypes described in the literature,

however some of the serotypes fail to meet the cross-reactivity requirement i.e. AAV6 can cross-react with AAV1 while AAV10 and AAV11 are not fully characterized [143]. Furthermore there are number of AAV variants for which serological data are not available. Each AAV serotype has diverse tissue tropism and therefore specific tissues can be targeted by using a particular AAV serotype. Another interesting approach is to generate hybrid viruses or create new serotypes in order to change tissue tropism or overcome pre-existing or acquired antibody response [144]. Tissue specificity is determined by the capsid composition and expression of AAV receptors, however apart from AAV2 all other serotypes' receptors are not very well characterized.

The most common organ transduced by AAV following tail-vein injection in mice is liver. Biodistribution studies of different AAV serotypes vectors demonstrated superiority of some AAV serotypes in the context of liver targeting [145]. AAV serotypes that preferentially target mice hepatocytes after tail-vein injection are serotypes 1, 2, 5, 6, 7, and 8 [145]. Among them AAV7 has the strongest tropism to the liver, followed by AAV6. AAV1, 2, and 5 transduce also preferentially the liver, however with lower efficiency compared to AAV7 and AAV6. Additionally AAV8 and AAV9 demonstrate robust expression in the liver; however they also transduce other tissues more ubiquitously [145]. It is extremely important to understand that tissue specificity is species-specific and vectors which transducer murine liver do not necessary transduce human liver with the same efficiency.

Immune response to AAV capsid or the transgene

Side effects associated with gene therapy can originate from different sources and in the case of gene silencing; the outcome may be a combination of toxicity resulting from both RNAi and the delivery vehicle. rAAV has been shown to stably express many genes *in vivo* [146]. Surprisingly initial studies in humans led to identification of immune responses not to the transgene but to the AAV capsid [102]. A complete understanding of the interactions of rAAV with the immune system is pivotal for all gene therapy applications and both innate and adaptative immune responses should be taken into account.

In contrast to dsRNA, AAV does not appear to be recognized by any pattern recognitions receptors such as TLR [147] and AAV does not activate the classical complement reaction [148]. Nonetheless AAV virus interacts with complement and it is likely that it can be coated with serum opsonins [148]. AAV capsid has been shown to co-precipitate with factors H and C3b of the complement and it is likely that the mechanism by which AAV abrogates innate response involves conversion C3b into iC3b. AAV particles opsonized with iC3b are subject to adherence to other immune cells such as B-cells, which enhances their response and neutralizing antibody production. Most humans display naturally acquired neutralizing antibodies to AAV capsid due to initial AAV infection and activation of B-cell antibody production.

Another important aspect is the cellular response to AAV [142], which is mounted after the presentation of AAV derived antigen by mature presenting cells in lymph nodes to T cells. The manner in which the antigen is presented and the nature of the antigen itself determines the activation of antigen specific T cells. Antigen presentation can occur in two distinct manners: Antigens that are endogenously generated by the cellular machinery are presented on the Major histocompatibility complex (MHC) class I molecules which are present on all nucleated cells. Proteins exogenous to the cells are presented in context of MHC class II molecules exclusively on APC after phagocytosis or endocytosis of the pathogen [149]. During AAV infection, virus-derived antigens can be presented by APCs on both MHC class molecules. Opsonized AAVs can be phagocyted by APCs [150] and antigens will presented on MHC class II molecules. However it does not lead to CTL response as the iC3b and factor H influence APC chemokines and cytokies microenvironment. Additionally APCs are not natural targets of AAV which minimizes presentation of AAV derived antigens on MHC class I molecules. However, exogenous antigen can also be presented on MHC class I molecules via cross-presentation. Cross-presentation is the predominant mechanism by which AAV induces T cell immune response. Co-administration of an immunosuppressive regimen with AAV injection can be a good option to impede immune response to AAV [151,152]. It was shown that short-term immunosuppression did not lead to toxicity and does not interfere with AAV transduction of hepatocytes [152]. Application of immunosuppression prior injection may provide a solution for patients with pre-existing antibody response to AAV or for re-injecting patients with the same rAAV serotype as this strategy has already been validated in animal models [153,154].

Overview

Safe and long-term expression of siRNA is necessary for the treatment of patients with liver diseases that fail to respond to conventional treatment. This thesis addresses important questions about delivery of RNAi therapeutics to the liver, the efficacy of gene silencing and possible side effects. These aspects were considered in terms of constitutive and inducible expression of RNAi therapeutics in liver (Fig. 4). First, we show that ApoB can be inhibited *in vivo* using AAV vectors delivering shRNA expressed from pol III promoters. By inhibiting ApoB, a stable reduction of total plasma cholesterol and LDL-C was achieved. To minimize possible toxic effects caused by shRNA overexpression pol II-driven expression of shRNA was optimized and compared to artificial miRNA expression *in vitro*. As the latter appeared to be more potent, an artificial miRNA construct targeting ApoB was developed, allowing expression from the weaker liver-specific LP1 promoter. Subsequently the long-term efficacy and safety of shApoB and miApoB was assessed *in vivo*. Initially both shApoB and miApoB were equally efficient in knocking down ApoB in plasma and concomitant with reduction

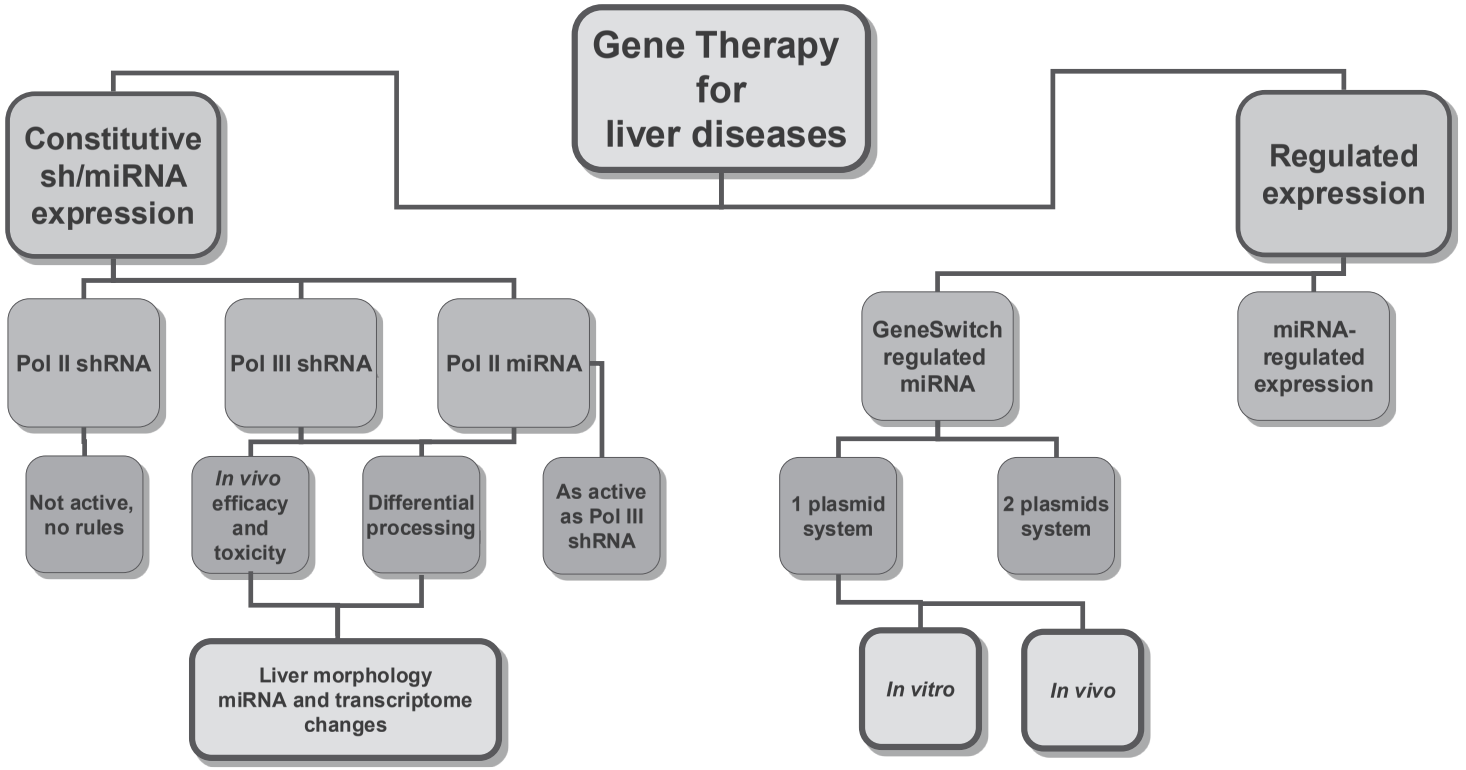
Gene Therapy for liver diseases
Constitutive sh/miRNA expression
Regulated expression
Pol II shRNA
Pol III shRNA
Pol II miRNA
GeneSwitch regulated miRNA
miRNA-regulated expression
Not active, no rules
In vivo efficacy and toxicity
Differential processing
As active as Pol III shRNA
1 plasmid system
2 plasmids system
Liver morphology miRNA and transcriptome changes
In vitro
In vivo

of total cholesterol. Surprisingly, the effect diminished over the time over the course of 27 weeks and the loss was associated with virally delivered DNA loss. To address this issue we investigated liver function and morphology 8 weeks post injection with AAV encoding shApoB or miApoB. We showed differences in processing of shApoB and miApoB, which may have serious implications for RNAi therapy of liver diseases.

A second part of this thesis was to investigate the possibility of regulated expression using two separate approaches: inducible expression of artificial miRNA and transgene regulation using endogenous miRNA. We have shown expression of miRNA targeting ApoB using the GeneSwitch inducible system which allowed time-dependent expression of siApoB when the inducer was administered and no expression in its absence. A detailed analysis of the inducible promoter was performed in order to optimize induction rate and minimize leakiness. We also optimized an expression cassette for inducible expression of miRNA, combining two structural components of the GeneSwitch system. This is important safety measure to avoid possible side-effects resulting from miRNA overexpression.

In this thesis we discuss future developments of RNAi-based gene therapy strategies for liver diseases and their potential for clinical applications. Particular emphasis is put on safety issues of the different strategies for RNAi induction in cells. Some of these topics including tissue specific expression of artificial miRNA and in a detailed analysis of *in vitro* processing have never been previously investigated, but can have serious implication if future applications of RNAi for treatment of liver diseases.

Reference list

1. Pillai, RS (2005). MicroRNA function: multiple mechanisms for a tiny RNA? *RNA*; **11:** 1753-1761.
2. Stark, A, Brennecke, J, Bushati, N, Russell, RB and Cohen, SM (2005). Animal MicroRNAs confer robustness to gene expression and have a significant impact on 3'UTR evolution. *Cell*; **123:** 1133-1146.
3. Castanotto, D and Rossi, JJ (2009). The promises and pitfalls of RNA-interference-based therapeutics. *Nature*; **457:** 426-433.
4. Ecker, JR and Davis, RW (1986). Inhibition of gene expression in plant cells by expression of antisense RNA. *Proc Natl Acad Sci U S A*; **83:** 5372-5376.
5. Napoli, C, Lemieux, C and Jorgensen, R (1990). Introduction of a chimeric chalcone synthase gene into petunia results in reversible co-suppression of homologous genes in trans. *The Plant Cell Online*; **2:** 279-289.
6. Romano, N and Macino, G (1992). Quelling: transient inactivation of gene expression in Neurospora crassa by transformation with homologous sequences. *Mol Microbiol*; **6:** 3343-3353.
7. Guo, S and Kemphues, KJ (1995). Par-1, a gene required for establishing polarity in C. elegans embryos, encodes a putative Ser/Thr kinase that is asymmetrically distributed. *Cell*; **81:** 611-620.
8. Fire, A, Xu, S, Montgomery, MK, Kostas, SA, Driver, SE and Mello, CC (1998). Potent and specific genetic interference by double-stranded RNA in Caenorhabditis elegans. *Nature*; **391:** 806-811.
9. Borchert, GM, Lanier, W and Davidson, BL (2006). RNA polymerase III transcribes human microRNAs. *Nat Struct Mol Biol*; **13:** 1097-1101.
10. Zeng, Y, Yi, R and Cullen, BR (2005). Recognition and cleavage of primary microRNA precursors by the nuclear processing enzyme Drosha. *EMBO J*; **24:** 138-148.
11. MacRae, IJ, Zhou, K and Doudna, JA (2007). Structural determinants of RNA recognition and cleavage by Dicer. *Nat Struct Mol Biol*; **14:** 934-940.
12. Gu, S, Jin, L, Zhang, F, Huang, Y, Grimm, D, Rossi, JJ, et al. (2011). Thermodynamic stability of small hairpin RNAs highly influences the loading process of different mammalian Argonautes. *Proc Natl Acad Sci U S A*; **108:** 9208-9213.
13. zuma-Mukai, A, Oguri, H, Mituyama, T, Qian, ZR, Asai, K, Siomi, H, et al. (2008). Characterization of endogenous human Argonautes and their miRNA partners in RNA silencing. *Proc Natl Acad Sci U S A*; **105:** 7964-7969.
14. Gregory, RI, Chendrimada, TP, Cooch, N and Shiekhattar, R (2005). Human RISC couples microRNA biogenesis and posttranscriptional gene silencing. *Cell*; **123:** 631-640.
15. Lewis, BP, Shih, Ih, Jones-Rhoades, MW, Bartel, DP and Burge, CB (2003). Prediction of Mammalian MicroRNA Targets. *Cell*; **115:** 787-798.
16. Lewis, BP, Burge, CB and Bartel, DP (2005). Conserved seed pairing, often flanked by adenosines, indicates that thousands of human genes are microRNA targets. *Cell*; **120:** 15-20.
17. Kini, HK and Walton, SP (2007). In vitro binding of single-stranded RNA by human Dicer. *FEBS Letters*; **581:** 5611-5616.
18. Aliyari, R and Ding, SW (2009). RNA-based viral immunity initiated by the Dicer family of host immune receptors. *Immunol Rev*; **227:** 176-188.
19. Tenllado, F and Díaz-Ruíz, JR (2001). Double-stranded RNA-mediated interference with plant virus infection. *J Virol*; **75:** 12288-12297.
20. Kumar, A (2008). RNA interference: a multifaceted innate antiviral defense. *Retrovirology*; **5:** 17.
21. Umbach, JL and Cullen, BR (2009). The role of RNAi and microRNAs in animal virus replication and antiviral immunity. *Genes Dev*; **23:** 1151-1164.
22. Elbashir, SM, Harborth, J, Lendeckel, W, Yalcin, A, Weber, K and Tuschl, T (2001). Duplexes of 21-nucleotide RNAs mediate RNA interference in cultured mammalian cells. *Nature*; **411:** 494-498.
23. Burnett, JC, Rossi, JJ and Tiemann, K (2011). Current progress of siRNA/shRNA therapeutics in clinical trials. *Biotechnol J*; **6:** 1130-1146.
24. Rettig, GR and Behlke, MA (2012). Progress toward in vivo use of siRNAs-II. *Mol Ther*; **20:** 483-512.
25. Paddison, PJ, Caudy, AA, Bernstein, E, Hannon, GJ and Conklin, DS (2002). Short hairpin RNAs (shRNAs) induce sequence-specific silencing in mammalian cells. *Genes Dev*; **16:** 948-958.
26. Konstantinova, P, de Vries, W, Haasnoot, J, ter Brake, O, de Haan, P and Berkhout, B (2006).

Inhibition of human immunodeficiency virus type 1 by RNA interference using long-hairpin RNA. *Gene Ther*; **13:** 1403-1413.

27. Konstantinova, P, ter Brake, O, Haasnoot, J, de Haan, P and Berkhout, B (2007). Trans-inhibition of HIV-1 by a long hairpin RNA expressed within the viral genome. *Retrovirology*; **4:** 15.
28. Weinberg, MS, Ely, A, Barichievy, S, Crowther, C, Mufamadi, S, Carmona, S, et al. (2007). Specific inhibition of HBV replication in vitro and in vivo with expressed long hairpin RNA. *Mol Ther*; **15:** 534-541.
29. Boudreau, RL, Martins, I and Davidson, BL (2009). Artificial microRNAs as siRNA shuttles: improved safety as compared to shRNAs in vitro and in vivo. *Mol Ther*; **17:** 169-175.
30. Couto, LB and High, KA (2010). Viral vector-mediated RNA interference. *Current Opinion in Pharmacology*; **10:** 534-542.
31. Chen, M, Du, Q, Zhang, HY, Wahlestedt, C and Liang, Z (2005). Vector-based siRNA delivery strategies for high-throughput screening of novel target genes. *J RNAi Gene Silencing*; **1:** 5-11.
32. Siolas, D, Lerner, C, Burchard, J, Ge, W, Linsley, PS, Paddison, PJ, et al. (2005). Synthetic shRNAs as potent RNAi triggers. *Nat Biotech*; **23:** 227-231.
33. Xia, H, Mao, Q, Paulson, HL and Davidson, BL (2002). siRNA-mediated gene silencing in vitro and in vivo. *Nat Biotech*; **20:** 1006-1010.
34. Song, J, Pang, S, Lu, Y, Yokoyama, KK, Zheng, JY and Chiu, R (2004). Gene silencing in androgen-responsive prostate cancer cells from the tissue-specific Prostate-specific antigen promoter. *Cancer Research*; **64:** 7661-7663.
35. Giering, JC, Grimm, D, Storm, TA and Kay, MA (2008). Expression of shRNA from a tissue-specific pol II promoter is an effective and safe RNAi therapeutic. *Mol Ther*; **16:** 1630-1636.
36. Saayman, S, Arbuthnot, P and Weinberg, MS (2010). Deriving four functional anti-HIV siRNAs from a single Pol III-generated transcript comprising two adjacent long hairpin RNA precursors. *Nucl Acids Res*; **38:** 6652-6663.
37. Han, J, Lee, Y, Yeom, KH, Kim, YK, Jin, H and Kim, VN (2004). The Drosha-DGCR8 complex in primary microRNA processing. *Genes Dev*; **18:** 3016-3027.
38. Zhou, H, Huang, C and Xia, XG (2008). A tightly regulated Pol III promoter for synthesis of miRNA genes in tandem. *Biochim Biophys Acta*; **11:** 773-9.
39. Gregory, RI and Shiekhattar, R (2005). MicroRNA biogenesis and cancer. *Cancer Res*; **65:** 3509-3512.
40. Sullivan, CS and Ganem, D (2005). MicroRNAs and viral infection. *Mol Cell*; **20:** 3-7.
41. Coulouarn, C, Factor, VM, Andersen, JB, Durkin, ME and Thorgeirsson, SS (2009). Loss of miR-122 expression in liver cancer correlates with suppression of the hepatic phenotype and gain of metastatic properties. *Oncogene*; **28:** 3526-3536.
42. Valastyan, S, Reinhardt, F, Benaich, N, Calogrias, D, Szász, AM, Wang, ZC, et al. (2009). A pleiotropically acting microRNA, miR-31, inhibits breast cancer metastasis. *Cell*; **137:** 1032-1046.
43. Karali, M, Manfredi, A, Puppo, A, Marrocco, E, Gargiulo, A, Allocca, M, et al. (2011). MicroRNA-Restricted Transgene Expression in the Retina. *PLoS ONE*; **6:** e22166.
44. Brown, BD, Gentner, B, Cantore, A, Colleoni, S, Amendola, M, Zingale, A, et al. (2007). Endogenous microRNA can be broadly exploited to regulate transgene expression according to tissue, lineage and differentiation state. *Nat Biotechnol*; **25:** 1457-1467.
45. Brown, BD, Cantore, A, Annoni, A, Sergi, LS, Lombardo, A, Della, VP, et al. (2007). A microRNA-regulated lentiviral vector mediates stable correction of hemophilia B mice. *Blood*; **110:** 4144-4152.
46. Sjouke, B, Kusters, D, Kastelein, J and Hovingh, G (2011). Familial Hypercholesterolemia: Present and Future Management. *Curr Cardiol Rep*; **13:** 527-536.
47. van Aalst-Cohen, ES, Jansen, ACM, Tanck, MWT, Defesche, JC, Trip, MD, Lansberg, PJ, et al. (2006). Diagnosing familial hypercholesterolaemia: the relevance of genetic testing. *Eur Heart J*; **27:** 2240-2246.
48. Myant, NB (1993). Familial defective apolipoprotein B-100: a review, including some comparisons with familial hypercholesterolaemia. *Atherosclerosis*; **104:** 1-18.
49. Tosi, I, Toledo-Leiva, P, Neuwirth, C, Naoumova, RP and Soutar, AK (2007). Genetic defects causing familial hypercholesterolaemia: Identification of deletions and duplications in the LDL-receptor gene and summary of all mutations found in patients attending the Hammersmith Hospital Lipid Clinic. *Atherosclerosis*; **194:** 102-111.
50. Austin, MA, Hutter, CM, Zimmern, RL and Humphries, SE (2004). Genetic Causes

of Monogenic Heterozygous Familial Hypercholesterolemia: A HuGE Prevalence Review. *Am J Epidemiol*; **160:** 407-420.

51. Cohen, MS (2004). Fetal and childhood onset of adult cardiovascular diseases. *Pediatr Clin North Am*; **51:** 1697-1719.
52. Rader, DJ, Cohen, J and Hobbs, HH (2003). Monogenic hypercholesterolemia: new insights in pathogenesis and treatment. *J Clin Invest*; **111:** 1795-1803.
53. Brown, MS and Goldstein, JL (1986). A receptor-mediated pathway for cholesterol homeostasis. *Science*; **232:** 34-47.
54. Al-Allaf, F, Coutelle, C, Waddington, S, David, A, Harbottle, R and Themis, M (2010). LDLR-Gene therapy for familial hypercholesterolaemia: problems, progress, and perspectives. *Int Arch Med*; **3:** 36.
55. Chen, SJ, Rader, DJ, Tazelaar, J, Kawashiri, M, Gao, G and Wilson, JM (2000). Prolonged correction of hyperlipidemia in mice with familial hypercholesterolemia using an adeno-associated viral vector expressing very-low-density lipoprotein receptor. *Mol Ther*; **2:** 256-261.
56. Frank-Kamenetsky, M, Grefhorst, A, Anderson, NN, Racie, TS, Bramlage, B, Akinc, A, et al. (2008). Therapeutic RNAi targeting PCSK9 acutely lowers plasma cholesterol in rodents and LDL cholesterol in nonhuman primates. *Proc Natl Acad Sci U S A*; **105:** 11915-11920.
57. Soutschek, J, Akinc, A, Bramlage, B, Charisse, K, Constien, R, Donoghue, M, et al. (2004). Therapeutic silencing of an endogenous gene by systemic administration of modified siRNAs. *Nature*; **432:** 173-178.
58. Zimmermann, TS, Lee, AC, Akinc, A, Bramlage, B, Bumcrot, D, Fedoruk, MN, et al. (2006). RNAi-mediated gene silencing in non-human primates. *Nature*; **441:** 111-114.
59. Gettins, PGW (2002). Serpin Structure, Mechanism, and Function. *Chem Rev*; **102:** 4751-4804.
60. DeMeo, DL and Silverman, EK (2004). Alpha1-antitrypsin deficiency. 2: genetic aspects of alpha(1)-antitrypsin deficiency: phenotypes and genetic modifiers of emphysema risk. *Thorax*; **59:** 259-264.
61. Schlade-Bartusiak, K and Cox, DW (1993). Alpha1-antitrypsin deficiency.
62. Lomas, DA and Mahadeva, R (2002). Alpha1-antitrypsin polymerization and the serpinopathies: pathobiology and prospects for therapy. *J Clin Invest*; **110:** 1585-1590.
63. Perlmutter, DH (2002). Liver injury in alpha1-antitrypsin deficiency: an aggregated protein induces mitochondrial injury. *J Clin Invest*; **110:** 1579-1583.
64. Li, C, Xiao, P, Gray, SJ, Weinberg, MS and Samulski, RJ (2011). Combination therapy utilizing shRNA knockdown and an optimized resistant transgene for rescue of diseases caused by misfolded proteins. *Proc Natl Acad Sci U S A*; **108:** 14258-14263.
65. Mueller, C, Tang, Q, Gruntman, A, Blomenkamp, K, Teckman, J, Song, L, et al. (2012). Sustained miRNA-mediated knockdown of mutant AAT with simultaneous augmentation of wild-type AAT has minimal effect on global liver miRNA profiles. *Mol Ther*; **20:** 590-600.
66. Wang, XW, Hussain, SP, Huo, TI, Wu, CG, Forgues, M, Hofseth, LJ, et al. (2002). Molecular pathogenesis of human hepatocellular carcinoma. *Toxicology*; **181;182:** 43-47.
67. Bonin, S, Pascolo, L, Croce, LS, Stanta, G and Tiribelli, C (2002). Gene expression of ABC proteins in hepatocellular carcinoma, perineoplastic tissue, and liver diseases. *Mol Med*; **8:** 318-325.
68. Borel, F, van Logtenstein R., Koornneef, A, Maczuga, P, Ritsema, T, Petry, H, et al. (2011). In vivo knock-down of multidrug resistance transporters ABCC1 and ABCC2 by AAV-delivered shRNAs and by artificial miRNAs. *J RNAi Gene Silencing*; **7:** 434-442.
69. Borel, F, Han, R, Visser, A, Petry, H, van Deventer, SJH, Jansen, PLM, et al. (2012). Adenosine triphosphate-binding cassette transporter genes up-regulation in untreated hepatocellular carcinoma is mediated by cellular microRNAs. *Hepatology*; **55:** 821-832.
70. Coulouarn, C, Factor, VM, Andersen, JB, Durkin, ME and Thorgeirsson, SS (2009). Loss of miR-122 expression in liver cancer correlates with suppression of the hepatic phenotype and gain of metastatic properties. *Oncogene*; **28:** 3526-3536.
71. Xia, L, Zhang, D, Du, R, Pan, Y, Zhao, L, Sun, S, et al. (2008). miR-15b and miR-16 modulate multidrug resistance by targeting BCL2 in human gastric cancer cells. *Int J Cancer*; **123:** 372-379.
72. Zhu, H, Wu, H, Liu, X, Evans, BR, Medina, DJ, Liu, CG, et al. (2008). Role of MicroRNA miR-27a and miR-451 in the regulation of MDR1/P-glycoprotein expression in human cancer cells. *Biochem Pharmacol*; **76:** 582-588.

73. Ayoub, WS and Keeffe, EB (2011). Review article: current antiviral therapy of chronic hepatitis B. *Aliment Pharmacol Ther*; **34:** 1145-1158.
74. Williams, R (2006). Global challenges in liver disease. *Hepatology*; **44:** 521-526.
75. Seeger, C and Mason, WS (2000). Hepatitis B Virus Biology. *Microbiol Mol Biol Rev*; **64:** 51-68.
76. McCaffrey, AP, Nakai, H, Pandey, K, Huang, Z, Salazar, FH, Xu, H, et al. (2003). Inhibition of hepatitis B virus in mice by RNA interference. *Nat Biotech*; **21:** 639-644.
77. Gao, YF, Yu, L, Wei, W, Li, JB, Luo, QL and Shen, JL (2008). Inhibition of hepatitis B virus gene expression and replication by artificial microRNA. *World J Gastroenterol*; **14:** 4684-4689.
78. Snyder, LL, Ahmed, I and Steel, LF (2009). RNA polymerase III can drive polycistronic expression of functional interfering RNAs designed to resemble microRNAs. *Nucleic Acids Res*; **37:** e127.
79. Lee, LY, Tong, CYW, Wong, T and Wilkinson, M (2012). New therapies for chronic hepatitis C infection: a systematic review of evidence from clinical trials. *Int J Clin Pract*; **66:** 342-355.
80. Chevaliez, S and Pawlotsky, JM (2006). HCV genome and life cycle.
81. Pawlotsky, JM, Chevaliez, S and McHutchison, JG (2007). The hepatitis C virus life cycle as a target for new antiviral therapies. *Gastroenterology*; **132:** 1979-1998.
82. Yokota, T, Sakamoto, N, Enomoto, N, Tanabe, Y, Miyagishi, M, Maekawa, S, et al. (2003). Inhibition of intracellular hepatitis C virus replication by synthetic and vector-derived small interfering RNAs. *EMBO Rep*; **4:** 602-608.
83. Sen, A, Steele, R, Ghosh, AK, Basu, A, Ray, R and Ray, RB (2003). Inhibition of hepatitis C virus protein expression by RNA interference. *Virus Res*; **96:** 27-35.
84. Krönke, J, Kittler, R, Buchholz, F, Windisch, MP, Pietschmann, T, Bartenschlager, R, et al. (2004). Alternative approaches for efficient inhibition of hepatitis C virus RNA replication by small interfering RNAs. *J Virol*; **78:** 3436-3446.
85. Ashfaq, U, Yousaf, M, Aslam, M, Ejaz, R, Jahan, S and Ullah, O (2011). siRNAs: Potential therapeutic agents against Hepatitis C Virus. *Virol J*; **8:** 276.
86. Wilson, JA and Richardson, CD (2005). Hepatitis C virus replicons escape RNA interference induced by a short interfering RNA directed against the NS5b coding region. *J Virol*; **79:** 7050-7058.
87. Akashi, H, Miyagishi, M, Yokota, T, Watanabe, T, Hino, T, Nishina, K, et al. (2005). Escape from the interferon response associated with RNA interference using vectors that encode long modified hairpin-RNA. *Mol BioSyst*; **1:** 382-390.
88. Watanabe, T, Sudoh, M, Miyagishi, M, Akashi, H, Arai, M, Inoue, K, et al. (2006). Intracellular-diced dsRNA has enhanced efficacy for silencing HCV RNA and overcomes variation in the viral genotype. *Gene Ther*; **13:** 883-892.
89. Chang, J, Guo, JT, Jiang, D, Guo, H, Taylor, JM and Block, TM (2008). Liver-specific microRNA miR-122 enhances the replication of hepatitis C virus in nonhepatic cells. *J Virol*; **82:** 8215-8223.
90. Lanford, RE, Hildebrandt-Eriksen, ES, Petri, A, Persson, R, Lindow, M, Munk, ME, et al. (2010). Therapeutic silencing of microRNA-122 in primates with chronic hepatitis C virus infection. *Science*; **327:** 198-201.
91. Haussecker, D and Kay, MA (2010). miR-122 continues to blaze the trail for microRNA therapeutics. *Mol Ther*; **18:** 240-242.
92. Lee, CA, Kessler, CM, Varon, D, Martinowitz, U, Heim, M and Lillicrap, D (1998). The molecular basis of haemophilia B. *Haemophilia*; **4:** 350-357.
93. Manno, CS, Arruda, VR, Pierce, GF, Glader, B, Ragni, M, Rasko, J, et al. (2006). Successful transduction of liver in hemophilia by AAV-Factor IX and limitations imposed by the host immune response. *Nat Med*; **12:** 342-347.
94. Margaritis, P (2010). Long-term expression of canine FVIIa in hemophilic dogs. *Thrombosis Research*; 125, Supplement **1:** S60-S62.
95. Hasbrouck, NC and High, KA (2008). AAV-mediated gene transfer for the treatment of hemophilia B: problems and prospects. *Gene Ther*; **15:** 870-875.
96. Harding, TC, Koprivnikar, KE, Tu, GH, Zayek, N, Lew, S, Subramanian, A, et al. (0 AD). Intravenous administration of an AAV-2 vector for the expression of factor IX in mice and a dog model of hemophilia B. *Gene Ther*; **11:** 204-213.
97. Dai, Y, Schwarz, EM, Gu, D, Zhang, WW, Sarvetnick, N and Verma, IM (1995). Cellular and humoral immune responses to adenoviral vectors containing factor IX gene: tolerization of factor IX and vector antigens allows for long-term expression. *Proc Natl Acad Sci U S A*; **92:** 1401-1405.
98. Tsui, LV, Kelly, M, Zayek, N, Rojas, V, Ho, K, Ge, Y, et al. (2002). Production of human clotting Factor IX without toxicity in mice

after vascular delivery of a lentiviral vector. *Nat Biotech*; **20:** 53-57.

99. Mingozzi, F, Liu, YL, Dobrzynski, E, Kaufhold, A, Liu, JH, Wang, Y, et al. (2003). Induction of immune tolerance to coagulation factor IX antigen by in vivo hepatic gene transfer. *J Clinical Investig*; **111:** 1347-1356.
100. Follenzi, A, Battaglia, M, Lombardo, A, Annoni, A, Roncarolo, MG and Naldini, L (2004). Targeting lentiviral vector expression to hepatocytes limits transgene-specific immune response and establishes long-term expression of human antihemophilic factor IX in mice. *Blood*; **103:** 3700-3709.
101. Brown, BD, Venneri, MA, Zingale, A, Sergi, SL and Naldini, L (2006). Endogenous microRNA regulation suppresses transgene expression in hematopoietic lineages and enables stable gene transfer. *Nat Med*; **12:** 585-591.
102. Nathwani, AC, Tuddenham, EGD, Rangarajan, S, Rosales, C, McIntosh, J, Linch, DC, et al. (2011). Adenovirus-associated virus vector-mediated gene transfer in Hemophilia B. *N Engl J Med*; **365:** 2357-2365.
103. Judge, AD, Sood, V, Shaw, JR, Fang, D, McClintock, K and MacLachlan, I (2005). Sequence-dependent stimulation of the mammalian innate immune response by synthetic siRNA. *Nat Biotech*; **23:** 457-462.
104. Balachandran, S, Roberts, PC, Brown, LE, Truong, H, Pattnaik, AK, Archer, DR, et al. (2000). Essential role for the dsRNA-dependent protein kinase PKR in innate immunity to viral infection. *Immunity*; **13:** 129-141.
105. Bridge, AJ, Pebernard, S, Ducraux, A, Nicoulaz, AL and Iggo, R (2003). Induction of an interferon response by RNAi vectors in mammalian cells. *Nat Genet*; **34:** 263-264.
106. Kleinman, ME, Yamada, K, Takeda, A, Chandrasekaran, V, Nozaki, M, Baffi, JZ, et al. (2008). Sequence- and target-independent angiogenesis suppression by siRNA via TLR3. *Nature*; **452:** 591-597.
107. Li, XL, Ezelle, HJ, Hsi, TY and Hassel, BA (2011). A central role for RNA in the induction and biological activities of type 1 interferons. *WIREs RNA*; **2:** 58-78.
108. Alexopoulou, L, Holt, AC, Medzhitov, R and Flavell, RA (2001). Recognition of double-stranded RNA and activation of NF-[kappa]B by Toll-like receptor 3. *Nature*; **413:** 732-738.
109. Diebold, SS (2008). Recognition of viral single-stranded RNA by Toll-like receptors. *Adv Drug Deliv Rev*; **60:** 813-823.
110. Honey, K (2004). TLR ligands from the natural world. *Nat Rev Immunol*; **4:** 247.
111. Jackson, AL and Linsley, PS (2010). Recognizing and avoiding siRNA off-target effects for target identification and therapeutic application. *Nat Rev Drug Discov*; **9:** 57-67.
112. Qiu, S, Adema, CM and Lane, T (2005). A computational study of off-target effects of RNA interference. *Nucl Acids Res*; **33:** 1834-1847.
113. Brown, K and Samarsky, D (2006). RNAi off-targeting: Light at the end of the tunnel. *J RNAi Gene Silencing*; **2:** 175-177.
114. Snøve, J and Holen, T (2004). Many commonly used siRNAs risk off-target activity. *Biochem Biophys Res Commun*; **319:** 256-263.
115. Gredell, JA, Dittmer, MJ, Wu, M, Chan, C and Walton, SP (2010). Recognition of siRNA asymmetry by TAR RNA binding protein. *Biochemistry*; **49:** 3148-3155.
116. Wei, JX, Yang, J, Sun, JF, Jia, LT, Zhang, Y, Zhang, HZ, et al. (2009). Both strands of siRNA have potential to guide posttranscriptional gene silencing in mammalian cells. *PLoS ONE*; **4:** e5382.
117. Wu, H, Ma, H, Ye, C, Ramirez, D, Chen, S, Montoya, J, et al. (2011). Improved siRNA/shRNA Functionality by Mismatched Duplex. *PLoS ONE*; **6:** e28580.
118. Fedorov, Y, Anderson, EM, Birmingham, A, Reynolds, A, Karpilow, J, Robinson, K, et al. (2006). Off-target effects by siRNA can induce toxic phenotype. *RNA*; **12:** 1188-1196.
119. Ebert, MS and Sharp, PA (2010). Emerging roles for natural microRNA sponges. *Curr Biol*; **20:** R858-R861.
120. Bish, LT, Sleeper, MM, Reynolds, C, Gazzara, J, Withnall, E, Singletary, GE, et al. (2011). Cardiac gene transfer of short hairpin RNA directed against phospholamban effectively knocks down gene expression but causes cellular toxicity in canines. *Hum Gene Ther*; **22:** 969-977.
121. Grimm, D, Streetz, KL, Jopling, CL, Storm, TA, Pandey, K, Davis, CR, et al. (2006). Fatality in mice due to oversaturation of cellular microRNA/short hairpin RNA pathways. *Nature*; **441:** 537-541.
122. Ahn, M, Witting, SR, Ruiz, R, Saxena, R and Morral, N (2011). Constitutive expression of shRNA in vivo triggers build up of mature hairpin molecules. *Hum Gene Ther*; **22:** 1483-1497.
123. McBride, JL, Boudreau, RL, Harper, SQ, Staber, PD, Monteys, AM, Martins, I, et al. (2008). Artificial miRNAs mitigate shRNA-

mediated toxicity in the brain: Implications for the therapeutic development of RNAi. *Proc Natl Acad Sci U S A*; **105:** 5868-5873.

124. Castanotto, D, Sakurai, K, Lingeman, R, Li, H, Shively, L, Aagaard, L, et al. (2007). Combinatorial delivery of small interfering RNAs reduces RNAi efficacy by selective incorporation into RISC. *Nucleic Acids Res*; **35:** 5154-5164.
125. Liu, YP, Haasnoot, J, Ter, BO, Berkhout, B and Konstantinova, P (2008). Inhibition of HIV-1 by multiple siRNAs expressed from a single microRNA polycistron. *Nucleic Acids Res*; **36:** 2811-2824.
126. Boudreau, RL, Monteys, AM and Davidson, BL (2008). Minimizing variables among hairpin-based RNAi vectors reveals the potency of shRNAs. *RNA*; **14:** 1834-1844.
127. Kappel, S, Matthess, Y, Zimmer, B, Kaufmann, M and Strebhardt, K (2006). Tumor inhibition by genomically integrated inducible RNAi-cassettes. *Nucleic Acids Res*; **34:** 4527-4536.
128. McJunkin, K, Mazurek, A, Premsrirut, PK, Zuber, J, Dow, LE, Simon, J, et al. (2011). Reversible suppression of an essential gene in adult mice using transgenic RNA interference. *Proc Natl Acad Sci U S A*; **108:** 7113-7118.
129. Premsrirut, P, Dow, L, Kim, S, Camiolo, M, Malone, C, Miething, C, et al. (2011). A rapid and scalable system for studying gene function in mice using conditional RNA interference. *Cell*; **145:** 145-158.
130. Rangasamy, D, Tremethick, DJ and Greaves, IK (2008). Gene knockdown by ecdysone-based inducible RNAi in stable mammalian cell lines. *Nat Protocols*; **3:** 79-88.
131. Kay, MA, Glorioso, JC and Naldini, L (2001). Viral vectors for gene therapy: the art of turning infectious agents into vehicles of therapeutics. *Nat Med*; **7:** 33-40.
132. Grieger, J and Samulski, R (2005). Adeno-associated virus as a gene therapy vector: vector development, production and clinical applications. *Gene Therapy and Gene Delivery Systems*; **99:** 119-145
133. Goncalves, M (2005). Adeno-associated virus: from defective virus to effective vector. *Virol J*; **2:** 43.
134. Surosky, RT, Urabe, M, Godwin, SG, McQuiston, SA, Kurtzman, GJ, Ozawa, K, et al. (1997). Adeno-associated virus Rep proteins target DNA sequences to a unique locus in the human genome. *J Virol*; **71:** 7951-7959.
135. Kotin, RM, Siniscalco, M, Samulski, RJ, Zhu, XD, Hunter, L, Laughlin, CA, et al. (1990). Site-specific integration by adeno-associated virus. *Proc Natl Acad Sci U S A*; **87:** 2211-2215.
136. Berns, KI and Linden, RM (1995). The cryptic life style of adeno-associated virus. *BioEssays*; **17:** 237-245.
137. Geoffroy, MC, Epstein, AL, Toublanc, E, Moullier, P and Salvetti, A (2004). Herpes simplex virus type 1 ICP0 protein mediates activation of adeno-associated virus type 2 rep gene expression from a latent integrated form. *J Virol*; **78:** 10977-10986.
138. Geoffroy, MC and Salvetti, A (2005). Helper functions required for wild type and recombinant adeno-associated virus growth. *Curr Gene Ther*; **5:** 265-271.
139. Penaud-Budloo, M, Le Guiner, C, Nowrouzi, A, Toromanoff, A, Chérel, Y, Chenuaud, P, et al. (2008). Adeno-associated virus vector genomes persist as episomal chromatin in primate muscle. *J Virol*; **82:** 7875-7885.
140. Inagaki, K, Piao, C, Kotchey, NM, Wu, X and Nakai, H (2008). Frequency and spectrum of genomic integration of recombinant adeno-associated virus serotype 8 vector in neonatal mouse liver. *J Virol*; **82:** 9513-9524.
141. Coura, R and Nardi, N (2007). The state of the art of adeno-associated virus-based vectors in gene therapy. *Virol J*; **4:** 99.
142. Vandenberghe, LH and Wilson, JM (2007). AAV as an immunogen. *Curr Gene Ther*; **7:** 325-333.
143. Wu, Z, Asokan, A and Samulski, RJ (2006). Adeno-associated virus serotypes: vector toolkit for human gene therapy. *Mol Ther*; **14:** 316-327.
144. Wang, J, Faust, SM and Rabinowitz, JE (2011). The next step in gene delivery: Molecular engineering of adeno-associated virus serotypes. *J Mol Cell Cardiol*; **50:** 793-802.
145. Zincarelli, C, Soltys, S, Rengo, G and Rabinowitz, JE (2008). Analysis of AAV serotypes 1-9 mediated gene expression and tropism in mice after systemic injection. *Mol Ther*; **16:** 1073-1080.
146. Mingozzi, F and High, KA (2011). Therapeutic in vivo gene transfer for genetic disease using AAV: progress and challenges. *Nat Rev Genet*; **12:** 341-355.
147. Hensley, SE and Amalfitano, A (2007). Toll-like receptors impact on safety and efficacy of gene transfer vectors. *Mol Ther*; **15:** 1417-1422.
148. Zaiss, AK, Cotter, MJ, White, LR, Clark, SA, Wong, NCW, Holers, VM, et al. (2008). Complement is an essential component of the immune response to adeno-associated virus vectors. *J Virol*; **82:** 2727-2740.

149. Robinson, JH and Delvig, AA (2002). Diversity in MHC class II antigen presentation. *Immunology*; **105:** 252-262.

150. Rogers, GL, Martino, AT, Aslanidi, G, V, Jayandharan, GR, Srivastava, A and Herzog, RW (2011). Innate immune responses to AAV vectors. *Frontiers in Microbiology*; **2:** 194

151. Haurigot, V, Mingozzi, F, Buchlis, G, Hui, DJ, Chen, Y, Basner-Tschakarjan, E, et al. (2010). Safety of AAV factor IX peripheral transvenular gene delivery to muscle in hemophilia B dogs. *Mol Ther*; **18:** 1318-1329.

152. Jiang, H, Couto, LB, Patarroyo-White, S, Liu, T, Nagy, D, Vargas, JA, et al. (2006). Effects of transient immunosuppression on adenoassociated, virus-mediated, liver-directed gene transfer in rhesus macaques and implications for human gene therapy. *Blood*; **108:** 3321-3328.

153. Wang, Z, Kuhr, CS, Allen, JM, Blankinship, M, Gregorevic, P, Chamberlain, JS, et al. (2007). Sustained AAV-mediated dystrophin expression in a canine model of Duchenne muscular dystrophy with a brief course of immunosuppression. *Mol Ther*; **15:** 1160-1166.

154. McIntosh, JH, Cochrane, M, Cobbold, S, Waldmann, H, Nathwani, SA, Davidoff, AM, et al. (2012). Successful attenuation of humoral immunity to viral capsid and transgenic protein following AAV-mediated gene transfer with a non-depleting CD4 antibody and cyclosporine. *Gene Ther*; **19:** 78-85.

CHAPTER 2

Apolipoprotein B knockdown by AAV-delivered shRNA lowers plasma cholesterol in mice

Annemart Koornneef[1], Piotr Maczuga[1,2], Richard van Logtenstein[1], Florie Borel[1,3], Bas Blits[1], Tita Ritsema[1], Sander van Deventer[2], Harald Petry[1] and Pavlina Konstantinova[1]

[1]Research & Development, Amsterdam Molecular Therapeutics, Amsterdam, the Netherlands; [2]Department of Gastroenterology and Hepatology, Leiden University Medical Center, Leiden, the Netherlands; [3]Department of Gastroenterology and Hepatology, Academic Medical Center, Amsterdam, the Netherlands

Molecular Therapy (2011); 19: *731–740*

Abstract

Serum low-density lipoprotein cholesterol (LDL-C) levels are proportionate to the risk of atherosclerotic cardiovascular disease. In order to reduce serum total cholesterol and LDL-C levels in mice, RNA interference was used to inhibit expression of the structural protein of LDL-C, apolipoprotein B100 (ApoB). We developed and screened 19 short hairpin RNAs targeting conserved sequences in human, mouse, and macaque ApoB mRNAs (shApoB) and subsequently narrowed our focus to one candidate for *in vivo* testing. Self-complementary adeno-associated virus serotype 8 (scAAV8) was used for long-term transduction of murine liver with shApoB. A strong dose-dependent knockdown of ApoB mRNA and protein was observed, which correlated with a reduction in total cholesterol levels, without obvious signs of toxicity. Furthermore, shApoB was found to specifically reduce LDL-C in diet-induced dyslipidemic mice, while high-density lipoprotein cholesterol (HDL-C) remained unaffected. Finally, elevated lipid accumulation was shown in murine liver transduced with shApoB, a known phenotypic side effect of lowering ApoB levels. These results demonstrate a robust dose-dependent knockdown of ApoB by AAV-delivered shRNA in murine liver, thus providing an excellent candidate for development of RNAi-based gene therapy for the treatment of hypercholesterolemia.

Introduction

Elevated levels of serum total cholesterol and low-density lipoprotein cholesterol (LDL-C) are major risk factors and contributors to the development of atherosclerosis and cardiovascular disease (CVD). Currently, hydroxymethylglutaryl coenzyme A reductase inhibitors (statins) are the preferred pharmacologic agents for hypercholesterolemia treatment due to their superior efficacy in lowering LDL-C, proven ability to reduce CVD morbidity and mortality, and a low incidence of adverse events. However, statins are not uniformly effective in all patients and some patients can be relatively refractory to treatment due to absent or diminished LDL-C receptor activity [1]. Furthermore, ten to fifteen percent of patients are unable to take statins due to intolerable muscle symptoms like myalgias, myositis, or mitochondrial injury [2]. Thus, effective therapeutic alternatives with a different mechanism of action are needed.

Apolipoprotein B (ApoB) is required for the assembly of lipoprotein particles and is a constituent of all classes of lipoproteins that are considered atherogenic [3]. ApoB exists in two isoforms, ApoB100 and ApoB48, which are transcribed from a single gene. ApoB100 is the full-length ApoB protein and is synthesized by the liver. It forms the structural protein in very low-density lipoprotein cholesterol (VLDL-C) and LDL-C particles, which are essential for the transport and metabolism of cholesterol. ApoB48 contains the amino-terminal 2152 amino acids of ApoB100 as a result of ApoB mRNA editing which yields an early stop codon. In humans, ApoB is edited solely in the small intestine where ApoB48 plays a role in dietary fat absorption as part of chylomicrons. By contrast, some species such as mice and rats also edit ApoB in their liver and hence synthesize both ApoB100 and ApoB48 [4].

Elevated ApoB levels correlate with increased risk of coronary artery disease [5]. As a large, lipid-associated protein, ApoB belongs to the so-called "non-druggable" targets, which are not amenable to conventional therapies. However, ApoB is a highly validated target for treatment of increased LDL-C levels and subsequent CVD [6]. An approach targeting ApoB with second-generation antisense oligonucleotides (ASO) has progressed into Phase III clinical trials for treatment of homozygous familial hypercholesterolemia [6]. Another therapeutic approach that holds great promise for silencing ApoB is based on RNA interference (RNAi).

RNAi is an evolutionary conserved sequence-specific post-transcriptional gene silencing mechanism in eukaryotes that results in the degradation of mRNA and subsequently in decrease of protein synthesis [7]. Therapeutic RNAi can be induced by synthetic small interfering RNAs (siRNA) or by intracellular expression of short hairpin RNAs (shRNAs) and artificial microRNAs (miRNA) that target a disease-causing gene [8,9,10]. shRNAs are typically expressed from a constitutive strong polymerase III (pol III) promoter, and are processed intracellularly by Dicer, rendering a mature siRNA which interacts with the cytosolic multiprotein RNA-induced silencing complex

(RISC). The RISC-incorporated siRNA binds to the complementary mRNA sequence and mediates its sequence-specific degradation [11].

The largest obstacle in using synthetic siRNAs as therapeutics *in vivo* is the need for efficient and specific delivery to target cells and organs. Chemical modifications and conjugations resulting in lower effective dose and longer half-life of the siRNA have improved their efficacy [12,13]. Chemically modified ApoB-specific siRNAs, when delivered systemically, can silence ApoB expression up to 90% in murine liver [8,14,15]. Inclusion of siApoB in liposomal formulations is another highly effective approach for ApoB silencing in the liver [16]. However, even with current improvements, siRNAs need to be delivered monthly or bi-monthly, which is not achievable for many diseases, especially in the brain, eye, heart, or other internal organs. An alternative for delivery of small RNAs is administration of a single dose of recombinant viral vectors based on lentivirus or adeno-associated virus (AAV), which yield long-term expression [17,18]. The latter holds a unique set of advantages over other vector systems, including the complete lack of pathogenicity and low immunogenicity [19]. AAV induces efficient and long-term transduction of non-dividing cells, an important facet for liver-based gene therapeutic strategies [20]. Unlike the use of synthetic siRNA molecules, AAV gene therapy allows long-term efficacy with a single dose.

In this study, we evaluated the potential of AAV-delivered shRNA for long-term silencing of ApoB in murine liver. A single intravenous injection of AAV-shA10 resulted in prolonged ApoB knockdown with no obvious signs of toxicity, concomitant with a reduction in plasma cholesterol levels. In addition, in mice fed on an atherogenic diet there was a significant reduction of LDL-C, while high density lipoprotein cholesterol (HDL-C) levels remained unchanged.

Results

Design and validation of shRNAs targeting conserved ApoB sequences

Three conserved regions in the last exon of the human, macaque, and mouse ApoB mRNA sequences were selected to design 19 anti-ApoB shRNAs. shApoB expression plasmids (A1-A19) were constructed with the H1 pol III promoter based on a 19-nucleotide target sequence (Table S1). Some of the shRNAs were targeting partly overlapping sequences. For example, shRNAs A9 to A14 were designed by sliding the ApoB target sequence with one nucleotide. All shRNA sequences had identical five-nucleotide loop sequences and the top two basepairs of the pSuper system, and ended with a 3' UU overhang derived from the pol III termination signal.

To evaluate the suppressive activities of the 19 shApoB constructs *in vitro*, we co-transfected them in HEK293T cells with renilla luciferase reporter constructs containing the last ApoB exon in the 3'UTR (Luc-ApoB). An shRNA construct targeting GFP was included as a negative control and firefly luciferase expression was measured

to control for transfection efficiency. Firefly and renilla luciferase expression were measured two days post-transfection and their ratio was used to calculate the relative luciferase activity. The renilla/firefly ratio in the presence of shGFP was set at 100% (Fig. 1a). Four shApoB constructs (A9, A10, A14, and A15) were highly effective and inhibited relative Luc-ApoB expression more than 75%. Ten shApoB constructs (A4, A5, A6, A7, A11, A12, A16, A17, A18, and A19) showed moderate activity and induced 50-75% inhibition of Luc-ApoB. The remaining shApoB constructs were not active. Interestingly, A13 was inactive, whereas the following shRNA construct A14 was highly active, indicating that a single nucleotide shift can render an shRNA ineffective. In total, one out of five tested shApoB constructs was highly active against the Luc-ApoB reporter.

The ability of several shApoB constructs to knockdown endogenous ApoB was assessed *in vitro*. The mouse hepatoma Hepa 1-6 and human hepatoma Huh7 cell lines were transfected with the highly active shApoB constructs A9, A10, A14, and the intermediately active A4, A5, A17, and A18 constructs. As a negative control the shGFP construct was transfected. The three highly active shApoB constructs inhibited murine endogenous ApoB mRNA by approximately 60% while the others were less effective (Fig. 1b). Similar results were obtained for human ApoB knockdown in the Huh7 cell line (data not shown). Generally, the inhibitory effect of the shApoB constructs on endogenous ApoB showed a similar trend to the Luc-ApoB knockdown results.

The highly active shApoB construct A10 (shA10) was selected for further analysis, and siRNA expression from this construct (siA10) was determined *in vitro*. HEK293T cells were transfected with increasing amounts of shA10 plasmid, and two days post-transfection total RNA was isolated and siA10-specific small RNA Taqman assay was performed (Fig. 1c). To calculate the copy number per cell, we used a standard line based on serial dilutions of the guide strand from a synthetic siA10 RNA oligo. Increasing the amount of transfected shA10 construct clearly correlated with an increase in expression of siA10 (Fig. 1c). For example, transfection with 5 ng and 100 ng shA10 construct resulted in approximately 125 and 970 siA10 copies per cell, respectively. Having established a good correlation between shA10 activity and siA10 expression *in vitro*, we proceeded to test the *in vivo* efficacy of this shRNA construct.

Efficient shRNA-mediated knockdown of ApoB and decrease of cholesterol *in vivo*

To test the *in vivo* efficacy of shA10, self-complementary AAV serotype 8 (scAAV8) viral vectors were produced encoding anti-ApoB shA10 or a control shScramble (shScr). C57BL/6 mice were injected via the tail vein with scAAV8-shA10 (AAV-shA10) or the control vector scAAV8-shScramble (AAV-shScr) at four different concentrations: 10^8, 10^9, 10^{10}, and 10^{11} genome copies (gc) per animal. Two weeks after injection, mice

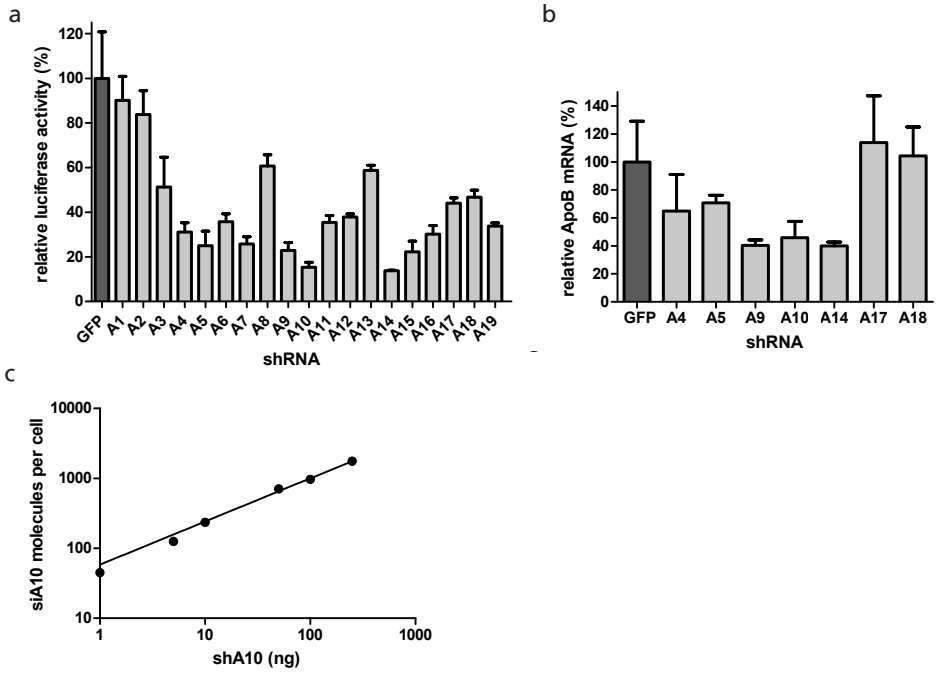

Figure 1. Inhibition of Luc-ApoB reporter and endogenous ApoB mRNA by shApoB constructs *in vitro.* (a) Luc-ApoB knockdown efficiency of anti-ApoB shRNAs expressed from the H1 promoter. HEK293T cells were co-transfected with 10 ng Luc-ApoB reporter and 50 ng different shApoB constructs (A1-A19). The shGFP construct was used as a negative control. Two days post-transfection, firefly and renilla luciferase expression was measured. Renilla luciferase expression was normalized to firefly luciferase expression and shGFP-treated cells were set at 100%. (b) Endogenous ApoB mRNA knockdown by shApoB constructs A4, A5, A9, A10, A14, A17, and A18. The shGFP construct was used as a negative control. Hepa 1-6 cells were transfected with 1 µg shApoB construct. Two days post-transfection, RNA was isolated and qRT-PCR was performed with ApoB- and actin-specific primers. ApoB mRNA levels were calculated relative to actin mRNA and shGFP-treated cells were set at 100%. (c) Small RNA Taqman detection of siA10 expression from shA10. HEK293T cells were transfected with 1, 5, 10, 50, 100, and 250 ng A10 expression construct. Two days post-transfection, RNA was isolated and siA10 Taqman was performed. The transfected amount shA10 correlates well with siA10 expression (R^2=0.997). Data are represented as mean values ±SD from a representative experiment conducted with three technical replicates. Luc, luciferase; ApoB, apolipoprotein B100; shApoB, short hairpin RNA against apolipoprotein B100; shGFP, short hairpin RNA against green fluorescent protein; Hepa 1-6, hepatoma; siA10, small interfering RNA against apolipoprotein B100.

were sacrificed and liver and plasma were analyzed for ApoB knockdown. A dose-dependent increase in AAV transduction efficiency was demonstrated by monitoring GFP fluorescence intensity and GFP mRNA expression in the liver (Figs. 2a and S1), and this correlated with a dose-dependent increase in siA10 and siScr expression (Fig. 2b and data not shown). ApoB mRNA expression in the liver was strongly reduced by administration of increasing doses of AAV-shA10 and reached up to 95% knockdown compared to PBS-injected controls at the highest administered AAV dose

(Fig. 2c). In contrast, the AAV-shScr control vector did not affect ApoB mRNA levels, apart from an unexpected inhibitory effect at the highest dose of 10^{11} gc.

To compare the effect of AAV-shA10 on ApoB mRNA with changes in ApoB protein levels, we assayed plasma and liver ApoB protein levels by Western blot at two weeks post-transduction. AAV-shA10 strongly reduced secreted ApoB100 in a dose-dependent manner, while AAV-shScr did not affect ApoB100 protein expression (Fig. 2d). Similar results were observed for liver ApoB100 protein knockdown (data not shown). In mice, unlike humans, 60-70% of hepatic ApoB mRNA is edited to form truncated ApoB48. Similar to ApoB100, we found that ApoB48 protein levels in plasma and liver were reduced (Fig. 2d and data not shown).These results indicate that a single AAV-shA10 dose achieves a potent knockdown of ApoB mRNA and protein in murine liver and plasma. Furthermore, knockdown of ApoB was associated with changes in total cholesterol levels. Being the structural protein of LDL-C, lowering of ApoB is expected to reduce cholesterol levels. Indeed, dose-dependent ApoB knockdown correlated tightly with reduction in total cholesterol levels, resulting in a maximal cholesterol decrease of 79% compared to PBS-treated controls (Fig. 2e). Profiling of cholesterol distribution over the lipoprotein subclasses revealed a major reduction in HDL-C by AAV-shA10, concomitant with a decrease in VLDL-C and LDL-C levels (Fig. 2f).

AAV-shA10 administration does not cause severe toxicity in mice

It has been reported that high levels of shRNA expression can lead to severe liver toxicity symptoms like weight loss, activation of liver-specific transaminases, changes in liver morphology, or oversaturation of the cellular miRNA machinery [21]. We monitored alanine aminotransferase (ALT) and aspartate aminotransferase (AST) levels two weeks post-transduction with AAV-shA10 and AAV-shScr and observed no significant increase in liver transaminases for the lower viral doses of 10^8, 10^9, and 10^{10} gc per animal. However, the group injected with 10^{11} gc AAV-shScr per animal showed a ten- to thirty-fold increase in ALT and AST levels, indicating liver damage (Fig. 3a). AAV-shA10 injection at a dose of 10^{11} gc per animal gave rise to a two- to five-fold increase in liver transaminases (Fig. 3a). Histological analysis of liver sections revealed no gross changes in liver morphology except for the 10^{11} gc AAV-shScr dose where abnormal morphology was observed (Fig. S2).

shRNAs and miRNAs share the same processing pathway and nuclear export machinery and overexpression of shRNAs can modify the processing of cellular miRNA transcripts [22]. We investigated whether high expression of shRNA in the liver competes with the intracellular processing of miRNAs. mir-122 was selected because it represents 70% of all liver miRNAs and is expressed almost exclusively in the liver [23]. mir-122-specific Taqman analysis was performed on RNA samples isolated from mice two weeks after administration of increasing doses of AAV-shScr

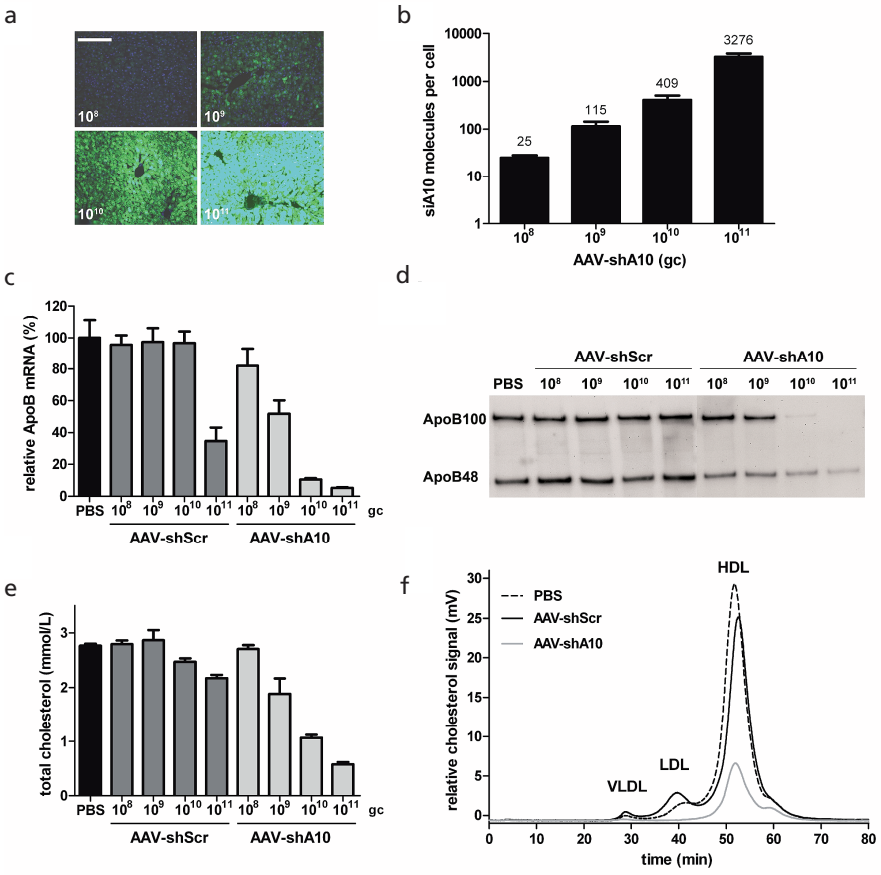

Figure 2. AAV-delivered shA10 strongly inhibits ApoB and plasma cholesterol levels two weeks post-transduction. Mice were intravenously injected with 10^8, 10^9, 10^{10}, and 10^{11} gc AAV-shA10 or control AAV-shScr per animal. Two weeks after transduction, animals were sacrificed and liver and plasma were collected for analysis. (a) Representative image of GFP fluorescence in picric-acid fixed liver, which was transduced with 10^8, 10^9, 10^{10}, or 10^{11} gc AAV-shA10 per animal, co-expressing GFP under control of the liver-specific LP1 promoter. Nuclei were visualized in blue by staining with Hoechst. Photos were taken using the same exposure and magnification settings. Scale bar=10 µm. (b) Small RNA Taqman detection of siA10 expression from liver transduced with 10^8, 10^9, 10^{10}, or 10^{11} gc AAV-shA10 per animal. Total RNA was isolated from snap-frozen livers and siA10-specific Taqman was performed. (c) Relative ApoB mRNA expression in transduced liver. Total RNA was isolated from snap-frozen liver tissue and qRT-PCR was performed with ApoB- and actin-specific primers. ApoB mRNA levels were calculated relative to actin mRNA and the PBS-treated group was set at 100%. (d) Western blot analysis of secreted ApoB100 and ApoB48 protein in 0.1 µL plasma. ApoB protein was detected using a polyclonal anti-ApoB antibody, and antibody binding was visualized by a chemiluminescence detection kit. (e) Total cholesterol levels in plasma collected from fasted mice. Cholesterol levels were analyzed on the automated clinical chemistry analyzer Modular Analytics P800 from Roche. (f) Plasma cholesterol distribution over lipoprotein subclasses in FPLC-separated pooled plasma from mice injected with 10^{11} gc AAV-shA10 or AAV-shScr per animal. Data are represented as mean ±SE, treatment groups are n=5. gc, genome copies; AAV-shA10, adeno-associated virus expressing short hairpin RNA against apolipoprotein B100; AAV-shScr, adeno-associated virus expressing short hairpin RNA scramble; GFP, green fluorescent protein; LP1, liver-specific regulatory element; siA10, small interfering RNA against apolipoprotein B100; FPLC, Fast Protein Liquid Chromatography.

and AAV-shA10. Expression profiles revealed that there was no significant decrease in mir-122 expression except for the group transduced with 10^{11} gc AAV-shScr per animal (Fig. 3b). In this group, mir-122 expression decreased more than 50%. Therefore, we analysed for increased expression levels of AldoA, Bckdk, and Ndrg3, because these genes have been reported as target genes of mir-122 [24]. Gene expression was not significantly affected in murine liver transduced with 10^{11} gc AAV-shScr or AAV-shA10 (Fig. S3). We further monitored the expression of the less abundant liver miRNAs let-7a and mir-29a (Fig. 3b). The expression profile of these miRNAs was similar to mir-122, indicating that there were no severe toxic effects induced by AAV-shA10 or AAV-shScr. Finally, the level of induction of markers of the interferon response (STAT1, TNFα, IFNβ, IFNγ) was examined by qRT-PCR on RNA isolated from murine white blood cells one week after viral administration. No significant induction of the interferon-pathway genes was observed upon viral administration indicating lack of shRNA toxicity at this time-point (data not shown).

ApoB knockdown results in fat accumulation in murine liver

ApoB suppression results in decreased cholesterol levels due to impairment of VLDL-C and LDL-C assembly, but can also lead to hepatic triglyceride accumulation. Triglycerides are normally incorporated into VLDL-C, and hepatic accumulation of these lipids can potentially cause steatosis [14]. To assess the effect of ApoB knockdown on hepatic lipid accumulation, we performed Oil red O staining on liver sections obtained from mice injected with 10^8, 10^9, 10^{10}, or 10^{11} gc AAV-shScr and AAV-shA10 per animal at two weeks post-administration (Fig. 3c). Analysis of the liver sections revealed increased accumulation of hepatic lipid content at the effective 10^9, 10^{10}, and 10^{11} gc AAV-shA10 doses compared with PBS- and AAV-shScr-injected mice (Fig. 3c). In addition, plasma triglyceride levels were also decreased after AAV-shA10 transduction, demonstrating diminished hepatic triglyceride export capacity in these mice (data not shown). These results indicate that a single AAV-shA10 administration in mice results in a dramatically decreased ApoB expression in murine liver with expected phenotypic side effects.

Long-term efficacy of AAV-shA10 in murine liver

In order to monitor the viral persistence and robustness of ApoB knockdown by AAV-shA10, a second group of mice was injected with 10^9 and 10^{11} gc AAV-shA10 or control AAV-shScr and sacrificed at eight weeks post-injection. At this time-point, we observed a significant reduction in ApoB mRNA for both AAV-shA10 viral doses confirming stable transduction of scAAV8 in murine liver (Fig. 4a). However, maximum ApoB mRNA knockdown was slightly less than at two weeks post-transduction (Figs. 2c and 4a). Similarly, GFP and siA10 expression was lower at the eight-week time-point, compared to two weeks post-injection. This effect was most pronounced in the group

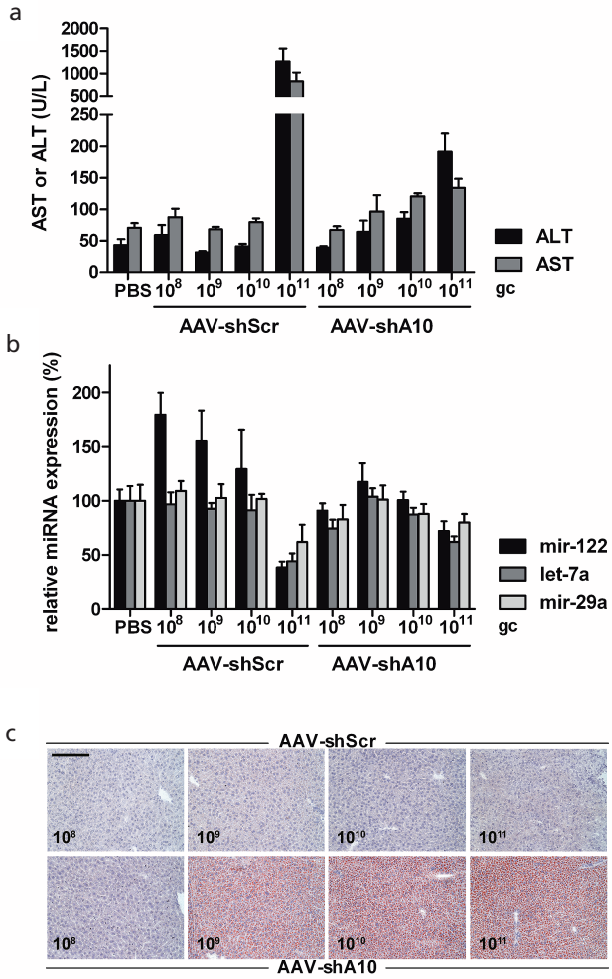

Figure 3. Effect of AAV-delivered shA10 on liver transaminases, cellular miRNA expression, and hepatic fat accumulation. Mice were intravenously injected with 10^8, 10^9, 10^{10}, and 10^{11} gc AAV-shA10 or control AAV-shScr per animal. Two weeks after transduction, animals were sacrificed and liver and plasma were collected for analysis. (a) Liver transaminases ALT and AST at two weeks post-injection. Transaminases were analyzed on the automated clinical chemistry analyzer Modular Analytics P800 from Roche. (b) Relative expression of liver-specific mir-122, let-7a, and mir-29a. Total RNA was isolated from snap-frozen livers and miRNA-specific Taqmans were performed. miRNA expression levels were calculated relative to actin mRNA and the PBS-treated group was set at 100%. Data are represented as mean ±SE, treatment groups are n=5. (c) Representative image of hepatic lipid accumulation. Frozen liver sections were stained with Oil red O for lipids, and nuclei were counterstained with hematoxylin solution. Fat accumulation was visible starting at a dose of 10^9 gc AAV-shA10. Photos were taken using the same exposure and magnification settings. Scale bar=10 µm. gc, genome copies; AAV-shA10, adeno-associated virus expressing short hairpin RNA against apolipoprotein B100; AAV-shScr, adeno-associated virus expressing short hairpin RNA scramble; ALT, alanine aminotransferase; AST, aspartate aminotransferase; mir-122, microRNA 122; let-7a, microRNA let-7a; mir-29a, microRNA 29a; miRNA, microRNA.

of animals injected with the 10^{11} dose (Figs. S4a,b). Nevertheless, AAV-shA10 was still effective at lowering ApoB100 and ApoB48 protein and cholesterol levels (Figs 4b and S4c). AAV-shA10 injection at a dose of 10^{11} gc per animal gave rise to a two- to five-fold increase in liver transaminases, which was most pronounced for ALT levels at three weeks post-injection and transaminases were still above baseline after eight weeks (Fig. 4c). During the eight week period the highest dose of 10^{11} gc AAV-shScr did not induce a dramatic increase in ALT and AST levels, as was observed in the group of animals sacrificed at two weeks post-injection (Figs. 3b and 4c). We next tested for altered expression of mir-122, mir-29a, let-7a, and mir-122 target genes at eight weeks post-injection. No significant changes were measured in liver miRNA or mir-122 target gene expression, although a trend was observed for lower miRNA levels in the animals injected with 10^{11} gc AAV-shA10 (Figs. S4 d,e).

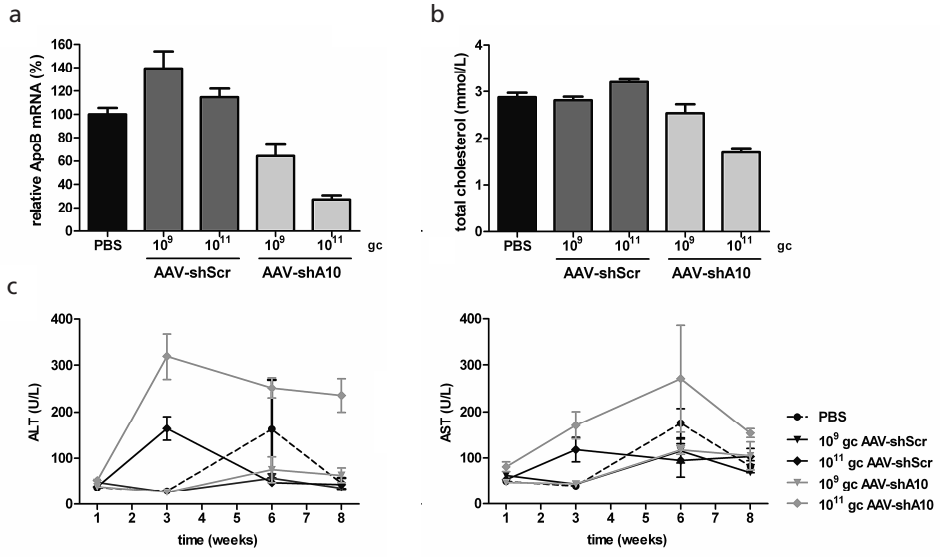

Figure 4. ApoB mRNA and cholesterol decrease eight weeks post-transduction with AAV-shA10. Mice were intravenously injected with 10^9 and 10^{11} gc AAV-shA10 or control AAV-shScr per animal. Eight weeks after transduction, animals were sacrificed and liver and plasma were collected for analysis. (a) Relative ApoB mRNA expression in liver. Total RNA was isolated from snap-frozen liver tissue and qRT-PCR was performed with ApoB- and actin-specific primers. ApoB mRNA levels were calculated relative to actin mRNA and the PBS-treated group was set at 100%. (b) Total cholesterol levels in plasma collected from fasted mice. Cholesterol levels were analyzed on the automated clinical chemistry analyzer Modular Analytics P800 from Roche. (c) Plasma ALT (left panel) and AST (right panel) levels at 1, 3, 6, and 8 weeks post-injection. Transaminases were analyzed on the automated clinical chemistry analyzer Modular Analytics P800 from Roche. Data are represented as mean ±SE, treatment groups are n=5. gc, genome copies; AAV-shA10, adeno-associated virus expressing short hairpin RNA against apolipoprotein B100; AAV-shScr, adeno-associated virus expressing short hairpin RNA scramble; ALT, alanine aminotransferase; AST, aspartate aminotransferase.

AAV-shA10 specifically reduces LDL-C in mice fed on an atherogenic diet

Mice are refractory to atherosclerosis because they have small amounts of VLDL-C and LDL-C, while HDL-C is their major lipoprotein [25]. To specifically elevate VLDL-C and LDL-C levels, mice were fed on an atherogenic diet. Nine weeks after starting on the atherogenic diet, murine livers were grossly enlarged and pale in color, and liver transaminases were elevated compared to lean control animals, as described previously [26] (data not shown). In addition, total cholesterol, VLDL-C, and LDL-C levels increased substantially compared to lean controls (Figs. 2e, 5a-b, S5a). Seven weeks after starting on the atherogenic diet, animals were injected with the effective and non-toxic dose of 10^{10} gc AAV-shA10 or control AAV-shScr per animal, and two weeks later mice were sacrificed and liver and plasma were analyzed for ApoB knockdown. Transduction efficiency in liver cells was lower in atherogenic diet-fed mice compared to lean animals, since GFP mRNA and siA10 expression was respectively hundred- and eight-fold lower (Figs. S5b,c). Nonetheless, AAV-shA10 reduced ApoB mRNA levels by 62% compared to PBS-injected controls, concomitant with a reduction in secreted ApoB100 and ApoB48 protein, whereas AAV-shScr had no effect (Figs. 4d and S5d). Furthermore, ApoB knockdown correlated with a significant reduction in plasma total cholesterol (Fig. 5a). More importantly, AAV-shA10 reduced only VLDL-C and LDL-C levels significantly, while HDL-C concentrations remained unaffected (Figs. 5b-c and S5a).

Discussion

The major challenge for RNAi-based therapies is the delivery of siRNAs to the target tissue or organ. In the last few years much progress has been made in optimizing the specificity and tissue-tropism of AAV viral vectors. AAV vectors mediating expression of shRNAs have proven to be valuable vehicles for RNAi research and therapy of various diseases in the liver, brain, and the eye [9]. However, detailed studies analyzing the dynamics and putative side effects of AAV-shRNA-mediated knockdown of ApoB *in vivo* have not been carried out. To address this issue, we have employed self-complementary AAV serotype 8 that expresses shApoB (AAV-shA10) and have studied prolonged inhibition of ApoB in murine liver. With a single injection of 10^{10} gc per animal of this vector, ApoB expression was inhibited dramatically for up to eight weeks without inducing severe toxicity or disturbance of miRNA processing.

Murine liver was transduced with increasing doses of AAV-shA10 and a good correlation between the administered viral dose and expression of siA10 and GFP mRNA was observed. ApoB knockdown occurred in a dose-dependent fashion and was already detected at a low dose of 10^{9} gc AAV-shA10 per animal, demonstrating the potency of this shRNA construct. Maximal suppression of ApoB led to 95% inhibition of ApoB mRNA and undetectable ApoB100 protein levels, concomitant

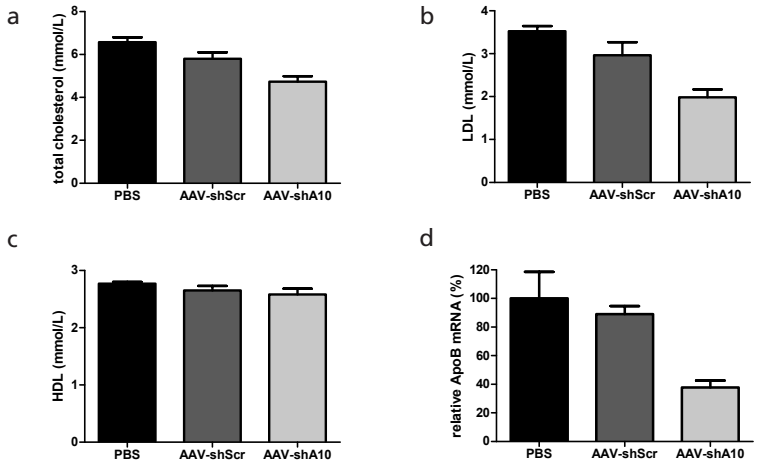

Figure 5. AAV-delivered shA10 specifically lowers total cholesterol and LDL-C levels in mice fed on an atherogenic diet. Mice were fed on an atherogenic diet for seven weeks, before intravenously receiving 10^{10} gc AAV-shA10 or control AAV-shScr per animal. Animals continued feeding on the atherogenic diet and were sacrificed at two weeks post-transduction. (a) Total cholesterol levels in plasma collected from fasted mice. (b) LDL-C levels in plasma collected from fasted mice. LDL-C levels were calculated using the Friedewald formula. AAV-shA10 significantly reduces LDL-C levels compared with PBS (p=0.001) and AAV-shScr (p=0.039) injected animals. (c) HDL-C levels in plasma collected from fasted mice. Cholesterol and HDL-C levels were analyzed on the automated clinical chemistry analyzer Modular Analytics P800 from Roche. (d) Relative ApoB mRNA expression in liver. Total RNA was isolated from snap-frozen liver tissue and qRT-PCR was performed with ApoB- and actin-specific primers. ApoB mRNA levels were calculated relative to actin mRNA and the PBS-treated group was set at 100%. Data are represented as mean ±SE, treatment groups are n=5. gc, genome copies; AAV-shA10, adeno-associated virus expressing short hairpin RNA against apolipoprotein B100; AAV-shScr, adeno-associated virus expressing short hairpin RNA scramble; HDL-C, high-density lipoprotein cholesterol; LDL-C, low-density lipoprotein cholesterol.

with a 79% reduction in plasma total cholesterol. Protein levels of ApoB48 were also reduced by AAV-shA10 in murine plasma and liver. Inhibition of ApoB48 can potentially affect dietary fat absorption in the small intestine. However, AAV-shA10 is not expected to reduce murine intestinal ApoB48, as AAV8 has a manifold higher tropism for liver than intestine [27,28]. Moreover, 85% of intestinal human ApoB transcripts have been shown to terminate after the edited stop codon, which excludes the shA10 target sequence [29]. Hence, AAV-shA10 is not likely to affect the uptake of dietary fats in humans.

We observed a strong reduction in the major lipoprotein in mice, HDL-C, along with a decrease in VLDL-C and LDL-C. The reduction of HDL-C has been attributed to the requirement of components from VLDL-C and LDL-C for the formation of mature HDL-C; hence a significant loss of VLDL-C and LDL-C should result in a similar reduction of HDL-C [30]. There is a debate on to what extent LDL-C levels need to be lowered to achieve optimal cardiovascular risk reduction. It is argued that the

most effective LDL-C intervention is a reduction of at least 30% from baseline, rather than reaching a predefined low LDL-C concentration [31]. Our data show a 32% reduction of plasma total cholesterol after a single intravenous injection with a low dose of 10^9 gc AAV-shA10 per animal, thus signifying potential therapeutic benefit for reducing cardiovascular risk by using this shRNA. To study the specific effect of AAV-shA10 on VLDL-C and LDL-C levels, C57BL/6 mice were fed an atherogenic diet. These mice had elevated levels of plasma total cholesterol, VLDL-C, and LDL-C compared with lean animals. A single administration of 10^{10} gc AAV-shA10 per animal specifically reduced total cholesterol, VLDL-C, and LDL-C levels, while HDL-C remained unaffected, demonstrating the specificity of our approach since ApoB participates only in the formation of VLDL-C and LDL-C, and not HDL-C particles. Similar data have been obtained from human subjects with mild dyslipidemia that were treated with an ApoB ASO [32].

The initial excitement around RNAi as a therapeutic of chronic diseases has been tempered by skepticism related to off-targeting and toxic effects of the shRNA. Recently, it was reported that AAV-expressed shRNAs, when administered to mice, can result in profound liver toxicity, presumably by saturation of the cellular miRNA-processing factors exportin-5 and RISC [21]. shRNA-mediated toxic effects were marked by reductions in cytoplasmic levels of mature miRNA, and were independent of the shRNA sequence. However, toxic effects were due to the injected viral vector dose of 10^{11} and 10^{12} gc per animal, which led to accumulation of extremely high cytoplasmic concentration of the shRNA. The authors discovered that ~10-fold lower viral dose and subsequently lower levels of shRNA expression was effective and well-tolerated, and had no adverse effects [21]. In our study, we were able to achieve a 90% ApoB knockdown at 10^{10} gc AAV-shA10 per animal. At this effective viral dose we did not observe any signs of toxic effects or disturbance of liver mir-122 expression. Similar to the previously published observations of Grimm *et al.* [21], we were able to reach toxic levels of shRNA expression with 10^{11} gc AAV-shScr per animal that was associated with ten to thirty times higher ALT and AST levels, decrease in cellular mir-122 expression, and changes in liver morphology. This strong liver toxicity was probably dependent on the shScr sequence because there was not such a dramatic toxic effect when 10^{11} gc AAV-shA10 per animal was used. The latter induced milder, but persistent ALT and AST activation within the eight-week period, which might be a consequence of the almost complete ApoB inhibition and hepatic fat accumulation at this viral dose. For both AAV-shA10 and AAV-shScr we observed a gradual loss of GFP expression following transduction with the high 10^{11} gc dose, while at 10^9 gc GFP expression persisted more stably within the eight-week study period. These results match previous observations that describe a reduction in transgene expression after transduction with over-expressing shRNAs due to hepatocyte death and subsequent liver repopulation by non-transduced

cells [21,33]. An alternative strategy to avoid shRNA toxicity with no sacrifice in gene-silencing efficacy is to incorporate the siRNA into an artificial miRNA scaffold [34]. It has been suggested that miRNAs are better substrates for Dicer and RISC and therefore get processed more efficiently than shRNAs [10]. Furthermore, they are more amenable to tissue-specific or inducible expression systems than pol III-expressed shRNAs [35]. We are currently testing this hypothesis *in vivo* by incorporating the shA10 sequence in a miRNA backbone (miA10) and correlating the efficacy of miA10 with the concentration of siA10 molecules in mouse livers.

Individuals with the autosomal dominant disorder familial hypobetalipoproteinemia (FHBL) have very low plasma levels of LDL-C and ApoB that are <30% of the normal, and approximately 50% of FHBL subjects carry mutations that result in truncated forms of ApoB. Although these subjects are often clinically asymptomatic, non-alcoholic fatty liver disease (NAFLD) is common due to reduced capacity for hepatic triglyceride export [36,37]. Reduction of ApoB by AAV-shA10 was found to increase the accumulation of hepatic fat content, as determined by Oil red O staining of frozen liver sections, which already occurred at the lowest effective dose of 10^9 gc AAV-shA10 per animal. These results corroborate studies that demonstrated an increase in hepatic lipid content concomitant with ApoB knockdown [14,38,39]. Steatosis was not observed in murine studies with an ApoB ASO [30]. However, treatment of subjects with familial hypercholesterolemia with the human ApoB ASO did reveal a trend toward an increase in intra-hepatic triglyceride content [40]. The clinical relevance of increased hepatic fat content has not been fully elucidated, since follow-up data is lacking on the progression of NAFLD in FHBL patients toward more severe chronic liver diseases, such as steatohepatitis, fibrosis, and cirrhosis [37]. Careful consideration and investigation of this potential consequence of lowering ApoB is warranted. A possible solution to prevent fat accumulation in the liver as a consequence of ApoB knockdown is the use of inducible shRNA expression, for example by the tetracycline inducible (tetO) promoter [41]. Expression of the shApoB can be temporarily "switched on" by addition of doxycycline and when sufficient cholesterol decrease is achieved due to ApoB knockdown, the shRNA expression can be again "switched off". This approach may prevent accumulation of fat in the liver while maintaining the effectiveness of the shApoB in lowering plasma cholesterol levels.

In summary, we showed that ApoB can be almost completely silenced in murine liver by AAV-delivered shRNA. A single injection of 10^{10} gc per animal AAV-shA10 rendered prolonged gene silencing of ApoB that was associated with clear decrease in total plasma cholesterol levels without signs of severe toxicity. Optimization of the shA10 RNA structure by inserting the sequences in a miRNA backbone and obtaining an inducible expression system will be further steps towards a successful gene therapeutic approach for the treatment of hypercholesterolemia.

Matherials and methods

DNA constructs

Nineteen shRNA constructs simultaneously targeting mouse, macaque, and human ApoB, and an shRNA targeting eGFP were made by annealing of complementary oligonucleotides and ligation into the BglII and XhoI site of the pSuper vector (OligoEngine, Seattle, WA). The sequence for constructing the negative control hairpin shScr has been described previously [42]. The sequences of the oligonucleotides used in this study are listed in Table S1. Luciferase reporter Luc-ApoB containing in the 3'UTR 1851 nucleotides of the last exon from human ApoB (NM_000384, 12255-14105) was made by cloning of the ApoB sequence, that was PCR amplified with primers LucApoBf and LucApoBr (Table S1), in the NotI and XhoI sites of the renilla luciferase gene in the psiCHECK-2 vector (Promega, Madison, WI). The Mfold program [43] was used to determine the secondary structure of the RNA transcripts.

For cloning in the AAV backbone, the H1-shRNA expression cassettes were subcloned in pCR-Blunt II-TOPO vector (Invitrogen, Carlsbad, CA), digested with SpeI and XbaI and ligated in the SpeI site of the pVD287 vector. pVD287 contains the eGFP gene under the control of the liver-specific LP1 promoter and generates scAAV due to a mutation in one terminal repeat [44]. Sense orientation of the shRNA cassette was verified by sequencing and the presence of the two ITRs was verified by restriction digestion with SmaI.

Cell culture and transfections

The human embryonic kidney (HEK) 293T, human hepatoma (Huh7), and mouse hepatoma (Hepa1-6) cell lines were maintained in Dulbecco's modified Eagle's medium (DMEM; Invitrogen, Carlsbad, CA) containing 10% fetal calf serum, 100 U/ml penicillin and 100 U/ml streptomycin, at 37°C and 5% CO_2. For luciferase assays, endogenous ApoB knockdown assays, and siRNA expression analysis, cells were seeded in 96- or 24-well plates at a density of 6×10^4 or 1.5×10^5 cells per well, respectively, in DMEM one day prior transfection. Transfections were performed with Lipofectamine 2000 reagent (Invitrogen, Carlsbad, CA) according to the manufacturer's instructions.

Luciferase assays

For luciferase assays, cells were co-transfected with 10 ng Luc-ApoB that contains both firefly and renilla luciferase genes, and 50 ng shApoB expression constructs. Transfected cells were assayed at 48 hr post-transfection in 20 μl 1 x passive lysis buffer (Promega, Madison, WI) by gentle rocking for 15 min at room temperature. The cell lysates were centrifuged for 5 min at 4000 rpm and 10 μl of the supernatant was used to measure firefly and renilla luciferase activities with the Dual-Luciferase Reporter Assay System (Promega, Madison, WI). The relative luciferase activity was calculated as the ratio between the renilla and firefly luciferase activities.

RNA isolation and quantitative real-time RT-PCR

To determine endogenous ApoB mRNA knockdown by the shApoB hairpins *in vitro*, Huh7 and Hepa1-6 cells were transfected with 1 μg shApoB-expressing constructs using Lipofectamine 2000 reagent and total RNA was isolated from cells 48 hr post-transfection using the Nucleospin kit (Clontech, Mountain View, CA). To determine ApoB mRNA knockdown and mir-122 target gene expression *in vivo*, total RNA was isolated from frozen liver sections at two and eight weeks post-transduction with AAV-shA10 using Trizol (Invitrogen, Carlsbad, CA) according to the manufacturer's protocol. Genomic DNA was removed by DNase treatment using TURBO DNase (Ambion, Austin, TX). First strand cDNA was reverse transcribed using random hexamer primers with the Dynamo kit (Finnzymes, Espoo, Finland) and 700 ng of total RNA. Real time PCR amplification was performed with ApoB-, AldoA (Aldolase A)-, Bckdk (Branched-chain α-ketoacid dehydrogenase kinase)-, Ndrg3 (N-myc downstream regulated gene 3)-, and beta actin-specific primers (Table S1). PCR reaction conditions were: 95°C for 10 min, followed by 40 cycles of 15 sec at 95°C and 1 min at 60°C. The assays were performed on ABI 7000 or ABI 7500 (Applied Biosystems, Foster City, CA). ApoB, AldoA, Bckdk, and Ndrg3 expression levels were normalized to beta actin, and the relative gene expression $2^{-\Delta\Delta Ct}$ method of Livak and Schmittgen was used for analysis of PCR data [45].

siRNA and miRNA detection by small RNA Taqman assay

RT reactions for siA10, mir-122, mir-29a, and let-7a expression were performed with the TaqMan MicroRNA Reverse Transcription Kit (Applied Biosystems, Foster City, CA) using 10 ng RNA and 3 μl custom-made specific RT-stem-loop primer (Applied Biosystems, Foster City, CA) according to the manufacturer's instructions. The Taqman assay was done in 20 μl using 1 μl cDNA (15x diluted), 1 μl custom-made siRNA-specific primer with FAM-labelled fluorogenic probe (Applied Biosystems, Foster City, CA) and 10 μl Taqman 2x Universal PCR Master Mix (Applied Biosystems, Foster City, CA). Amplification of the beta actin gene was used as a RNA quality and loading control. siRNA copy number per cell was calculated based on the amplification plot of a dilution series of synthetic siA10 RNA standard (IDT, Coralville, IA). Ten-fold dilutions (100 pg – 1 fg) of the guide strand of a synthetic siA10 RNA oligo were used to create a standard line. The copy number of each dilution was calculated according to the formula 1 mole = 6.02×10^{23} molecules. The trend line value of the standard line was used to calculate the siA10 copy number cell, assuming 15 pg RNA per cell [46]. mir-122, mir-29a, and let-7a expression levels were normalized to beta actin, and the relative gene expression $2^{-\Delta\Delta Ct}$ method of Livak and Schmittgen was used for analysis of PCR data [45].

Western blot analysis for detection of ApoB100 and ApoB48 protein

Murine plasma proteins (0.1 µL) were separated by electrophoresis on a 3-8% Tris-Actetate gel (Invitrogen, Carlsbad, CA) and blotted onto a 0.45 µm nitrocellulose membrane (Invitrogen, Carlsbad, CA). The blot was incubated with a 1:2000 dilution of a rabbit polyclonal anti-ApoB antibody (ab31992, Abcam, Cambrigde, UK), followed by incubation with a 1:2000 dilution of goat anti-rabbit antibody conjugated to horseradish peroxidase (P0448, Dako, Glostrup, Denmark). Antibody binding was detected by the Lumi-Light^{PLUS} chemiluminescent detection kit (Roche Diagnostics, Basel, Switzerland). Equal loading of protein samples was confirmed by Ponceau S staining (Sigma, St. Louis, MO).

AAV vector production

AAV viral vectors were produced encoding shA10 or control shScr and co-expressing the GFP reporter gene under control of the liver-specific LP1 promoter [47]. To maximize efficacy in the murine liver, AAV serotype 8 was employed because it can transduce 100% of hepatocytes in mice when delivered peripherally at high doses [48]. Secondly, a self-complementary AAV (scAAV) vector was used because it shows faster onset of gene expression and 10- to 100-fold higher expression levels than conventional single-stranded vectors [44]. In addition, the scAAV vector is well-suited for expression of short pol III shRNA cassettes, since it cannot accommodate inserts longer than ~2 kb. Self-complementary AAV serotype 8 vectors were produced by calcium phosphate-mediated co-transfection in HEK293T cells, using the three-plasmid based system described by Gao *et al*. [49]. The cells were lysed 48 hr after transfection and virus was released by addition of Tris lysis buffer. Crude lysate from all batches was treated with Benzonase (50 U/mL) (Merck, Darmstadt, Germany) for 1 hr at 37°C. AAV vector particles were purified by iodixanol (Sigma, St. Louis, MO) gradient centrifugation as described previously [50]. Purified batches were concentrated by passage through Vivaspin 15R tubes (Sartorius Stedim, Aubagne, France) to a final concentration of 8-11x10^{11} genome copies (gc) per mL as determined by quantitative PCR with LP1f and LP1r primers amplifying a 95-bp fragment from the LP1 promoter region (Table S1).

In vivo experiments

All animal experiments were conducted according to the guidelines of the local animal welfare committee. Six-to-eight-week-old male C57BL/6 mice received 10^8, 10^9, 10^{10}, or 10^{11} gc AAV-shScr or AAV-shApoB per animal intravenously via the tail vein, corresponding to approximately 4x10^9, 4x10^{10}, 4x10^{11}, or 4x10^{12} gc/kg. Heparinized blood samples were taken at 1, 2, 3, 6, and 8 weeks post-injection from fasted mice for plasma analysis. Mice were sacrificed at two and eight weeks post-injection and livers

and plasma were examined for ApoB knockdown. Feeding was performed *ad libitum* with either regular chow or the atherogenic Paigen diet (TD.88051, Harlan, Madison, WI). Plasma levels of alanine aminotransferase (ALT), aspartate aminotransferase (AST), cholesterol, and high-density lipoprotein cholesterol (HDL-C) were analyzed on the automated clinical chemistry analyzer Modular Analytics P800 (Roche Diagnostics, Basel, Switzerland) at the Academic Medical Center (Amsterdam, the Netherlands). Lipoprotein profiling using FPLC separation of pooled plasma was carried out at the Academic Medical Center (Amsterdam, the Netherlands). GFP expression was analyzed in liver sections that were fixed with 4% formalin, 7% picric acid, and 10% sucrose in PBS. Livers were cryosectioned at 5 µm and eGFP signal was visualized using standard fluorescence microscopy on a Leica fluorescent microscope (Leica Microsystems GmbH, Wetzlar, Germany). Nuclei were visualized by staining with Hoechst. For analysis of liver fat accumulation, snap-frozen liver sections were cryosectioned at 5 µm, fixed in 10% formalin and stained for 25 min in filtered 0.3 % Oil red O (Sigma, St. Louis, MO) solution in 60% isopropanol. Nuclei were counterstained for 5 min in hematoxylin solution (Sigma, St. Louis, MO). Liver histology was assessed by hematoxylin-eosin (H&E) staining of frozen liver sections. Statistical analysis was performed by ANOVA testing and $p<0.05$ was considered significant.

Acknoledgments

The authors thank Han Levels (Academic Medical Center, Amsterdam, the Netherlands) for the FPLC analyses and Eric Timmermans (AMT) and Angelina Huseinovic (AMT) for technical assistance and support. We also thank Jaap Twisk (AMT), Mark Chadwick (AMT), and Wim Hermens (AMT) for critically reviewing the manuscript. The self-complementary AAV vector containing the LP1 promoter was kindly provided by Amit C. Nathwani (St. Jude Children's Research Hospital, Memphis, TN). The authors declare no conflict of interest.

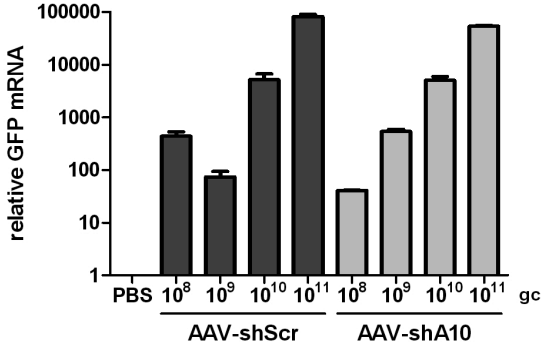

Figure S1. GFP mRNA expression in liver transduced with AAV-shA10 and AAV-shScr. Relative GFP mRNA expression in mice intravenously injected with 10^8, 10^9, 10^{10}, and 10^{11} gc AAV-shA10 or control AAV-shScr per animal. Two weeks post-transduction, RNA was isolated from snap-frozen liver tissue and qRT-PCR was performed with GFP- and actin-specific primers. GFP mRNA levels were calculated relative to actin mRNA and the PBS-treated group was set at 1. Data are represented as mean ±SE, treatment groups are n=5.

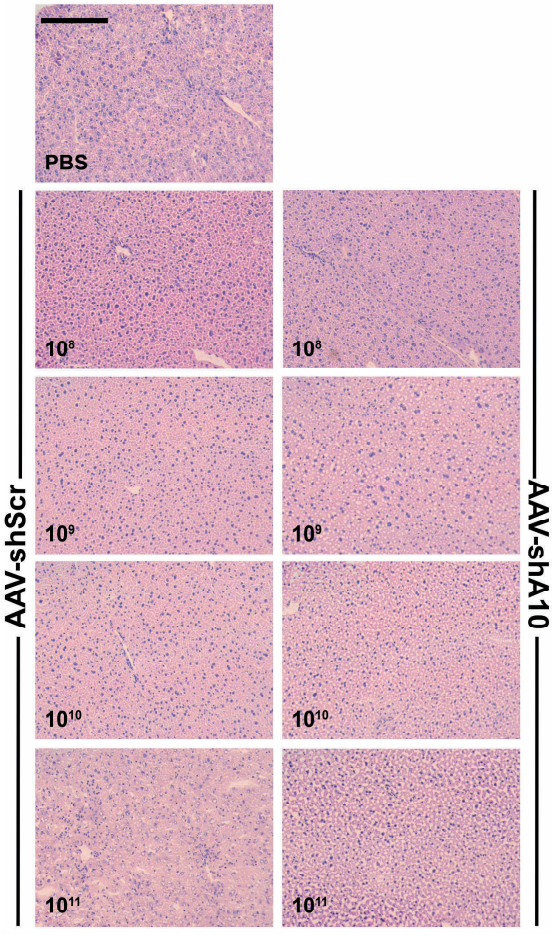

Figure S2. Transduction with 1011 gc AAV-shScr results in abnormal liver tissue morphology, as determined by H&E staining. Representative image of liver sections from mice transduced with 108, 109, 1010, and 1011 gc AAV-shA10 or control AAV-shScr per animal. Animals were sacrificed at two weeks post-transduction and frozen liver tissue was cryosectioned at 5 µm and used for hematoxylin and eosin (H&E) staining. Photos were taken using the same exposure and magnification settings. Scale bar = 10 µm.

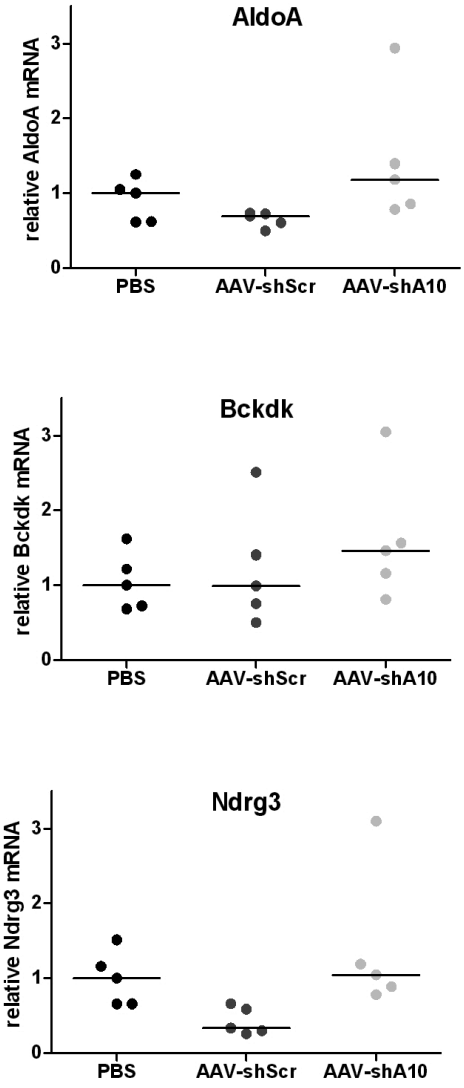

Figure S3. Expression of mir-122 target genes at two weeks post-transduction. Relative expression of mir-122 target genes AldoA, Bckdk, and Ndrg3 in mice transduced with 10^{11} gc AAV-shA10 or control AAV-shScr per animal. Two weeks post-transduction, RNA was isolated from snap-frozen liver tissue and qRT-PCR was performed with AldoA-, Bckdk-, Ndrg3-, and actin-specific primers. AldoA, Bckdk, and Ndrg3 mRNA levels were calculated relative to actin mRNA. Data are represented as individual measurements with median plotted, treatment groups are n=5.

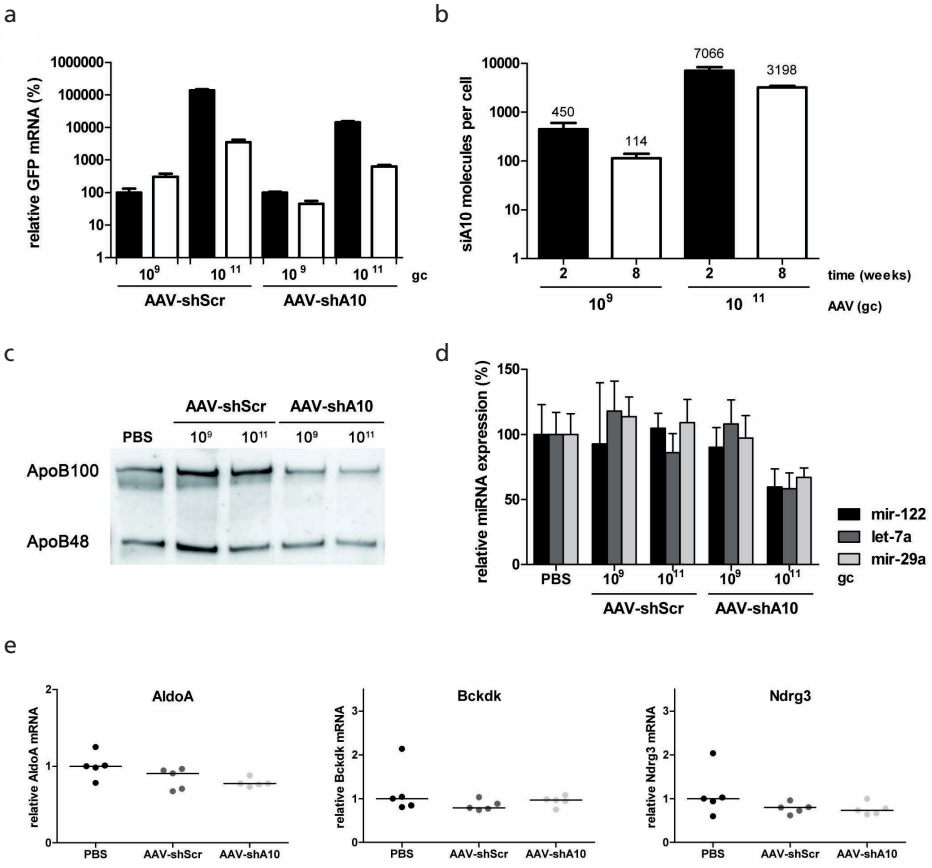

Figure S4. AAV-shA10 persistence, robustness of ApoB knockdown, and off-target effects at eight weeks post-transduction. (a) Comparison of GFP expression in murine liver at two (black bars) and eight (white bars) weeks post-transduction with 10^9 and 10^{11} gc AAV-shA10 or control AAV-shScr per animal. Both viruses co-express the GFP reporter gene under control of a liver-specific LP1 promoter. RNA was isolated from snap-frozen liver tissue, followed by qRT-PCR with GFP- and actin-specific primers. GFP mRNA levels were calculated relative to actin mRNA and the groups injected with 10^9 gc were set at 100%. (b) Comparison of siA10 expression in murine liver at two (black bars) and eight (white bars) weeks post-transduction with 10^9 and 10^{11} gc AAV-shA10 per animal. Total RNA was isolated from snap-frozen livers and siA10-specific small RNA Taqman was performed. The copy number siA10 per cell was calculated as described in Fig. 1c. (c) Western blot analysis of secreted ApoB100 and ApoB48 protein in 0.1 µL plasma eight weeks post-transduction with 10^9 and 10^{11} gc AAV-shA10 or control AAV-shScr per animal. ApoB100 and ApoB48 protein was detected using a polyclonal anti-ApoB antibody, and antibody binding was visualized by a chemiluminescence detection kit. (d) Relative expression of mir-122, let-7a, and mir-29a in murine liver eight weeks post-transduction with 10^9 and 10^{11} gc AAV-shA10 or control AAV-shScr. miRNA-specific Taqmans were performed on RNA isolated from snap-frozen livers, and miRNA expression levels were calculated relative to actin mRNA and the PBS-treated group was set at 100%. Data are represented as mean ±SE, treatment groups are n=5. (e) Relative expression of mir-122 target genes AldoA, Bckdk, and Ndrg3 in mice transduced with 10^{11} gc AAV-shA10 or control AAV-shScr per animal. Eight weeks post-transduction, RNA was isolated from snap-frozen liver tissue and qRT-PCR was performed with AldoA-, Bckdk-, Ndrg3-, and actin-specific primers. AldoA, Bckdk, and Ndrg3 mRNA levels were calculated relative to actin mRNA. Data are represented as individual measurements with median plotted, treatment groups are n=5.

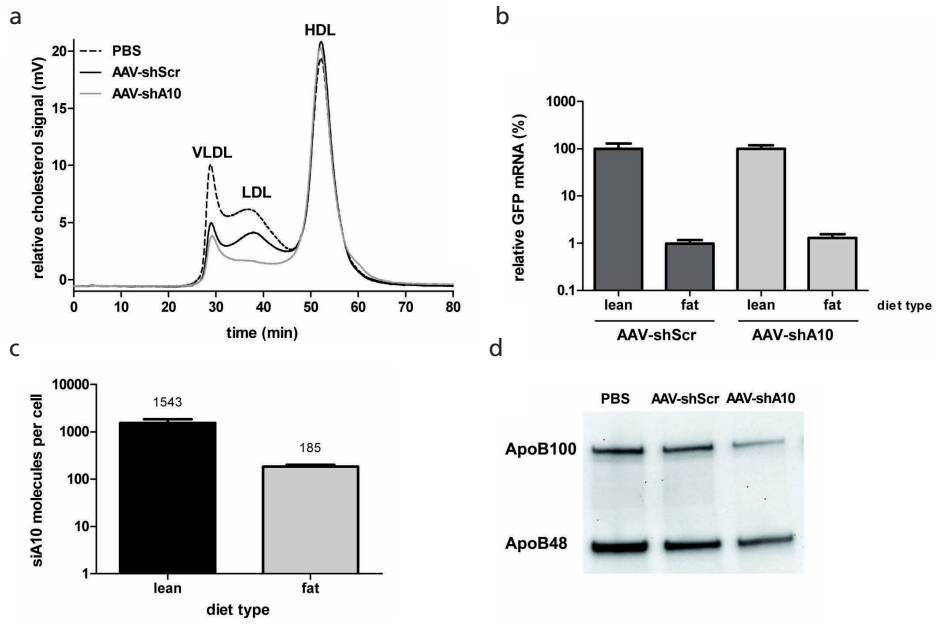

Figure S5. AAV-shA10 persistence and robustness of ApoB knockdown in mice fed on an atherogenic diet. Mice were fed on regular chow (lean) or on an atherogenic diet (fat) containing approximately 15.8% fat, 1.25% cholesterol, and 0.5% sodium cholate for seven weeks, before being injected via the tail vein with 10^{10} gc AAV-shA10 or control AAV-shScr per animal. Animals continued feeding on the atherogenic diet and were sacrificed at two weeks post-transduction. (a) Plasma cholesterol distribution over lipoprotein subclasses in FPLC-separated pooled plasma. (b) Comparison of GFP expression in liver from AAV-transduced mice fed on a regular (lean) or atherogenic (fat) diet. Both AAV-shA10 and AAV-shScr co-express the GFP reporter gene under control of a liver-specific LP1 promoter. Total RNA was isolated from snap-frozen liver tissue and qRT-PCR was performed with GFP- and actin-specific primers. GFP mRNA levels were calculated relative to actin mRNA and the groups of lean mice were set at 100%. (c) Comparison of siA10 expression in liver from AAV-shA10 transduced mice fed on a regular (lean) or atherogenic (fat) diet. Total RNA was isolated from snap-frozen livers and siA10-specific small RNA Taqman assay was performed. The copy number siA10 per cell was calculated as described in Fig. 1c. (d) Western blot analysis of secreted ApoB100 and ApoB48 protein in 0.1 µL plasma from mice that were fed on an atherogenic diet and transduced with 10^{10} gc AAV-shA10 or control AAV-shScr. ApoB100 and ApoB48 protein was detected using a polyclonal anti-ApoB antibody, and antibody binding was visualized by a chemiluminescence detection kit. Data are represented as mean ±SE, treatment groups are n=5.

Table S1. Oligonucleotides used in this study

name	Sequence (5′-3′)	Target
shA1f	GATCCCC**TTAATTGGGAAGAAGAGGC**TTCAAGAGA**GCCTCTTCTTCCCAATTAA**TTTTTC	ApoB,12295-12313
shA1r	TCGAGAAAAATTAATTGGGAAGAAGAGGCTCTCTTGAAGCCTCTTCTTCCCAATTAAGGG	
shA2f	GATCCCC**TAATTGGGAAGAAGAGGCA**TTCAAGAGA**TGCCTCTTCTTCCCAATTA**TTTTTC	ApoB,12296-12314
shA2r	TCGAGAAAAATAATTGGGAAGAAGAGGCATCTCTTGAATGCCTCTTCTTCCCAATTAGGG	
shA3f	GATCCCC**TTGGGAAGAAGAGGCAGCT**TTCAAGAGA**AGCTGCCTCTTCTTCCCAA**TTTTTC	ApoB,12299-12317
shA3r	TCGAGAAAAATTGGGAAGAAGAGGCAGCTTCTCTTGAAAGCTGCCTCTTCTTCCCAAGGG	
shA4f	GATCCCC**TGGGAAGAAGAGGCAGCTT**TTCAAGAGA**AAGCTGCCTCTTCTTCCCA**TTTTTC	ApoB,12300-12318
shA4r	TCGAGAAAAATGGGAAGAAGAGGCAGCTTTCTCTTGAAAAGCTGCCTCTTCTTCCCAGGG	
shA5f	GATCCCC**GGGAAGAAGAGGCAGCTTC**TTCAAGAGA**GAAGCTGCCTCTTCTTCCC**TTTTTC	ApoB,12301-12319
shA5r	TCGAGAAAAAGGGAAGAAGAGGCAGCTTCTCTCTTGAAGAAGCTGCCTCTTCTTCCCGGG	
shA6f	GATCCCC**TGGACAGTGAAATATTATG**TTCAAGAGA**CATAATATTTCACTGTCCA**TTTTTC	ApoB,13314-13332
shA6r	TCGAGAAAAATGGACAGTGAAATATTATGTCTCTTGAACATAATATTTCACTGTCCAGGG	
shA7f	GATCCCC**GGACAGTGAAATATTATGA**TTCAAGAGA**TCATAATATTTCACTGTCC**TTTTTC	ApoB,13315-13333
shA7r	TCGAGAAAAAGGACAGTGAAATATTATGATCTCTTGAATCATAATATTTCACTGTCCGGG	
shA8f	GATCCCC**GACAGTGAAATATTATGAA**TTCAAGAGA**TTCATAATATTTCACTGTC**TTTTTC	ApoB,13316-13334
shA8r	TCGAGAAAAAGACAGTGAAATATTATGAATCTCTTGAATTCATAATATTTCACTGTCGGG	
shA9f	GATCCCC**AGATTGATTGACCTGTCCA**TTCAAGAGA**TGGACAGGTCAATCAATCT**TTTTTC	ApoB,13683-13701
shA9r	TCGAGAAAAAAGATTGATTGACCTGTCCATCTCTTGAATGGACAGGTCAATCAATCTGGG	
shA10f	GATCCCC**GATTGATTGACCTGTCCAT**TTCAAGAGA**ATGGACAGGTCAATCAATC**TTTTTC	ApoB,13684-13702
shA10r	TCGAGAAAAAGATTGATTGACCTGTCCATTCTCTTGAAATGGACAGGTCAATCAATCGGG	
shA11f	GATCCCC**ATTGATTGACCTGTCCATT**TTCAAGAGA**AATGGACAGGTCAATCAAT**TTTTTC	ApoB,13685-13703
shA11r	TCGAGAAAAAATTGATTGACCTGTCCATTTCTCTTGAAAATGGACAGGTCAATCAATGGG	
shA12f	GATCCCC**TTGATTGACCTGTCCATTC**TTCAAGAGA**GAATGGACAGGTCAATCAA**TTTTTC	ApoB,13686-13704
shA12r	TCGAGAAAAATTGATTGACCTGTCCATTCTCTCTTGAAGAATGGACAGGTCAATCAAGGG	
shA13f	GATCCCC**TGATTGACCTGTCCATTCA**TTCAAGAGA**TGAATGGACAGGTCAATCA**TTTTTC	ApoB,13687-13705
shA13r	TCGAGAAAAATGATTGACCTGTCCATTCATCTCTTGAATGAATGGACAGGTCAATCAGGG	
shA14f	GATCCCC**GATTGACCTGTCCATTCAA**TTCAAGAGA**TTGAATGGACAGGTCAATC**TTTTTC	ApoB,13688-13706
shA14r	TCGAGAAAAAGATTGACCTGTCCATTCAATCTCTTGAATTGAATGGACAGGTCAATCGGG	
shA15f	GATCCCC**TGACCTGTCCATTCAAAAC**TTCAAGAGA**GTTTTGAATGGACAGGTCA**TTTTTC	ApoB,13691-13709
shA15r	TCGAGAAAAATGACCTGTCCATTCAAAACTCTCTTGAAGTTTTGAATGGACAGGTCAGGG	

shA16f	GATCCCC**GACCTGTCCATTCAAAACT**TTCAAGAGA**AGTTTTGAATGGACAGGTC**TTTTTC	ApoB,13692-13710
shA16r	TCGAGAAAAAGACCTGTCCATTCAAAACTTCTCTTGAAAGTTTTGAATGGACAGGTCGGG	
shA17f	GATCCCC**CCTGTCCATTCAAAACTAC**TTCAAGAGA**GTAGTTTTGAATGGACAGG**TTTTTC	ApoB,13694-13712
shA17r	TCGAGAAAAACCTGTCCATTCAAAACTACTCTCTTGAAGTAGTTTTGAATGGACAGGGGG	
shA18f	GATCCCC**CTGTCCATTCAAAACTACC**TTCAAGAGA**GGTAGTTTTGAATGGACAG**TTTTTC	ApoB,13695-13713
shA18r	TCGAGAAAAACTGTCCATTCAAAACTACCTCTCTTGAAGGTAGTTTTGAATGGACAGGGG	
shA19f	GATCCCC**GTCCATTCAAAACTACCAC**TTCAAGAGA**GTGGTAGTTTTGAATGGAC**TTTTTC	ApoB,13697-13715
shA19r	TCGAGAAAAAGTCCATTCAAAACTACCACTCTCTTGAAGTGGTAGTTTTGAATGGACGGG	
shScr-f	GATCCCCGATCGAATGTGTACTTCGATTCCAAGAGATCGAAGTACACATTCGATCTTTTTGCATGCC	Doege *et al*., 2008
shScr-r	TCGAGGCATGCAAAAAGATCGAATGTGTACTTCGATCTCTTGGAATCGAAGTACACATTCGATCGGG	
shGFPf	GATCCCC**AGCTGGAGTACAACTACAAC**CTTCCTGTCA**GTTGTAGTTGTACTCCAGCT**TTTTGCATGCC	eGFP
shGFPr	TCGAGGCATGCAAAAAGCTGGAGTACAACTACAACTGACAGGAAGGTTGTAGTTGTACTCCAGCTGGG	
LucApoBf	CGACTCGAGTTGAGGGTCCGGGAAT	ApoB,12255-12271
LucApoBr	CGAGCGGCCGCGACTCCATTTATTTGTTCCTCCTC	ApoB,14105-14081
ApoBf	TGGTTACTGCGCTGAGAGG	ApoB qRT-PCR
ApoBr	CCACACTGAACCAAGGCTT	
m-act-f	ACGGCCAGGTCATCACTATTG	Mouse actin qRT-PCR
m-act-r	CAAGAAGGAAGGCTGGAAAAGA	
h-act-f	CAGCCATGTACGTTGCTATCCAGG	Human actin qRT-PCR
h-act-r	AGGTCCAGACGCAGGATGGCATG	
LP1f	CCCTGTTTGCTCCTCCGATAA	LP1 qRT-PCR
LP1r	GTCCGTATTTAAGCAGTGGATCCA	
eGFPf	GGGCACAAGCTGGAGTACAACTA	eGFP qRT-PCR
eGFPr	ATGTTGTGGCGGATCTTGAAG	
AldoA-f	GCTGTGCCCAGTATAAGAAG	AldoA qRT-PCR
AldoA-r	GCTCCACAATGGGTACAATG	
Bckdk-f	TGCTGGCTACTCACCACTTG	Bckdk qRT-PCR
Bckdk-r	ATGTCCGTTGATGCGGACTC	

ApoB (NM_000384) and GFP sequences in the shRNA oligos are bold
Accession numbers of the genes are: mmu-AldoA NM_001177307, mmu-Bckdk NM_009739, mmuNdrg3 NM_013865

Reference list

1. Rader, DJ, Cohen, J and Hobbs, HH (2003). Monogenic hypercholesterolemia: new insights in pathogenesis and treatment. *J Clin Invest*; **111:** 1795-1803.
2. Kashani, A, Phillips, CO, Foody, JM, Wang, Y, Mangalmurti, S, Ko, DT, et al. (2006). Risks associated with statin therapy: a systematic overview of randomized clinical trials. *Circulation*; **114:** 2788-2797.
3. Young, SG (1990). Recent progress in understanding apolipoprotein B. *Circulation*; **82:** 1574-1594.
4. Greeve, J, Altkemper, I, Dieterich, JH, Greten, H and Windler, E (1993). Apolipoprotein B mRNA editing in 12 different mammalian species: hepatic expression is reflected in low concentrations of apoB-containing plasma lipoproteins. *J Lipid Res*; **34:** 1367-1383.
5. Zambon, A, Brown, BG, Deeb, SS and Brunzell, JD (2006). Genetics of apolipoprotein B and apolipoprotein AI and premature coronary artery disease. *J Intern Med*; **259:** 473-480.
6. Raal, FJ, Santos, RD, Blom, DJ, Marais, AD, Charng, MJ, Cromwell, WC, et al. (2010). Mipomersen, an apolipoprotein B synthesis inhibitor, for lowering of LDL cholesterol concentrations in patients with homozygous familial hypercholesterolaemia: a randomised, double-blind, placebo-controlled trial. *Lancet*; **375:** 998-1006.
7. Fire, A, Xu, S, Montgomery, MK, Kostas, SA, Driver, SE and Mello, CC (1998). Potent and specific genetic interference by double-stranded RNA in Caenorhabditis elegans. *Nature*; **391:** 806-811.
8. Soutschek, J, Akinc, A, Bramlage, B, Charisse, K, Constien, R, Donoghue, M, et al. (2004). Therapeutic silencing of an endogenous gene by systemic administration of modified siRNAs. *Nature*; **432:** 173-178.
9. Grimm, D (2009). Small silencing RNAs: State-of-the-art. *Adv Drug Deliv Rev*; **61:** 672-703.
10. Liu, YP, Haasnoot, J, ter Brake, O, Berkhout, B and Konstantinova, P (2008). Inhibition of HIV-1 by multiple siRNAs expressed from a single microRNA polycistron. *Nucleic Acids Res*; **36:** 2811-2824.
11. Zamore, PD, Tuschl, T, Sharp, PA and Bartel, DP (2000). RNAi: Double-stranded RNA directs the ATP-dependent cleavage of mRNA at 21 to 23 nucleotide intervals. *Cell*; **101:** 25-33.
12. Love, KT, Mahon, KP, Levins, CG, Whitehead, KA, Querbes, W, Dorkin, JR, et al. (2010). Lipid-like materials for low-dose, in vivo gene silencing. *Proc Natl Acad Sci U S A*; **107:** 1864-1869.
13. Semple, SC, Akinc, A, Chen, J, Sandhu, AP, Mui, BL, Cho, CK, et al. (2010). Rational design of cationic lipids for siRNA delivery. *Nat Biotech*; **28:** 172-176.
14. Rozema, DB, Lewis, DL, Wakefield, DH, Wong, SC, Klein, JJ, Roesch, PL, et al. (2007). Dynamic PolyConjugates for targeted in vivo delivery of siRNA to hepatocytes. *Proc Natl Acad Sci U S A*; **104:** 12982-12987.
15. Wolfrum, C, Shi, S, Jayaprakash, KN, Jayaraman, M, Wang, G, Pandey, RK, et al. (2007). Mechanisms and optimization of in vivo delivery of lipophilic siRNAs. *Nat Biotech*; **25:** 1149-1157.
16. Zimmermann, TS, Lee, ACH, Akinc, A, Bramlage, B, Bumcrot, D, Fedoruk, MN, et al. (2006). RNAi-mediated gene silencing in non-human primates. *Nature*; **441:** 111-114.
17. Manjunath, N, Wu, H, Subramanya, S and Shankar, P (2009). Lentiviral delivery of short hairpin RNAs. *Adv Drug Deliv Rev*; **61:** 732-745.
18. Grimm, D, Pandey, K and Kay, MA (2005). Adeno-associated virus vectors for short hairpin RNA expression. *Methods Enzymol*; **392:** 381-405.
19. Daya, S and Berns, KI (2008). Gene therapy using adeno-associated virus vectors. *Clin Microbiol Rev*; **21:** 583-593.
20. Vaessen, SF, Veldman, RJ, Comijn, EM, Snapper, J, Sierts, JA, van den Oever, K, et al. (2009). AAV gene therapy as a means to increase apolipoprotein (Apo) A-I and high-density lipoprotein-cholesterol levels: correction of murine ApoA-I deficiency. *J Gene Med*; **11:** 697-707.
21. Grimm, D, Streetz, KL, Jopling, CL, Storm, TA, Pandey, K, Davis, CR, et al. (2006). Fatality in mice due to oversaturation of cellular microRNA/short hairpin RNA pathways. *Nature*; **441:** 537-541.
22. Kim, VN (2005). Small RNAs: Classification, biogenesis, and function. *Mol Cells*; **19:** 1-15.
23. Lagos-Quintana, M, Rauhut, R, Yalcin, A, Meyer, J, Lendeckel, W and Tuschl, T (2002). Identification of tissue-specific microRNAs from mouse. *Curr Biol*; **12:** 735-739.
24. Elmen, J, Lindow, M, Silahtaroglu, A, Bak, M, Christensen, M, Lind-Thomsen, A, et al. (2007). Antagonism of microRNA-122

in mice by systemically administered LNA-antimiR leads to up-regulation of a large set of predicted target mRNAs in the liver. *Nucleic Acid Res*; **36:** 1153-1162.

25. Jiao, S, Cole, TG, Kitchens, RT, Pfleger, B and Schonfeld, G (1990). Genetic heterogeneity of lipoproteins in inbred strains of mice: analysis by gel-permeation chromatography. *Metabolism*; **39:** 155-160.
26. Matsuzawa, N, Takamura, T, Kurita, S, Misu, H, Ota, T, Ando, H, et al. (2007). Lipid-induced oxidative stress causes steatohepatitis in mice fed an atherogenic diet. *Hepatology*; **46:** 1392-1403.
27. Nakai, H, Fuess, S, Storm, TA, Muramatsu, Si, Nara, Y and Kay, MA (2005). Unrestricted hepatocyte transduction with adeno-associated virus serotype 8 vectors in mice. *J Virol*; **79:** 214-224.
28. Shen, X, Storm, T and Kay, MA (2007). Characterization of the relationship of AAV capsid domain swapping to liver transduction efficiency. *Mol Ther*; **15:** 1955-1962.
29. Chen, SH, Habib, G, Yang, CY, u, ZW, Lee, BR, eng, SA, et al. (1987). Apolipoprotein B-48 is the product of a messenger RNA with an organ-specific in-frame stop codon. *Science*; **238:** 363-366.
30. Crooke, RM, Graham, MJ, Lemonidis, KM, Whipple, CP, Koo, S and Perera, RJ (2005). An apolipoprotein B antisense oligonucleotide lowers LDL cholesterol in hyperlipidemic mice without causing hepatic steatosis. *J Lipid Res*; **46:** 872-884.
31. Fazio, S and Linton, M (2001). Debate: "How low should LDL cholesterol be lowered?" Viewpoint: "It doesn't need to be very low". *Curr Control Trials in Cardiovasc Med*; **2:** 8-11.
32. Kastelein, JJP, Wedel, MK, Baker, BF, Su, J, Bradley, JD, Yu, RZ, et al. (2006). Potent reduction of apolipoprotein B and low-density lipoprotein cholesterol by short-term administration of an antisense inhibitor of apolipoprotein B. *Circulation*; **114:** 1729-1735.
33. Giering, JC, Grimm, D, Storm, TA and Kay, MA (2008). Expression of shRNA from a tissue-specific pol II promoter is an effective and safe RNAi therapeutic. *Mol Ther*; **16:** 1630-1636.
34. McBride, JL, Boudreau, RL, Harper, SQ, Staber, PD, Monteys, AM, Martins, I, et al. (2008). Artificial miRNAs mitigate shRNA-mediated toxicity in the brain: Implications for the therapeutic development of RNAi. *Proc Natl Acad Sci U S A*; **105:** 5868-5873.
35. Amendola, M, Passerini, L, Pucci, F, Gentner, B, Bacchetta, R and Naldini, L (2009). Regulated and multiple miRNA and siRNA delivery into primary cells by a lentiviral platform. *Mol Ther*; **17:** 1039-1052.
36. Schonfeld, G, Lin, X and Yue, P (2005). Familial hypobetalipoproteinemia: genetics and metabolism. *Cell Mol Life Sci*; **62:** 1372-1378.
37. Tarugi, P, Averna, M, Di Leo, E, Cefalu, AB, Noto, D, Magnolo, L, et al. (2007). Molecular diagnosis of hypobetalipoproteinemia: An ENID review. *Atherosclerosis*; **195:** e19-e27.
38. Straarup, EM, Fisker, N, Hedtjarn, M, Lindholm, MW, Rosenbohm, C, Aarup, V, et al. (2010). Short locked nucleic acid antisense oligonucleotides potently reduce apolipoprotein B mRNA and serum cholesterol in mice and non-human primates. *Nucl Acids Res*; **38:** 7100-7111.
39. Nishina, K, Unno, T, Uno, Y, Kubodera, T, Kanouchi, T, Mizusawa, H, et al. (2008). Efficient in vivo delivery of siRNA to the liver by conjugation of [alpha]-tocopherol. *Mol Ther*; **16:** 734-740.
40. Visser, ME, Akdim, F, Tribble, DL, Nederveen, AJ, Kwoh, TJ, Kastelein, JJP, et al. (2010). Effect of apolipoprotein-B synthesis inhibition on liver triglyceride content in patients with familial hypercholesterolemia. *J Lipid Res*; **51:** 1057-1062.
41. Kappel, S, Matthess, Y, Kaufmann, M and Strebhardt, K (2007). Silencing of mammalian genes by tetracycline-inducible shRNA expression. *Nat Protocols*; **2:** 3257-3269.
42. Doege, H, Grimm, D, Falcon, A, Tsang, B, Storm, TA, Xu, H, et al. (2008). Silencing of hepatic fatty acid transporter protein 5 in vivo reverses diet-induced non-alcoholic fatty liver disease and improves hyperglycemia. *J Biol Chem*; **283:** 22186-22192.
43. Zuker, M (2003). Mfold web server for nucleic acid folding and hybridization prediction. *Nucleic Acids Res*; **31:** 3406-3415.
44. McCarty, DM, Fu, H, Monahan, PE, Toulson, CE, Naik, P and Samulski, RJ (2003). Adeno-associated virus terminal repeat (TR) mutant generates self-complementary vectors to overcome the rate-limiting step to transduction in vivo. *Gene Ther*; **10:** 2112-2118.
45. Livak, KJ and Schmittgen, TD (2001). Analysis of relative gene expression data using real-time quantitative PCR and the 2-[delta][delta] CT method. *Methods*; **25:** 402-408.
46. Chen, C, Ridzon, DA, Broomer, AJ, Zhou, Z, Lee, DH, Nguyen, JT, et al. (2005). Real-time

quantification of microRNAs by stem-loop RT-PCR. *Nucl Acids Res*; **33:** e179.

47. Nathwani, AC, Gray, JT, Ng, CYC, Zhou, J, Spence, Y, Waddington, SN, et al. (2006). Self-complementary adeno-associated virus vectors containing a novel liver-specific human factor IX expression cassette enable highly efficient transduction of murine and nonhuman primate liver. *Blood*; **107:** 2653-2661.
48. Grimm, D, Pandey, K, Nakai, H, Storm, TA and Kay, MA (2006). Liver transduction with recombinant adeno-associated virus is primarily restricted by capsid serotype not vector genotype. *J Virol*; **80:** 426-439.
49. Gao, GP, Alvira, MR, Wang, L, Calcedo, R, Johnston, J and Wilson, JM (2002). Novel adeno-associated viruses from rhesus monkeys as vectors for human gene therapy. *Proc Natl Acad Sci U S A*; **99:** 11854-11859.
50. Zolotukhin, S, Byrne, BJ, Mason, E, Zolotukhin, I, Potter, M, Chesnut, K, et al. (1999). Recombinant adeno-associated virus purification using novel methods improves infectious titer and yield. *Nucleic Acids Res*; **6:** 973-985.

CHAPTER 3

Optimization and comparison of knockdown efficacy between polymerase II expressed shRNA and artificial miRNA targeting luciferase and Apolipoprotein B100

Piotr Maczuga[1,2], Annemart Koornneef[1], Florie Borel [1,3], Harald Petry[1], Sander van Deventer[2] Tita Ritsema[1] and Pavlina Konstantinova[1]

[1]Research & Development, Amsterdam Molecular Therapeutics, Amsterdam, the Netherlands; [2]Department of Gastroenterology and Hepatology, Leiden University Medical Center, Leiden, the Netherlands; [3]Department of Gastroenterology and Hepatology, Academic Medical Center, Amsterdam, the Netherlands

BMC Biotechnology (2012); 12*:42*

Abstract

Controlling and limiting the expression of short hairpin RNA (shRNA) by using constitutive or tissue-specific polymerase II (pol II) expression can be a promising strategy to avoid RNAi toxicity. However, to date detailed studies on requirements for effective pol II shRNA expression and processing are not available. We investigated the optimal structural configuration of shRNA molecules, namely: hairpin location, stem length and termination signal required for effective pol II expression and compared it with an alternative strategy of avoiding toxicity by using artificial microRNA (miRNA) scaffolds.

Highly effective shRNAs targeting luciferase (shLuc) or Apolipoprotein B100 (shApoB1 and shApoB2) were placed under the control of the pol II CMV promoter and expressed at +5 or +6 nucleotides (nt) with reference to the transcription start site (TSS). Different transcription termination signals (TTS), namely minimal polyadenylation (pA), poly T (T5) and U1 were also used. All pol II-expressed shRNA variants induced mild inhibition of Luciferase reporters carrying specific targets and none of them showed comparable efficacy to their polymerase III-expressed H1-shRNA controls, regardless of hairpin position and termination signal used. Extending hairpin stem length from 20 basepairs (bp) to 21, 25 or 29 nt yielded only slight improvement in the overall efficacy. When shLuc, shApoB1 and shApoB2 were placed in an artificial miRNA scaffold, two out of three were as potent as the H1-shRNA controls. Quantification of small interfering RNA (siRNA) molecules showed that the artificial miRNA constructs expressed less molecules than H1-shRNAs and that CMV-shRNA expressed the lowest siRNA molecules suggesting that RNAi processing in this case is least effective. Furthermore, CMV-miApoB1 and CMV-miApoB2 were as effective as the corresponding H1-shApoB1 and H1-shApoB2 in inhibiting endogenous ApoB mRNA.

Our results demonstrate that artificial miRNA have a better efficacy profile than shRNA expressed either from H1 or CMV promoter and will be used in the future for RNAi therapeutic development.

Introduction

RNA interference (RNAi) is an evolutionary conserved mechanism for regulating gene expression. It plays an important role in defense against viruses but also in development and in normal functioning of the cell [1,2]. The natural RNAi mechanism functions by endogenous microRNA (miRNA) molecules, which are synthesized in cells as part of longer primary RNA transcripts (pri-miRNAs). Pri-miRNAs are cleaved by the nuclear Drosha-DGCR8 complex to produce miRNA precursors (pre-miRNAs) of 70 nucleotides (nt), which are then transported by Exportin 5 to the cytoplasm and processed by the RNAse III endonuclease family enzyme Dicer to produce a mature miRNA duplex of ~21,22 basepairs (bp). The guide strand of the miRNA enters a multiprotein RNA-induced silencing complex (RISC) where it is used for sequence-specific recognition of target messenger RNA (mRNA). RISC binding to complementary sequences on the target mRNA results in transcript degradation or translational repression [3].

By introducing molecules that constitute substrates for the endogenous RNAi pathway disease-related mRNA and thus protein translation can be inhibited. RNAi in cells can be induced in different ways. Generally this is achieved by delivery of 20-25 bp-long small interfering RNAs (siRNAs) [4] which serve as substrates for the RISC complex. Alternatively, siRNAs can be generated by expressing short hairpin RNA (shRNA) [5] or artificial microRNA (miRNA) structures [6]. Both enter the endogenous RNAi pathway and are processed into mature siRNAs. The crucial difference between shRNAs and artificial miRNAs is in their secondary structure and processing in the RNAi pathway. shRNAs are normally expressed from polymerase III (pol III) promoters and directly generate a mature product which is exported and processed by Dicer, while miRNAs require an additional step of excision from the longer pre-miRNA sequence by the Drosha-DGCR8 complex. Moreover, miRNAs are expressed from polymerase II (pol II) promoters that allow for the use of tissue-specific or regulated expression systems.

To date, shRNA expression from pol III promoters is the most common way to induce RNAi in cells, which provides potent and stable target inhibition. Several pol III promoters are being used for expression of shRNAs, such as H1 or U6, and transcription initiation and termination sites together with the structural requirements for effective expression of the hairpins are well described [7,8]. However, there are serious disadvantages of pol III expression systems which question their possible application as therapeutic agents. There are cases reporting severe toxicity after administration of high doses of vectors encoding shRNA [9,10]. Toxicity was shown to be associated with oversaturation of the cellular RNAi machinery and changes in endogenous miRNA expression.

This toxicity problem may be circumvented by using weaker pol II promoter to express shRNAs or by embedding siRNA into artificial miRNA scaffolds. The CMV promoter has been the first pol II promoter shown to express active shRNA and

initial requirements for this approach have been established: the shRNA has to be juxtaposed to the transcription start site (TSS) (within 6 nt) and followed by the minimal polyadenylation signal (pA) [11]. When these two conditions were not met, the shRNA was found to be inactive. Additionally, to limit toxicity tissue-specific pol II promoters which restrict expression to the target tissue can be applied. This approach has been used to safely express shRNAs targeting JNK1, JNK2, and PI3 under the control of the prostate-specific antigen pol II promoter in androgen-responsive cancer cells [12]. Furthermore, *in vivo* toxicity related to high shRNA expression levels from a pol III promoter was abolished when the shRNA was expressed from the liver-specific pol II hAAT promoter and U1 termination signal was used [13]. Incorporation of a siRNA sequence in an artificial miRNA scaffold has been shown to abolish shRNA-induced neuronal cell death and to avoid disruption of the endogenous RNAi pathway [14,15].

In the current study we focused on the structural requirements to determine the optimal configuration for pol II shRNA expression and compared it to the pol II expression of artificial miRNA. To date, no detailed studies on the hairpin positions, transcription termination signal (TTS) and shRNA stem length requirements for efficient pol II shRNA expression have been performed. Varying positions of the hairpin relative to the TSS +5 or +6, stem length of 20, 21, 25, 29 bp, and different TTS (pA, U1 and T5) have been tested for a shRNA targeting luciferase (shLuc) and expressed from the pol II CMV promoter. shLuc at +6 location relative to TSS, with stem length of 20 nt with either pA or U1 termination signal was found to yield optimal results. However, the average luciferase inhibition of 40% was still lower than the control pol III H1-shRNA, which inhibited luciferase up to 90%. Additionally, two shRNAs targeting ApoB (shApoB1 and shApoB2) were found inactive when expressed from CMV using the same configuration. In contrast, when the three shRNAs were incorporated in an artificial miRNA scaffold, two were equally active to their respective H1-shRNA controls while expressing much less siRNA molecules. This indicates that using artificial miRNA scaffolds has a greater therapeutic potential than direct expression of shRNAs from pol II promoters.

Results

Design and knockdown efficacy of CMV-shLuc with different transcription start and transcription termination signals

Previously, we have identified a highly effective siRNA potent in knocking down luciferase when expressed as shLuc from the pol III H1 promoter [16]. To minimize the risk of inducing toxic effects due to siRNA overexpression we wanted to express the same shLuc sequence under the control of the pol II CMV promoter. In contrast to pol III, most pol II transcripts undergo posttranscriptional modification at the 5'

and 3' ends, which enhances their stability and protects them from degradation [17]. However, both 5' and 3' overhangs of the shRNA are important for correct recognition and processing by Dicer [18] therefore these sequences needed to be optimized. A panel of shLuc constructs with perfect complementary 20-bp shRNA stem and 9-nt loop was expressed from the pol II CMV promoter (Fig. 1a). Initially, shLuc was placed behind the CMV promoter, followed by a minimal pA signal. The beginning of the passenger strand of the shLuc sequence was placed at positions +5 or +6 relative to the TSS generating CMV+5shLuc-pA and CMV+6shLuc-pA, respectively (Fig. 1a). It has been reported that T5 TTS can be used instead of pA signal in a CMV-shRNA expression cassette [19]. Therefore, this termination signal was used in the +5shLuc and +6shLuc constructs instead of pA, resulting in CMV+5shLuc-T5 and CMV+6shLuc-T5. Finally, the U1 termination signal was cloned behind +6shLuc, resulting in CMV+6shLuc-U1. To compare their inhibitory effect, HEK293T cells were co-transfected with the different variants of CMV-shLuc together with the firefly luciferase reporter. shRNA targeting GFP (shGFP) was included as a negative control and renilla luciferase expression was measured to correct for experimental conditions. The ratio firefly/renilla in the negative control was set as 100% and relative inhibition of the luciferase reporter was calculated. All CMV-shLuc constructs appeared less effective in inhibiting luciferase compared to the pol III H1-shLuc control (Fig. 1b). The maximum inhibition of luciferase achieved was 22% and 36% for CMV+5shLuc-pA and CMV+6shLuc-pA constructs, respectively. CMV+6shLuc-U1 inhibited luciferase expression with only 18%. CMV+5shLuc-T5 and CMV+6shLuc-T5 constructs were not effective at all.

Design and knockdown efficacy of CMV-shLuc with different hairpin stem length

The length of the stem in the shRNA has been found to be important for Dicer processing resulting in enhancement of the silencing potential of a given hairpin [20]. Dicer recognizes double-stranded RNA and cleaves 21-22 nt to produce mature siRNA. To check whether extending stem length of shLuc would improve its efficacy as a result of better Dicer processing, constructs with 20, 21, 25, and 29 bp stem were designed by extending the 5' end of the guide strand, resulting in shLuc20, shLuc21, shLuc25, and shLuc29 variants (Fig. 2a). Based on our previous findings shLuc was placed at +6 site and followed by pA or U1 termination signal. Luciferase knockdown was measured to determine the efficacy of the extended stem length constructs (Fig. 2b,c). Improved efficacy was observed when extending hairpin stem to 21 nt for both pA (Fig. 2b) and U1 TTS (Fig. 2c). This improvement was statistically significant for pA TTS ($p < 0,05$) while change for U1 TTS was not significant ($p > 0,05$). Further lengthening of the shLuc hairpin stem to 25 and 29 bp did not change the inhibitory effect of these constructs (Fig. 2b,c).

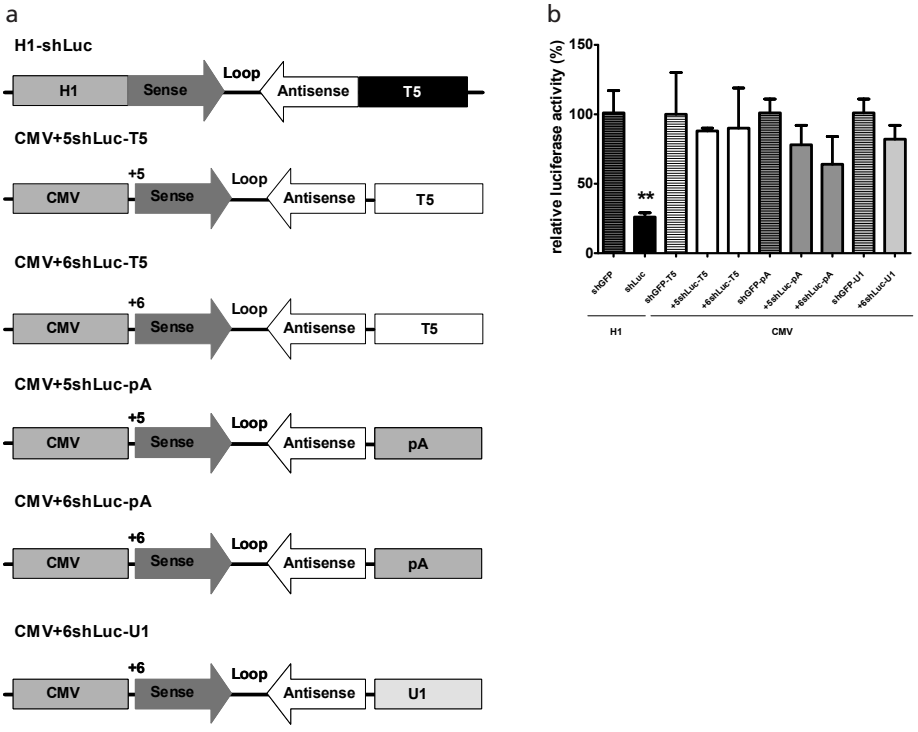

Figure 1. Structure and knockdown efficacy of short hairpins targeting luciferase (shLuc) with TSS and TTS. (a) Schematic representation of shLuc constructs expressed from H1 and CMV promoters. Different TTS (pA, T5 and U1) are presented. Hairpin location (+5 or +6) is shown with reference to the TSS (set as +1). The shLuc consists of 20 nt perfectly complementary hairpin structure and a loop of 9 nt. (b) Luciferase knockdown by CMV-shLuc with different TSS and different TTS. Renilla and firefly luciferase were measured two days post-transfection with 2,5 ng Firefly luciferase reporter, 0,5 ng Renilla luciferase and 100 ng shLuc expressing plasmids. Firefly luciferase expression was normalized to Renilla luciferase expression. H1-shLuc was used as a positive control, H1-shGFP and CMV-shGFP served as negative controls and were set at 100%. Data are represented as mean values ±SD from three independent experiments analyzed with the factor correction method [35]. **p < 0.01 versus negative control One-way ANOVA test with Bonferroni post test.

Design and knockdown efficacy of CMV-shRNA and artificial miRNA targeting luciferase or apolipoprotein B100 (ApoB)

Previously, H1-shApoB1 and H1-shApoB2 have been used to inhibit *in vitro* and *in vivo* the expression of ApoB that is the structural protein of low density lipoprotein cholesterol (LDL-C) [21](and data not shown). To evaluate whether the structural requirements for expression of shRNA from the CMV promoter, +6 TSS and pA TTS apply not only to luciferase-targeting constructs, two CMV-shRNAs targeting ApoB were designed and named CMV-shApoB1 and CMV-shApoB2, respectively. As an alternative strategy for direct pol II expression of shRNA, artificial miRNA scaffolds

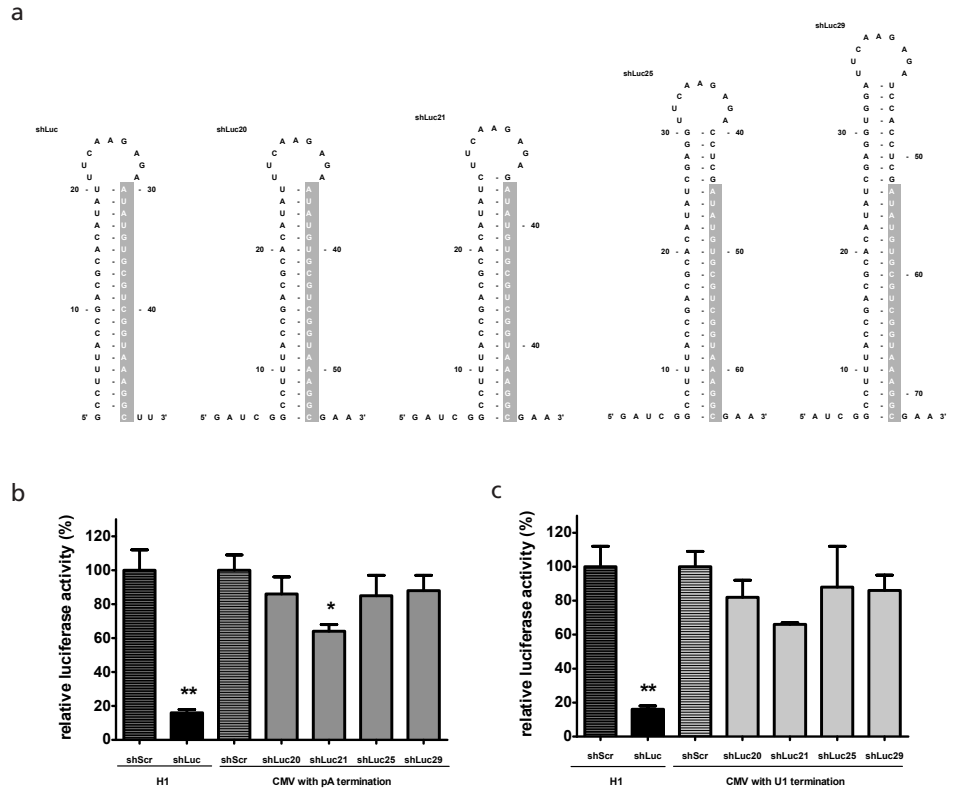

Figure 2. Structure and knockdown efficacy of CMV-shLuc with different stem length and polyadenylation (pA) or U1 transcription termination signals (U1). (a) Predicted stem-loop structure of CMV-shLuc with different stem lengths (20, 21, 25 and 29 nt). Guide strand is highlighted in grey (b) Luciferase knockdown by CMV-shLuc20, CMV-shLuc21, CMv-shLuc25, CMV-shLuc29 with pA transcription termination signal. (c) Luciferase knockdown by CMV-shLuc20, CMV-shLuc21, CMV-shLuc25, CMV-shLuc29 with U1 transcription termination signal. Renilla and firefly luciferase were measured two days post-transfection with 2,5 ng Firefly luciferase reporter, 0,5 ng Renilla luciferase and 100 ng short hairpin expressing plasmid. Firefly luciferase expression was normalized to Renilla luciferase expression. H1-shLuc was used as a positive control. H1-shScr and CMV-shScr served as negative controls and were set at 100%. Data are represented as mean values ±SD from three independent experiments analyzed with the factor correction method [35]. *$p < 0.05$, **$p < 0.01$ versus negative control (One-way ANOVA test with Bonferroni post test).

incorporating siRNA targeting luciferase or ApoB were designed by substituting the mature miRNA sequence with luciferase and ApoB target sequences, resulting in CMV-miLuc, CMV-miApoB1 and CMV-miApoB2 (Fig. 3a,b,c). The pri-miRNA structure contains additional flanking sequences at the 5′ and 3′ ends of the hairpin, which enables correct recognition and processing by the RNAi pathway enzymes Drosha and Dicer. The 5′ and 3′ flanking sequences of pri-mir155 were used, therefore design and optimization of the sequences up- or downstream of the miRNA hairpin are not required

for effective knockdown. Knockdown efficacy of CMV-shRNAs and CMV-miRNAs was determined on their specific luciferase reporters, containing ApoB target sequences in case of shApoB and miApoB constructs. H1-shLuc, H1-shApoB1 and H1-shApoB2 were used as positive controls and H1-shScr, CMV-shScr and CMV-miScr, not targeting any sequence in the human genome, were used as negative controls. Luciferase expression in the negative controls was set at 100% and the relative inhibition of luciferase reporters was calculated (Fig. 3d,e,f). CMV-shApoB1 and CMV-shApoB2 inhibited luciferase reporters by 22% and 8% respectively (Fig. 3e,f), which is similar to the knockdown observed with CMV+6shLuc20-pA (Fig. 3d). By contrast, CMV-miApoB1 and CMV-miApoB2 were found to inhibit luciferase reporters up to 57% and 75% respectively (Fig. 3e,f). CMV-miLuc was not more active than CMV+6shLuc20-pA even though it was designed the same way as CMV-miApoB1 and CMV-miApoB2 (Fig. 3d).

Quantification of siRNA molecules processed from the different shRNA and miRNA scaffolds

Next, we wanted to determine if the inhibitory effect of the shRNA and artificial miRNA constructs correlates with the amount of processed siRNA molecules in the cell. For siLuc, siApoB1 and siApoB2 sequences, small RNA specific Taqman assay was designed for detecting the guide strand (Table S1). Ten-fold dilutions (100 pg – 1 fg) of the guide strand of each synthetic siRNA oligo were used to create a standard line (Fig. 4a). All siRNA assays showed a clear exponential correlation between the amplification pattern and the amount of siRNA standard. The small RNA Taqman assay relies on the hybridization of stem-loop RT primers to the mature guide strand and in some cases the method could show insufficient specificity, amplifying the precursor shRNA hairpin or nonspecifically binding to another siRNA molecule. To

Figure 3. Structure and knockdown efficacy of shRNA and miRNA hairpin constructs targeting luciferase and Apolipoprotein B100 (ApoB). (a,b,c) Predicted stem-loop structures of shRNA and miRNA targeting luciferase: shLuc or miLuc and ApoB: shApoB or miApoB with guide strand highlighted in grey. shRNA structure is described in Fig. 1. miApoB consists of pri-mir-155 precursor sequence, where the mature mir-155 sequence was replaced with the target sequence for luciferase or ApoB. ApoB1 and ApoB2 target different sequences in the ApoB gene. (d) Luciferase knockdown by CMV-shLuc and CMV-miLuc. Renilla and firefly luciferase were measured two days post-transfection with 100 ng shRNA or miRNA expressing plasmid and 2,5 ng Firefly luciferase and 0,5 ng Renilla luciferase. H1-shLuc was used as a positive control. shScr and miScr served as negative controls and were set at 100%. Firefly luciferase expression was normalized to Renilla luciferase expression. Data are represented as mean values ±SD from three independent experiments analyzed with the factor correction method [35] (e) Knockdown of Luc-ApoB1 reporter, containing in its 3′ UTR ApoB1 target sequence, by CMV-shApoB1 and CMV-miApoB1. Experimental setup was as described in (d) H1-shApoB1 was used as a positive control. (f) Knockdown of Luc-ApoB2 reporter, containing in its 3′ UTR ApoB2 target sequence, by CMV-shApoB2 and CMV-miApoB2. Experimental setup was as described in (d) with the exception that in this Renilla luciferase contained target sequence for ApoB2 and its expression was normalized to Firefly luciferase expression H1-shApoB2 was used as a positive control. **$p < 0.01$ versus negative control (One-way ANOVA test with Bonferroni post test). ►

a

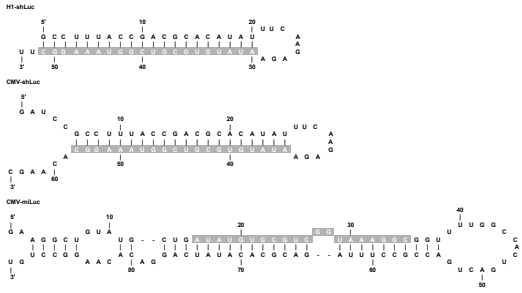
H1-shLuc
CMV-shLuc
CMV-miLuc

d

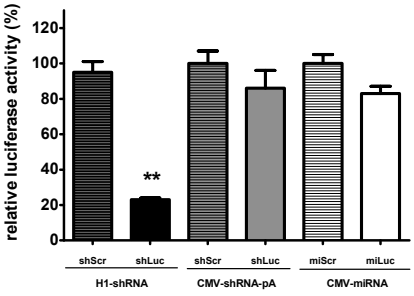
relative luciferase activity (%)
shScr
shLuc
shScr
shLuc
miScr
miLuc
H1-shRNA
CMV-shRNA-pA
CMV-miRNA

b

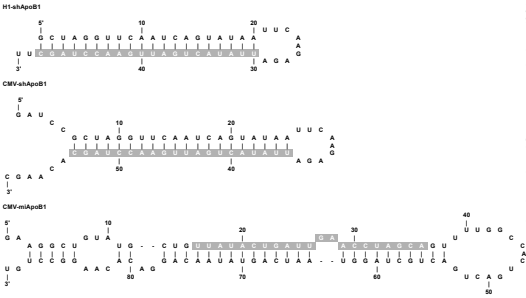
H1-shApoB1
CMV-shApoB1
CMV-miApoB1

e

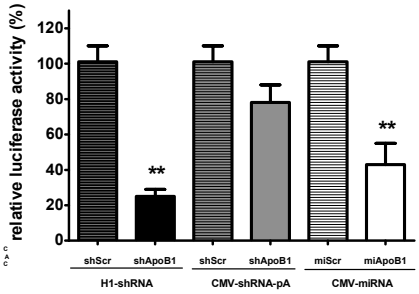
relative luciferase activity (%)
shScr
shApoB1
shScr
shApoB1
miScr
miApoB1
H1-shRNA
CMV-shRNA-pA
CMV-miRNA

c

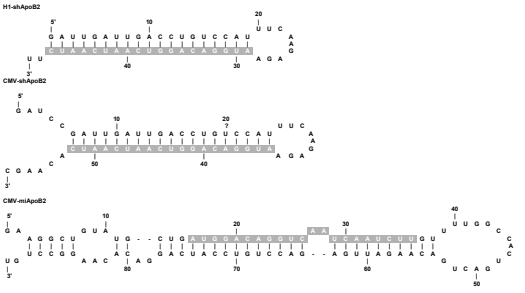
H1-shApoB2
CMV-shApoB2
CMV-miApoB2

f

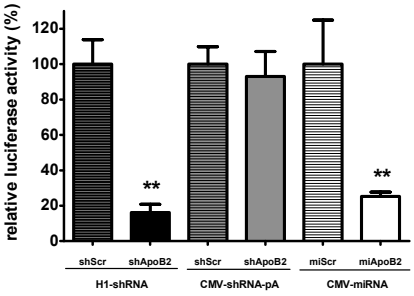
relative luciferase activity (%)
shScr
shApoB2
shScr
shApoB2
miScr
miApoB2
H1-shRNA
CMV-shRNA-pA
CMV-miRNA

exclude this possibility, we investigated the ability of the siApoB1 and siApoB2 assays to differentiate between the mature siRNA molecules, their shApoB1 or shApoB2 hairpin precursors and expression plasmids by performing additional Taqman experiments. The primers and probes specifically amplified only the corresponding synthetic siRNA standard and no aspecific amplification was detected for the shRNA hairpin oligo or expression plasmid suggesting that the small RNA Taqman assays were highly specific for the mature siApoB1 or siApoB2 (Tables S2 and S3). Having confirmed that properly processed siRNA molecules can be specifically detected, we proceeded with detection and quantification of the siRNA molecules per cell for H1-shRNA, CMV-shRNA and CMV-miRNA constructs (Fig. 4b,c,d). For all constructs an amplification chart was created and the amount of molecules was calculated. The exponential amplification for H1-shLuc began at 25 cycles, while it began later for both CMV-shLuc and CMV-miLuc (32 and 29 cycles respectively) (Fig. 4b left panel). The expression of siLuc molecules was 125-fold lower when expressed as CMV-shLuc and 10-fold lower when expressed as CMV-miLuc compared to H1-shLuc, which resulted in 16686 siRNA molecules per cell (Fig. 4b right panel). The exponential amplification for H1-shApoB1 began at 26 cycles, at cycles 32 for CMV-shApoB1 and at 27 cycles for CMV-miApoB1 (Fig. 4c left panel). This represents 12-fold less molecules expressed with CMV-shApoB1 and 2-fold less for CMV-miApoB1 compared to H1-shApoB1, which resulted in 14838 siRNA molecules (Fig. 4c right panel). siApoB2 molecules were not detected as efficiently as siLuc and siApoB1 thus the exponential amplification started later: for H1-shApoB2, it began at 29 cycles, at 36 cycles for CMV-shApoB2 and at 34 cycles for CMV-miApoB2 (Fig. 4d left panel). This represented 49-fold less molecules expressed with CMV-shApoB2 and 32-fold less for CMV-miApoB2 compared to H1-shApoB2, which resulted in 1764 molecules per cell (Fig. 4d right panel).

Figure 4. Quantification of siRNA molecules expressed from H1-shRNA, CMV-shRNA and CMV-miRNA targeting luciferase and Apolipoprotein B100. (a) Synthetic siRNA standard lines. siRNA- specific small RNA Taqman was performed with dilution series of synthetic siLuc, siApoB1 or siApoB2 molecules. Based on molecular weight of the synthetic siLuc, siApoB1 and siApoB2, the amount of molecules for each point of standard line was calculated and plotted against CT value. Data are represented as mean values from 2 independent experiments conducted with two technical replicates. (b) siLuc amplification plot (left panel) and expression in HEK293T cells (right panel). RNA was isolated two days post-transfection with 1 µg H1-shLuc, CMV-shLuc or CMV-miLuc expressing constructs and siLuc-specific small RNA TaqMan was performed. siRNA copy number was calculated using the synthetic RNA oligo standard line as described in (a) Data are presented from representative experiment from two independent experiments conducted with two technical replicates (c) siApoB1 amplification plot (left panel) and expression in HEK293T cells (right panel) after transfection with 1 µg H1-shApoB1, CMV-shApoB1 or CMV-miApoB1 expressing constructs. Experimental set up as described in (b) (d) siApoB2 amplification plot (left panel) and expression in HEK293T cells (right panel) after transfection with 1 µg H1-shApoB2, CMV-shApoB2 or CMV-miApoB2 expressing constructs. Experimental set up as described in (b). Data are represented as mean values from 2 independent experiments conducted with two technical replicates. ►

a

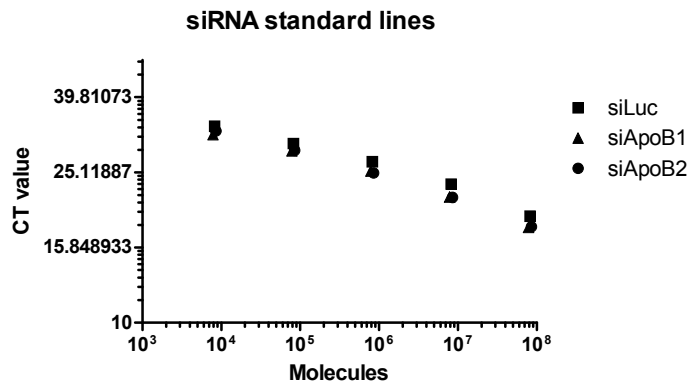
siRNA standard lines
39.81073
25.11887
15.848933
10
CT value
10^3
10^4
10^5
10^6
10^7
10^8
Molecules
siLuc
siApoB1
siApoB2

b

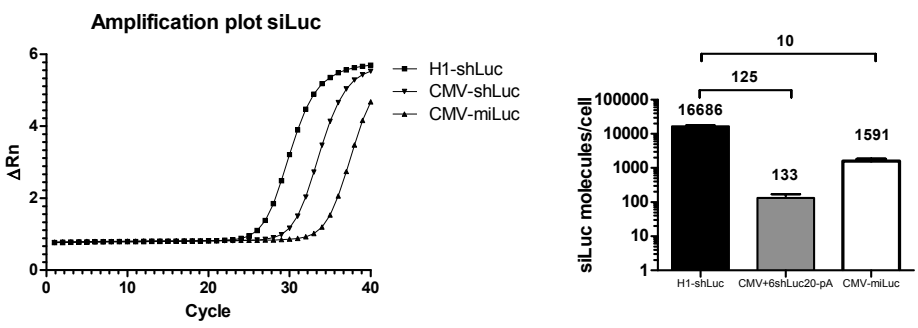
Amplification plot siLuc
ΔRn
Cycle
H1-shLuc
CMV-shLuc
CMV-miLuc
siLuc molecules/cell
16686
133
1591
10
125
H1-shLuc
CMV+6shLuc20-pA
CMV-miLuc

c

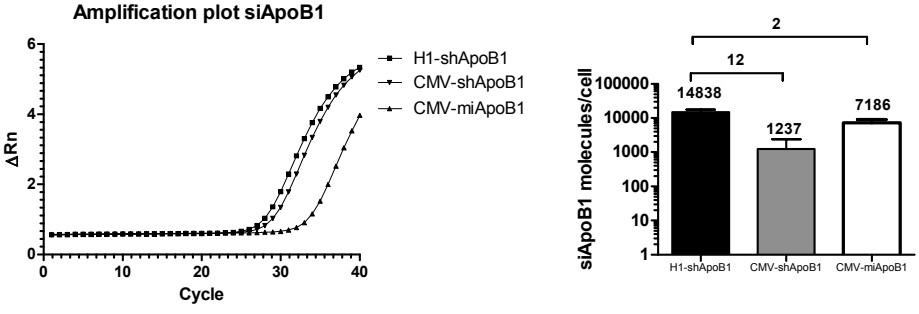
Amplification plot siApoB1
ΔRn
Cycle
H1-shApoB1
CMV-shApoB1
CMV-miApoB1
siApoB1 molecules/cell
14838
1237
7186
2
12
H1-shApoB1
CMV-shApoB1
CMV-miApoB1

d

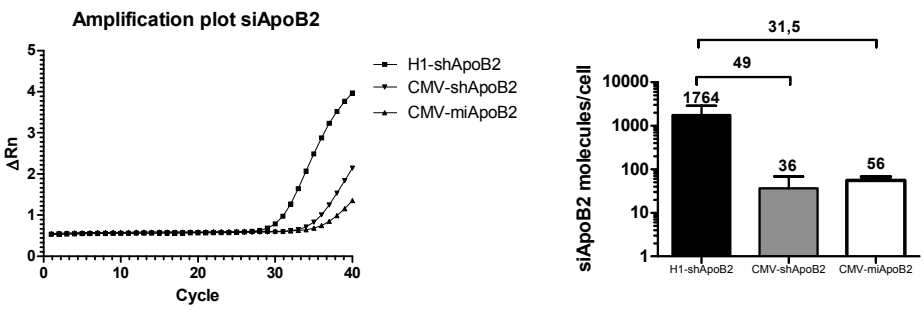
Amplification plot siApoB2
ΔRn
Cycle
H1-shApoB2
CMV-shApoB2
CMV-miApoB2
siApoB2 molecules/cell
1764
36
56
31,5
49
H1-shApoB2
CMV-shApoB2
CMV-miApoB2

Endogenous ApoB mRNA knockdown

In order to assess the inhibitory effect of shApoB1, shApoB2, miApoB1 and miApoB2 constructs on endogenous ApoB expression the mouse hepatoma Hepa1-6 cell line was selected. Cells were transfected with H1-shApoB1, CMV-shApoB1 and CMV-miApoB1 or with their equivalent constructs having ApoB2 as a target. Two days post transfection RNA was isolated and ApoB mRNA expression was determined by RT-qPCR. Both H1-shApoB1 and CMV-miApoB1 efficiently inhibited ApoB mRNA up to 70% and 50% respectively (Fig. 5a). An even stronger effect was observed for H1-shApoB2 and CMV-miApoB2 which inhibited ApoB mRNA both up to 85% (Fig. 5b). CMV-shApoB1 and CMV-shApoB2 showed no inhibition of endogenous ApoB expression, which confirms the results on luciferase reporters inhibition (Fig. 3e,f) and shows the specificity of the designed constructs.

Discussion

There are few examples of successful shRNA expression using pol II promoters. Although several requirements for pol II shRNA expression have been established, optimization and direct assessment of different hairpin stem lengths, TSS and TTS have not been performed. In the current study we evaluated the relevance of these factors by positioning shRNAs targeting luciferase or ApoB at +5 or +6 relative to the CMV TSS and added the T5, pA or U1 TTS at the 3' end of the hairpins. Additionally, the same siRNA sequences were incorporated in artificial miRNA scaffolds and direct

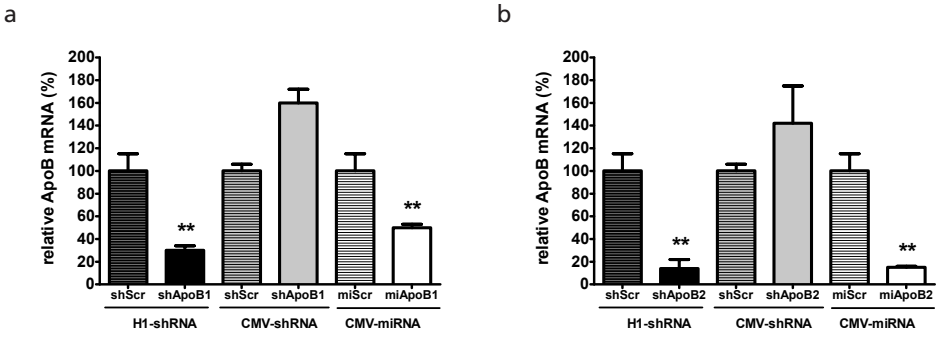

Figure 5. Comparison of endogenous ApoB mRNA knockdown by shApoB1, shApoB2, miApoB1 and miApoB2in Hepa1-6 cells. (a) Endogenous ApoB mRNA knockdown by H1-shApoB1, CMV-shApoB1 and CMV-miApoB1 constructs (b) Endogenous ApoB mRNA knockdown by H1-shApoB2, CMV-shApoB2 and CMV-miApoB2 constructs qRT-PCR was performed two days post-transfection with 1 µg of shRNA or miRNA expressing constructs and ApoB mRNA levels were calculated relative to actin mRNA. H1-shApoB1 and H1-ApoB1 served as positive control. shScr and miScr served as negative controls and were set at 100%. Data are represented as mean values ±SD from three independent experiments analyzed with factor correction method [35]. **$p < 0.01$ versus negative control (One-way ANOVA test with Bonferroni post test).

evaluation between the silencing efficacy and processing of pol II-expressed shRNA and miRNA was performed.

The nucleotide distance between the promoter, the shRNA structure and the TTS determines the length and sequence composition of the 5′ and 3′ overhangs of the expressed hairpin. Both ends act as reference points for recognition and proper processing by Dicer [18]. Initial rules published by Xia *et al.* include shRNA location within 6 nt from the TSS and pA TTS [11]. Later shRNA containing T5 and U1 TTS where also found to be active when substituted for pA [13,19]. These settings were used in our study to express shRNA from the CMV promoter. The shLuc, shApoB1 and shApoB2 sequences have been previously validated as potent inhibitors of their targets when expressed from the pol III H1 promoter [16,21]. Surprisingly, all CMV-shLuc constructs induced only a mild target inhibition when the hairpin was placed at +6 TSS and T5 or pA TTS were used. In contrast to previously published data, the use of U1 TTS did not improve silencing efficacy. By shifting the hairpin from +6 to +5 from TSS, thus minimizing the 5′ overhang, no significant improvement was achieved and the effect was not dependent of TTS used. Additionally, the CMV-shApoB1 and CMV-shApoB2 hairpins were ineffective when the initial settings of +6 TSS and pA TTS were used, indicating that those settings cannot be used as a general rule for pol II-shRNA expression.

The length of the shRNA hairpin stem has been shown to play an important role in silencing efficacy as it can lead to differential processing into multiple siRNAs [8,22,23]. In the current study we optimized the pol II shRNA expression by testing stem lengths of 20, 21, 25, and 29 bp. Slight increase in silencing efficacy was observed only when extending hairpin stem from 20 to 21 bp but not when the stem length was further extended to 25 or 29 bp. Mcintyre *et al.* performed a similar study by extending the shRNA stem length from 16 to 41 bp and looked at the core placement of the shRNA [23]. While the processing of hairpins was clearly dependent on the stem length, the activity was primarily dependent on the sequence of processed products. Consistent with their data, our results suggest that there is no strict correlation between the increase in stem length and better silencing activity of the shRNAs. Here, we focused only on pol II expression of shRNA but an alternative approach would be to express long hairpin RNA (lhRNA) where the stem length is extended up to 300 bp [24-26]. Using lhRNA allows generating multiple siRNA from a single transcript, which can be used for viral infections or cancer, where multiple sequences have to be targeted. To date, expression of active lhRNA from pol II promoter has not been successful due to inefficient processing of the hairpins by the RNAi machinery, and detailed studies on TSS, TTS and hairpin location, similar to those for shRNA are lacking.

An alternative to optimizing pol II expression of shRNA is to use pre-miRNA scaffolds and replace the mature miRNA sequence with siRNA targeting a gene of interest.

Cellular miRNAs are naturally expressed from pol II promoters [1,27]. Therefore, when shLuc, shApoB1 and shApoB2 were expressed from the pri-mir-155 scaffold the knockdown efficacy was significantly improved. Importantly, artificial miRNA have been found to be less toxic *in vitro* and *in vivo* compared to shRNA as they do not disrupt the endogenous RNAi pathway. McBride *et al.* used this approach to target Huntingtin mRNA and to avoid neurotoxicity caused by overexpression of shRNA [15]. Similarly, incorporation of a siRNA against Spinocerebellar ataxia 1 protein into an artificial miRNA abolished neuronal cell death observed with a shRNA harboring the same siRNA sequence [28]. In a previous study we have provided evidence for the efficacy of liver-specific expression of artificial miRNA targeting ApoB *in vivo* and demonstrated its advantages over the pol III-expressed shRNA [29]. In conclusion, we and others have shown that pol II expression of artificial miRNA scaffolds is a more robust and promising approach than pol II shRNA expression, probably due to the specific structural characteristics of the miRNA.

An additional advantage of the use of artificial miRNAs is that several precursors can be expressed as clusters from longer transcripts, allowing simultaneous targeting of multiple genes [30]. This feature of the miRNA is very important when mutation-prone viruses, such as HIV-1 or HCV, are targeted or when several disease-related genes need to be simultaneously silenced. Moreover, miRNAs can be linked to the 3' untranslated region of a therapeutic gene, which is an additional advantage for therapeutic applications since it allows co-delivery of a codon-optimized gene together with a miRNA targeting the disease-causing version of the same gene. Such combinational therapy has been shown for alpha1-antitrypsin (A1AT) deficiency, in which a hairpin RNA targeting mutated A1AT transcript was delivered together with codon-optimized A1AT gene [31].

Quantification of the siRNA molecules expressed from the H1-shRNA, CMV-shRNA or CMV-miRNA constructs was highly specific and revealed differences in the amount of processed siRNA molecules per cell. As expected, highest siRNA amounts were detected when the shRNAs were expressed from the strong H1 promoter. However, when the same shRNAs were expressed from the CMV promoter, 12- to 125-fold less siRNA molecules were detected indicating that either the shRNA was not efficiently transcribed from the CMV promoter or that there was impaired siRNA processing by the RNAi machinery. Surprisingly, the amount of processed siRNA from the CMV-miRNA constructs did not correlate with efficacy. For example, CMV-miLuc yielded 1591 siLuc molecules per cell and was completely ineffective in target knockdown while CMV-miApoB2 yielded only 56 siApoB2 molecules per cell and was highly efficient. A possible explanation for this discrepancy is that the small RNA Taqman assay detects only one variant of the guide strand and although identical predicted siRNA sequences were incorporated in the CMV-shRNA and CMV-miRNA

scaffolds, they can still be processed differently. Indeed, our newest data based on Next Generation Sequencing (NGS) of small RNAs from cells transfected with H1-shApoB2 and CMV-miApoB2 indicates differential processing and different mature sequences from the two scaffolds [29]. The siRNAs originating from the H1-shRNA were more heterogeneous in cleavage sites and length compared to the products originating from the CMV-miRNA scaffold supporting the notion that Dicer cleavage is less precise than the combination of Drosha and Dicer. Unfortunately, NGS data from pol II-expressed shRNA, which would allow verifying the processed siRNA variants and their abundance, are still not available.

Conclusions

In summary, our results demonstrate that it is currently difficult to draw rules for efficient pol II shRNA expression and processing. Optimization of the shRNA stem length, TSS and TTS did not result in better silencing efficacy for any of the CMV-expressed shRNAs. On the other hand, when identical predicted sequences were incorporated in miRNA scaffolds, two out of three sequences resulted in potent inhibition of luciferase reporters and endogenous mRNA. Our data question the application of the previously published rules for pol II shRNA expression as general standards. The rules for design of potent shRNA expressed from pol II promoters are still far from clear and they can be used rather as reference points. Still detailed empirical optimization of hairpin location seems to be required for every target and pol II promoter used. We consider that embedding siRNA in artificial miRNA scaffold and expression from pol II promoter is a better and approach than direct pol II shRNA expression due to the intrinsic characteristics of the miRNA structure rendering it a better substrate for the RNAi machinery.

Metherials and methods

DNA constructs

H1-shRNAs were made by annealing complementary oligonucleotides and ligating them into the BglII and XhoI sites of the pSuper vector (OligoEngine, Seattle, WA, USA). The vector contains a stretch of five thymidines (T5), which acts as the transcription termination signal. Panel of shRNAs were designed to act as positive controls: one shRNAs was designed that target firefly luciferase (H1-shLuc), two shRNAs were made that target different regions of human ApoB gene (H1-shApoB1 and H1-shApoB2). Additionally two negative controls shRNA were deigned: one that do not target any gene in human and mouse genome (H1-shScr) and one that target the GFP (H1-shGFP). All the sequences of oligonucleotides used in this study are listed in Table S1.

CMV-shRNA with different termination signals were designed as followed. First different TTS (T5, pA or U1) were annealed from complementary oligonucleotides and ligated into the AccI and SphI sites of pVD23 which includes the CMV promoter. Next, plasmids were digested with SacI and NheI and complementary oligonucleotides containing shRNA targeting GFP (shGFP) or Luciferase (shLuc) were inserted. shLuc oligonucleotides were designed to allow the hairpin transcription to start at +5 or +6 nucleotides after the TSS, which was considered as +1. The final constructs were CMV+5shLuc-T5, CMV+6shLuc-T5, CMV+5shLuc-pA and CMV+6shLuc-pA. For U1 termination signal only CMV+6shLuc-U1 was created. As negative controls CMV-shGFP-T5, CMV-shGFP-pA and CMV-shGFP-U1 were made. GFP oligonucleotides were designed that hairpin started at +6 from the TSS.

CMV-shRNAs with different stem length of the hairpin were designed as followed. CMV-shLuc20, CMV-shLuc21, CMV-shLuc25 or CMV-shLuc29 were made by annealing complementary oligonucleotides that create the stem-loop structure of 20, 21, 25 and 29 bp respectively and ligating them into the BamHI and XhoI sites of the pSilencer 4.1 CMV vector (Life Technologies, Grand Island, NY). Constructs contained either the pA or the U1 termination signal. To create the CMV-shApoB1 and CMV-siApoB2, siRNA sequences from shApoB1 and shApoB2 were cloned by annealing complementary oligonucleotides and ligating them into the BamHI and XhoI sites of the pSilencer 4.1 CMV vector with pA termination signal. As the negative control, pSilencer 4.1 CMV control (Life Technologies, Grand Island, NY) plasmid was used, named CMV-shScr.

To create the artificial miRNA expressing vectors, siRNA sequences from shLuc, shApoB1 and shApoB2 were cloned into the pri-mir-155 backbone of pcDNA6.2-GW/EmGFP-miR (Life Technologies, Grand Island, NY) by annealing complementary oligonucleotides and ligation into BamHI- and XhoI-digested pcDNA6.2 plasmid and named respectively CMV-miLuc, CMV-miApoB1and CMV-miApoB2. As the negative control pcDNA6.2-GW/EmGFP-miR-neg control (Life Technologies, Grand Island, NY) was used, named CMV-miScr. The Mfold program was used to determine the secondary structure of all RNA transcripts [32].

Reporter constructs that were used for luciferase knockdown are Firefly luciferase pGL4 (Promega, Madison, WI) and pRL Renilla (Promega, Madison, WI) under control of the CMV promoter. Luc-ApoB1 reporter, containing in its 3' UTR a fragment of 239 nucleotides of human ApoB (NM_000384, 9362-9600) sequence was made, by cloning of the ApoB sequence, that was PCR amplified with primers pr565f and pr566r in the XhoI and NheI sites of pGL4 plasmid. For The Luc-ApoB2 containing in the 3'UTR of siCheck2 vector (Promega, Madison, WI) 1851 nucleotides of the last exon from the human ApoB has been described previously.

Cell culture and transfections

The human embryonic kidney (HEK)293T and mouse hepatoma Hepa1-6 cell lines were maintained in Dulbecco's modified Eagle's medium (DMEM; Life Technologies,

Grand Island, NY) containing 10% fetal calf serum, 100 U/ml penicillin and 100 U/ml streptomycin, at 37°C and 5% CO_2. For luciferase assays, endogenous ApoB knockdown assays, and siRNA expression analysis, cells were seeded in 96- or 24-well plates at a density of 3×10^4 or 1.2×10^5 cells per well, respectively, in DMEM one day prior transfection. Transfections were performed with Lipofectamine 2000 reagent (Life Technologies, Grand Island, NY) according to the manufacturer's instructions.

Luciferase assays

Cells were co-transfected with 100 ng shRNA or miRNA expressing plasmid and respectively 2,5 ng Firefly luciferase or Luc-ApoB1 and 0,5 ng Renilla or 50 ng Luc-ApoB2 reporter.Transfected cells were assayed at 48 hr post-transfection in 20 µl 1x passive lysis buffer (Promega, Madison, WI) firefly and renilla were measured luciferase activities with the Dual-Luciferase Reporter Assay System (Promega, Madison, WI). For luciferase knockdown calculations, H1-shLuc was used as a positive control. CMV-shScr, CMV-shGFP or CMV-miScr served as negative controls and were set at 100%. For luciferase- and ApoB1-targeting constructs Firefly luciferase expression was normalized to Renilla luciferase expression. For ApoB2-targeting constructs Renilla luciferase expression was normalized to Firefly luciferase expression since the siCheck2 plasmid was used.

RNA isolation and quantitative real-time RT-PCR

To determine endogenous ApoB mRNA knockdown by shApoB and miApoB constructs *in vitro*, Hepa1-6 cells were transfected with 1 µg shApoB1, shApoB2, miApoB1 or miApoB2 and total RNA was isolated from cells 48 hr post-transfection using the Nucleospin kit (Clontech, Mountain View, CA). Genomic DNA (gDNA) was removed by DNase treatment using TURBO DNase (Ambion, Austin, TX). First strand cDNA was reverse transcribed using random hexamer primers with the Dynamo kit (Finnzymes, Espoo, Finland). Real time PCR amplification was performed with ApoB- and beta actin-specific primers (Table S1). PCR reaction conditions were: 95°C for 10 min, followed by 40 cycles of 15 sec at 95°C and 1 min at 60°C. The assays were performed on ABI 7000 or ABI 7500 (Applied Biosystems, Foster City, CA). ApoB expression levels were normalized to beta actin as an internal control, and the relative gene expression $2^{-\Delta\Delta Ct}$ method of Livak and Schmittgen was used for analysis of PCR data [33].

siRNA detection by Small RNA Taqman assay

RT reactions for siLuc, siApoB1 and siApoB2 expression were performed with the TaqMan MicroRNA Reverse Transcription Kit (Applied Biosystems, Foster City, CA) using 10 ng RNA isolated from cells transfected with shRNA or miRNA expression plasmids and 3 µl custom-made specific RT-stem-loop primers (Applied Biosystems, Foster City, CA) according to the manufacturer's instructions. The TaqMan assay was

done in 20 µl using 1,33 µl cDNA , 1 µl custom-made siRNA-specific primer with FAM-labeled fluorogenic probe (Applied Biosystems) and 10 µl TaqMan 2× Universal PCR Master Mix (Applied Biosystems). For determining the assay specificity, 10 ng of the indicated oligo or expression plasmid was added to the Taqman reaction. Amplification of the beta actin gene was used as a RNA quality and loading control. siRNA copy number per cell was calculated based on the amplification plot of a dilution series of synthetic siRNA standards (IDT, Coralville, IA). Tenfold dilutions (100 pg – 1 fg) of the guide strand of the synthetic siRNA oligo were used to create a standard line. The copy number of each dilution was calculated according to the formula 1 mol = 6.02×10^{23} molecules. The trend line value of the standard line was used to calculate the siRNA copy number per cell, assuming 15 pg RNA per cell [34].

Competing interests

PM, FB, HP, SvD and PK are employees of Amsterdam Molecular Therapeutics. AK and TR are former employees of Amsterdam Molecular Therapeutics. The authors declare that they have no competing interests.

Authors' contributions

PM carried out the experiments, designed the study and prepared the manuscript; AK, FB, HP, SvD and TR participated in the study design and drafting of the manuscript; PK designed and interpreted the research and participated in preparing of the manuscript. All authors read and approved the final manuscript.

Acknowledgments

This work was carried out and funded by Amsterdam Molecular Therapeutics, Amsterdam.

Table S1. Oligonucleotides used in this study

name	Sequence (5'-3')
pA forward	AGACGCTAGCTAATAAAGGCATGCTTATTTTCATTGGATCCGTGTGTGTTGGTTTTTTCCTAGGGCATG
pA reverse	CCCTAGGAAAAAACCAACACACACGGATCCAATGAAAATAAGCATGCCTTTATTAGCTAGCGT
T5 forward	AGACGCTAGCTATTTTTGGCATGCTTATTTTCATTGGATCCGTGTGTGTTGGTTTTTTCCTAGGGCATG
T5 reverse	CCCTAGGAAAAAACCAACACACACGGATCCAATGAAAATAAGCATGCCAAAAATAGCTAGCGT
H1-shScr-F	GATCCCCGATCGAATGTGTACTTCGATTCAAGAGATCGAAGTACACATTCGATCTTTTTGCATGCC
H1-shScr-R	TCGAGGCATGCAAAAAGATCGAATGTGTACTTCGATCTCTTGGAATCGAAGTACACATTCGATCGGG
H1-shGFP-F	GATCCCCAGCTGGAGTACAACTACAACCTTCCTGTCAGTTGTAGTTGTACTCCAGCTTTTTGCATGCC
H1-shGFP-R	TCGAGGCATGCAAAAAGCTGGAGTACAACTACAACTGACAGGAAGGTTGTAGTTGTACTCCAGCTGGG
CMV+6shGFP-F	CGGTTTAGTCGACCGTCAGATTAGCTGGAGTACAACTACAACTTCAAGAGAGTTGTAGTTGTACTCCAGCTG
CMV+6shGFP-R	CTAGCAGCTGGAGTACAACTACAACTCTCTTGAAGTTGTAGTTGTACTCCAGCTAATCTGACGGTCGACTAAACCGAGCT
H1-shLucF	GATCCCCGCCTTTACCGACGCACATATTTCAAGAGAATATGTGCGTCGGTAAAGGCTTTTTGCATGCC
H1-shLucR	TCGAGGCATGCAAAAAGCCTTTACCGACGCACATATTCTCTTGGAAATATGTGCGTCGGTAAAGGCGGG
CMV+6shLucF	CTAGTCAGATTGCCTTTACCGACGCACATATTTCAAGAGAATATGTGCGTCGGTAAAGGCG
CMV+6shLucR	CTAGCGCCTTTACCGACGCACATATTCTCTTGAAATATGTGCGTCGGTAAAGGCAATCTGA
CMV-shLuc20F	GATCGGCCTTTACTGACGTACATATTTCAAGAGATATGTGCGTCGGTAAAGGCGAA
CMV-shLuc20R	AGCTTTCGCCTTTACCGACGCACATATCTCTTGAATATGTACGTCAGTAAAGGCC
CMV-shLuc21F	GATCGGCCTTTACTGACGTACATATCTCAAGAGGATATGTGCGTCGGTAAAGGCGAA
CMV-shLuc21R	AGCTTTCGCCTTTACCGACGCACATATCCTCTTGAGATATGTACGTCAGTAAAGGCC
CMV-shLuc25F	GATCGGCCTTTACTGACGTACATATCGAGGTTCAAGAGCCTCGATATGTGCGTCGGTAAAGGCGAA
CMV-shLuc25R	AGCTTTCGCCTTTACCGACGCACATATCGAGGCTTCTTGACCTCGATATGTACGTCAGTAAAGGCC
CMV-shLuc29F	GATCGGCCTTTACTGACGTACATATCGAGGTGGATTCAAGAGTCCACCTCGATATGTGCGTCGGTAAAGGCGAA
CMV-shLuc29R	AGCTTTCGCCTTTACCGACGCACATATCGAGGTGGACTCTTGATCCACCTCGATATGTACGTCAGTAAAGGCC
CMV-shLuc20U1F	GATCGGCCTTTACTGACGTACATATTTCAAGAGATATGTGCGTCGGTAAAGGCGAAGGAGTTTCAAAAGTAGAGCGGCCGCAA
CMV-shLuc20U1R	TGCGGCCGCTCTACTTTTGAAACTCCTTCGCCTTTACCGACGCACATATCTCTTGAATATGTACGTCAGTAAAGGCC
CMV-shLuc21U1F	GATCGGCCTTTACTGACGTACATATCTTCAAGAGGATATGTGCGTCGGTAAAGGCGAAGGAGTTTCAAAAGTAGAGCGGCCGCAA
CMV-shLuc21U1R	AGCTTTGCGGCCGCTCTACTTTTGAAACTCCTTCGCCTTTACCGACGCACATATCCTCTTGAGATATGTACGTCAGTAAAGGCC
CMV-shLuc25U1F	GATCGGCCTTTACTGACGTACATATCGAGGTTCAAGAGCCTCGATATGTGCGTCGGTAAAGGCGAAGGAGTTTCAAAAGTAGAGCGGCCGCAA
CMV-shLuc25U1R	AGCTTTGCGGCCGCTCTACTTTTGAAACTCCTTCGCCTTTACCGACGCACATATCGAGGCTCTTGACCTCGATATGTACGTCAGTAAAGGCC
CMV-shLuc29U1F	GATCGGCCTTTACTGACGTACATATCGAGGTGGATTCAAGAGTCCACCTCGATATGTGCGTCGGTAAAGGCGAAGGAGTTTCAAAAGTAGAGCGGCCGCAA

CMV-shLuc29U1R	AGCTTTGCGGCCGCTCTACTTTTGAAACTCCTTCGCCTTTACCGACGCACATATCGAGGTGGA CTCTTGA TCCACCTCGATATGTACGTCAGTAAAGGCC
CMV-miLucF1	GATCCTGGAGGCTTGCTGAAGGCTGTATGCTGATATGTGCGTCGGTAAAGGCGGTTTTGGCCACTGACTGACCGC
CMV-miLucF2	CTTTAGACGCACATATCAGGACACAAGGCCTGTTACTAGCACTCACATGGAACAAATGGCCCAGATCTGGCCGCAG
CMV-miLucR1	TCGACTGCGGCCAGATCTGGGCCATTTGTTCCATGTGAGTGCTAGTAACAGGCCTTGTGTCCTGATATGTGCGTCTAAAGGCGGTCAGTCAGTGGCCAAAACC
CMV-miLucR2	GCCTTTACCGACGCACATATCAGCATACAGCCTTCAGCAAGCCTCCAG
H1-shApoB1F	GATCCCCGCTAGGTTTAATTAGTATGATTCAAGAGATTATACTGATTGAACCTAGCTTTTTGCATGCC
H1-shApoB1R	TGCAAAAAGCTAGGTTCAATCAGTATAATCTCTTGAATCATACTAATTAAACCTAGCGGG
CMV-shApoB1F	GATCGGCTAGGTTCAATCAGTATAAGTCAAGAGCTTATACTGATTGAACCTAGCACA
CMV-shApoB1R	AGCTTGTGCTAGGTTCAATCAGTATAAGCTCTTGACTTATACTGATTGAACCTAGCC
CMV-miApoB1F1	GATCCTGGAGGCTTGCTGAAGGCTGTATGCTGTTATACTGATTGAACCTAGCAGTTTTGGCCACTGACTGACTGC
CMV-shApoB1F2	TAGGTAATCAGTATAACAGGACACAAGGCCTGTTACTAGCACTCACATGGAACAAATGGCCCAGATCTGGCCGCAG
CMV-miApoB1R1	TCGACTGCGGCCAGATCTGGGCCATTTGTTCCATGTGAGTGCTAGTAACAGGCCTTGTGTCCTGTTATACTGATTACCTAGCAGTCAGTCAGTGGCCAAAACT
CMV-shApoB1R2	GCTAGGTTCAATCAGTATAACAGCATACAGCCTTCAGCAAGCCTCCAG
H1-shApoB2f	GATCCCCGATTGATTGACCTGTCCATTTCAAGAGAATGGACAGGTCAATCAATCTTTTTC
H1-shApoB2r	TCGAGAAAAAGATTGATTGACCTGTCCATTCTCTTGAAATGGACAGGTCAATCAATCGGG
CMV-shApoB2F	GATCTGATTGATTGACCTGTCCATTCTCAAGAGGAATGGACAGGTCAATCAATCTTA
CMV-shApoB2R	AGCTTAAGATTGATTGACCTGTCCATTCCTCTTGAGAATGGACAGGTCAATCAATCA
CMV-miApoB2F1	GATCCTGGAGGCTTGCTGAAGGCTGTATGCTGATGGACAGGTCAATCAATCTTGTTTTGGCCACTGACTGACAAG
CMV-miApoB2F2	ATTGAGACCTGTCCATCAGGACACAAGGCCTGTTACTAGCACTCACATGGAACAAATGGCCCAGATCTGGCCGCAG
CMV-miApoB2R1	TCGACTGCGGCCAGATCTGGGCCATTTGTTCCATGTGAGTGCTAGTAACAGGCCTTGTGTCCTGATGGACAGGTCTCAATCTTGTCAGTCAGTGGCCAAAACA
CMV-miApoB2R2	AGATTGATTGACCTGTCCATCAGCATACAGCCTTCAGCAAGCCTCCAG
Pr565f	CAGCTCGAGTCCCAGTGCCCAGCAAGC
Pr566r	CGTGCTAGCCTGTTTTTTCCCATAGAG
ApoBf	TGGTTACTGCGCTGAGAGG
ApoBr	CCACACTGAACCAAGGCTT
m-act-f	ACGGCCAGGTCATCACTATTG
m-act-r	CAAGAAGGAAGGCTGGAAAAGA
shApoB1 oligo	GATCCCCGCTAGGTTTAATTAGTATGATTCCAAGAGATTATACTGATTGAACCTAGCTTTTTC
miApoB1 oligo	TTATACTGATTGAACCTAGCAGTTTTGGCCACTGACTGACTGCTAGGTAATCAGTATAACAGG
shApoB2 oligo	GATCCCCGATTGATTGACCTGTCCATTTCAAGAGAATGGACAGGTCAATCAATCTTTTTC
miApoB2 oligo	ATGGACAGGTCAATCAATCTTGTTTTGGCCACTGACTGACAAGATTGAGACCTGTCCATCAGG

Table S2. Determination of siApoB1 RT primers and Taqman probe specificity on siApoB1, shApoB1 hairpin precursor, shApoB1- and miApoB1-expression plasmid and siApoB2

Sample	Amount	RT primer	Taqman probe	CT value	Molecules per cell
siApoB1 synthetic standard	10 pg	ApoB1	ApoB1	15,1	1,23E+05
siApoB1 synthetic standard	1 pg	ApoB1	ApoB1	17,2	1,23E+04
siApoB1 synthetic standard	0,1 pg	ApoB1	ApoB1	21,5	1,23E+03
siApoB1 synthetic standard	0,01 pg	ApoB1	ApoB1	24,9	1,23E+02
siApoB1 synthetic standard	0,001pg	ApoB1	ApoB1	29,0	1,23E+01
siApoB1 synthetic standard	10 pg	ApoB2	ApoB1	ND	ND
siApoB1 synthetic standard	1 pg	ApoB2	ApoB1	ND	ND
siApoB1 synthetic standard	0,1 pg	ApoB2	ApoB1	ND	ND
siApoB1 synthetic standard	0,01 pg	ApoB2	ApoB1	ND	ND
siApoB1 synthetic standard	0,001pg	ApoB2	ApoB1	ND	ND
siApoB2 synthetic standard	10 pg	ApoB1	ApoB1	ND	ND
siApoB2 synthetic standard	1 pg	ApoB1	ApoB1	ND	ND
siApoB2 synthetic standard	0,1 pg	ApoB1	ApoB1	ND	ND
siApoB2 synthetic standard	0,01 pg	ApoB1	ApoB1	ND	ND
siApoB2 synthetic standard	0,001pg	ApoB1	ApoB1	ND	ND
H1-shApoB1 plasmid	10 ng	-	ApoB1	ND	ND
CMV-shApoB1 plasmid	10 ng	-	ApoB1	ND	ND
CMV-miApoB1 plasmid	10 ng	-	ApoB1	ND	ND
shApoB1 oligo	10 ng	-	ApoB1	ND	ND
miApoB1 oligo	10 ng	-	ApoB1	ND	ND

siApoB1- specific assay was tested against synthetic RNA standards, shApoB1-expression plasmids and shApoB1 hairpin oligonucleotides using different configuration of RT primer and Taqman probe. Average CT values lower than 40 cycles are presented. The amount of molecules per cell was calculated, assuming that 15 pg RNA was isolated per cell [34]. Data are presented from one representative experiment from two independent experiments conducted with two technical replicates. ND, not detected

Table S3. Determination of siApoB2 RT primers and Taqman probe specificity on siApoB2, shApoB2 hairpin precursor, shApoB2- and miApoB2-expression plasmid and siApoB1

Sample	Amount	RT primer	Taqman probe	CT value	Molecules per cell
siApoB2 synthetic standard	10 pg	ApoB2	ApoB2	12,7	1,28E+05
siApoB2 synthetic standard	1 pg	ApoB2	ApoB2	16,2	1,28E+04
siApoB2 synthetic standard	0,1 pg	ApoB2	ApoB2	19,4	1,28E+03
siApoB2 synthetic standard	0,01 pg	ApoB2	ApoB2	23,2	1,28E+02
siApoB2 synthetic standard	0,001pg	ApoB2	ApoB2	23,7	1,28E+01
siApoB2 synthetic standard	10 pg	ApoB1	ApoB2	28,7	7,13E+00
siApoB2 synthetic standard	1 pg	ApoB1	ApoB2	32,0	5,26E-01
siApoB2 synthetic standard	0,1 pg	ApoB1	ApoB2	36,4	1,72E-02
siApoB2 synthetic standard	0,01 pg	ApoB1	ApoB2	ND	ND
siApoB2 synthetic standard	0,001pg	ApoB1	ApoB2	ND	ND
siApoB2 synthetic standard	10 pg	ApoB2	ApoB1	ND	ND
siApoB2 synthetic standard	1 pg	ApoB2	ApoB1	ND	ND
siApoB2 synthetic standard	0,1 pg	ApoB2	ApoB1	ND	ND
siApoB2 synthetic standard	0,01 pg	ApoB2	ApoB1	ND	ND
siApoB2 synthetic standard	0,001pg	ApoB2	ApoB1	ND	ND
H1-shApoB2 plasmid	10 ng	-	ApoB2	ND	ND
CMV-shApoB2 plasmid	10 ng	-	ApoB2	ND	ND
CMV-miApoB2 plasmid	10 ng	-	ApoB2	ND	ND
shApoB2 oligo	10 ng	-	ApoB2	ND	ND
miApoB2 oligo	10 ng	-	ApoB2	ND	ND

siApoB2- specific assay was tested against synthetic RNA standards, shApoB2-expression plasmids and shApoB1 hairpin oligonucleotides using different configuration of RT primer and Taqman probe. Average CT values lower than 40 cycles are presented. The amount of molecules per cell was calculated, assuming that 15 pg RNA was isolated per cell [34]. Data are presented from one representative experiment from two independent experiments conducted with two technical replicates. ND, not detected

Reference list

1. Pillai, RS (2005). MicroRNA function: multiple mechanisms for a tiny RNA? *RNA*; **11:** 1753-1761.
2. Stark, A, Brennecke, J, Bushati, N, Russell, RB and Cohen, SM (2005). Animal MicroRNAs confer robustness to gene expression and have a significant impact on 3'UTR evolution. *Cell*; **123:** 1133-1146.
3. Fire, A, Xu, S, Montgomery, MK, Kostas, SA, Driver, SE and Mello, CC (1998). Potent and specific genetic interference by double-stranded RNA in Caenorhabditis elegans. *Nature*; **391:** 806-811.
4. Elbashir, SM, Harborth, J, Lendeckel, W, Yalcin, A, Weber, K and Tuschl, T (2001). Duplexes of 21-nucleotide RNAs mediate RNA interference in cultured mammalian cells. *Nature*; **411:** 494-498.
5. Paddison, PJ, Caudy, AA, Bernstein, E, Hannon, GJ and Conklin, DS (2002). Short hairpin RNAs (shRNAs) induce sequence-specific silencing in mammalian cells. *Genes Dev*; **16:** 948-958.
6. Boudreau, RL, Martins, I and Davidson, BL (2009). Artificial microRNAs as siRNA shuttles: improved safety as compared to shRNAs in vitro and in vivo. *Mol Ther*; **17:** 169-175.
7. Henriksen, JR, Lřkke, C, Hammerř, M, Geerts, D, Versteeg, R, Flřgstad, T, et al. (2007). Comparison of RNAi efficiency mediated by tetracycline-responsive H1 and U6 promoter variants in mammalian cell lines. *Nucleic Acids Res*; 35: e67.
8. Li, L, Lin, X, Khvorova, A, Fesik, SW and Shen, Y (2007). Defining the optimal parameters for hairpin-based knockdown constructs. *RNA*; **13:** 1765-1774.
9. Borel, F, van Logtenstein R., Koornneef, A, Maczuga, P, Ritsema, T, Petry, H, et al. (2011). In vivo knock-down of multidrug resistance transporters ABCC1 and ABCC2 by AAV-delivered shRNAs and by artificial miRNAs. *J RNAi Gene Silencing*; **7:** 434-442.
10. Grimm, D, Streetz, KL, Jopling, CL, Storm, TA, Pandey, K, Davis, CR, et al. (2006). Fatality in mice due to oversaturation of cellular microRNA/short hairpin RNA pathways. *Nature*; **441:** 537-541.
11. Xia, H, Mao, Q, Paulson, HL and Davidson, BL (2002). siRNA-mediated gene silencing in vitro and in vivo. *Nat Biotech*; **20:** 1006-1010.
12. Song, J, Pang, S, Lu, Y, Yokoyama, KK, Zheng, JY and Chiu, R (2004). Gene silencing in androgen-responsive prostate cancer cells from the tissue-specific Prostate-specific antigen promoter. *Cancer Res*; **64:** 7661-7663.
13. Giering, JC, Grimm, D, Storm, TA and Kay, MA (2008). Expression of shRNA from a tissue-specific pol II promoter is an effective and safe RNAi therapeutic. *Mol Ther*; **16:** 1630-1636.
14. Boudreau, RL, Martins, I and Davidson, BL (2009). Artificial microRNAs as siRNA shuttles: improved safety as compared to shRNAs in vitro and in vivo. *Mol Ther*; **17:** 169-175.
15. McBride, JL, Boudreau, RL, Harper, SQ, Staber, PD, Monteys, AM, Martins, I, et al. (2008). Artificial miRNAs mitigate shRNA-mediated toxicity in the brain: Implications for the therapeutic development of RNAi. *Proc Natl Acad Sci U S A*; **105:** 5868-5873.
16. Koornneef, A, van Logtenstein, R, Timmermans, E, Pisas, L, Blits, B, Abad, X, et al. (2011). AAV-mediated in vivo knockdown of luciferase using combinatorial RNAi and U1i. *Gene Ther*; **18:** 929-935.
17. Guhaniyogi, J and Brewer, G (2001). Regulation of mRNA stability in mammalian cells. *Gene*; **265:** 11-23.
18. Park, JE, Heo, I, Tian, Y, Simanshu, DK, Chang, H, Jee, D, et al. (2011). Dicer recognizes the 5[prime] end of RNA for efficient and accurate processing. *Nature*; **475:** 201-205.
19. Song, J, Pang, S, Lu, Y and Chiu, R (2004). Poly(U) and polyadenylation termination signals are interchangeable for terminating the expression of shRNA from a pol II promoter. *Biochemical Biophys Res Commun*; **323:** 573-578.
20. Vermeulen, A, Behlen, L, Reynolds, A, Wolfson, A, Marshall, WS, Karpilow, J, et al. (2005). The contributions of dsRNA structure to Dicer specificity and efficiency. *RNA*; **11:** 674-682.
21. Koornneef, A, Maczuga, P, van, LR, Borel, F, Blits, B, Ritsema, T, et al. (2011). Apolipoprotein B knockdown by AAV-delivered shRNA lowers plasma cholesterol in mice. *Mol Ther*; **19:** 731-740.
22. Ge, Q, Ilves, H, Dallas, A, Kumar, P, Shorenstein, J, Kazakov, SA, et al. (2010). Minimal-length short hairpin RNAs: The relationship of structure and RNAi activity. *RNA*; **16:** 106-117.
23. Mcintyre, G, Yu, YH, Lomas, M and Fanning, G (2011). The effects of stem length and core placement on shRNA activity. *BMC Molecular Biology*; **12:** 34.
24. Konstantinova, P, de Vries, W, Haasnoot, J, ter Brake, O, de Haan, P and Berkhout, B (2006). Inhibition of human immunodeficiency virus

type 1 by RNA interference using long-hairpin RNA. *Gene Ther*; **13:** 1403-1413.

25. Konstantinova, P, ter Brake, O, Haasnoot, J, de Haan, P and Berkhout, B (2007). Trans-inhibition of HIV-1 by a long hairpin RNA expressed within the viral genome. *Retrovirology*; **4:** 15.
26. Weinberg, MS, Ely, A, Barichievy, S, Crowther, C, Mufamadi, S, Carmona, S, et al. (2007). Specific Inhibition of HBV Replication In Vitro and In Vivo With Expressed Long Hairpin RNA. *Mol Ther*; **15:** 534-541.
27. He, L and Hannon, GJ (2004). MicroRNAs: small RNAs with a big role in gene regulation. *Nat Rev Genet*; **5:** 522-531.
28. Boudreau, RL, Martins, I and Davidson, BL (2009). Artificial microRNAs as siRNA shuttles: improved safety as compared to shRNAs in vitro and in vivo. *Mol Ther*; **17:** 169-175.
29. Maczuga, P, Lubelski, J, van Logtenstein, R, Borel, F, Blits, B, Fakkert, E, et al. (2013). Embedding siRNA sequences targeting Apolipoprotein B100 in shRNA and miRNA scaffolds results in differential processing and in vivo efficacy. *Mol Ther*; **21:** 217-227.
30. Zhou, H, Huang, C and Xia, XG (2008). A tightly regulated Pol III promoter for synthesis of miRNA genes in tandem. *Biochim Biophys Acta*; **11:** 773-779
31. Li, C, Xiao, P, Gray, SJ, Weinberg, MS and Samulski, RJ (2011). Combination therapy utilizing shRNA knockdown and an optimized resistant transgene for rescue of diseases caused by misfolded proteins. *Proc Natl Acad Sci U S A*; **108:** 14258-14263.
32. Zuker, M (2003). Mfold web server for nucleic acid folding and hybridization prediction. *Nucleic Acids Res*; **31:** 3406-3415.
33. Livak, KJ and Schmittgen, TD (2001). Analysis of relative gene expression data using real-time quantitative PCR and the 2-[delta][delta] CT method. *Methods*; **25:** 402-408.
34. Chen, C, Ridzon, DA, Broomer, AJ, Zhou, Z, Lee, DH, Nguyen, JT, et al. (2005). Real-time quantification of microRNAs by stem-loop RT-PCR. *Nucl Acids Res*; **33:** e179.
35. Ruijter, J, Thygesen, H, Schoneveld, O, Das, A, Berkhout, B and Lamers, W (2006). Factor correction as a tool to eliminate between-session variation in replicate experiments: application to molecular biology and retrovirology. *Retrovirology*; **3:** 2.

CHAPTER 4

Embedding siRNA sequences targeting Apolipoprotein B100 in shRNA and miRNA scaffolds results in differential processing and *in vivo* efficacy

Piotr Maczuga[1,2], Jacek Lubelski[1], Richard van Logtenstein[1], Florie Borel[1,3], Bas Blits[1], Erwin Fakkert[4], Adalberto Costessi[4], Derek Butler[4], Sander van Deventer[2], Harald Petry[1], Annemart Koornneef[1] and Pavlina Konstantinova[1]

[1]Department of Research & Development, uniQure Biopharma b.v., Amsterdam, the Netherlands; [2]Department of Gastroenterology and Hepatology, Leiden University Medical Center, Leiden, the Netherlands; [3]Department of Gastroenterology and Hepatology, Academic Medical Center, Amsterdam, the Netherlands; [4] Department of Genome Analysis, BaseClear b.v., Leiden, The Netherlands

Molecular Therapy (2013); 21: 217–227

Abstract

Overexpression of short hairpin RNA (shRNA) often causes cytotoxicity and using microRNA (miRNA) scaffolds can circumvent this problem. In the current study identical predicted small interfering RNA (siRNA) sequences targeting Apolipoprotein B100 (siApoB) were embedded in shRNA (shApoB) or miRNA (miApoB) scaffolds and a direct comparison of the processing and long-term *in vivo* efficacy was performed. Next generation sequencing (NGS) of small RNAs originating from shApoB- or miApoB-transfected cells revealed substantial differences in processing, resulting in different siApoB length, 5' and 3' cleavage sites and abundance of the guide or passenger strands. Murine liver transduction with adeno-associated virus (AAV) vectors expressing shApoB or miApoB resulted in high levels of siApoB expression associated with strong decrease of plasma ApoB protein and cholesterol. Expression of miApoB from the liver-specific LP1 promoter was restricted to the liver, while the H1 promoter-expressed shApoB was ectopically present. Delivery of 1×10^{11} genome copies AAV-shApoB or AAV-miApoB led to a gradual loss of ApoB and plasma cholesterol inhibition, which was circumvented by delivering a 20-fold lower vector dose. In conclusion, incorporating identical siRNA sequences in shRNA or miRNA scaffolds results in differential processing patterns and *in vivo* efficacy that may have serious consequences for future RNAi-based therapeutics.

Introduction

RNA interference (RNAi) is an evolutionary conserved mechanism for post-transcriptional regulation of gene expression. It plays an important role in defense against viruses but also in development and in normal functioning of the cell [1,2]. Since its discovery RNAi has become a valuable research tool for functional analysis of gene expression and a promising therapeutic approach for treatment of many disorders by silencing disease-related genes [3]. Significant progress has been made towards improving the specificity of RNAi-mediated target inhibition and minimizing its potential side-effects, yet more insight is needed on the exact small interfering RNA (siRNA) processing pattern when identical predicted sequences are incorporated in a short-hairpin RNA (shRNA) or artificial microRNA (miRNA) scaffold for therapeutic applications.

Processing of miRNA by RNAse III family endonucleases plays a central role in their proper functioning in the cell [4]. In the nucleus, Drosha cleaves primary miRNA precursors (pri-miRNAs) to produce ~70 nucleotides (nt) miRNA precursors (pre-miRNAs) with 2 nt 3′ overhang [5]. Pre-miRNAs are transported by Exportin 5 to the cytoplasm where Dicer, another member of the RNAse III endonuclease family produces a mature miRNA duplex of ~21-28 nt basepairs (bp) [6]. Dicer also recognizes and processes shRNAs, which resemble the pre-miRNA structure. shRNAs with 19 bp or shorter stem may also be processed independently from Dicer cleavage, however the detailed mechanism has not been described [7-9]. The ~21-28 nt cleavage products enter a multiprotein RNA-induced silencing complex (RISC) where one of the strands is used for the sequence-specific recognition of target messenger RNA (mRNA) [10]. Drosha and Dicer cleavage is determined by certain RNA structures like a terminal loop region, a central stem bulge and single-stranded RNA (ssRNA) flanking sequences, which are recognized and serve as reference points for endonuclease digestions [5,6,11-13]. In the case of miRNA processing by Drosha, the stem-ssRNA junction is recognized by the Drosha cofactor DGCRG8 and cleavage occurs ~11 nt away from this structure [13]. Dicer anchors to both 5′ and 3′ ends of processed molecules and cleaves ~21-28 nt measured from one of the termini of the pre-miRNA or shRNA [11]. For Dicer cleavage mainly, the 5′ counting rules apply, meaning that the 5′ end acts as the primary reference point for the cleavage. The terminal loop is important as its disruption inhibits Drosha pri-miRNA processing as well as pre-miRNA and shRNA processing by Dicer [13]. Precise cleavage is critical for shRNA and miRNA functions because alterations in cleavage sites can change the abundance and thermodynamic stability of the shRNA and miRNA duplex, which is important for RISC loading [14].

shRNAs are generally expressed from polymerase III (pol III) promoters, which provide constitutive high expression levels necessary for potent knockdown of target mRNA. Although these features are valuable for research purposes, they can be disadvantageous for therapeutic applications. It has been reported that pol

III-expressed shRNA can lead to severe toxicity when high doses are used [15-17]. Grimm *et al.* observed liver failure and mortality in mice injected with different AAV-expressed shRNAs irrespective of hairpin length, sequence and target [17]. Toxic side-effects were associated with saturation of the cellular RNAi machinery and changes in endogenous miRNA expression. Toxicity may be circumvented by using lower doses of vectors encoding shRNA. However, this approach may result in loss of RNAi silencing efficacy and therapeutic effect [18]. Alternatively, toxicity resulting from shRNA overexpression can be resolved by embedding the siRNA sequence into an artificial miRNA scaffold and expressing it from weaker polymerase II (pol II) promoters [19,20]. Incorporation of a siRNA sequence in an artificial miRNA scaffold has been shown to abolish shRNA-induced neuronal cell death and to avoid disruption of the endogenous RNAi pathway [18,21]. However, in some cases miRNAs were found to be less potent compared to shRNAs [22].

Another disadvantage of pol III-expressed shRNAs is their constitutive expression in all cell types and organs. In order to limit their expression to target organs, the use of tissue-specific promoters has been applied for shRNAs [23,24]. However, this has been achieved with limited success as the rules for efficient transcription of shRNAs from poll II promoters are poorly understood and these constructs show only mild knockdown efficacy. Others have used inducible systems regulated by tetracycline or by ecdysone for expression of shRNAs or artificial miRNAs, which allows time- and dose-dependent expression when the inducer is administered and no expression in its absence [25-29]. Proof of concept has been established in transgenic mice enabling inducible and reversible suppression of gene expression by a tetracycline-regulated shRNA which also resulted in phenotypic changes [27]. However, the use of such systems in preclinical and clinical studies is limited because they include two additional components; elements encoding regulatory proteins that often induce an immune response and inducer molecules which need to be safe for long-term applications.

To date, no detailed analyses have been performed on the processing of identical predicted siRNA sequences embedded in shRNA or artificial miRNA scaffolds and the consequences for *in vivo* applications. Moreover, long-term efficacy *in vivo* and the use of miRNA expressed from a tissue-specific promoter have not been described. We addressed these issues by incorporating identical predicted siRNA targeting Apolipoprotein B (ApoB) in a shRNA (shApoB) or artificial miRNA scaffold (miApoB) and performed Next Generation Sequencing (NGS) analysis of the processed small RNAs. Additionally, aspecific off-target effects of shApoB and miApoB *in vivo* were investigated using NGS transcriptome analysis of the murine livers. ApoB is a constituent of all classes of lipoproteins that are considered atherogenic and elevated ApoB levels have been demonstrated to correlate with increased risk of cardiovascular disease (CVD) [30]. Therefore, ApoB is a highly validated target for treatment of increased low-

density lipoprotein cholesterol levels and subsequent CVD [31,32]. Injection of AAV-shApoB and AAV-miApoB yielded a long-term strong reduction of total cholesterol and ApoB expression. However, AAV-miApoB expressed from the liver-specific LP1 promoter induced stronger knockdown and its expression was restricted to the targeted hepatocytes in contrast to AAV-shApoB, which was ubiquitously expressed. Our results demonstrate that incorporation of identical predicted siRNA sequences in a shRNA or miRNA scaffolds yields differential processing and long-term efficacy *in vivo* that might have implications for future therapeutic applications.

Results

In vitro efficacy of shApoB and miApoB

Previously, we have reported that AAV delivery of shApoB expressed from the H1 pol III promoter is highly effective in knocking down ApoB and in reducing plasma cholesterol in mice [33]. However, the AAV-shApoB effect measured at 8 weeks p.i. decreased compared to week 2 p.i., which was associated with lower expression of anti-ApoB siRNA (siApoB) [33]. For clinical applications, stringent control of shRNA expression and restriction to the target organs is desirable. Therefore, the 21 nt-long siApoB guide sequence was embedded in an artificial miRNA scaffold using pri-mir-155 (miApoB, Fig. 1a) and expressed from the liver-specific LP1 promoter. The mature miApoB sequence was predicted to be identical as the one expressed from the shApoB scaffold (Fig. 1a).

Initially, the efficacy of miApoB was tested *in vitro* using the CMV promoter instead of the liver-specific LP1 promoter since the latter has low activity *in vitro* [34] The inhibitory effect of shApoB and miApoB was compared by co-transfecting human embryonic kidney 293T (HEK 293T) cells with a reporter expressing renilla luciferase that contained the ApoB target sequence in its 3'UTR (Luc-ApoB). Scrambled controls for both shRNA and miRNA (shScr and miScr) were included as negative controls and firefly luciferase expression was measured to correct for transfection efficiency. The renilla/firefly luciferase ratio in the negative controls was set at 100% and relative inhibition of the Luc-ApoB reporter was calculated. Both shApoB and miApoB showed similar efficacy and reduced luciferase expression by approximately 80% (Fig. 1b).

Since the identical predicted siApoB sequence was embedded in the shApoB or miApoB scaffold the number of processed molecules per cell was determined by small RNA Taqman assay (Fig. 1c). HEK 293T cells were transfected with either shApoB- or miApoB-expression constructs and two days post-transfection total RNA was isolated and siApoB copies were measured. Processing of siApoB from the miApoB scaffold was ~30-fold lower compared to shApoB (Fig. 1c). In order to assess the effect of the inhibitory constructs on endogenous ApoB expression, the mouse hepatoma Hepa1-6 cell line was transfected with shApoB or miApoB and ApoB mRNA knockdown was

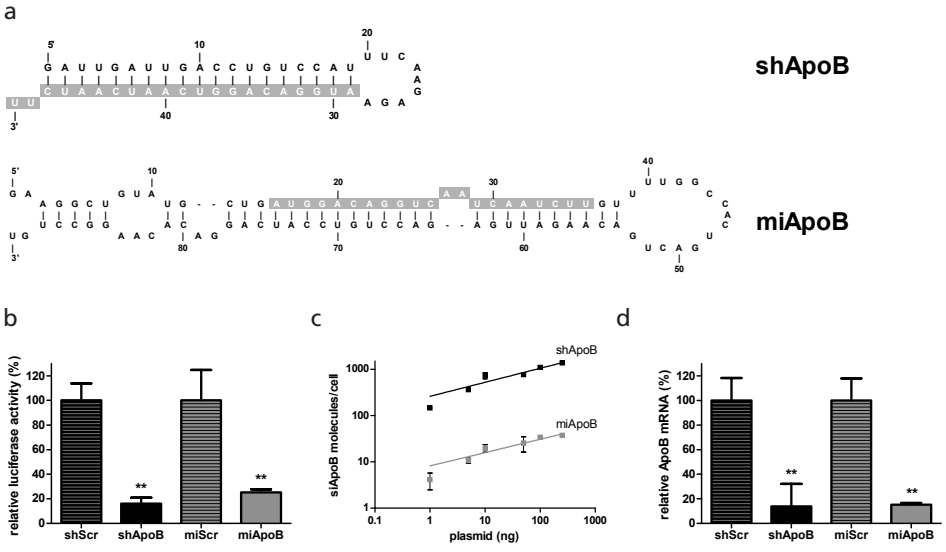

Figure 1. Structure and knockdown efficacy of shApoB and miApoB *in vitro*. (a) Predicted stem-loop structure for shApoB and miApoB with the guide strand shown in grey. (b) Knockdown of Luc-ApoB by shApoB and miApoB in HEK293T cells. Renilla and firefly luciferase were measured two days post-transfection with 50 ng Luc-ApoB reporter and 50 ng shApoB or miApoB, and renilla luciferase expression was normalized to firefly luciferase expression. shScr and miScr served as negative controls and were set at 100%. Data are represented as mean values ±SD from three independent experiments analyzed with factor correction [52] **p < 0.01 versus shScr or miScr. (c) siApoB expression from shApoB and miApoB in HEK293T cells. RNA was isolated two days post-transfection with 1, 5, 10, 50, 100 and 250 ng of shApoB or miApoB and siApoB-specific small RNA TaqMan was performed. siApoB copy number was calculated using a siApoB synthetic RNA oligo standard line. Data are represented as mean values from two independent experiments conducted with two technical replicates. (d) Endogenous ApoB mRNA knockdown by shApoB and miApoB in Hepa1-6 cells. qRT-PCR was performed two days post-transfection with 1 µg shApoB or miApoB and ApoB mRNA levels were calculated relative to actin mRNA. shScr and miScr served as negative controls and were set at 100%. Data are represented as mean values ±SD from a representative experiment conducted with three technical replicates. **p < 0.01 versus shScr or miScr.

measured two days post transfection (Fig. 1d). Both shApoB and miApoB efficiently inhibited ApoB mRNA up to 80% confirming the efficacy and specificity of the hairpin constructs. Our results indicate that shApoB and miApoB are equally effective in inhibiting Luc-ApoB and endogenous ApoB mRNA expression *in vitro*.

NGS analysis of siApoB processed from shApoB or miApoB scaffolds reveals guide and passenger strand heterogeneity

So far, the "golden standard" for siRNA detection has been the small RNA Taqman assay that relies on amplification of the predicted processed guide strand, which is normally 21 nt long. In the current research we investigated whether exactly identical siRNA sequences are processed by the cellular RNAi machinery from shRNA and

miRNA scaffolds. This is an important issue since it may have serious implications for future therapeutic development. NGS sequencing was performed on small RNAs isolated from HEK 293T cells transfected with shApoB or miApoB. A total of ~ 16 mln reads were obtained for each sample, which were further processed by applying the selection criteria described in Materials and Methods. For the NGS data analysis, all reads smaller than 15 nt or larger than 55 nt and all reads that were read less than 10 times were excluded from the analysis. Cellular miRNA expression pattern were compared between the miApoB and shApoB samples and are shown in Table S2. The small RNAs were aligned against their reference sequence resulting in 541.939 reads matching shApoB and 1.525.211 reads matching miApoB (Fig. S1 and S2). Analysis of the length distribution of the reads indicated that siApoB guide strand originating from shApoB ranged between 19 and 23 nt, with the most abundant one being 21 nt-long (Fig. 2a). Surprisingly, siApoB guide from miApoB scaffold ranged from 23 to 25 nt with the 24 nt-long strand being the predominant variant. This finding was rather unexpected considering that the predicted guide strand of siApoB was 21 nt long for both shApoB and miApoB scaffolds. Analysis of the processed 5' ends of the siApoB guide strand indicated that most of the reads matched position +1 relative to the predicted cleavage site for shApoB, while all the reads matched position 0 for miApoB (Fig. 2b). The 3' ends of the siApoB guide strand had a more heterogeneous pattern and ranged from -1 to +3 for shApoB and +1 to +4 for miApoB (Fig. 2c).

Next, we looked at the sequence distribution and percentage of reads for both the guide and passenger siApoB strands originating from the shApoB and miApoB scaffolds (Fig. 2d). A substantial difference between the two is that the guide from shApoB is in the 3' arm and hence Dicer [6] or other endonuclease [7-9] defines the cleavage position while the guide is present in the 5' arm of miApoB, where Drosha defines the cleavage [5]. Thus, defining the length and exact cleavage position for the guide and passenger strands is very important since even single nucleotide differences may result in significant changes in the predicted targets of the siRNAs. Moreover, the passenger siRNA* strand, if not degraded efficiently, may bind to unanticipated targets and cause off-target effects. As expected, 44.4% of the reads originating from shApoB matched the siApoB guide strand but processing was shifted at position +1 (Fig. 2d, upper panel). Surprisingly only 12.1% of the reads matched perfectly the predicted siApoB guide strand of 21 nt and starting at position 0. The reads matching the passenger siApoB* strand were represented in much lower percentage with the predominant one being only 5.3%.

Analysis of the guide strand from the siApoB reads originating from the miApoB scaffold indicated that they all started at the predicted cleavage site (Fig. 2d, lower panel). Surprisingly, the predominant, 22.3% of reads were 24 nt-long. Furthermore 5.1% reads were 23 nt- and 1.9% were 25 nt-long. A substantial number of 62% of the reads was found matching the passenger siApoB* strand and ranged between

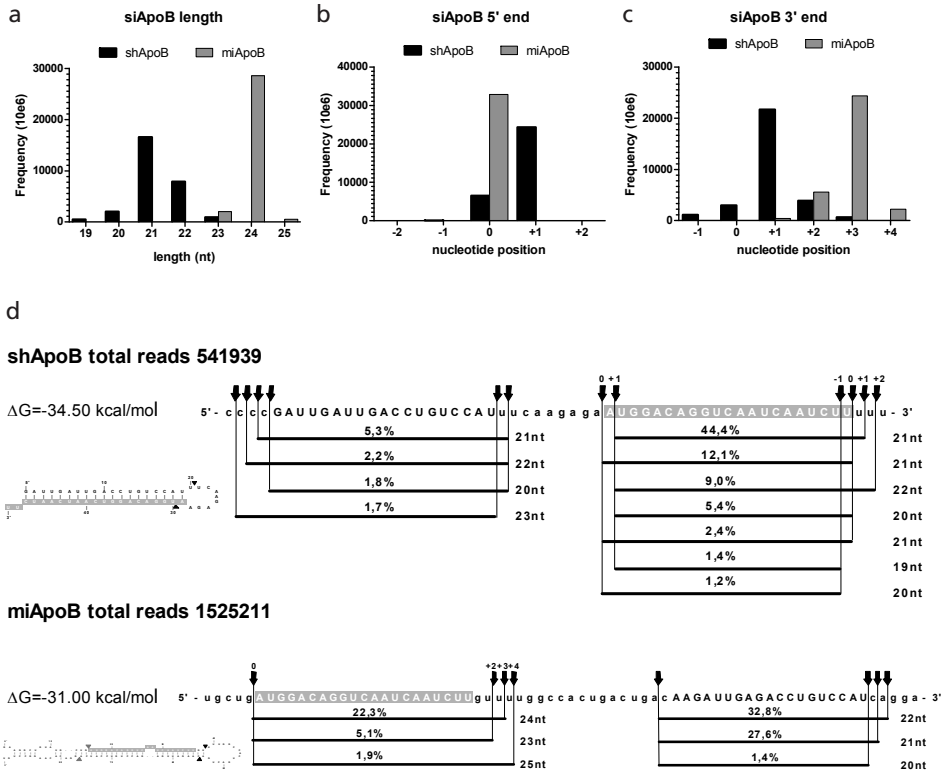

Figure 2. Small RNA NGS analysis reveals differential siApoB guide and siApoB* passenger strand processing from shApoB and miApoB scaffolds. (a) Sequence length distribution of the siApoB guide strand recovered from small RNA NGS of HEK293T cells transfected with shApoB- or miApoB-expression plasmids. The frequency on the *y* axis represents the reads per million. (b) Sequence variation in the 5′ end of the mature siApoB guide strand. Nucleotide position 0 was designated as the 5′ end of the predicted siApoB guide and other forms are numbered accordingly. (c) Sequence variation in the 3′ end of the mature siApoB guide strand. Nucleotide position 0 was designated as the 3′ end of the predicted siApoB guide and other forms are numbered accordingly. (d) Sequence distribution and percentage of reads from siApoB guide and siApoB* passenger strands aligned to the reference shApoB (upper panel) or miApoB (lower panel) sequence. ApoB sequences are presented in upper case, the loop and flanking sequences are in lower case, the predicted 21 nt siApoB guide strand is shaded in grey. The percentage of reads was calculated based on the total number of reads matching the reference shApoB or miApoB sequence. Sequences represented with less than 1% were excluded from the figure and can be found in Figures S1 and S2.

20 and 22 nt in length. In conclusion, both shApoB and miApoB scaffolds did not yield the predicted siApoB guide or siApoB* passenger sequences after processing from the cellular RNAi machinery. The guide from miApoB was cleaved much more precisely by Drosha at its 5′ end compared to shApoB that gave more heterogeneous pools of sequences following processing. Cellular miRNA expression profiles were also not identical for cells transfected with shApoB or miApoB (Table S2).

Long-term knockdown efficacy of AAV-delivered shApoB and miApoB in murine liver

Having shown that CMV-expressed miApoB, although differentially processed, is as effective in inhibiting ApoB as shApoB *in vitro*, we replaced the constitutive CMV promoter with the liver-specific LP1 promoter for *in vivo* applications. The use of LP1 limits miApoB expression to hepatocytes, thereby avoiding siApoB accumulation in non-target tissues. Male C57Bl/6 mice were injected with 1×10^{11} gc self-complementary AAV8 (scAAV8) per animal encoding shApoB, miApoB, shScr or miScr. All viruses co-expressed enhanced green fluorescent protein (eGFP) for monitoring of liver transduction efficacy. At week 27 p.i. mice were sacrificed and siApoB small RNA Taqman was performed on RNA isolated from the liver, spleen, ileum, lung, heart, and kidney. Four times less siApoB molecules were detected from the AAV-miApoB-injected animals in the liver compared to AAV-shApoB-injected animals (1163 vs. 399 copies per cell respectively) (Fig. 3a). In addition, in AAV-miApoB-injected animals siApoB expression was restricted to the liver in contrast to AAV-shApoB-injected mice where expression was detected in non-target organs (Fig. 3a).

At week 27 p.i. ApoB mRNA was reduced by 55% in AAV-miApoB-injected animals while no mRNA decrease was detected in the AAV-shApoB group (Fig. 3b). The inhibitory effect of AAV-shApoB and AAV-miApoB on ApoB protein was determined every two weeks up to week 27 p.i. by Western blot (Fig. 3c and data not shown). Initially, a strong inhibition of ApoB protein was achieved by both AAV-shApoB and AAV-miApoB. However, the effect decreased at week 10 p.i. for AAV-shApoB and at week 20 p.i. for AAV-miApoB. At week 27 p.i. ApoB concentrations in plasma were decreased by 25% in animals injected with AAV-shApoB and by 60% in mice treated with AAV-miApoB (Fig. 3c). Next, the phenotypic effect of ApoB knockdown was measured every two weeks by biochemical lipid profiling of cholesterol in murine plasma (Fig. 3d). Similar to the ApoB protein knockdown, initially a strong ~ 70% cholesterol decrease was induced by both AAV-shApoB and AAV-miApoB. However, the effect decreased gradually and at week 27 p.i. total cholesterol levels were reduced in both groups by only 25% compared to scrambled controls (Fig. 3d). Two-way ANOVA analysis revealed that AAV-miApoB performed significantly better than AAV-shApoB in reducing plasma cholesterol over the course of the experiment ($p= 0.0018$). In addition, there was a clear trend of a slower loss of plasma ApoB and cholesterol inhibition in mice injected with AAV-miApoB compared to AAV-shApoB indicating that miApoB had a better long-term efficacy than shApoB (Fig. 3c,d).

Based on our previous observations that shApoB and miApoB are differentially processed and that miApoB has a different passenger, we checked for possible aspecific off-target effects *in vivo*. NGS liver transcriptome analysis was performed 8 weeks p.i. for animals injected with $1x10^{11}$ gc AAV encoding shScr, shApoB, miScr and miApoB. We investigated whether shApoB and miApoB processing differences translate into

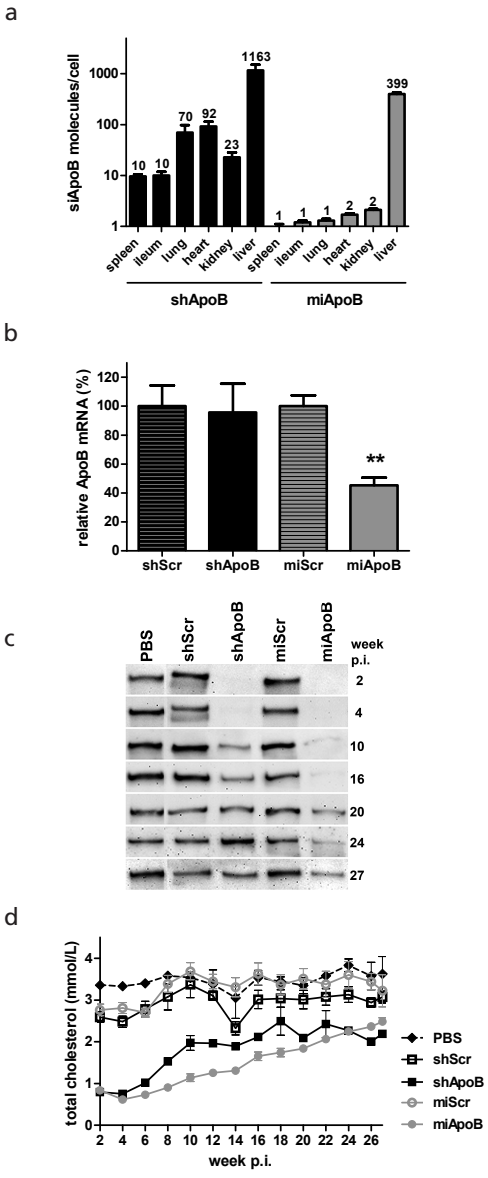

Figure 3. Long-term reduction of ApoB and plasma cholesterol levels by 1×10^{11} gc AAV-shApoB and AAV-miApoB. Mice were intravenously injected with 1×10^{11} gc AAV-shApoB or AAV-miApoB, or their respective controls AAV-shScr, AAV-miScr or PBS. Plasma was collected every two weeks p.i. and animals were sacrificed at 27 weeks p.i. (a) siApoB expression in murine spleen, ileum, lung, heart, kidney, and liver 27 weeks p.i. Total RNA was isolated from snap-frozen tissue and siApoB-specific small RNA TaqMan was performed. siApoB copy number was calculated using a siApoB synthetic RNA oligo standard line. Data are represented as mean values ±SE, treatment groups are n=4-5 for AAV-shApoB, AAV-shScr, AAV-miApoB or AAV-miScr and n=2 for PBS-injected animals. (b) Relative ApoB mRNA expression in murine liver 27 weeks p.i. Total RNA was isolated from snap-frozen liver tissue and qRT-PCR was performed using ApoB- and actin-specific primers. ApoB mRNA levels were calculated relative to actin mRNA and scrambled controls were set at 100 %. **p < 0.01 versus shScr or miScr (c) Western blot analysis of plasma ApoB at 2, 4, 10, 16, 20, 24, and 27 weeks p.i. ApoB protein was detected in 0.1 µl plasma using a polyclonal antibody against ApoB. (d) Total cholesterol levels in plasma collected from fasted mice over the course of 27 weeks p.i. Cholesterol levels were analyzed on the automated clinical chemistry analyzer Modular Analytics P800.

differences in gene expression in injected animals. A total number of 266 genes were significantly changing (p <0,05) in miApoB-injected mice compared to miScr (Table S3). Additionally 106 genes were found to be significantly up or down-regulated (p<0,05) in the shApoB mice compared to shScr (Table S4). Off-target predictions using Smith-Waterman algorithm [35] for the most abundant guide and passenger strand variants were performed to investigate if any of the observed changes results from aspecific

interactions. None of the changing genes had predicted targets for the guide or passenger strands of shApoB or miApoB (Table S3 and S4).

Decrease of ApoB knockdown is due to gradual AAV vector DNA loss

To follow up on the loss of ApoB and cholesterol inhibitory effect *in vivo*, AAV vector DNA copies were determined in murine liver at 2, 8, and 27 weeks p.i. from mice injected with AAV-shApoB and AAV-shScr. In both animal groups a clear gradual decrease in AAV vector DNA was observed over time indicating that the effect was not dependent on the shRNA target sequence (Fig. 4a). At week 8 and 27 p.i. the amount of AAV vector DNA copies in murine livers from AAV-miApoB and AAV-miScr were similar to AAV-shApoB and AAV-shScr indicating similar kinetics of vector loss irrespective of the promoter type (pol III or pol II), target sequence (Scr or ApoB), or of the shApoB or miApoB scaffolds (Fig. 4b).

The loss of AAV vector DNA occurs presumably as a result of cell death due to liver toxicity. In line with this assumption, transient activation of liver transaminases aspartate aminotransferase (AST) and alanine aminotransferase (ALT) were measured in all AAV-injected animals during the course of the experiment (Fig. S3). To explore the mechanism behind the DNA loss in more detail liver morphology was examined by hematoxylin and eosin staining. In addition, immunohistochemistry was performed to detect markers for apoptosis, T-regulatory cells, cytotoxic T lymphocytes, macrophages, and B lymphocytes. With none of those markers obvious differences between the treatment and PBS groups were found (data not shown). ELISA assay for antibodies against eGFP was performed to explore the possibility that these could have contributed to the loss of AAV vector DNA. No immune response against eGFP was found in any of the animals (data not shown). Together, these results indicate that there was no acute inflammatory effect responsible for the loss of AAV vector DNA.

A possible reason for the observed AAV vector DNA loss is oversaturation of the endogenous RNAi machinery resulting in changes of cellular miRNA processing. Previously, we have shown that cellular mir-122, mir-29a and let-7a expression does not change in murine livers at 2 and 8 weeks p.i. with 1×10^{11} gc AAV-shApoB or AAV-shScr [33]. To exclude the possibility that the loss of AAV vector DNA is due to oversaturation of the endogenous miRNA pathway, we determined the amount of the most abundant liver miRNA mir-122 at week 27 p.i. for animals injected with AAV-shApoB, AAV-miApoB and the two control viruses. There were no significant changes in mir-122 expression between all animal groups indicating that there was no oversaturation of the RNAi machinery caused by the injected AAVs (Fig. S4).

Lower AAV dose results in sustained ApoB and plasma cholesterol decrease

A possible reason for the observed AAV vector DNA loss and decrease in ApoB knockdown effect is the use of a too high viral dose. Previously we have shown

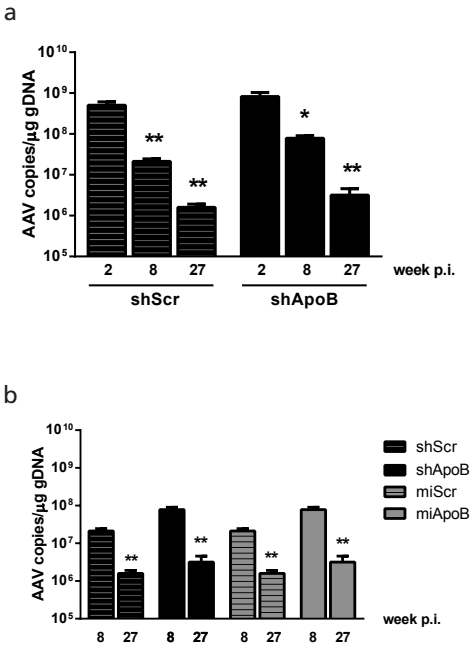

4

Figure 4. Gradual loss of AAV vector DNA *in vivo* over a time course of 27 weeks p.i. Mice were intravenously injected with 1×10^{11} gc AAV-shApoB or AAV-miApoB, or their respective controls AAV-shScr and AAV-miScr and livers were collected at 2, 8 or 27 weeks p.i. Genomic DNA (gDNA) was isolated from snap-frozen liver tissue and qPCR was performed using LP1-specific primers. AAV copy number was calculated using a LP1 plasmid standard line. (a) AAV copy number per microgram gDNA in murine liver of animals injected with AAV-shScr or AAV-shApoB at 2, 8, and 27 weeks p.i. *$p < 0.05$, **$p < 0.01$ versus shScr wk2 or shApoB wk2. (b) AAV copy number per microgram gDNA in murine liver 8 and 27 weeks p.i. with AAV-shScr, AAV-shApoB, AAV-miScr or AAV-miApoB. Data are represented as mean values ±SE, treatment groups are n=4-5.

that when 1×10^9 gc AAV-shApoB or AAV-shScr was injected in mice, ~90% liver transduction can be achieved that was not associated with viral loss at 8 weeks p.i [33]. In the current study a 12 week mouse experiment was initiated with a dose of 5×10^9 gc AAV-shApoB, AAV-miApoB, AAV-shScr, AAV-miScr and an additional control group AAV-eGFP expressing only eGFP (Fig. 5). The experiment was restricted to 12 weeks based on our previous observations [33] and the results presented in Figure 3 showing that a 12-week time period is sufficient to observe a significant loss of AAV vector DNA and knockdown efficacy.

Inhibition of ApoB mRNA was observed in the groups injected with AAV-shApoB or AAV-miApoB at 12 weeks p.i, 57% for AAV-miApoB and 43% for AAV-shApoB, respectively (Fig. 5a). Subsequently a decrease in ApoB protein levels was observed at week 4 and the effect remained stable during the 12-week course of the experiment (Fig. 5b). Plasma cholesterol levels were determined every two weeks to study

the kinetics and longevity of ApoB knockdown (Fig. 5c). Two weeks p.i., plasma cholesterol levels were decreased by 53% and 39% for AAV-miApoB- and AAV-shApoB-injected animals and the effect remained stable until week 12 p.i. Finally, equal amounts of AAV vector DNA copies were measured in mice livers for all animal groups (Fig. 5d). The animals injected with AAV-eGFP control had similar ApoB, and cholesterol levels as well as AAV vector DNA copies as the AAV-shScr or AAV-miScr controls indicating that there were no hairpin-related non-specific toxic effects in the current study. Importantly, over the 12-week time course, liver transaminases were not significantly elevated for all treatment groups (Fig. S5). Again, there was a trend for a stronger ApoB and cholesterol decrease in AAV-miApoB injected animals compared to AAV-shApoB (Fig. 5 b,c).

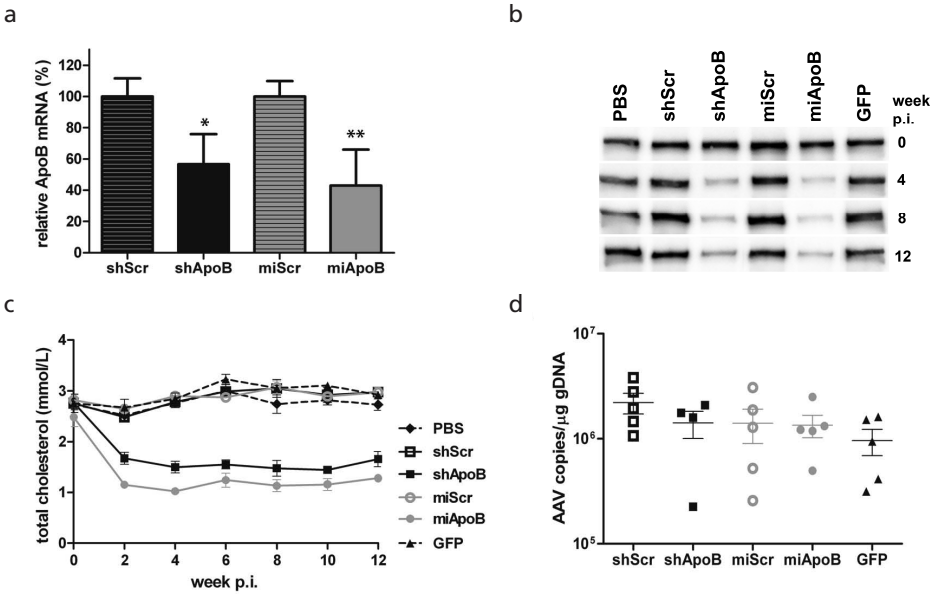

Figure 5. Sustained decrease of ApoB and plasma cholesterol levels by 5×10^9 gc AAV-shApoB and AAV-miApoB. Mice were intravenously injected with 5×10^9 gc AAV-shApoB, AAV-miApoB, AAV-shScr, AAV-miScr, AAV-GFP, or PBS. Plasma was collected every two weeks p.i. and animals were sacrificed at 12 weeks p.i. (a) Relative ApoB mRNA expression in murine liver 12 weeks p.i. Total RNA was isolated from snap-frozen liver tissue and qRT-PCR was performed using ApoB- and actin-specific primers. ApoB mRNA levels were calculated relative to actin mRNA and scrambled controls were set at 100%.*$p < 0.05$, **$p < 0.01$ versus shScr or miScr (b) Western blot analysis of plasma ApoB at 0, 4, 8, and 12 weeks p.i. ApoB protein was detected in 0.1 µl plasma using a polyclonal antibody against ApoB. (c) Total cholesterol levels in plasma collected from fasted mice over the course of 12 weeks p.i. Cholesterol levels were analyzed on the automated clinical chemistry analyzer Modular Analytics P800. (d) AAV copy number per microgram gDNA in murine liver 12 weeks p.i. gDNA was isolated from snap-frozen liver tissue and qPCR was performed using GFP-specific primers. AAV copy number was calculated using a GFP plasmid standard line. Data are represented as mean values ±SE, treatment groups are n=4-5.

Discussion

RNAi technology is one of the fastest developing scientific fields and holds a great promise for development of therapeutics of various diseases in the liver, brain, and the eye [36]. AAV vectors mediating expression of shRNAs or artificial miRNAs have proven to be valuable vehicles for RNAi research and therapy. However, induction of severe toxicity and/or off-target effects remains a major hurdle to be overcome before a long-term inhibition of a disease-related gene in the target tissue or organ can be accomplished. So far, detailed studies analyzing the precise processing of siRNA molecules expressed from shRNA or miRNA scaffolds and the consequences for *in vivo* applications have not been carried out. To address this issue, we have performed detailed NGS analysis of the siRNA processing when identical predicted sequences targeting ApoB have been embedded in shRNA or miRNA scaffolds. By using AAV delivery, we compared the efficacy and toxicity profiles of a constitutively expressed shRNA to tissue-specific expressed artificial miRNA in long-term *in vivo* studies.

An unexpected discovery in the current study was that siRNA processing by the cellular RNAi machinery did not follow the generally accepted and described cleavage sites for both molecules shApoB and miApoB siApoB guide strand originating from the shApoB scaffold was more heterogeneous in cleavage sites and length compared to the product originating from the miApoB scaffold. Most likely, differential cleavage mechanism defined the heterogeneity in the guide and passenger strands. Additionally, shRNAs with 19 bp stem or less are not necessarily recognized by Dicer and maybe be processed differently [7-9]. The heterogeneity seen with the shApoB can also be explained by the potential for 2 or 3 uridines to be added following termination of pol III transcription [37]. The main pool of guide sequences originating from miApoB was 24 nt-long although we used the scaffold of cellular pri-mir-155 that produces a 23 nt mature miRNA. However, a 24 nt-long siApoB sequence did not compromise efficacy because when placed in the miApoB scaffold, the ApoB target sequence was extended at the 3' end with 4 nt until the loop (Fig. 1a).

Another important observation is that the siApoB* passenger strand was present in a very high percentage of the reads from miApoB. Our results are in accordance with Gu *et al*. [14] who recently reported that mainly the guide siRNA strand of an shRNA was pulled down with Ago2 while both guide and passenger strands were detected from a miRNA scaffold associated with Ago1/2/3/4 [14]. Moreover, the passenger strand from the miRNA scaffold was not cleaved and eliminated as efficiently as from the shRNA. However, reporter assays revealed that the passenger siRNA* strand was mainly loaded into non-activated Ago complexes rendering those sequences ineffective at inducing knockdown. Our findings, together with the previously reported ones indicate that differential Ago loading of siRNAs originating from different scaffolds may have serious implications for future design of RNAi-based therapeutics.

There are important consequences of our findings for the small RNA Taqman that is being used for routine detection of siRNA expression. In our opinion this assay cannot be directly applied for sequences originating from shRNA or miRNA scaffolds because it amplifies only the predicted 21 nt guide strand and conclusions based on such data should be drawn with caution. Considering the different siApoB processing pattern from shApoB or miApoB scaffolds, the small RNA Taqman that was performed *in vivo* has only an indicative value rather than a precise estimation of the number of molecules per cell.

The use of the liver-specific LP1 promoter for miApoB limited the expression of siApoB to hepatocytes, thus providing an additional safety level for future clinical applications compared to the ubiquitously expressed shApoB. So far it has been suggested that the use of tissue-specific promoters for miRNA expression will not be feasible *in vivo* as the expression would be too low to achieve significant therapeutic effect [36]. In the current study we provide evidence for the efficacy of such an approach *in vivo* and demonstrate its advantages over the pol III-expressed shRNA. Although it has been reported that expression of shRNA can be achieved from liver-specific hAAT promoter and tetracycline-inducible promoter [23,27], the rules for design of potent shRNA expressed from pol II promoters are still far from clear. An additional advantage is that several miRNAs can be expressed as clusters from longer transcripts, allowing simultaneous targeting of multiple genes [20,38,39]. This feature of the miRNA is very important when mutation-prone viruses, such as HIV-1 or HCV, are targeted or when several disease-related genes need to be simultaneously silenced. Moreover, miRNAs can be linked to the 3' untranslated region of a therapeutic gene, which is an additional advantage for therapeutic applications since it allows co-delivery of a codon-optimized gene together with a miRNA targeting the disease-causing version of the same gene. Such combinational therapy has been shown for alpha1-antitrypsin (A1AT) deficiency, in which a hairpin RNA targeting mutated A1AT transcript was delivered together with codon-optimized A1AT gene [40,41].

In the current study, we have demonstrated a more sustained ApoB target knockdown by miApoB over the shApoB in long-term *in vivo* experiments. Although differential processing resulting in different siApoB families from the two scaffolds should be kept in mind, this study provides indication that limiting siRNA expression to the target cells or organ holds greater promises for future therapeutic applications. Oversaturation of the RNAi machinery and competition with cellular miRNA transport from nucleus to cytoplasm have been described for both siRNA and shRNA and this toxicity problem was circumvented when the siRNA sequence was expressed from a miRNA scaffold by the CMV pol II promoter [20,42]. Grimm *et al.* reported that delivery of a high dose of 1×10^{12} gc per animal scAAV8 expressing shRNA led to hepatocyte death, often severe enough to cause liver failure and morbidity [17]. This

was associated with accumulation of shRNA precursor, which saturated Exportin 5 and led to deregulation of the endogenous RNAi pathway. Toxic effects were reduced without compromising knockdown efficacy of the shRNA when a 10-fold lower viral dose or liver-specific expression of the shRNA were used [23]. Several other studies revealed neurotoxicity following AAV delivery of a shRNA targeting Huntingtin mRNA [18,21,22]. Subsequently, when siRNA sequences were incorporated in an artificial miRNA scaffold and expressed from the U6 pol III promoter neurotoxicity was abolished [21]. To our knowledge, no long-term head-to-head comparison has been performed to evaluate the processing and efficacy of siRNA sequences incorporated as identical predicted guide strand in a pol III-shRNA or liver-specific LP1 pol II-miRNA scaffolds. In contrast to the above-mentioned studies, our current data demonstrate that LP1-expressed miApoB did not circumvent liver toxicity and vector DNA loss when high doses of AAV were injected into mice. In our case AAV-shApoB and AAV-miApoB delivery initially showed strong inhibition of ApoB protein and plasma cholesterol levels *in vivo* and the effects diminished due to gradual AAV vector DNA loss. Interestingly, the NGS small RNA analysis indicated that the number of processed siApoB molecules from the shApoB or miApoB scaffolds was almost identical indicating that we might have reached a threshold above which no more siRNA molecules are being processed. Indeed, it has been calculated that in a typical mammalian cell the number of active RISC complexes ranges from 10^3 to 10^4 and the number of ectopic RNAi triggers should be kept in this range [43]. An important observation was that none of the changes in gene expression in AAV-miApoB and AAV-shApoB can be explained by possible aspecific down-regulation of non-target transcripts. Because of the complexity of sh/miRNA processing and RISC loading, off-targeting interactions are difficult to predict and evaluate. Although we could not explain the changes in gene expression by off-target prediction with Smith-Waterman algorithm, we cannot exclude that other prediction methods like screening 3' UTRs of genes for perfect complementarity to siRNA seed region may be more accurate [44]. miRNAs may regulate their targets by translational repression, therefore we might speculate that the off-target effects may be stronger at protein level.

By lowering the viral dose 20-fold a stable reduction of ApoB protein and plasma cholesterol was achieved by both AAV-shApoB and AAV-miApoB. Ongoing research including detailed liver histology to determine liver damage and small RNA NGS from murine livers will further investigate the exact cause of loss of RNAi inhibitory effect. For example, it is still unclear why after 27 weeks substantial amounts of siApoB can be detected from the AAV-shApoB-injected animals without observing ApoB knockdown effect. GFP fluorescence microscopy analysis demonstrated that only a few positive cells were still present at 27 weeks p.i. Most likely, only those few cells still expressed siApoB, which was not enough to achieve overall ApoB inhibition effect since the majority of

hepatocytes lost the siApoB due to liver regeneration. AAV itself is not likely to cause liver toxicity as it was shown not to be pathogenic or immunogenic in rodents [45] and in our studies we could not detect toxicity resulting from GFP expression, therefore excluding those two possibilities as reasons for AAV viral DNA loss.

In summary, our results demonstrate that incorporating identical predicted sequences in shRNA or miRNA scaffolds results in differential siRNA processing patterns that may have serious consequences for future RNAi-based therapeutic applications. However, we consider that tissue-specific expression and embedding siRNA in artificial miRNA scaffold can contribute to a better and safer gene therapy approach due to the intrinsic characteristics of the miRNA structure rendering it a better substrate for the RNAi machinery.

Materials and methods

DNA constructs

Cloning of shApoB constructs (shA10) and shScr in the pSuper and AAV backbone has been described previously [33]. To create the miApoB vector, the siRNA sequence from shApoB was cloned into the mir-155 backbone of pcDNA6.2-GW/EmGFP-miR (Invitrogen, Carlsbad, CA) by annealing complementary oligonucleotides and ligation into BamHI- and XhoI-digested pcDNA6.2 plasmid. As a negative control for miApoB pcDNA6.2-GW/EmGFP-miR-neg control (Invitrogen, Carlsbad, CA) was used, named miScr. The luciferase reporter Luc-ApoB containing in the 3'UTR 1851 nucleotides of the last exon from human ApoB has been described previously [33]. The sequences of the oligonucleotides used in this study are listed in Table S1.

Cell culture and transfections

The HEK293T and Hepa1-6 cell lines were maintained in Dulbecco's modified Eagle's medium (DMEM; Invitrogen, Carlsbad, CA) containing 10% fetal calf serum, 100 U/ml penicillin and 100 U/ml streptomycin, at 37°C and 5% CO_2. For luciferase assays, endogenous ApoB knockdown assays, siRNA expression analysis, and small RNA NGS cells were seeded in 96-, 24- or 6-well plates at a density of 3×10^4, 1.2×10^5 or 4.5×10^5 cells per well, respectively, in DMEM one day prior transfection. Transfections were performed with Lipofectamine 2000 reagent (Invitrogen, Carlsbad, CA) according to the manufacturer's instructions.

Luciferase assays

Cells were co-transfected with 50 ng Luc-ApoB that contains both firefly and renilla luciferase genes, and 50 ng shApoB or miApoB expression constructs. Transfected cells were assayed at 48 hr post-transfection in 20 µl 1x passive lysis buffer (Promega, Madison, WI) by gentle rocking for 15 min at room temperature. The cell lysates

were centrifuged for 5 min at 4000 rpm and 10 µl of the supernatant was used to measure firefly and renilla luciferase activities with the Dual-Luciferase Reporter Assay System (Promega, Madison, WI). Relative luciferase activity was calculated as the ratio between renilla and firefly luciferase activities.

RNA isolation and quantitative real-time RT-PCR

To determine endogenous ApoB mRNA knockdown by shApoB and miApoB constructs *in vitro*, Hepa1-6 cells were transfected with 1 µg shApoB- or miApoB-expression plasmids using Lipofectamine 2000 reagent and total RNA was isolated from cells 48 hr post-transfection using the Nucleospin kit (Clontech, Mountain View, CA). For NGS analysis and Small RNA Taqman HEK293T cells were transfected with 4 µg shApoB- or miApoB-expression plasmids using Lipofectamine 2000 reagent and total RNA was isolated from cells 48 hr post-transfection using Trizol (Invitrogen, Carlsbad, CA) according to the manufacturer's protocol. To determine ApoB mRNA knockdown *in vivo*, total RNA was isolated from frozen liver sections at 27 and 12 weeks p.i. using Trizol (Invitrogen, Carlsbad, CA). Genomic DNA (gDNA) was removed by DNase treatment using TURBO DNase (Ambion, Austin, TX). First strand cDNA was reverse transcribed using random hexamer primers with the Dynamo kit (Finnzymes, Espoo, Finland). Real time PCR amplification was performed with ApoB- and beta actin-specific primers (Table S1). PCR reaction conditions were: 95°C for 10 min, followed by 40 cycles of 15 sec at 95°C and 1 min at 60°C. The assays were performed on ABI 7000 or ABI 7500 (Applied Biosystems, Foster City, CA). ApoB expression levels were normalized to beta actin as an internal control, and the relative gene expression $2^{-\Delta\Delta Ct}$ method of Livak and Schmittgen was used for analysis of PCR data [46].

siRNA and miRNA detection by small RNA Taqman assay

RT reactions for siApoB and murine mir-122 expression were performed with the TaqMan MicroRNA Reverse Transcription Kit (Applied Biosystems, Foster City, CA) using 10 ng RNA and 3 µl custom-made specific RT-stem-loop primer (Applied Biosystems, Foster City, CA) according to the manufacturer's instructions. Amplification of the beta actin gene was used as a RNA quality and loading control.siRNA copy number per cell was calculated based on the amplification plot of a dilution series of synthetic siApoB RNA standard (IDT, Coralville, IA). The trend line value of the standard line was used to calculate the siApoB copy number cell, assuming 15 pg RNA per cell [47].

Next Generation Sequencing (NGS) of small RNA

Small RNA sequencing libraries were generated using high-quality total RNA as input and the NEXTflex Small RNA Sequencing kit (Bioo Scientific, USA). Briefly, the small RNA species were subjected to ligation with 3' and 5' RNA adapters, first strand reverse transcription, and PCR amplification. Sample-specific barcodes

were introduced in the PCR step. The PCR products were separated on TBE-PAGE electrophoresis and the expected band around 140-160bp was recovered for each sample. The resulting sequencing libraries were quantified on a BioAnalyzer (Agilent). The libraries were multiplexed, clustered, and sequenced on an Illumina HiSeq 2000 (TruSeq v3 chemistry) with a single-read 36 cycles sequencing protocol and indexing. The sequencing run was analyzed with the Illumina CASAVA pipeline (v1.8.0), with demultiplexing based on sample-specific barcodes. The raw sequencing data produced was processed removing the sequence reads which were of too low quality (only "passing filter" reads were selected), and discarding reads that aligned against the PhiX control. In total, we generated 16016701 reads for sample miApoB, and 15843150 reads for sample shApoB.

The NGS small RNA raw data set was analyzed using the CLC_bio genomic workbench (CLC Bio, Aarhus, Denmark). The obtained reads were adaptor-trimmed, which decreased the average read size from ~36bp to ~25bp. The custom adapter sequenced used for trimming all the bases extending 5' was: GTGACTGGAGTTCCTTGGCACCCGAGAATTCCA. All reads containing ambiguity N symbols, reads shorter than 15 nt, longer than 55 nt in length and reads represented less than 10 times were discarded. Next, both data sets from shApoB and miApoB samples were grouped based on the match to the reference sequence and the obtained unique small RNAs were aligned to the sequence of pre-miApoB: GATCCTGGAGGCTTGCTGAAGGCTGTATGCTGATGGACAGGTCAATCAATCT TGTTTTGGCCACTGACTGACAAGATTGAGACCTGTCCATCAGGACACAAGGCC TGTTACTAGCACTCACATGGAACAAATGGCCCAGATCTGGCCGCAG or shApoB: GA TCCCCGATTGATTGACCTGTCCATTTCAAGAGAATGGACAGGTCAATCAATCT TTTTCAGCTT sequence, respectively. To relatively represent the expression counts for the small RNAs obtained in the experiment, reads per million (rpm) [48] or percentage of reads based on the total number of reads matching the reference shApoB or miApoB sequence were calculated Finally, to identify the differences in cellular miRNA reads between the miApoB and shApoB samples the small RNA data sets were annotated to miRBase, Release 18 and grouped based on the mature miRNA sequences, the rpm were calculated and the fold change between miApoB and shApoB samples was calculated.

Total RNA sequencing libraries for the Illumina sequencing platform were generated using high-quality total RNA as input and the Illumina TrueSeq RNA v2 Sample preparation kit according to the manufacturer's protocol. Each read file (sample), in the FASTQ format, was individually aligned against the mouse reference genome (15 May 2012 NCBI build 38.1) using CLC Bio-Genomic Workbench and the expression abundance for each gene (RPKM) was calculated according to Montazavi *et al*. [49]. Smith-Waterman algorithm [35] was used to predict off-target genes in the mouse reference genome and mouse RNA Refseq for the most abundant expressed passenger and guide strands variants of shApoB and miApoB.

The NGS data discussed in this publication have been deposited in NCBI's Gene Expression Omnibus [50] and are accessible through GEO Series accession number GSE39187 (http://www.ncbi.nlm.nih.gov/geo/query/acc.cgi?acc=GSE39187).

Western blot analysis for detection of ApoB protein

Murine plasma proteins (0.1 µl) were separated by electrophoresis on a 3-8% Tris-Actetate gel (Invitrogen, Carlsbad, CA) and blotted onto a 0.45 µm nitrocellulose membrane (Invitrogen, Carlsbad, CA). The blot was incubated with a 1:2000 dilution of a rabbit polyclonal anti-ApoB antibody (ab31992, Abcam, Cambrigde, UK), followed by incubation with a 1:2000 dilution of goat anti-rabbit antibody conjugated to horseradish peroxidase (P0448, Dako, Glostrup, Denmark). Antibody binding was detected by the Lumi-LightPLUS chemiluminescent detection kit (Roche Diagnostics, Basel, Switzerland).

AAV vector production

Production of scAAV8 vectors encoding shApoB and shScr has been described previously [33]. The eGFP-expressing scAAV8 vector was created by digestion of a pTRCGW vector with XbaI and AflII restriction enzymes, blunting and ligation into a pro-AAV vector. The product of this cloning was named pVD287 and contains the eGFP gene under the control of the liver-specific LP1 promoter and generates scAAV due to a mutation in one terminal repeat For cloning the miRNA constructs, expression cassettes were amplified using PCR with specific primers miRf and miRr containing respectively EcoRI and PstI restriction sites at the 5' end. Digested PCR product was ligated into EcoRI and PstI sites of pVD287. Constructs were sequence-verified and the presence of two ITRs was confirmed by restriction digestion with SmaI. scAAV8 vectors were produced by calcium phosphate-mediated co-transfection in HEK293T cells, using the three-plasmid based system described by Gao *et al*. [51] Cells were lysed 48 hr after transfection and virus was released by addition of Tris lysis buffer. Crude lysate from all batches was treated with Benzonase (50 U/ml) (Merck, Darmstadt, Germany) for 1 hr at 37°C. AAV vector particles were purified by iodixanol (Sigma, St. Louis, MO) gradient centrifugation as described previously Purified batches were concentrated by passage through Vivaspin 15R tubes (Sartorius Stedim, Aubagne, France) and final concentration was determined by quantitative PCR with LP1f and LP1r primers amplifying a 95-bp fragment from the LP1 promoter region (Table S1). All viruses used in this study were simultaneously quantified three times to ensure that equal amount of gc per animal was injected.

Genomic DNA isolation and PCR

Genomic DNA (gDNA) was isolated using the DNeasy Blood & Tissue Kit (QIAGEN Inc., Chatsworth, CA) according to the manufacturer's protocol. The amount of viral

DNA in 250 ng gDNA was quantified using quantitative PCR using Lp1fv and Lp1rv primers (Table S1) amplifying 95-bp fragment from LP1 region or primers eGFPf and eGFPr (Table S1) amplifying a 101-bp fragment from the eGFP region. As a standard line, serial dilutions of plasmid DNA containing LP1 or GFP respectively were used.

In vivo experiments

All animal experiments were conducted according to the guidelines of the local animal welfare committee. Six-to-eight-week-old male C57BL/6 mice received an intravenous AAV injection of 1×10^{11} gc per animal (~4×10^{12} gc/kg) or 5×10^{9} gc per animal (~2×10^{10} gc/kg) via the tail vein. Treatment groups were n=4-5 for AAV-shRNA and AAV-miRNA and n=2 for PBS-injected animals. In the AAV-shApoB group sacrificed at 12 weeks n=4 because one animal died during blood sampling. Heparinized blood samples were taken every two weeks p.i. from fasted mice. Mice were sacrificed at 2, 8, 12 or 27 weeks p.i. and liver, heart, lung, kidney, ileum, spleen, and plasma were collected for analysis. Liver samples from 2 and 8 weeks p.i. were obtained from a previous experiment where mice were injected with 1×10^{11} gc of identical preparation of AAV-shScr or AAV-shApoB. Mice were housed 6 per cage and feeding was performed *ad libitum* with regular chow. Plasma levels of ALT, AST, and total cholesterol were analyzed on the automated clinical chemistry analyzer Modular Analytics P800 (Roche Diagnostics, Basel, Switzerland) at the Academic Medical Center (Amsterdam, the Netherlands). Statistical analysis was performed by ANOVA testing and $p<0.05$ was considered significant.

Acknowledgments

The authors thank Valerie Sier-Ferreira (uniQure), Karin Kwikkers (uniQure) and Lizzy Comijn (uniQure) for their expertise on immunology aspects of this paper. We also thank Wim Hermens (uniQure) and Tita Ritsema (uniQure) for critically reviewing the manuscript. The self-complementary AAV vector containing the LP1 promoter was kindly provided by Amit C. Nathwani (St. Jude Children's Research Hospital, Memphis, TN) and the pTRCGW vector was kindly provided by Wim Hermens (uniQure) and Paul Dijkhuizen (The Netherlands Institute for Brain Research, Amsterdam, The Netherlands). The authors declare no conflict of interest.

Supplementary material

Figure S1. Sequence annotation of siApoB reads matching shApoB sequences (available online). siApoB reads were annotated against shApoB reference sequence with the following settings: 2 additional upstream bases, 2 maximum mismatches, 2 missing downstream bases, 2 missing upstream bases. There were 793 from 26,848 small RNAs sequence variants annotated to shApoB sequence (541,939 of 14,491,210 reads). The match type can be exact or a sequence variant with mismatches and the numbers represent number of reads for each sequence. For calculating of frequency 10e6 (rpm), the numbers of reads have to be multiplied by a factor of 0,690.

Figure S2. Sequence annotation of siApoB reads matching miApoB sequences (available online). siApoB reads for miApoB sample were annotated against pre-miApoB reference sequence with the following settings: additional 2 additional upstream bases, 2 maximum mismatches, 2 missing downstream bases, 2 missing upstream bases. There were 741 from 33,164 small RNAs sequence variants annotated to miApoB sequence (1,525,211 of 14,524,958 reads). The match type can be exact or a sequence variant with mismatches and the numbers represents number of reads for each sequence. For calculating of frequency 10e6 (rpm), numbers of reads have to be multiplied by a factor of 0,688.

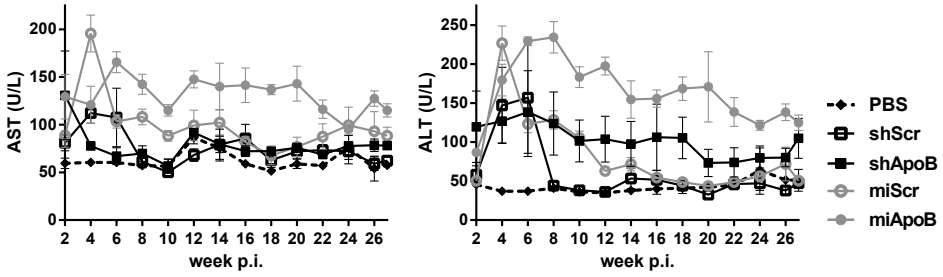

Figure S3. Transient increase in liver transaminases after injection with 1x10^{11} gc AAV. Liver transaminases AST (left) and ALT (right) over the course of 27 weeks p.i. Mice were intravenously injected with 1x10^{11} gc AAV-shApoB or AAV-miApoB, or their respective controls AAV-shScr and AAV-miScr or PBS. Plasma was collected every two weeks p.i. and animals were sacrificed at 27 weeks p.i. Transaminases were analyzed on the automated clinical chemistry analyzer Modular Analytics P800 from Roche. Data are represented as mean values ±SE, treatment groups are n=4-5 for AAV-shRNA or AAV-miRNA and n=2 for PBS-injected animals.

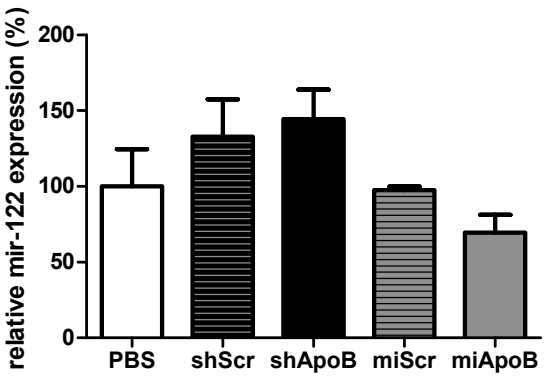

Figure S4. No significant change in mir-122 expression after injection with AAV-shRNA and AAV-miRNA. Relative expression of liver-specific mir-122. Total RNA was isolated from snap-frozen livers at 27 weeks p.i. and miRNA-specific Taqman was performed. mir-122 expression level was calculated relative to actin mRNA and the PBS control was set at 100%. Data are represented as mean ±SE, treatment groups are n=4-5 for AAV-shRNA or AAV-miRNA and n=2 for PBS.

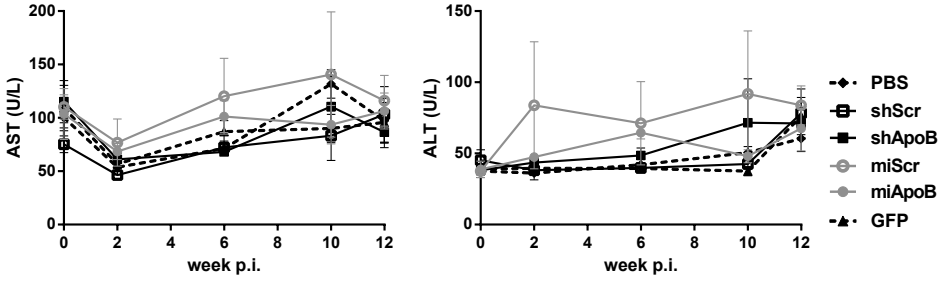

Figure S5. Stable liver transaminases after injection with $5x10^9$ gc AAV. Liver transaminases AST (left) and ALT (right) over the course of 12 weeks p.i. Mice were intravenously injected with $5x10^9$ gc AAV-shApoB, AAV-miApoB, AAV-shScr, AAV-miScr, AAV-GFP, or PBS. Plasma was collected every two weeks p.i. and animals were sacrificed at 12 weeks p.i. Transaminases were analyzed every 2-4 weeks p.i. on the automated clinical chemistry analyzer Modular Analytics P800 from Roche. Data are represented as mean values ±SE, treatment groups are n=4-5.

Table S1. Oligonucleotides used in this study

Name	Sequence (5′-3′)	Description
shApoBf	GATCCCCGATTGATTGACCTGTCCATTTCAAGAGAATGG ACAGGTCAATCAATCTTTTTC	ApoB,13684-13702
shApoBr	TCGAGAAAAAGATTGATTGACCTGTCCATTCTCTTGAAAT GGACAGGTCAATCAATCGGG	
shScr-f	GATCCCCGATCGAATGTGTACTTCGATTCCAAGAGATCG AAGTACACATTCGATCTTTTTGCATGCC	Doege *et al*., 2008
shScr-r	TCGAGGCATGCAAAAAGATCGAATGTGTACTTCGATCTCT TGGAATCGAAGTACACATTCGATCGGG	
miApoBf	GATCCTGGAGGCTTGCTGAAGGCTGTATGCTGATGGACA GGTCAATCAATCTTGTTTTGGCCACTGACTGACAAGATTG AGACCTGTCCATCAGGACACAAGGCCTGTTACTAGCACTC ACATGGAACAAATGGCCCAGATCTGGCCGCAG	ApoB,13684-13702
miApoBr	TCGACTGCGGCCAGATCTGGGCCATTTGTTCCATGTGAGT GCTAGTAACAGGCCTTGTGTCCTGATGGACAGGTCTCAAT CTTGTCAGTCAGTGGCCAAAACAAGATTGATTGACCTGTC CATCAGCATACAGCCTTCAGCAAGCCTCCA	
ApoBf	TGGTTACTGCGCTGAGAGG	ApoB qRT-PCR
ApoBr	CCACACTGAACCAAGGCTT	
m-act-f	ACGGCCAGGTCATCACTATTG	Mouse actin qRT-PCR
m-act-r	CAAGAAGGAAGGCTGGAAAAGA	
LP1f	CCCTGTTTGCTCCTCCGATAA	LP1 qPCR
LP1r	GTCCGTATTTAAGCAGTGGATCCA	
eGFPf	GGGCACAAGCTGGAGTACAACTA	eGFP qRT-PCR
eGFPr	ATGTTGTGGCGGATCTTGAAG	

Table S2. Changes in miRNA expression in shApoB versus miApoB samples (available online). Cellular small RNA data sets were annotated to miRBase (release 18, November 2011) and grouped based on the mature miRNA sequences and reads per million (rpm) were calculated. For each miRNA, proportion of the reads and the fold change between shApoB and miApoB samples were calculated. If the proportion of the given miRNA from the shApoB sample was lower than proportion of the same miRNA in the miApoB sample then this was represented by the negative value. All miRNAs with sequential numerical identifiers up to 500 and fold change more than two were included in statistical comparison. Kal's test (Z-test) with Bonferroni correction was used to compare the proportions of miRNAs in the miApoB versus shApoB sample. *$p < 0.05$, **$p < 0.01$.

Table S3. Expression changes in miApoB versus miScr murine liver samples (available online). Total RNA from murine livers was isolated 8 wk p.i. with 1×10^{11} gc AAV encoding miScr and miApoB and NGS analysis was performed for a representative animal of each group. Data sets were annotated to mouse reference genome (15 May 2012 NCBI build 38.1) and the expression abundance was quantified using the Reads per kilobase of exon model per million mapped reads (RPKM) measure: RPKM of (i) gene = 10^9 x Ci/(Ni x Li), where i is the gene, Ci is the sum of short read counts mapped to exons and Ni represents all mapped read counts in the lane, and Li is the sum of exon lengths [47]. For each entry the fold change between miApoB and miScr samples were calculated. If expression of given gene (RPKM) in the miApoB sample was lower than expression of the same gene in the miScr sample then this was represented by a negative value. Kal's test (Z-test) with Bonferroni correction was used to compare the RPKM value in the miApoB versus miScr sample. *$p < 0.05$, **$p < 0.01$.

Table S4. Expression changes in shApoB versus shScr murine liver samples (available online). Total RNA from livers was isolated 8 wk p.i. with 1×10^{11} gc AAV encoding shScr or shApoB and NGS analysis was performed for one representative animal of each group. Data sets were annotated to mouse reference genome (15 May 2012 NCBI build 38.1) and the expression abundance was quantified using the Reads per kilobase of exon model per million mapped reads (RPKM) measure: RPKM of (i) gene = 10^9 x Ci/(Ni x Li), where i is the gene, Ci is the sum of short read counts mapped to exons and Ni represents all mapped read counts in the lane, and Li is the sum of exon lengths [47]. For each entry the fold change between shApoB and shScr samples were calculated. If expression of given gene (RPKM) in the shApoB sample was lower than expression of the same gene in the shScr sample then this was represented by the negative value. Kal's test (Z-test) with Bonferroni correction was used to compare the RPKM value in the shApoB versus shScr sample. *$p < 0.05$, **$p < 0.01$.

Reference list

1. Pillai, RS (2005). MicroRNA function: multiple mechanisms for a tiny RNA? *RNA*; **11:** 1753-1761.
2. Stark, A, Brennecke, J, Bushati, N, Russell, RB and Cohen, SM (2005). Animal MicroRNAs confer robustness to gene expression and have a significant impact on 3'UTR evolution. *Cell*; **123:** 1133-1146.
3. Castanotto, D (2009). The promises and pitfalls of RNA-interference-based therapeutics. *Nature;* **457:** 426-433.
4. Mockenhaupt, S, Schürmann, N and Grimm, D (2011). When cellular networks run out of control: global dysregulation of the RNAi machinery in human pathology and therapy. *Prog Mol Biol Transl Sci;* **102:** 165-242.
5. Zeng, Y, Yi, R and Cullen, BR (2005). Recognition and cleavage of primary microRNA precursors by the nuclear processing enzyme Drosha. *EMBO J*; **24:** 138-148.
6. MacRae, IJ, Zhou, K and Doudna, JA (2007). Structural determinants of RNA recognition and cleavage by Dicer. *Nat Struct Mol Biol*; **14:** 934-940.
7. Ge, Q, Ilves, H, Dallas, A, Kumar, P, Shorenstein, J, Kazakov, SA, et al. (2010). Minimal-length short hairpin RNAs: The relationship of structure and RNAi activity. *RNA*; **16:** 106-117.
8. Ge, Q, Dallas, A, Ilves, H, Shorenstein, J, Behlke, MA and Johnston, BH (2010). Effects of chemical modification on the potency, serum stability, and immunostimulatory properties of short shRNAs. *RNA*; **16:** 118-130.
9. Siolas, D, Lerner, C, Burchard, J, Ge, W, Linsley, PS, Paddison, PJ, et al. (2005). Synthetic shRNAs as potent RNAi triggers. *Nat Biotech*; **23:** 227-231
10. Fire, A, Xu, S, Montgomery, MK, Kostas, SA, Driver, SE and Mello, CC (1998). Potent and specific genetic interference by double-stranded RNA in Caenorhabditis elegans. *Nature*; **391:** 806-811
11. Park, JE, Heo, I, Tian, Y, Simanshu, DK, Chang, H, Jee, D, et al. (2011). Dicer recognizes the 5[prime] end of RNA for efficient and accurate processing. *Nature*; **475:** 201-205.
12. Vermeulen, A, Behlen, L, Reynolds, A, Wolfson, A, Marshall, WS, Karpilow, J, et al. (2005). The contributions of dsRNA structure to Dicer specificity and efficiency. *RNA*; **11:** 674-682
13. Zhang, X and Zeng, Y (2010). The terminal loop region controls microRNA processing by Drosha and Dicer. *Nucl Acids Res*; **38:** 7689-7697
14. Gu, S, Jin, L, Zhang, F, Huang, Y, Grimm, D, Rossi, JJ, et al. (2011). Thermodynamic stability of small hairpin RNAs highly influences the loading process of different mammalian Argonautes. *Proc Natl Acad Sci USA*; **108:** 9208-9213
15. Bish, LT, Sleeper, MM, Reynolds, C, Gazzara, J, Withnall, E, Singletary, GE, et al. (2011). Cardiac gene transfer of short hairpin RNA directed against phospholamban effectively knocks down gene expression but causes cellular toxicity in Canines. *Hum Gene Ther*; **22:** 969-977
16. Borel, F, van Logtenstein, R, Koornneef, A, Maczuga, P, Ritsema, T, Petry, H, et al. (2011). In vivo knock-down of multidrug resistance transporters ABCC1 and ABCC2 by AAV-delivered shRNAs and by artificial miRNAs. *J RNAi Gene Silencing*; **7:** 434-442
17. Grimm, D, Streetz, KL, Jopling, CL, Storm, TA, Pandey, K, Davis, CR, et al. (2006). Fatality in mice due to oversaturation of cellular microRNA/short hairpin RNA pathways. *Nature*; **441:** 537-541
18. McBride, JL, Boudreau, RL, Harper, SQ, Staber, PD, Monteys, AM, Martins, I, et al. (2008). Artificial miRNAs mitigate shRNA-mediated toxicity in the brain: Implications for the therapeutic development of RNAi. *Proc Natl Acad Sci USA*; **105:** 5868-5873
19. Castanotto, D, Sakurai, K, Lingeman, R, Li, H, Shively, L, Aagaard, L, et al. (2007). Combinatorial delivery of small interfering RNAs reduces RNAi efficacy by selective incorporation into RISC. *Nucl Acids Res*; **35:** 5154-5164
20. Liu, YP, Haasnoot, J, Ter, BO, Berkhout, B and Konstantinova, P (2008). Inhibition of HIV-1 by multiple siRNAs expressed from a single microRNA polycistron. *Nucleic Acids Res*; **36:** 2811-2824
21. Boudreau, RL, Martins, I and Davidson, BL (2009). Artificial microRNAs as siRNA shuttles: improved safety as compared to shRNAs in vitro and in vivo. *Mol Ther*; **17:** 169-175.
22. Boudreau, RL, Monteys, AM and Davidson, BL (2008). Minimizing variables among hairpin-based RNAi vectors reveals the potency of shRNAs. *RNA*; **14:** 1834-1844
23. Giering, JC, Grimm, D, Storm, TA and Kay, MA (2008). Expression of shRNA from a tissue-specific pol II promoter is an effective and safe RNAi therapeutic. *Mol Ther*; **16:** 1630-1636

24. Song, J, Pang, S, Lu, Y, Yokoyama, KK, Zheng, JY and Chiu, R (2004). Gene silencing in androgen-responsive prostate cancer cells from the tissue-specific prostate-specific antigen promoter. *Cancer Res*; **64:** 7661-7663
25. Aagaard, L, Amarzguioui, M, Sun, G, Santos, LC, Ehsani, A, Prydz, H, et al. (2007). A facile lentiviral vector system for expression of doxycycline-inducible shRNAs: knockdown of the pre-miRNA processing enzyme drosha. *Mol Ther*; **15:** 938-945
26. Kappel, S, Matthess, Y, Zimmer, B, Kaufmann, M and Strebhardt, K (2006). Tumor inhibition by genomically integrated inducible RNAi-cassettes. *Nucleic Acids Res*; **34:** 4527-4536
27. McJunkin, K, Mazurek, A, Premsrirut, PK, Zuber, J, Dow, LE, Simon, J, et al. (2011). Reversible suppression of an essential gene in adult mice using transgenic RNA interference. *Proc Natl Acad Sci USA*; **108:** 7113-7118
28. Premsrirut, P, Dow, L, Kim, S, Camiolo, M, Malone, C, Miething, C, et al. (2011). A rapid and scalable system for studying gene function in mice using conditional RNA interference. *Cell*; **145:** 145-158
29. Rangasamy, D, Tremethick, DJ and Greaves, IK (2008). Gene knockdown by ecdysone-based inducible RNAi in stable mammalian cell lines. *Nat Protoc*; **3:** 79-88
30. McQueen, MJ, Hawken, S, Wang, X, Ounpuu, S, Sniderman, A, Probstfield, J, et al. (2008). Lipids, lipoproteins, and apolipoproteins as risk markers of myocardial infarction in 52 countries (the INTERHEART study): a case-control study. *The Lancet*; **372:** 224-233
31. Crooke, RM, Graham, MJ, Leonidis, KM, Whipple, CP, Koos, S, Perera, RJ (2005). An apolipoprotein B antisense oligonucleotide lowers LDL cholesterol in hyperlipidemic mice without causing hepatic steatosis. *J Lipid Res;* **46:** 872-884
32. Zimmermann, TS, Lee, AC, Akinc, A, Bramlage, B, Bumcrot, D, Fedoruk, MN, et al. (2006). RNAi-mediated gene silencing in non-human primates. *Nature*; **441:** 111-114
33. Koornneef, A, Maczuga, P, van Logtenstein, R, Borel, F, Blits, B, Ritsema, T, et al. (2011). Apolipoprotein B knockdown by AAV-delivered shRNA lowers plasma cholesterol in mice. *Mol Ther*; **19:** 731-740
34. Miao, CH, Ohashi, K, Patijn, GA, Meuse, L, Ye, X, Thompson, AR, et al. (2000). Inclusion of the hepatic locus control region, an intron, and untranslated region increases and stabilizes hepatic factor IX gene expression in vivo but not in vitro. *Mol Ther*; **1:** 522-532
35. Grimm, D (2009). Small silencing RNAs: State-of-the-art. *Adv Drug Deliv Rev*; **61:** 672-703
36. Braglia, P, Percudani, R and Dieci, G (2005). Sequence Context Effects on Oligo(dT) Termination signal recognition by Saccharomyces cerevisiae RNA polymerase III. *J Biol Chem.*; **280:** 19551-19562
37. Aagaard, LA, Zhang, J, von Eije, KJ, Li, H, Saetrom, P, Amarzguioui, M, et al. (2008). Engineering and optimization of the miR-106b cluster for ectopic expression of multiplexed anti-HIV RNAs. *Gene Ther*; **15:** 1536-1549
38. Ehsani, A, Saetrom, P, Zhang, J, Alluin, J, Li, H, Snove Jr, O, et al. (2010). Rational design of micro-RNA-like bifunctional siRNAs targeting HIV and the HIV coreceptor CCR5. *Mol Ther*; **18:** 796-802
39. Ely, A, Naidoo, T and Arbuthnot, P (2009). Efficient silencing of gene expression with modular trimeric Pol II expression cassettes comprising microRNA shuttles. *Nucl Acids Res*; **37:** e91
40. Li, C, Xiao, P, Gray, SJ, Weinberg, MS and Samulski, RJ (2011). Combination therapy utilizing shRNA knockdown and an optimized resistant transgene for rescue of diseases caused by misfolded proteins. *Proc Natl Acad Sci USA*; **108:** 14258-14263
41. Mueller, C, Tang, Q, Gruntman, A, Blomenkamp, K, Teckman, J, Song, L, et al. (2012). Sustained miRNA-mediated knockdown of mutant AAT with simultaneous augmentation of wild-type AAT has minimal effect on global liver miRNA profiles. *Mol Ther*; **20:** 590-600.
42. Ely, A, Naidoo, T and Arbuthnot, P (2009). Efficient silencing of gene expression with modular trimeric Pol II expression cassettes comprising microRNA shuttles. *Nucl Acids Res*; **37:** e91
43. Cuccato, G, Polynikis, A, Siciliano, V, Graziano, M, di Bernardo, M and di Bernardo, D (2011). Modeling RNA interference in mammalian cells. *BMC Syst Biol*; **5:** 19
44. Jackson, AL, Burchard, J, Schelter, J, Chau, BN, Cleary, M, Lim, L, et al. (2006). Widespread siRNA "off-target" transcript silencing mediated by seed region sequence complementarity. *RNA*; **12:** 1179-1187.
45. Vandenberghe, LH and Wilson, JM (2007). AAV as an immunogen. *Curr Gene Ther*; **7:** 325-333
46. Livak, KJ and Schmittgen, TD (2001). Analysis of relative gene expression data using real-time quantitative PCR and the 2-[delta][delta] CT method. *Methods*; **25:** 402-408

47. Chen, C, Ridzon, DA, Broomer, AJ, Zhou, Z, Lee, DH, Nguyen, JT, et al. (2005). Real-time quantification of microRNAs by stem-loop RT-PCR. *Nucl Acids Res*; **33:** e179

48. Motameny, S, Wolters, S, Nürnberg, P and Schumacher, B (2010). Next generation sequencing of miRNAs - strategies, resources and methods. *Genes*; **1:** 70-84

49. Mortazavi, A, Williams, BA, McCue, K, Schaeffer, L and Wold, B (2008). Mapping and quantifying mammalian transcriptomes by RNA-Seq. *Nat Meth*; **5:** 621-628

50. Edgar, R, Domrachev, M and Lash, AE (2002). Gene Expression Omnibus: NCBI gene expression and hybridization array data repository. *Nucleic Acids Res*; **30:** 207-210

51. Gao, GP (2002). Novel adeno-associated viruses from rhesus monkeys as vectors for human gene therapy. *Proc Natl Acad Sci USA.*; **99:** 11854-11859.

52. Ruijter, J, Thygesen, H, Schoneveld, O, Das, A, Berkhout, B and Lamers, W (2006). Factor correction as a tool to eliminate between-session variation in replicate experiments: application to molecular biology and retrovirology. *Retrovirology*; **3:** 2.

CHAPTER 5

Therapeutic expression of hairpins targeting Apolipoprotein B100 induces differential changes in murine liver

Piotr Maczuga[1,2], Joanne Verheij[3], Chris van der Loos[3], Richard van Logtenstein[1], Gerrit Hooijer[3], Florie Borel[1,4], Jacek Lubelski[1], Annemart Koornneef[1], Bas Blits[1], Sander van Deventer[2], Harald Petry[1] and Pavlina Konstantinova[1]

[1]Department of Research & Development, uniQure Biopharma B.V., Amsterdam, the Netherlands; [2]Department of Gastroenterology and Hepatology, Leiden University Medical Center, Leiden, the Netherlands; [3] Department of Pathology, Academic Medical Center, Amsterdam, the Netherlands; [4] Department of Gastroenterology and Hepatology, Academic Medical Center, Amsterdam, the Netherlands

Submitted to Gene Therapy

Abstract

Constitutive expression of short-hairpin RNAs (shRNAs) may cause cellular toxicity *in vivo* and using microRNA (miRNA) scaffolds can circumvent this problem. Here we show that embedding siRNA sequences targeting Apolipoprotein B100 (ApoB) in shRNA (shApoB) or miRNA (miApoB) scaffolds resulted in differential processing and efficacy, leading to changes in liver morphology, cellular miRNA and gene expression. Adeno-associated virus (AAV)-shApoB- or AAV-miApoB-mediated ApoB knockdown induced differential expression of 37 cellular miRNAs and significant deregulation of 106 and 266 genes, respectively. Overall, our data indicate that therapeutic expression of shApoB and miApoB results in alterations of different lipid metabolism genes despite the same phenotypic effect of plasma cholesterol reduction. Surprisingly, only in AAV-shApoB-injected animals, genes involved in immune system activation or cell growth and death were affected, which was represented with increased hepatocyte proliferation in this group. Subsequently, in AAV-miApoB-injected animals, changes of genes involved in oxidoreductase activity, oxidative phosphorylation and nucleic bases biosynthetic processes were observed indicating that shApoB and miApoB have a distinct side effect profile. Deregulation of cellular miRNA and liver transcriptome may have serious consequences for future RNAi therapeutics as it may result in cytotoxicity and loss of gene silencing.

Introduction

RNAi is an evolutionary conserved sequence-specific post-transcriptional gene silencing mechanism in eukaryotes that results in the degradation of mRNA and subsequently in decrease of protein synthesis [1]. Therapeutic RNAi can be induced by delivering synthetic small interfering RNAs (siRNAs) or by intracellular expression of short hairpin RNAs (shRNAs) and artificial microRNAs (miRNAs) that target a disease-causing gene [2,3,4]. shRNAs and miRNAs are typically expressed in the cell from pol III or pol II promoters, respectively and are processed by the RNAi machinery, rendering a mature siRNA, which interacts with the cytosolic multiprotein RNA-induced silencing complex (RISC). The RISC-incorporated siRNA binds to the complementary mRNA sequence and mediates its sequence-specific degradation or translational repression [5,6].

Because RNAi can interfere with normal functioning of the cells, the safety of RNAi therapeutics is a major issue. Non-specific effects resulting from the RNAi induction appear to have several main causes: oversaturation of the RNAi pathway, aspecific activation of the immune response and off-target effects due to miRNA-like binding [7-12]. These side effects are often associated with severe toxicity, which can be even fatal. High expression levels of therapeutic shRNA can saturate the endogenous RNAi machinery and in consequence lead to deregulation of the entire miRNA network. For example, mice injected with AAV expressing shRNAs against different targets, developed liver failure irrespective of hairpin length, sequence, and target [10]. Toxicity could be circumvented by using lower vector doses, but this approach in some cases resulted in loss of RNAi silencing efficacy and therapeutic effect [13]. Alternatively, toxicity resulting from shRNA overexpression can be resolved by embedding the siRNA sequence into an artificial miRNA scaffold and expressing it from weaker pol II promoters [4,14,15]. By using miRNA scaffolds disruption of the endogenous RNAi pathway is avoided and shRNA-induced cell death can be prevented. However, in some cases miRNA were found to be less potent compared to shRNA [13].

A second source of toxicity is immune system activation. Characteristically, the interferon (IFN) response to foreign double-stranded RNAs (dsRNAs) is either mediated by phosphorylation of the dsRNA-dependent protein kinase R (PKR) leading to a global inhibition of protein synthesis [16] or via Toll-like receptor (TLR) activation [17]. Recent studies showed that RNAi therapeutics, in particular siRNAs can be potent inducers of IFN and inflammatory cytokines both *in vivo* and *in vitro* [9,11]. Administration of siRNA for treatment of neovascular age-related macular degeneration (AMD) has been reported to induce retinal degeneration via non-specific activation of immune response, which was independent of siRNA or target sequence [18]. Although intracellulary expressed shRNAs are less prone to IFN activation because they can evade activation of TLR, several reports indicated immune reactions against vector delivered shRNA. For example, adenoviral delivery of shRNA targeting Fatty acid

binding protein 5 (Fabp5) activated IFN response in liver [19] and lentiviral vector delivery of shRNA targeting Cyclophilin resulted in IFN activation *in vitro* [20].

Another source of RNAi toxicity is aspecific deregulation of gene expression, when non-targeted transcripts are down-regulated based on sequence complimentarily to the shRNA or miRNA "seed" sequence [12,21]. Because of the complexity of shRNA and miRNA processing and RISC loading, these unanticipated interactions are difficult to predict and evaluate. Off-targeting can be minimized by adopting a stringent design filter both for sense and antisense strands of the RNAi efector molecules. This approach has been validated for siRNA targeting Huntingtin, where off-targeting effect was significantly minimized by avoiding complementarity of siRNA "seed" to 3'UTR, while a high silencing potential was maintained [22]. Additionally significant reduction of off-target effects can be achieved by reducing the dose of siRNA or by chemical modification which impairs siRNA binding to possible off-targets [23].

Previously we have identified differences in processing and efficacy of shRNA and artificial miRNA targeting Apolipoprotein B100 (ApoB) that resulted in differences in long-term gene silencing *in vivo* when delivered with self-complementary adeno-associated virus serotype 8 (AAV) [24]. In the present study we investigated the effect of AAV-shApoB and AAV-miApoB expression on liver morphology, cell proliferation, cellular miRNA and transcriptome changes. Using both approaches, a strong decrease of plasma cholesterol was observed *in vivo* without signs of serious side-effects. Although biochemical analysis showed no acute toxicity, the AAV-shApoB and AAV-miApoB induced differential changes in liver histology, miRNA and transcriptome profiles. Hepatic steatosis, which is known side-effect of ApoB inhibition, was observed with both molecules. However in AAV-shApoB-injected animals increased proliferation of hepatocytes was observed as compared to AAV-miApoB and only in AAV-shApoB-injected animals, genes involved in immune response, cell growth and death were found to be affected.

Results

Knockdown efficacy of AAV-delivered shApoB and miApoB in murine liver

We have previously reported that identical AAV-delivered siApoB sequences in shApoB and miApoB scaffolds (Fig. 1a) are differently processed and have a dissimilar knockdown efficacy *in vivo* [24]. miApoB had a better long-term efficacy and resulted in a more sustained reduction of plasma ApoB and cholesterol in mice. The reduction of therapeutic efficacy was associated with a loss of virally-delivered DNA, but no obvious signs of RNAi toxicity were observed. To directly compare the safety profile of shApoB and miApoB, male C57Bl/6 mice were injected with 1×10^{11} gc AAV per animal encoding shApoB, miApoB, shScr and miScr. All viruses co-expressed enhanced green fluorescent protein (eGFP) for monitoring of liver transduction efficacy and eGFP only

expressing virus (AAV-GFP) was used as an additional control. Mice were sacrificed at week 8 post injection (p.i.) and liver samples were collected for histological and molecular analysis. According to eGFP fluorescence intensity liver transduction efficacy was ~50% (Fig. 1b), and at week 8 ApoB mRNA was reduced by 80% in AAV-shApoB and 87% in AAV-miApoB-injected animals (Fig. 1c). This resulted in 60% and 70% inhibition of plasma cholesterol, respectively (Fig. 1d). Quantification of siApoB molecules expressed from both shApoB and miApoB showed that the knockdown effect correlated to siRNA expression in the liver and AAV-miApoB transduction resulted in significantly less siApoB molecules (Fig. 1e).

It has been reported that expression of shRNA may lead to severe liver toxicity symptoms that is associated with an increase of plasma levels of the transaminases alanine aminotransferase (ALT) and aspartate aminotransferase (AST). Mice injected with AAV-miScr eshowed a mild increase in ALT levels at weeks 4 and 6 p.i., which returned to baseline at week 8 p.i. (Fig. 1f). AAV-miApoB injection gave rise to a two- to three- fold increase in ALT at week 4 p.i. and AST at week 6 p.i. (Fig. 1f). In contrast, no significant increase in liver transaminases for the AAV-shScr, AAV-shApoB and AAV-GFP-injected animals was observed (Fig. 1f). Mouse body weight did not change in any groups and none of the animals displayed any signs of illness or discomfort (data not shown).

Expression of shApoB increases hepatocyte proliferation *in vivo*

A histological analysis was performed to evaluate the effect of stable expression of shApoB and miApoB on liver morphology. ApoB suppression results in decreased cholesterol levels due to impairment of VLDL-C and LDL-C assembly [25] but can also lead to hepatic triglyceride accumulation [26-28]. Triglycerides are normally incorporated into VLDL-C and hepatic accumulation of these lipids can potentially cause steatosis. To investigate the effect of ApoB knockdown on liver morphology, a scoring system was developed and was used to score hematoxylin and eosin (H&E) liver sections (Table S1). Histological analysis revealed no gross changes in liver morphology and no signs of lobular or portal inflammation or parenchymal necrosis were detected in any group (Fig. 2a). However in AAV-shApoB- and AAV-miApoB-injected animals, microvesicular steatosis affecting more than 67% of the liver tissue was apparent (Table 1 and Fig. 2a). In addition, an increase in the hepatocellular mitosis rate was found in AAV-shApoB-injected animals (Table 1). To confirm the scoring results and assess the effect of ApoB knockdown on hepatic lipid accumulation, Oil red O staining was performed on liver sections. Increased accumulation of hepatic lipid content in AAV-shApoB- and AAV-miApoB-injected animals compared to control groups was detected (Fig. 2b).

Previously we have demonstrated that the silencing effect of AAV-shApoB and AAV-miApoB waned over time and this was associated with a loss of virally delivered DNA [24]. We hypothesized that the loss of the (non-integrated) silencing construct

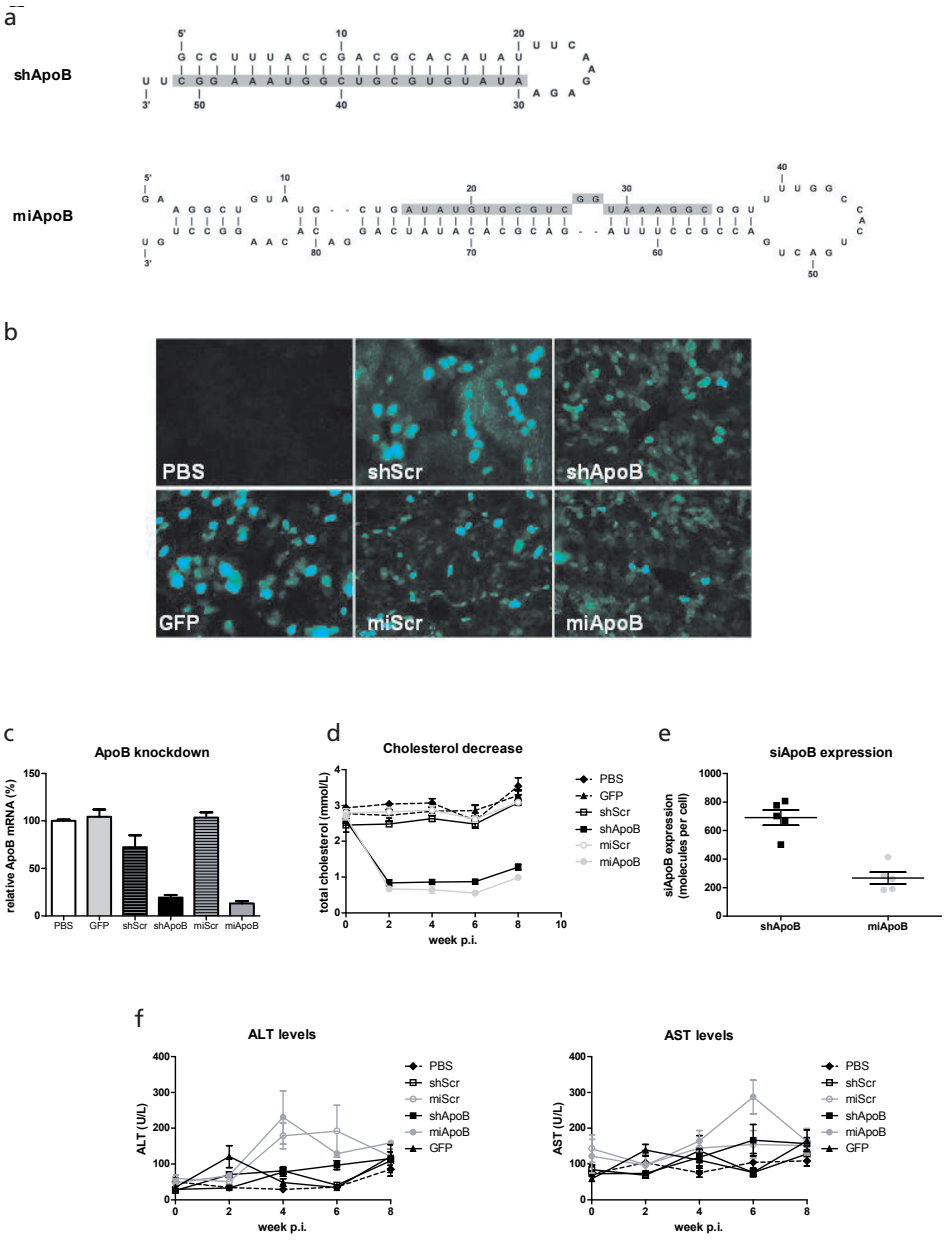

Figure 1. Structure, knockdown efficacy of AAV-shApoB and AAV-miApoB, siApoB expression and ALT/AST levels *in vivo*. Male C57BL/6 mice were intravenously injected with $1x10^{11}$ gc AAV-shApoB, AAV-miApoB, AAV-shScr, AAV-miScr, AAV-GFP or PBS. Plasma was collected every two weeks p.i., animals were sacrificed at 8 weeks p.i. and liver samples were collected for analysis (a) Predicted stem-loop structure for shApoB and miApoB with the guide strand shown in grey. (b) Representative image of GFP fluorescence in snap-frozen livers, transduced with 10^{11} gc of the indicated viruses. Photos were taken using the same exposure and magnification settings. (c) Relative ApoB mRNA expression in murine liver 8 weeks p.i. Total RNA was isolated from snap-frozen liver ►

► tissues and qRT-PCR was performed using ApoB- and actin-specific primers. ApoB mRNA levels were calculated relative to actin mRNA. ApoB mRNA levels in the PBS group was set at 100 %. Data are represented as mean values ±SE (d) Total cholesterol levels in plasma collected from fasted mice over the course of 8 weeks p.i. Cholesterol levels were analyzed on the automated clinical chemistry analyzer Modular Analytics P800. (e) siRNA expression in murine liver 8 weeks p.i. Total RNA was isolated from snap-frozen tissues and siApoB-specific small RNA TaqMan was performed. siApoB copy number was calculated using a siApoB synthetic RNA oligo standard line. Data are represented as mean values ±SE. (f) Plasma ALT (left panel) and AST (right panel) levels at 0, 2, 4, 6 and 8 weeks p.i. Transaminases were analyzed on the automated clinical chemistry analyzer Modular Analytics P800. Data are represented as mean ±SE, treatment groups are n = 5.

could have resulted from either cell division or cell death. Histological scoring showed an increase of proliferating hepatocytes in AAV-shApoB-injected animals, but no increase of apoptotic cells was observed in any of the groups (Table 1). To confirm these histological findings, we first examined whether AAV-shApoB or AAV-miApoB administration enhances the proliferative state of the liver cells. Two major types of cells populate the liver lobes: parenchymal referred as hepatocytes and non-parenchymal cells-sinusoidal cells. To distinguish between proliferating hepatocytes and sinusoidal cells slides were simultaneously stained with antibodies against cytokeratine 18 (CK18), which is a marker for hepatocytes, anti-CD31, a known marker for sinusoidal cells, and the Ki67 antigen, a known marker for cell proliferation (Fig. 2c). Surprisingly the number of proliferating hepatocytes was increased ~2 fold in AAV-shApoB animals compared to AAV-miApoB and control groups (Fig. 2d). When livers were stained for cleaved caspase 3, no increased apoptosis was detected in any of the animal groups (Fig. 2e).

Table 1. Histological scoring of H&E liver sections. Mice were intravenously injected with $1x10^{11}$ gc AAV-shApoB or AAV-miApoB, or their respective controls AAV-shScr, AAV-miScr, AAV-GFP and PBS. Animals were sacrificed at 8 weeks p.i. and liver samples were collected for analysis Paraffin embedded liver sections were stained with H&E and blind histological scoring was performed. Detailed information about the the scoring system used can be found in Table S1. *p<0,05 One-way ANOVA with Bonferroni post test against PBS.

	AVERAGE SCORE					
ITEM	shScr	shApoB	miScr	miApoB	shGFP	PBS
Macrovesicular steatosis	0	0	0	0	0	0
Microvesicular steatosis	1	3*	0	3*	0	0
Ballooning	0	0	0	0	0	0
Lobular inflammation	1	1	1	1	1	1
Portal inflammation	1	0	0	1	0	1
Sinusoidal dilatation	0	0	0	0	0	0
Parenchymal necrosis	0	0	0	0	0	0
Hepatocellular mitosis	1	2*	0	0	0	0
Councilman bodies	0	0	1	1	1	1

shApoB and miApoB expression induces differential cellular miRNA expression

Overexpression of therapeutic shRNAs and miRNAs can modify the processing of cellular miRNA transcripts since they share the same processing pathway and nuclear export machinery. We investigated whether high expression of shApoB and miApoB competes with the intracellular processing of miRNAs *in vitro* and *in vivo*. Next generation sequencing (NGS) of small RNAs was performed on HEK293T cells transfected with shApoB- or miApoB-expression constructs. Expression of endogenous miRNAs was normalized to mir-92 and expressed as number of reads per million (rpm). All conserved mammalian miRNAs with more than a 2-fold change between miApoB and shApoB were included in the statistical comparison. Kal's test (Z-test) with Bonferroni correction was used to compare the expression values of the cellular miRNAs in the miApoB- versus shApoB-transfected cells. A total of 37 cellular miRNAs, were found to be differentially expressed (Fig. 3a). A complete list of the differentially expressed miRNAs in the miApoB- versus shApoB-transfected cells can be found in Supplementary Table 2.

To determine whether shApoB and miApoB expression *in vivo* also results in different cellular miRNA profiles, endogenous levels of 7 miRNAs that are expressed in liver were measured *in vivo* 8 wk p.i. for all animal groups (Fig. 3b). The levels of the liver-specific mir-122 and the broadly expressed miRNAs let-7a, let-7e, mir-26a and mir-221 were not significantly changed in any of the groups expressing shApoB or miApoB. Expression levels for all miRNAs tested were in the range of 80% to 200% of the levels measured in PBS-treated animals. Mir-133a and mir-199a expression was 2-3 fold upregulated in AAV-miApoB-injected animals compared to PBS-injected animals. Importantly, mir-133a expression was significantly different in AAV-miApoB group compared to AAV-shApoB.

Figure 2. Effect of AAV-delivered shApoB and miApoB on liver morphology, proliferation and hepatic fat accumulation. Mice were intravenously injected with $1x10^{11}$ gc AAV-shApoB or AAV-miApoB, or their respective controls AAV-shScr, AAV-miScr, AAV-GFP and PBS. Animals were sacrificed at 8 weeks p.i. and liver samples were collected for analysis. (a) Representative image of H&E liver morphology staining. Paraffin embedded liver sections were stained with eosin for cytoplasm visualization, and nuclei were counterstained with hematoxylin solution. (b) Representative image of hepatic lipid accumulation. Frozen liver sections were stained with Oil Red O for lipids, and nuclei were counterstained with hematoxylin solution. (c) Representative image of liver proliferation. Paraffin embedded liver sections were simultaneously stained in red for hepatocytes (Rabbit anti-mouse CK18), in brown for sinusoidal cells (rabbit anti-mouse CD31) and in blue for antigen Ki67 (Rabbit ant-mouse Ki67). A nuclei counterstaining with hematoxylin was performed. (d) Representative image of liver apoptosis. Paraffin embedded liver sections were stained in blue for cleaved-Caspase 3 (Rabbit anti-mouse). Nuclei counterstaining with hematoxylin was performed. (e) Quantification of proliferating hepatocytes staining described in c). Spectral decomposition was done using inForm software v1.4 and the amount of proliferating hepatocytes (CK18+, Ki67+) was calculated for each animal in 5 different visual fields. Data are represented as mean values of 5 animals ±SE. ***$p < 0.001$ One-way ANOVA with Bonferroni post test against PBS. Bar = 5 µm ►

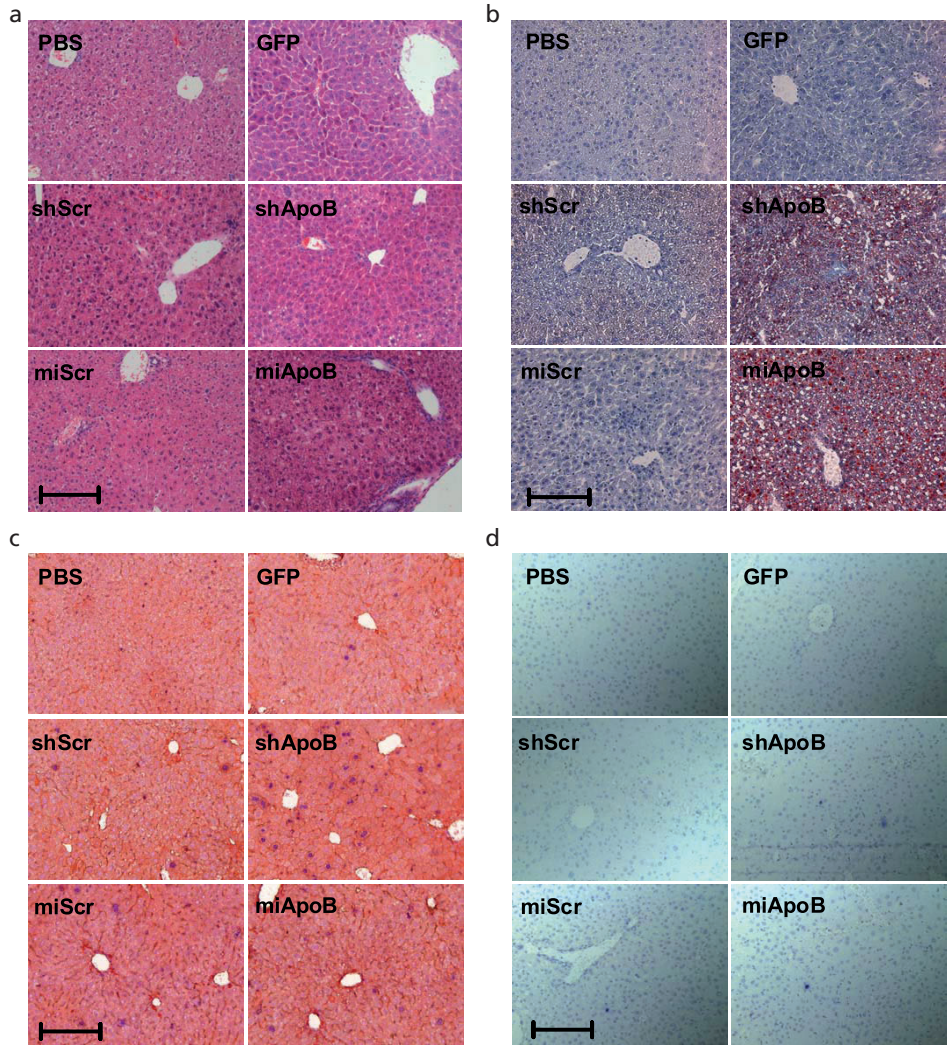
a
PBS
GFP
shScr
shApoB
miScr
miApoB
b
PBS
GFP
shScr
shApoB
miScr
miApoB
c
PBS
GFP
shScr
shApoB
miScr
miApoB
d
PBS
GFP
shScr
shApoB
miScr
miApoB

e

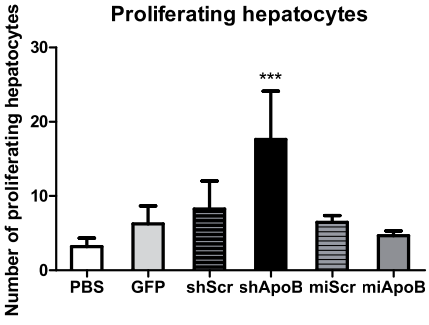
Proliferating hepatocytes
Number of proliferating hepatocytes
30
20
10
0
***
PBS
GFP
shScr
shApoB
miScr
miApoB

a

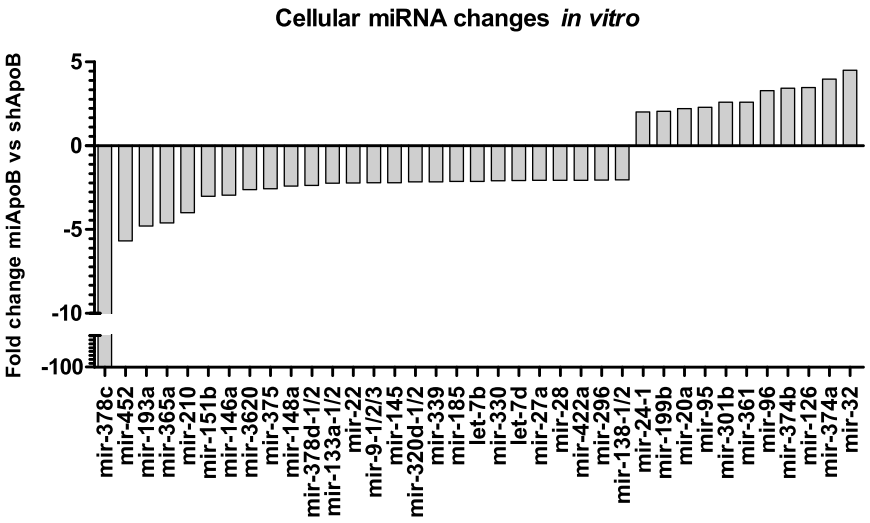

b

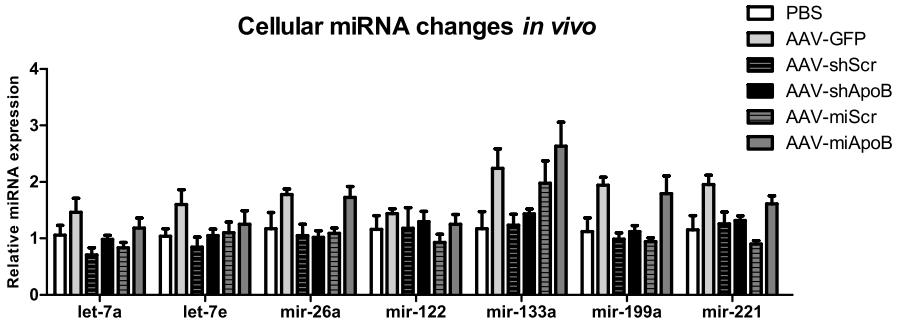

Figure 3. Effect of shApoB and miApoB expression on cellular miRNA levels *in vitro* and *in vivo.* (a) Cellular miRNA changes in miApoB vs. shApoB transfected cells. NGS analysis was performed on RNA isolated two days post-transfection with 1 µg shApoB or miApoB expression constructs. Cellular small RNA data sets were annotated to miRBase (release 18, November 2011) and grouped based on the mature miRNA sequences and reads per million (rpm) were calculated. For each miRNA, proportion of the reads and the fold change between shApoB and miApoB samples were calculated using Kal's test (Z-test) with Bonferroni correction. All miRNAs with sequential numerical identifiers up to 500 that are significantly changing are represented in the graph. (b) Verification of the NGS data *in vivo*. Relative expression of let-7a, let-7e, mir-26a, mir-122, mir-133a, mir-199b and mir-221 *in vivo* was measured by miRNA TaqMan. Mice were intravenously injected with 1×10^{11} gc AAV-shApoB or AAV-miApoB, or their respective controls AAV-shScr, AAV-miScr, AAV-GFP and PBS. Total RNA was isolated from snap-frozen livers. miRNA expression levels were calculated relative to actin mRNA and the PBS-treated group was set at 100%. Data are represented as mean ±SE, treatment groups are n = 5.

Table 2. Changes in predicted shApoB and miApoB off-target gene expression Smith-Waterman algorithm was used to predict shApoB and miApoB off-target genes for the most abundant expressed variants of passenger and guide strands in mouse reference genome (15 May 2012 NCBI build 38.1). Predicted targets were manually screened for genes expressed in the liver that were detected in NGS transcriptome analysis. For each entry the expression value RPKM and the fold change between samples relative to shScr or miScr control was calculated. If expression of a given gene in the shApoB or miApoB sample was lower than expression of the respective control sample shScr and miScr, the fold change had a negative value. ND- not detected NA-not applicable

Sequences	Strand	Targeted gene	Symbol	shApoB RPKM	miApoB RPKM	Fold change shApoB	Fold change miApoB
miApoB shApoB	guide	Apolipoprotein B (NM_009693)	ApoB	69,18	23,21	-3,1	-11,82
		Deltex 4 homolog (Drosophila) (NM_172442)	Dtx4	1,65	0,86	1,2	-1,58
		Ras responsive element binding protein 1, transcript variant 6 (NM_001177869)	Rreb1	3,63	1,87	2,4	-1,38
		Chaperonin containing Tcp1, subunit 2 (beta) (NM_007636)	Cct2	37,36	39,77	-1,2	-1,22
		Dipeptidase 1 (renal) (NM_007876)	Dpep1	0	0,59	NA	2,19
		RIKEN cDNA 2010305A19 gene (NM_027250)	2010305A19Rik	5,45	9,51	1	1,62
		PREDICTED: Uncharacterized LOC100862026 (XR_141568)	LOC100862026	ND	ND	NA	NA
miApoB	passenger	Protein kinase, AMP-activated, gamma 3 non-catatlytic subunit (NM_153744)	Prkag3	ND	0,3	NA	-2,03
		Mediator complex subunit 20 (NM_153744)	Med20	ND	5,77	NA	1,16
		A kinase anchor protein 6 (Akap6) (NM_198111)	Akap6	ND	0,01	NA	-2,35
		DNA segment, Chr 9, ERATO Doi 402, expressed (NM_001013405)	D9Ertd402e	ND	8,32	NA	1,33
		Predicted gene 4934 (NM_001167593)	Gm4934	ND	ND	NA	NA
		RIKEN cDNA 2310081J21 gene (NR_045474)	2310081J21Rik	ND	ND	NA	NA
shApoB	passenger	Regulator of G-protein signaling 12 (NM_001163512)	Rgs12	0,74	ND	1	NA
		Intraflagellar transport 52 homolog (Chlamydomonas) (NM_172150)	Ift52	10,86	ND	1,1	NA
		Budding uninhibited by benzimidazoles 1 homolog (S, cerevisiae) (Bub1), transcript variant 1 (NM_001113179)	Bub1	0,28	ND	5,8	NA
		Creatine kinase, mitochondrial 1, ubiquitous (NM_009897)	Ckmt1	0,11	ND	3,3	NA
		Tubulin tyrosine ligase-like family, member 11, transcript variant 1 (NM_029774)	Ttll11	0,11	ND	1,2	NA
		Visual system homeobox 1 homolog (zebrafish) (NM_054068)	Vsx1	ND	ND	NA	NA

NGS of liver transcriptome reveals differential gene expression in AAV-shApoB- and miApoB-injected animals

The differential siRNA processing from shRNA or miRNA scaffolds may have different consequences for induction of aspecific off-target effects. Therefore we investigated the effect of AAV-shApoB, AAV-shScr, AAV-miApoB, AAV-miScr or PBS on the liver transcriptome by performing NGS analysis. The expression abundance for each gene, represented in reads per kilobase of exon model per million mapped reads (RPKM) was calculated and Kal's test (Z-test) with Bonferroni correction was used to compare the RPKM values. We further focused on gene changes that are specific results of shApoB and miApoB expression, therefore we compared their profiles to the negative controls AAV-shScr and AAV-miScr. All AAV viruses co-expressed GFP therefore AAV-GFP sample was excluded from the NGS analysis. In the AAV-shApoB sample 106 genes were found to be significantly changed (68 were upregulated and 38 were downregulated; $p<0,05$) compared to AAV-shScr (Fig. 4a and 4b). A total of 266 genes were significantly changed ($p <0,05$) in AAV-miApoB-treated mice compared to AAV-miScr (Fig. 4a). Among them 154 genes were upregulated and 112 genes were found to be downregulated (Fig. 4b). Additionally gene expression of AAV-shApoB and AAV-miApoB samples was compared to the PBS and there was no significant difference in the amount of genes affected compared to shScr or miScr controls (Fig 4a). The number of genes affected in AAV-shApoB and AAV-miApoB samples when compared to PBS was 124 and 289, respectively (Fig. 4a). To confirm the changes observed in the NGS analysis, ApoB knockdown as measured with NGS, qRT-PCR and Western blot were compared (Fig. 4c). For both AAV-shApoB and AAV-miApoB animal groups ApoB knockdown detected with NGS correlated with qRT-PCR and Western blot data indicating that the NGS analysis is a reliable method for comparing gene expression between the different animal groups.

Next, we focused on genes that are specific results of ApoB inhibition in AAV-shApoB and AAV-miApoB-injected animals. Therefore we compared the expression of genes that are predicted to functionally interact with ApoB (Fig. 4d). Several consistently changing genes were observed like: Apobec2, Bgn and Lpl. However the majority of the ApoB-interacting genes were differentially changing between AAV-shApoB and AAV-miApoB and the expression of a number of genes remained unaltered.

Functional categorization of the NGS data

To generate a full functional profile for all genes altered by the *in vivo* expression of shScr, shApoB, miScr and miApoB, a web-based tool DAVID was used for the ontological analysis of large lists of genes (see Materials and Methods). Analysis of the 106 genes that were significantly changed in the AAV-shApoB group indicated that the most significant functional alterations were related to genes involved in lipid metabolism and

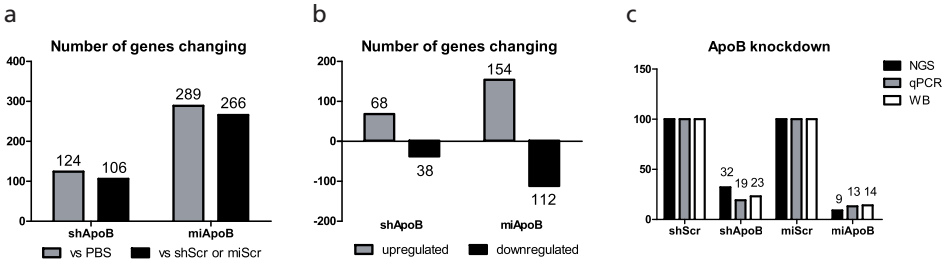

d

ApoB predicted partners' expression changes

	A1cf	Abca1	Abcg5	Acat1	ApoA1	ApoA2	ApoA4	ApoA5	Apobec1	Apobec2	Apobec3
shApoB	1,21	1,33	1,05	1,07	-1,13	-1,50	6,18	-1,20	1,77	-2,25	1,82
miApoB	-3,16	-1,95	-2,53	1,73	1,16	2,03	-8,86	-1,01	1,02	-2,50	1,32

	ApoC2	ApoC3	ApoE	ApoM	Bgn	Cd320	Cda	Ces3b	Cog2	Cyp7a1	Eif4g2
shApoB	1,56	-1,63	-1,23	-1,05	1,67	1,40	1,19	-1,68	1,54	1,76	1,26
miApoB	-1,08	1,26	1,50	1,15	1,77	2,44	1,94	1,25	1,09	1,27	-1,26

	Fgr	Hspg2	Lcat	Ldlr	Ldlrap1	Lipc	Lpl	Lsr	Mtp	Mvp	Nr1h4
shApoB	2,88	1,31	-1,35	1,23	1,66	1,08	1,88	1,02	1,21	1,48	-1,01
miApoB	1,31	-1,24	-1,31	-1,75	1,06	1,05	6,18	-1,24	-1,85	1,10	1,13

	P4hb	Pcsk9	Plg	Plk1	Pltp	Ppara	Scarb1	Sdc1	Srebf2	Txn1	Txnip
shApoB	-1,10	1,02	-1,10	4,16	1,14	1,06	1,42	1,62	1,35	-1,11	1,29
miApoB	-1,46	-2,69	-1,30	-2,07	1,03	-1,32	-1,79	1,45	-1,59	1,63	-1,09

Figure 4. NGS transcriptome analysis indicates differential gene expression profiles between AAV-shApoB- and AAV-miApoB-injected animals. To analyze liver transcriptome, total RNA was isolated from a representative animal 8 wk p.i. and NGS analysis was performed. The expression abundance for all genes was quantified using the reads per kilobase of exon model per million mapped reads (RPKM) measure. Expression data was compared using Kal's Z-test with Bonferroni correction. Genes significantly altered (p<0,05) were used in further analysis (a) Genes significantly altered (p<0,05) in AAV-shApoB- and AAV-miApoB-injected animals. Grey bars represent gene changes compared to PBS group and black bars represent gene changes compared to AAV-shScr or AAV-miScr controls (b) Genes significantly upregulated or downregulated in AAV-shApoB and AAV-miApoB injected animals. Grey and black bars represent number of genes upregulated and downregulated respectively compared to AAV-shScr or AAV-miScr controls (p<0,05) (c) Comparison of ApoB knockdown *in vivo* by NGS, qRT-PCR and protein Western blot. In all assays ApoB expression levels were calculated relative to AAV-shScr or AAV-miScr, which served as negative controls and were set at 100%. (d) Prediction of ApoB functional interactions was performed with STING software. Upregulated genes (fold change > 1,5) were marked in green and downregulated (fold change < -1,5) were marked in red.

transport and response to stimuli (Fig. 5a). In addition, expression of genes involved in drug metabolism, inflammation, cell growth and death and the MAPK signaling pathway were altered. In the AAV-miApoB animal group, the 266 significantly altered genes corresponded mainly to genes involved in drug metabolism, oxidoreductase activity and processes (Fig 5b). Other relevant pathways include lipid metabolism and transport, ion binding, response to stimuli and nucleobase, nucleoside and nucleotide biosynthetic process. A complete list of genes functionally annotated with DAVID

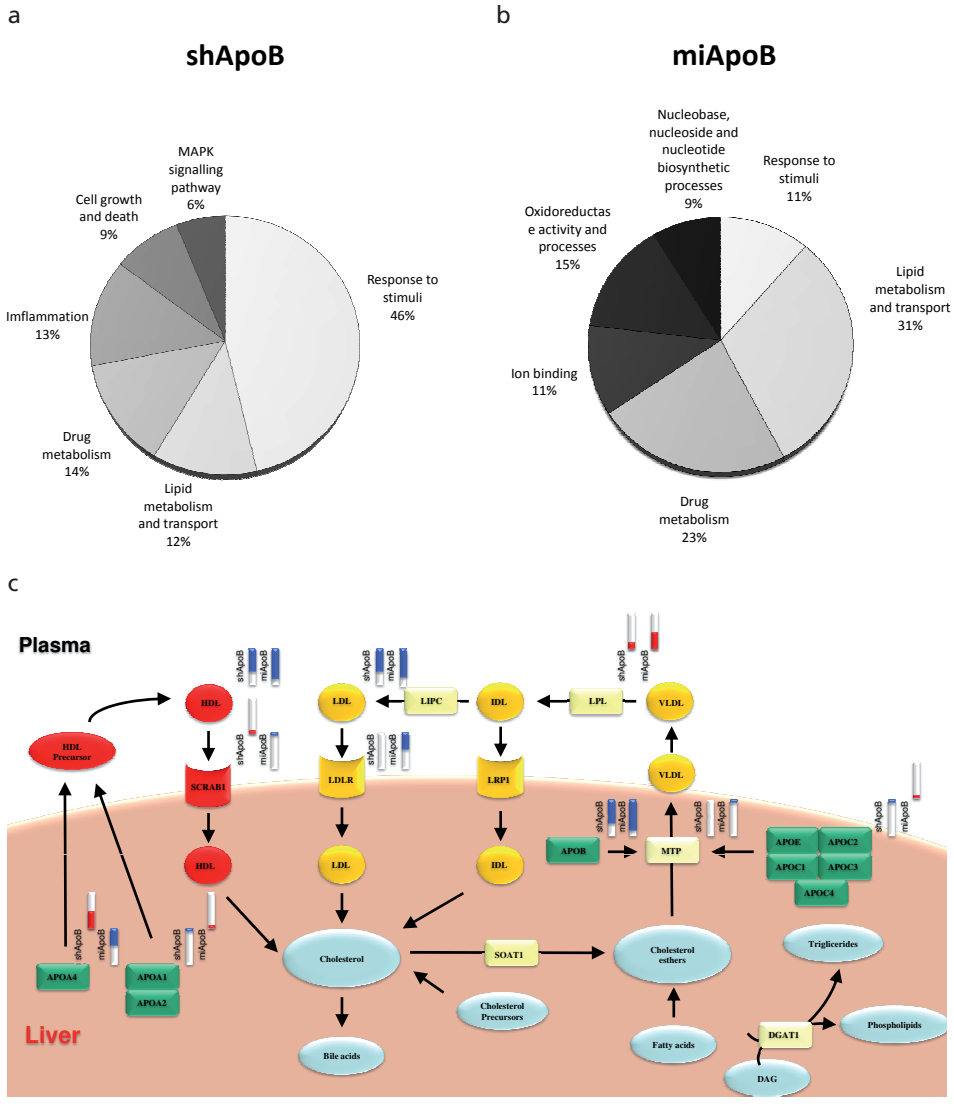

Figure 5. Functional categorization of gene expression changes in AAV-shApoB and AAV-miApoB injected animals. (a) Percentage and functional categorization of genes significantly changing in AAV-shApoB and AAV-miApoB animal groups. Genes significantly altered in AAV-shApoB and AAV-miApoB groups ($p<0,05$) were annotated to Gene Ontology (GOTERM_BP_FAT and GOTERM_MF_FAT) and KEGG (KEGG_PATHWAY) using the Database for Annotation, Visualization and Integrated Discovery (DAVID) v6.7 (National Institute of Allergy and Infectious Diseases (NIAID), NIH). Significant annotations ($p<0,05$) were grouped in 8 categories and the percentage of genes in each category was calculated with reference to all genes annotated in the DAVID analysis.(b) Outline of cholesterol pathway changes in AAV-miApoB and AAV-shApoB injected animals. There are several types of lipoproteins within blood: chylomicrons, very-low-density lipoprotein (VLDL), intermediate-density lipoprotein (IDL), low-density lipoprotein (LDL), and high-density lipoprotein (HDL). ApoB100 protein is synthesized in the liver and it forms the structural protein in VLDL and LDL particles. HDL is secreted by the gut and liver and receives additional components during the ►

► metabolism of triglyceride-rich lipoproteins. Therefore inhibition of ApoB affects VLDL-C, LDL-C and HDL levels-C. Genes significantly altered in the AAV-shApoB and AAV-miApoB groups were used ($p<0,05$) for toxicology prediction using Metacore software (Thomson Reuters) and the top scored map was generated. Experimental data from AAV-shApoB and AAV-miApoB groups are linked to and visualized on the image as thermometer-like figures place in the top right of respective gene or group of genes. Upward red colored thermometers indicate up-regulated components and downward blue thermometers indicate down-regulated components of the pathway.

for miApoB and shApoB samples can be found in Supplementary Tables 3 and 4, respectively. Although both shApoB and miApoB resulted in the same phenotypic effect as result of ApoB knockdown, the changes exerted on other lipid metabolism genes were rather dissimilar (Fig. 5c). Inhibition of ApoB in AAV-shApoB-injected mice resulted in a decrease of LDL-C and HDL-C associated genes: ApoA2, ApoE, ApoC1, ApoC3 and ApoC4. By contrast the same genes were upregulared in AAV-miApoB-injected samples. Furthermore miApoB was associated with downregulation of ApoA4, Ldlr, Pcsk9 and Scarb1, which are key components in cholesterol homeostasis. By contrast, ApoA4 and Scrab1 genes were upregulated in the AAV-shApoB sample. In both AAV-shApoB- and AAV-miApoB-injected animals Apobec2 gene was downregulated while Lpl gene was significantly upregulated (Fig 5c).

Although both shApoB and miApoB were found to affect response to stimuli and drug metabolism, only the serine protease inhibitors Serpina1b, Serpina1c, Serpina1d and Serpina3k were simultaneously affected in both groups. Serpins compose a large family of the functional diverse proteins which are involved in numerous intracellular and extracellular functions: blood clotting, inflammation, storage, hormone carriage and tumor suppression [29-31]. Only AAV-shApoB injection was found to upregulate genes involved in inflammatory response such as Serpina 8N which is induced during inflammation and Serum amyloid A1 (Saa1), a major acute phase reactant. shApoB but not miApoB expression also upregulated components of the MAPK signaling pathway: Fos, Jun, Nr4a1, Dusp1 and Dusp6. Fos, Jun, Nr4a1 are transcription factors involved a number of cellular processes including differentiation, proliferation, and apoptosis [32] and Nr4a1 plays a key role in mediating inflammatory responses in macrophages [33]. Dusp1 and Dusp6 negatively regulate the members of the MAPK family pathways JNK and p38, which results in cell apoptosis [34].

miApoB expression downregulated genes involved in drug metabolism such as members of alpha-glutathione-S-transferase Gsta1, Gsta2, Gsta4 and glutathione-S-transferase mu genes Gstm1, Gstm2, Gstm3 and Gstm3. By contrast, expression of those genes was upregulated in the AAV-shApoB-injected animal. Other genes that were upregulated in AAV-miApoB-injected animal are involved in oxidoreductase activity, oxidative phosphorylation and nucleic bases biosynthetic processes. Most of these are structural components of mitochondrial oxidative phosphorylation system: NADH-coenzyme Q oxidoreductase (complex I), Cytochrome bc1 complex

(complex III), Cytochrome c oxidase (complex IV) and ATP synthase (complex V). Finally, genes involved in lipid metabolism and transport that encode alcohol dehydrogenase (Adh1), Acetyl-Coenzyme A acyltransferase (Acaa1b, Acaa1a, Acaa2), Aldehyde dehydrogenase 3 family (Aldh3a2) and Cytochrome P450 family members (Cyp4a10, Cyp3a11, Cyp2c29, Cyp4a14) were upregulated in the AAV-miApoB sample.

shApoB and miApoB do not affect the expression of predicted off-target genes

A common source of RNAi toxicity is off-targeting, when non-targeted transcripts are down-regulated as a consequence of sequence complimentarily to the shRNA or miRNA sequence. In our previous study we have shown that shApoB and miApoB are differentially processed *in vivo* and that a pool of different guide and passenger strands was generated. To investigate possible off-target effects, the Smith-Waterman algorithm was used to predict the most abundant guide and passenger strand variants (Table 2). A total of 19 genes were predicted as off-targets in the liver for the guide and passenger strand of shApoB and 25 for miApoB. To investigate if any of the predicted interactions correlates with our experimental data, *in vivo* NGS data was manually screened for the predicted off-target gene expression and evaluation of the changes was performed (Table 2 and Fig. 6). From the 19 predicted off-target genes, 11 were expressed in AAV-shApoB animals and 10 in AAV-miApoB-injected animals. Surprisingly, the expression of none of the predicted off-targets for both shApoB and miApoB was significantly changed *in vivo* (Table 2 and Fig 6).

5 Discussion

The major challenge for the RNAi-based therapies is the delivery of siRNAs to the target tissue or organ for stable and long-term inhibition of a disease-related gene. Recent reports on the RNAi toxicity have initiated a discussion about the safety of such an approach. Although in the last few years much progress has been made in understanding the causes of toxicity and approaches to preclude adverse effects have been suggested, detailed studies on the differences between shRNA- or artificial miRNA-encoding constructs and the consequences for *in vivo* applications have not been reported. By using AAV delivery, we have compared the safety profiles of identical predicted siApoB sequences expressed as shApoB and miApoB in long-term *in vivo* studies. Detailed histological analyses, as well as comparison of endogenous miRNA and transcriptome expression revealed major differences between AAV-shApoB- and AAV-miApoB-injected animals, indicating that careful monitoring is necessary prior to proceeding clinical trials.

In vivo toxicity of shRNA was often linked to upregulation of liver enzymes ALT and AST in mice [8,10] and in non-human primates [35]. In our experiment, transient activation of liver transaminases was observed in AAV-miScr and AAV-miApoB animals

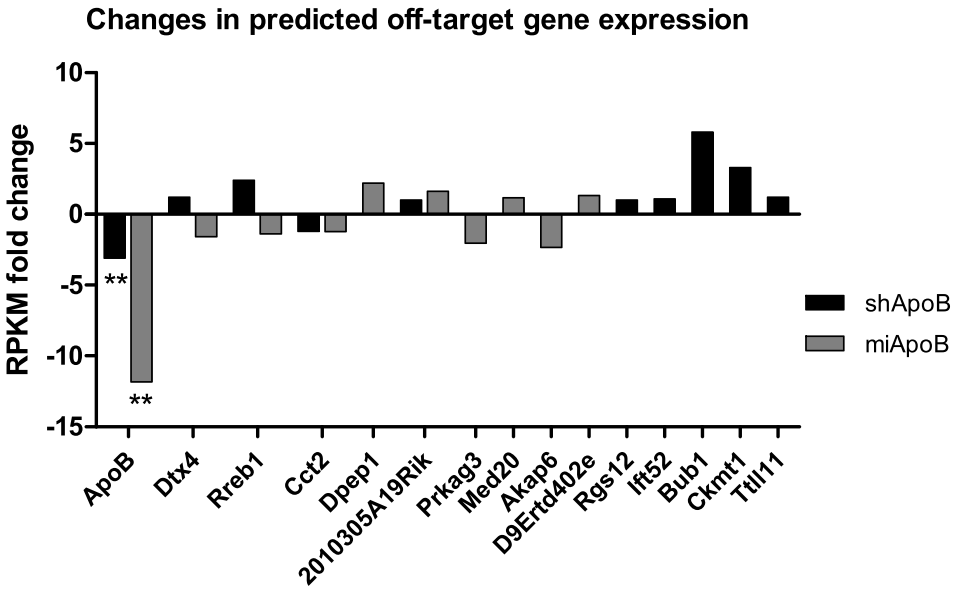

Figure 6. Changes in predicted shApoB and miApoB off-target gene expression. Smith-Waterman algorithm was used to predict shApoB and miApoB off-target genes for the most abundant expressed variants of passenger and guide strands in mouse reference genome (15 May 2012 NCBI build 38.1). Predicted targets were manually screened for genes expressed in the liver that were detected in NGS transcriptome analysis. Grey and black bars represent fold change in AAV-shApoB and AAV-miApoB relative to AAV-shScr or AAV-miScr controls respectively. Kal's test (Z-test) with Bonferroni correction was used to compare the RPKM value in the shApoB versus shScr or miApoB versus miScr. **$p < 0.01$

during the course of the experiment indicating mild dose-dependent toxicity. We have previously reported that such toxicity can be abolished by lowering the administered viral dose [24]. In contrast to our results, Ahn *et al.* described increased in ALT levels 3 weeks p.i. after injection of adenovirus encoding shRNA against transcription factor Srebp1 and lipid transporter Fatbp5 [7]. Interestingly in their study, scrambled control hairpin did also cause increase in ALT levels, indicating that toxicity was associated with shRNA expression and was not due to adenoviral vector. This also suggests that shRNA liver toxicity is probably sequence-dependent. In another study, three-fourths of the tested shRNAs resulted in liver injury, while expression of others was well tolerated [10]. Although transient ALT and AST increase was detected in AAV-miScr- and AAV-miApoB-injected animals, no acute inflammation and no gross-changes of liver morphology in these groups were detected.

Similar to previous studies, ApoB knockdown by AAV-shApoB and AAV-miApoB resulted in hepatic fat accumulation [36,37]. Surprisingly steatosis was not observed in murine studies with an ApoB antisense oligonucleotide [38]. By contrast, clinical trials with the human ApoB antisense oligonucleotide did reveal a trend toward an

increase in intrahepatic triglyceride content [39]. Steatosis may be associated with inflammation and may progress to cirrhosis, therefore careful consideration and investigation of this consequence of lowering ApoB is necessary. Tep *at al.* reported that simultaneous silencing of Mtp and Dgat2 rescues siRNA-induced hepatic steatosis [48]. However Dgat2 silencing resulted in a significant increase of plasma ketones making this approach not attractive for clinical applications as elevated serum ketones can cause medical emergency. By contrast, double knockdown of ApoB and Dgat2 or Fabp5 did not result in reduction of lipid accumulation.

We observed that injections of AAV-shApoB, but not AAV-miApoB, caused increased hepatocyte proliferation. The reason for the observed proliferation would be hepatocyte damage due to RNAi-induced toxicity. Increased apoptotic and proliferative activity has been observed in murine liver expressing AAV-delivered shRNA targeting human alpha-1-antitripsin [10] and adenoviral-expressed targeting Srebp1 and Fabp5 [7]. In our experiments we observed increased proliferation that was not associated with apoptosis, implying that apoptosis may have occurred earlier than 8 wk p.i. with AAV-shApoB. Another reason for the increased proliferation could be the hepatic steatosis. Indeed, It has been reported that increase in liver triglycerides may lead to increased oxidative stress in the hepatocytes and lipid-activated apoptosis [40]. The fact that miApoB does not affect liver proliferation excludes this possibility. Based on our data and previous reports, we can only conclude that increased liver proliferation due to shApoB expression is hairpin structure- and concentration-specific. It should be noted that AAV-miApoB- and AAV-miScr-injected animals did not reveal signs of increased liver proliferation, which could have important consequences for long-term correction, since AAV DNA forms episomal nuclear concatamers in the host cell nucleus, which are lost following cell division [41]. Those results also explain our previous observations where the silencing effect in AAV-shApoB-injected animals was less sustained than in AAV-miApoB-injected animals [24].

Saturation of the RNAi pathway and global de-regulation of endogenous miRNA processing as a consequence of overexpression of hairpin structures play an important role in RNAi-induced toxicity [8,10]. Castanotto *et al.* showed that both siRNAs and shRNAs against the HIV regulator gene Rev competed with the endogenous mir-21 expression *in vitro* in HEK293T cells [42]. However the siRNA sequences used in that setting did not show competition with endogenous miRNA when expressed as artificial miRNA. In another study mir-21 was shown to be affected by expression of artificial miRNA against the hepatitis virus B (HBV) genome in Huh7 cells [43]. The competition with endogenous miRNA was dose-dependent as potent silencing was also achieved with lower doses where RNAi saturation was not observed. It has also been reported that shRNA-induced toxicity resulted in inhibition of mir-122 and let-7a *in vitro* and *in vivo* [8,10]. Our NGS analysis of small RNA profiles showed significant divergence between shApoB- and miApoB-transfected cells. *In vivo* of 7 tested miRNAs only

mir-133a was differentially expressed in the AAV-miApoB-injected group compared to AAV-shApoB-injected group. However we cannot exclude that complete NGS profiling of miRNA expression *in vivo* would allow identification of other differentially expressed endogenous miRNAs. Importantly in both *in vitro* and *in vivo* experiments, we did not observe global downregulation of endogenous miRNA expression indicating that therapeutic delivery of AAV-shApoB and AAV-miApoB did not induce toxic effects.

The NGS analysis of liver transcriptome revealed differential gene expression in AAV-shApoB- and AAV-miApoB-injected animals. As anticipated, lipid metabolism and transport genes were affected for both molecules. Interestingly, Bgn, a proteoglycan which can bind ApoB-containing lipoproteins and is involved in atherosclerosis [44], and Lpl is one of the key enzymes for lipoprotein catabolism which hydrolyzes triglycerides and VLDL-C [45], were upregulated for both AAV-shApoB and AAV-miApoB. In addition to lipolysis, Lpl mediates the uptake and degradation of lipoproteins by cells. Our hypothesis is that the upregulation of these two genes might be a compensatory reaction to the strong ApoB decrease in murine liver but the biological significance of those changes needs to be determined. Apobec2, which is an ApoB mRNA editing enzyme, was downregulated in both treatment groups probably as a result of the low concentrations of ApoB in the liver of shApoB and miApoB animals. Although Abobec2 functions in liver are not fully investigated, its upregulation has been associated with tumorogenesis and development of hepatocellular carcinoma through hepatic inflammation [46]. By contrast Apobec2 deficient mice did not reveal any abnormalities on health and survival [47].

Surprisingly, the majority of the lipid metabolism genes were differentially affected in AAV-shApoB and AAV-shApoB animals despite the same phenotypic effect. Recently, significant changes in many lipid metabolism genes following ApoB silencing with siRNA have been reported using TaqMan analysis [48]. Out of 96 genes which were investigated, 53 were downregulated more than 1,5 fold while only 7 were upregulated. However when compared to our NGS data, only a few genes had a similar change in expression profile (Table S5). This may suggest that siRNA, shRNA and miRNA induce different gene expression profile despite the same phenotypic effect. However, it has to be noted that the siApoB used had a different sequence and the experiment was performed in LDL-R/CETP+/- hemizygous mice, which exhibit different lipid profile. Additionally the analysis was performed 2 wk p.i. with siApoB and at this time point gene expression changes may have been more pronounced. To our knowledge comparison of liver gene expression analysis after siRNA, shRNA and miRNA administration has not been performed.

Besides lipid metabolism and transport other functions were also altered in murine liver by expression of AAV-shApoB or AAV-miApoB. Response to stimuli and drug metabolism were found to be affected in both shApoB and miApoB groups, but the genes involved showed minimal overlap. shApoB was found to affect genes involved

in cell growth and death, inflammation and MAPK pathway, which correlated with our findings on increased liver proliferation. miApoB affected genes involved in ion binding, nucleobase biosynthetic process and oxidative activity and processes. Previously, Ahn *et al.* described significant transcriptomic changes in mice after adenoviral deliver of shRNA [7], where a total number of 181 genes, were found to be upregulated while only 32 genes were found to be downregulated as a consequence of shRNA expression. Data generated from their study suggested that shRNA expression also upregulated genes involved in the RNAi pathway and proliferation. In contrast, we did not see significant upregulation of those genes, which might be due to the fact that we performed our analysis 8 weeks p.i. and because we used AAV as a delivery vector. Importantly we detected upregulation of inflammatory related genes exclusively in the AAV-shApoB group although no signs of inflammation in the liver could be found and in our previous experiments we did not measure IFN response activation [49]. Immune activation might indeed have caused hepatocytes' damage in the AAV-shApoB sample resulting in increased proliferation and eventually loss of the knockdown effect. The consequences of the activation of genes involved in immune response solely by AAV-shApoB needs to be further investigated by careful monitoring their expression over time and when different shRNAs and AAV doses are used.

Another important observation was that none of the changes in gene expression in AAV-miApoB and AAV-shApoB resulted from aspecific down-regulation of off-target transcripts. Although we could not explain the changes in gene expression by off-target prediction using the Smith-Waterman algorithm, we cannot exclude that some of the interaction may have been missed and other prediction methods like screening 3' UTRs of genes for perfect complementarity to siRNA seed region may be more accurate. miRNAs may regulate their targets by translational repression, therefore we might speculate that the off-target effects may be stronger at protein level.

In summary, our findings demonstrate that the incorporation of identical siRNA sequences in shRNA or artificial miRNA scaffolds induces differential effects on liver morphology, transcriptome and cellular miRNA expression. Despite effective silencing, same phenotypic effect and no signs of severe toxicity, multiple genes and functions were de-regulated by AAV-shApoB or AAV-miApoB. Mir-133a was upregulated in AAV-miApoB animals and might be one of the mediators responsible for the observed differences between shApoB and miApoB. Furthermore only expression of shApoB resulted in increased hepatocyte proliferation indicating the miApoB is a better candidate for future development of RNAi therapeutics of familial hypercholesterolemia. Finally, miApoB expression was limited to the liver due to the use of a tissue-specific promoter, while the presence of shApoB-derived siApoB was detected in spleen, heart, lung, kidney, and ileum. All those features of AAV-miApoB makes us consider the use of tissue-specific expression of therapeutic siRNA from miRNA scaffolds a safer option than shRNA.

Materials and methods

DNA constructs AAV production and purification

The design and cloning of the shApoB, shScr, miScr, miApoB and GFP expression vectors, scAAV8 vector production and purification has been described previously [24,49].

In vivo experiments

All animal experiments were conducted according to the guidelines of the local animal welfare committee. Six-to-eight-week-old male C57BL/6 mice received an intravenous AAV injection of 1×10^{11} gc per animal (~4×10^{12} gc/kg) via the tail vein. Treatment groups were n=5, mice were housed 6 per cage and feeding was performed *ad libitum* with regular chow. Heparinized blood samples were taken every two weeks p.i. from fasted mice. Mice were sacrificed at 8 weeks p.i. and liver and plasma were collected for analysis. Plasma levels of ALT, AST, and total cholesterol were analyzed on the automated clinical chemistry analyzer Modular Analytics P800 (Roche Diagnostics, Basel, Switzerland) at the Academic Medical Center (Amsterdam, the Netherlands). Statistical analysis was performed by ANOVA testing with Bonferroni post test and $p<0.05$ was considered significant.

GFP expression was analyzed in snap-frozen liver sections. Livers were cryosectioned at 5 µm and eGFP signal was visualized using standard fluorescence microscopy on a Leica fluorescent microscope (Leica Microsystems GmbH, Wetzlar, Germany). For analysis of liver fat accumulation, snap-frozen liver sections were cryosectioned at 5 µm, fixed in 10% formalin and stained for 25 min in filtered 0.3 % Oil red O (Sigma, St. Louis, MO) solution in 60% isopropanol. Nuclei were counterstained for 5 min in hematoxylin solution (Sigma, St. Louis, MO). Liver histology was assessed by hematoxylin-eosin (H&E) staining of frozen liver sections.

Immunohistochemistry

Mouse liver samples were fixed with buffered 4% formalin (NBF) for 48 h and then routinely processed to paraffin blocks. Five-micrometer sections were cut, mounted on coated slides and dried overnight at 37°C. Slides were dewaxed in xylene and hydrated with the use of graded alcohols to tap water. Endogenous preoxidases were blocked by incubation in methanol supplemented with 0,3% peroxide. Heat induced endogenous antigen retrieval (HIER) was performed in the PreTreatment Module (PTModule; Thermo Fisher Scientific/Labvision, Fremont, CA) for 20 min at 98°C and a cool-down to 75°C in Tris-HCI + EDTA pH 9.0. After washing sections with running tap water, Ultra V Block (Thermo Fisher Scientific/Labvision, Fremont, CA) for 10 minutes at room temperature (RT). A sequential triple staining procedure [50] started with CD31 (LifeSpan Biosciences Inc., Seattle, WA) visualized by horseradish peroxidase (HRP) conjugated anti-rabbit IgG polymer and BrightDAB (both Immunologic, Duiven, The Netherlands). The DAB reaction product effectively shelters the first set of

antibodies and thus prohibits unwanted cross-reactions with later incubation steps. Staining was continued with anti-Ki67, clone SP6 (Thermo Fisher Scientific/Labvision, Fremont, CA) visualized by BrightVision alkaline phosphatase (AP) conjugated anti-rabbit IgG polymer (Immunologic, Duiven, Then Netherlands) and Vector Blue (Vector Laboratories, Burlingame, CA, USA). Next, a second HIER step (10 min, 98C) using citrate buffer pH6. 0 was applied to remove all antibodies used but leaving the chromogens unchanged. Finally, CK18 (Abcam, Cambridge, UK) was visualized by BrightVision AP conjugated anti-mouse IgG polymer (Immunologic) and Vector Red (Vector Labs). Slides were weakly counterstained with hematoxylin diluted 1:5 in distilled water for 3 min, washed with tap water, completely dried at a hot plate and non-aqueous coverslipped with VectaMount (Vector Labs). Primary and secondary antibodies used in this study are listed in Table 1. Antibodies and conjugates were diluted in antibody dilutent (Immunologic) and Tris-buffered saline (TBS) was used as washing buffer for all further steps (three changes, 3 min each). HRP activity in brown was developed with Bright DAB (Immunologic) according to manufacturer's instructions. Alkaline phosphatase (AP) activity in blue and in red was developed with the Vector Blue and Vector Red kits (Vector Laboratories, Burlingame, CA) with the use of a Tris-HCI buffer (100 mM, pH 8.2) according to manufacturer instructions.

Spectral Imaging and proliferation quantification

Specimens were observed with a Leica BM5000 microscope equipped with plan apochromatic objectives (Leica Microsystems, Wetzlar, Germany). From all IHC triple stained slides, multispectral data sets of five random fields with Ki67 positive nuclei at 200x were acquired using a Nuance imaging system (PerkinElmer/Caliper Life Science, Hopkinton, MA). Spectral libraries were created acquiring spectra from 420-720 nm at 20 nm intervals from single-staining with DAB, Vector Blue, Vector Red and Hematoxylin. Spectral data sets from triple staining and control slides were acquired at the same wavelengths. To analyze the frequency of proliferating hepatocytes, MSI data sets were analyzed with InForm 1.4 image analysis software (PerkinElmer/Caliper Life Science) as earlier described for proliferating hepatocytes in rabbit liver by Van der Loos *et al.* [50]. The learn-by-example interface from the software segments hepatocytic and sinusoidal tissue compartments. Next, the number of proliferating hepatocytes by analyzing the number of cells in the hepatocytic tissue compartment with co-expression for cytoplasmic CK18 (Vector Red) and nuclear Ki67 (Vector Blue) was calculated. For comparison and validation of the automated procedure, two observers independently manually counted all Ki67-positive hepatocytes in the images which were used to create the algorithm.

Western blot analysis for detection of ApoB100 protein

Murine plasma proteins from 8 wk p.i. (0.1 µl) were separated by electrophoresis on a 3–8% Tris-Actetate gel (Invitrogen) and blotted onto a 0.45-µm nitrocellulose

membrane (Invitrogen). The blot was incubated with a 1:2,000 dilution of a rabbit polyclonal anti-ApoB antibody (ab31992; Abcam, Cambridge, UK), followed by incubation with a 1:2,000 dilution of goat anti-rabbit antibody conjugated to horseradish peroxidase (P0448; Dako, Glostrup, Denmark). Antibody binding was detected by the Lumi-LightPLUS chemiluminescent detection kit (Roche Diagnostics, Basel, Switzerland). Equal loading of protein samples was confirmed by Ponceau S staining (Sigma, St Louis, MO).

Cell culture and transfections

The human embryonic kidney 293T (HEK293T) cell line was maintained in Dulbecco's modified Eagle's medium (DMEM; Invitrogen, Carlsbad, CA) containing 10% fetal calf serum, 100 U/ml penicillin and 100 U/ml streptomycin, at 37°C and 5% CO_2. For small RNA next generation sequencing (NGS) cells were seeded in 6-well plates at a density of 4.5×10^5 cells per well in DMEM one day prior transfection. Transfections were performed with Lipofectamine 2000 reagent (Invitrogen, Carlsbad, CA) according to the manufacturer's instructions. RT reactions for siApoB expression *in vivo* and let-7a, let-7e, mir-26a, mir122, mir-133a, mir-199a and mir-221 expressions *in vitro* were performed with the TaqMan MicroRNA Reverse Transcription Kit (Applied Biosystems, Foster City, CA) using 10 ng RNA and 3 µl custom-made specific RT-stem-loop primer (Applied Biosystems, Foster City, CA) according to the manufacturer's instructions. Amplification of the beta actin gene was used as a RNA quality and loading control. siApoB copy number per cell was calculated based on the amplification plot of a dilution series of synthetic siApoB RNA standard (IDT, Coralville, IA). The trend line value of the standard line was used to calculate the siApoB copy number cell, assuming 15 pg RNA per cell [51]. Let-7a, let-7e, mir-26a, mir122, mir-133a, mir-199a and mir-221 levels were normalized to β-actin and the relative gene expression $2^{-\Delta\Delta Ct}$ method of Livak and Schmittgen was used for analysis of PCR data [52].

RNA isolation, quantitative real-time RT-PCR (qRT-PCR), siRNA and miRNA Taqman assay

To determine ApoB mRNA knockdown and siApoB expression *in vivo* , total RNA was isolated from frozen liver sections at 8 weeks p.i. using Trizol (Invitrogen, Carlsbad, CA). Genomic DNA (gDNA) was removed by DNase treatment using TURBO DNase (Ambion, Austin, TX). First strand cDNA was reverse transcribed using random hexamer primers with the Dynamo kit (Finnzymes, Espoo, Finland). Real time PCR amplification was performed with ApoB- and beta actin-specific primers. PCR reaction conditions were: 95°C for 10 min, followed by 40 cycles of 15 sec at 95°C and 1 min at 60°C. The assays were performed on ABI 7000 or ABI 7500 (Applied Biosystems, Foster City, CA). ApoB expression levels were normalized to beta actin as an internal control, and the relative gene expression $2^{-\Delta\Delta Ct}$ method of Livak and Schmittgen was used for analysis of PCR data [52].

Next Generation Sequencing (NGS) of small RNA and liver transcriptome

For NGS analysis of small RNA, HEK293T cells were transfected with 4 µg shApoB- or miApoB-expression plasmids using Lipofectamine 2000 reagent and total RNA was isolated from cells 48 hr post-transfection using Trizol (Invitrogen, Carlsbad, CA) according to the manufacturer's protocol. Small RNA sequencing libraries were generated using high-quality total RNA as input and the NEXTflex Small RNA Sequencing kit (Bioo Scientific, USA). Briefly, the small RNA species were subjected to ligation with 3' and 5' RNA adapters, first strand reverse transcription, and PCR amplification. Sample-specific barcodes were introduced in the PCR step. The PCR products were separated on TBE-PAGE electrophoresis and the expected band around 140-160bp was recovered for each sample. The resulting sequencing libraries were quantified on a BioAnalyzer (Agilent). The libraries were multiplexed, clustered, and sequenced on an Illumina HiSeq 2000 (TruSeq v3 chemistry) with a single-read 36 cycles sequencing protocol and indexing. The sequencing run was analyzed with the Illumina CASAVA pipeline (v1.8.0), with demultiplexing based on sample-specific barcodes. The raw sequencing data produced was processed removing the sequence reads which were of too low quality (only "passing filter" reads were selected), and discarding reads that aligned against the PhiX control. In total, we generated 16016701 reads for sample miApoB, and 15843150 reads for sample shApoB. The NGS small RNA raw data set was analyzed using the CLC_bio genomic workbench (CLC Bio, Aarhus, Denmark). The obtained reads were adaptor-trimmed, which decreased the average read size from ~36bp to ~25bp. The custom adapter sequenced used for trimming all the bases extending 5' was: GTGACTGGAGTTCCTTGGCACCCGAGAATTCCA. All reads containing ambiguity N symbols, reads shorter than 15 nt, longer than 55 nt in length and reads represented less than 10 times were discarded. To relatively represent the expression counts for the small RNAs obtained in the experiment, reads per million (rpm) or percentage of reads based on the total number of reads matching the reference shApoB or miApoB sequence were calculated Finally, to identify the differences in cellular miRNA reads between the miApoB and shApoB samples the small RNA data sets were annotated to miRBase, Release 18 and grouped based on the mature miRNA sequences, the rpm were calculated and the fold change between miApoB and shApoB samples was calculated.

To analyze liver transcriptome, total RNA was isolated from frozen liver sections of representative animals at 8 weeks p.i. with AAV-shApoB, AAV-miApoB, AAV-shScr, AAV-miScr or PBS using Trizol (Invitrogen, Carlsbad, CA). RNA sequencing libraries for the Illumina sequencing platform were generated using high-quality RNA as input and the Illumina TrueSeq RNA v2 Sample preparation kit. Briefly, poly-A containing mRNA molecules were purified using poly-T oligo-attached magnetic beads. Following purification, the mRNA was fragmented via incubation for 5 min at 94°C with the

Illumina-supplied fragmentation buffer. The first strand of cDNA was next synthesized by reverse transcription using random oligo primers. Second-strand synthesis was conducted by incubation with RNase H and DNA polymerase I. The resulting double-stranded DNA fragments were subsequently endrepaired, and A-nucleotide overhangs were added by incubation with Taq Klenow lacking exonuclease activity. After the attachment of adaptor sequences, fragments were PCR-amplified using Illumina-supplied primers. The resulting sequencing libraries were quantified on a BioAnalyzer (Agilent). The libraries were multiplexed, clustered, and sequenced on an Illumina HiSeq 2000 (TruSeq v3 chemistry) with a single-read 36 cycles sequencing protocol and indexing. The sequencing run was analyzed with the Illumina CASAVA pipeline (v1.8.0), with demultiplexing based on sample-specific barcodes. The raw sequencing data produced was processed removing the sequence reads which were of too low quality (only "passing filter" reads were selected), and discarding reads that aligned against the PhiX control. Each read file (sample), in the FASTQ format, was individually aligned against the Mouse reference genome (15 May 2012 NCBI build 38.1) using CLC Bio- Genomic Workbench. The expression abundance for all genes was quantified using the reads per kilobase of exon model per million mapped reads (RPKM) measure [53]. Expression data was compared using Kal's Z-test with Bonferroni correction. Smith-Waterman algorithm was used to predict off-target genes in Mouse reference genome (15 May 2012 NCBI build 38.1) for the most abundant expressed variants of both passenger and guide strands of shApoB and miApoB. Small RNA and transcriptome NGS was carried out by Macrogen Inc. (Seoul, Korea).

The NGS data discussed in this publication have been deposited in NCBI's Gene Expression Omnibus [54] and are accessible through GEO Series accession number GSE39187 (http://www.ncbi.nlm.nih.gov/geo/query/acc.cgi?acc=GSE39187).

Functional analysis

For the ApoB functional interactions, online database resource search tool for the retrieval of interacting genes (STRING) was used, which allowed annotation of functional interactions of ApoB protein in cell (http://string-db.org/) [55]. For the genes that were identified RPKM gene expression values were compared to PBS or shScr and miScrand and fold change between sample and control was calculated. Upregulation of genes (fold change > 1,5) was marked in green and downregulations (fold change < -1,5) were marked in red.

For the transcriptome analysis, RPKM gene expression values were compared to PBS using Kal's test (Z-test) with Bonferroni correction. All genes that changed significantly ($p<0,05$) and were expressed higher than 0,1 (RPKM>0,1) were included in the further analysis. Functional analysis of the significantly changing genes was done with the functional annotation tool DAVID (Database for Annotation, Visualization and Integrated Discovery v6.7; National Institute of Allergy and Infectious Diseases,

NIH) that allows finding combination of genes under study with respect to a reference list [56,57]. The annotations were done simultaneously with the reference to Gene Ontology databases (GOTERM_BP_FAT and GOTERM_MF_FAT, www.geneontology.org) and to KEGG pathway database (KEGG_PATHWAY; www.genome.ad.jp/kegg/pathway.html). The redundancy in the gene list was manually analyzed and significant annotations were grouped in 8 categories and the percentage of genes in each category was calculated with reference to all genes that were annotated in DAVID analysis.

Supplementary material

Table S1. Description of histological scoring system of liver morphology

Macrovesicular steatosis Grade	<5% 5%-33% 34%-66% >67%	0 1 2 3
Microvesicular steatosis grade	<5% 5%-33% 34%-66% >67%	0 1 2 3
Ballooning Grade	none few cells prominent ballooning	0 1 2
Lobular Inflammation assessment of all foci per 10x objective	no foci <2 2-4 >4	0 1 2 3
Portal inflammation arbitrary	absent mild moderate severe	0 1 2 3
Sinusoidal dilatation Grade	absent mild; involving ≤ 1/3 of the (centro-) lobular area moderate; involving 1/3-2/3 of the liver parenchyma severe; involving > 2/3 of the liver parenchyma	0 1 2 3
Parenchymal necrosis grade	absent affecting <25% of the parenchyma affecting 25%-50% of the parenchyma affecting 51-75% of the parenchyma affecting >75% of the parenchyma	0 1 2 3 4
Hepatocellular mitosis Per 8 HPF	not present <2 foci 2-4 5-10 >10	0 1 2 3 4
Councilman bodies Per 10x objective	not present <2 foci 2-4 5-10 >10	0 1 2 3 4

Table S2. Changes in miRNA expression in shApoB versus miApoB samples. Cellular small RNA data sets were annotated to miRBase (release 18, November 2011) and grouped based on the mature miRNA sequences and reads per million (rpm) were calculated. For each miRNA, proportion of the reads and the fold change between shApoB and miApoB (rpm) samples were calculated. If the proportion of the given miRNA from the shApoB sample was lower than proportion of the same miRNA in the miApoB (rpm) sample then this was represented by the negative value. Kal's test (Z-test) with Bonferroni correction was used to compare the proportions of miRNAs in the miApoB (rpm) versus shApoB sample. **p < 0.01

Name	miApoB (rpm)	shApoB (rpm)	Fold change	p value
mir-4521	2829	15	-188,60	0
mir-378c	5146	51	-100,90	<0,01**
mir-4326	462	13	-35,54	0
mir-720	688	52	-13,23	0
mir-3182	171	13	-13,15	0
mir-4454	68347	5281	-12,94	0
mir-4791	116	12	-9,67	0
mir-877	910	106	-8,58	<0,01**
mir-483	91	11	-8,27	0
mir-1280	2104	264	-7,97	0
mir-4286	15254	2127	-7,17	0
mir-4484	691	106	-6,52	<0,01**
mir-1260a	15492	2454	-6,31	0
mir-1260b	2977	494	-6,03	0
mir-4455	592	100	-5,92	<0,01**
mir-452	176	31	-5,68	<0,01**
mir-3127	51	10	-5,10	<0,01**
mir-1250	203	40	-5,08	0
mir-1299	176	35	-5,03	0
mir-4713	208	42	-4,95	0
mir-585	54	11	-4,91	<0,01**
mir-193a	302	63	-4,79	<0,01**
mir-551b	67	14	-4,79	<0,01**
mir-365a	83	18	-4,61	<0,01**
mir-1246	1872	406	-4,61	<0,01**
mir-2110	470	105	-4,48	<0,01**
mir-1268a	110	25	-4,40	0
mir-1247	78	18	-4,33	<0,01**
mir-3176	121	28	-4,32	0
mir-4473	82	19	-4,32	<0,01**
mir-1268b	116	27	-4,30	0
mir-4485	216	51	-4,24	0
mir-760	201	50	-4,02	<0,01**
mir-1227	44	11	-4,00	<0,01**
mir-210	11150	2794	-3,99	<0,01**
mir-1262	95	24	-3,96	<0,01**
mir-627	87	22	-3,95	<0,01**
mir-4470	135	36	-3,75	0

Table S2. continued

Name	miApoB (rpm)	shApoB (rpm)	Fold change	p value
mir-1261	52	14	-3,71	<0,01**
mir-3074	104	30	-3,47	<0,01**
mir-378i	1134	329	-3,45	<0,01**
mir-29c	339	100	-3,39	0
mir-504	81	24	-3,38	<0,01**
mir-3615	300	89	-3,37	0
mir-4746	168	50	-3,36	<0,01**
mir-491	341	103	-3,31	0
mir-505	33	10	-3,30	<0,01**
mir-193b	125	38	-3,29	<0,01**
mir-1290	178	56	-3,18	<0,01**
mir-1269b	1747	566	-3,09	<0,01**
mir-320c-1/2	188	61	-3,08	<0,01**
mir-1914	52	17	-3,06	<0,01**
mir-151b	326	108	-3,02	<0,01**
mir-146a	655	222	-2,95	<0,01**
mir-326	863	293	-2,95	<0,01**
mir-320a	58157	19821	-2,93	0
mir-4687	92	32	-2,88	<0,01**
mir-1249	180	63	-2,86	<0,01**
mir-573	37	13	-2,85	<0,01**
mir-3928	60	22	-2,73	<0,01**
mir-940	245	91	-2,69	<0,01**
mir-671	6969	2624	-2,66	0
mir-92b	69	26	-2,65	<0,01**
mir-3620	559	213	-2,62	<0,01**
mir-211	26	10	-2,60	<0,01**
mir-375	1962	762	-2,57	<0,01**
mir-328	783	311	-2,52	<0,01**
mir-1343	170	68	-2,50	<0,01**
mir-1180	4978	1995	-2,50	0
mir-4423	52	21	-2,48	<0,01**
mir-3136	95	39	-2,44	<0,01**
mir-148a	2964	1231	-2,41	<0,01**
mir-1269a	12	5	-2,40	<0,01**
mir-378d-1/2	1454	611	-2,38	<0,01**
mir-24-2	45	19	-2,37	<0,01**
mir-423	11893	5028	-2,37	0
mir-1255a	90	39	-2,31	<0,01**
mir-642b	46	20	-2,30	<0,01**
mir-501	376	164	-2,29	<0,01**
mir-2277	187	82	-2,28	<0,01**

Table S2. continued

Name	miApoB (rpm)	shApoB (rpm)	Fold change	p value
mir-942	410	182	-2,25	0
mir-133a-1/2	90	40	-2,25	<0,01**
mir-22	78	35	-2,23	<0,01**
mir-9-1/2/3	18571	8401	-2,21	<0,01**
mir-145	42	19	-2,21	<0,01**
mir-3943	24	11	-2,18	<0,01**
mir-574	392	180	-2,18	<0,01**
mir-1468	26	12	-2,17	<0,01**
mir-320d-1/2	93	43	-2,16	<0,01**
mir-339	18019	8358	-2,16	<0,01**
mir-3173	47	22	-2,14	<0,01**
mir-185	19368	9097	-2,13	<0,01**
let-7b	516	243	-2,12	<0,01**
mir-330	328	157	-2,09	<0,01**
let-7d	243	117	-2,08	<0,01**
mir-27a	165	80	-2,06	<0,01**
mir-28	1355	657	-2,06	<0,01**
mir-422a	101	49	-2,06	<0,01**
mir-296	358	175	-2,05	<0,01**
mir-744	3109	1523	-2,04	<0,01**
mir-1306	128	63	-2,03	<0,01**
mir-138-1/2	731	360	-2,03	<0,01**
mir-589	1938	974	-1,99	0
mir-378a	2067	1040	-1,99	<0,01**
mir-425	17334	8748	-1,98	0
mir-378f	537	275	-1,95	0
mir-151a	18918	9890	-1,91	0
mir-106b	18130	9486	-1,91	0
mir-542	107	56	-1,91	<0,01**
let-7c	3092	1628	-1,90	<0,01**
mir-629	5082	2682	-1,89	0
mir-708	3957	2093	-1,89	0
mir-320b-1/2	706	374	-1,89	0
mir-769	17874	9484	-1,88	0
mir-551a	139	74	-1,88	<0,01**
mir-345	7651	4077	-1,88	0
mir-29b-2	75	40	-1,88	<0,01**
mir-3944	298	160	-1,86	0
mir-1303	24	13	-1,85	<0,01**
mir-590	230	126	-1,83	<0,01**
mir-25	1151	635	-1,81	0
mir-5008	79	44	-1,80	<0,01**

Table S2. continued

Name	miApoB (rpm)	shApoB (rpm)	Fold change	p value
let-7i	2615	1458	-1,79	0
mir-152	4037	2334	-1,73	0
mir-1266	38	22	-1,73	<0,01**
mir-98	797	462	-1,73	0
mir-129-1/2	1111	649	-1,71	0
mir-27b	195	114	-1,71	<0,01**
mir-34a	16816	9849	-1,71	0
mir-628	46	27	-1,70	<0,01**
mir-548ab	100	59	-1,69	<0,01**
mir-1910	44	26	-1,69	<0,01**
mir-103a-2	1171	694	-1,69	0
mir-146b	11389	6806	-1,67	0
mir-4421	35	21	-1,67	<0,01**
mir-497	633	380	-1,67	0
mir-324	1118	682	-1,64	0
mir-194-1/2	7139	4362	-1,64	0
mir-139	36	22	-1,64	<0,01**
let-7g	19609	12000	-1,63	0
mir-7-1/2/3	123822	76717	-1,61	0
mir-1285-2	534	331	-1,61	<0,01**
mir-31	4700	2916	-1,61	<0,01**
mir-1307	1418	880	-1,61	0
mir-616	32	20	-1,60	<0,01**
mir-486	28634	17950	-1,60	0
mir-132	408	258	-1,58	0
mir-1286	17	11	-1,55	0,11
mir-93	49978	32504	-1,54	0
mir-101-2	53740	34952	-1,54	0
mir-217	39	26	-1,50	<0,01**
mir-3065	240	161	-1,49	<0,01**
mir-346	392	263	-1,49	<0,01**
mir-605	59	40	-1,48	<0,01**
mir-502	63	43	-1,47	<0,01**
mir-550a-1/2	328	225	-1,46	<0,01**
mir-103a-1	53323	37037	-1,44	0
mir-181c	1037	721	-1,44	<0,01**
mir-874	6180	4320	-1,43	<0,01**
mir-484	22583	15790	-1,43	0
mir-503	2035	1445	-1,41	0
mir-128-1/2	5142	3663	-1,40	0
mir-4677	53	38	-1,39	<0,01**
mir-188	236	170	-1,39	<0,01**

Table S2. continued

Name	miApoB (rpm)	shApoB (rpm)	Fold change	p value
mir-5585	54	39	-1,38	<0,01**
mir-548j	22	16	-1,38	0,13
mir-3130-1/2	59	43	-1,37	<0,01**
mir-17	208165	151899	-1,37	0
mir-204	177	130	-1,36	<0,01**
mir-218-1/2	32185	23741	-1,36	0
mir-186	79819	58927	-1,35	0
mir-548an	125	93	-1,34	<0,01**
mir-548aa-1/2	165	124	-1,33	<0,01**
mir-149	7087	5329	-1,33	0
mir-30b	15097	11479	-1,32	<0,01**
mir-1252	13	10	-1,30	0,29
mir-500a	822	638	-1,29	<0,01**
mir-181b-1/2	4027	3128	-1,29	<0,01**
mir-182	53787	42345	-1,27	0
mir-191	156325	123307	-1,27	0
mir-92a-1	694	548	-1,27	<0,01**
mir-1305	29	23	-1,26	0,14
let-7a-1/2/3	17874	14242	-1,26	0,00
mir-3909	257	205	-1,25	<0,01**
mir-576	259	207	-1,25	<0,01**
mir-1915	15	12	-1,25	0,30
mir-3662	30	24	-1,25	0,14
mir-4467	15	12	-1,25	0,30
mir-935	572	459	-1,25	<0,01**
mir-192	24042	19301	-1,25	0
mir-3140	66	53	-1,25	<0,01**
mir-548f-1/2/3/4	353	286	-1,23	<0,01**
mir-196a-1/2	16566	13441	-1,23	0
mir-130b	3712	3073	-1,21	0
mir-5699	65	54	-1,20	<0,01**
mir-3157	49	41	-1,20	0,09
mir-625	247	208	-1,19	<0,01**
mir-3611	38	32	-1,19	0,14
mir-891a	13	11	-1,18	0,40
mir-125b-1/2	12077	10462	-1,15	<0,01**
mir-598	637	557	-1,14	<0,01**
mir-618	714	629	-1,14	<0,01**
let-7e	2670	2361	-1,13	<0,01**
mir-362	13573	12026	-1,13	<0,01**
mir-1292	89	79	-1,13	0,05
mir-556	45	40	-1,13	0,17

Table S2. continued

Name	miApoB (rpm)	shApoB (rpm)	Fold change	p value
mir-219-1	292	263	-1,11	<0,01**
mir-18a	20829	18939	-1,10	<0,01**
mir-26b	6658	6060	-1,10	0
mir-1257	213	195	-1,09	<0,01**
mir-30a	54010	49483	-1,09	0
mir-489	13	12	-1,08	0,52
mir-580	65	60	-1,08	0,15
mir-652	169	157	-1,08	<0,01**
mir-651	136	127	-1,07	<0,01**
mir-33a	153	143	-1,07	<0,01**
mir-4792	291	273	-1,07	<0,01**
mir-499a	37	35	-1,06	0,32
mir-1301	1479	1409	-1,05	<0,01**
mir-19b-1	581	555	-1,05	<0,01**
mir-190b	24	23	-1,04	0,45
mir-34c	2365	2286	-1,03	<0,01**
mir-532	4923	4763	-1,03	<0,01**
mir-195	957	930	-1,03	<0,01**
mir-16-1/2	30082	29378	-1,02	0
mir-181d	1926	1883	-1,02	<0,01**
mir-2355	359	352	-1,02	<0,01**
mir-20b	52	51	-1,02	0,31
mir-1287	64	63	-1,02	0,27
mir-449a	70	69	-1,01	0,25
mir-99b	726091	721490	-1,01	0
mir-30d	57480	57397	-1,00	<0,01**
let-7f-1/2	11474	11467	-1,00	0
mir-23b	10	10	1,00	0,69
mir-133b	4	4	1,00	0,80
mir-3150a	18	18	1,00	0,59
mir-3174	12	12	1,00	0,66
mir-222	171	173	1,01	0,12
mir-190a	160	162	1,01	0,13
mir-1296	1177	1197	1,02	<0,01**
mir-641	434	444	1,02	<0,01**
mir-455	629	647	1,03	<0,01**
mir-338	148	153	1,03	0,20
mir-4786	29	30	1,03	0,58
mir-181a-1/2	11483	11939	1,04	<0,01**
mir-30e	128424	133609	1,04	0
mir-424	6753	7108	1,05	<0,01**
mir-140	1893	2035	1,08	<0,01**

Table S2. continued

Name	miApoB (rpm)	shApoB (rpm)	Fold change	p value
mir-454	128	138	1,08	0,40
mir-215	681	738	1,08	0,06
mir-1298	10	11	1,10	0,85
mir-26a-1/2	41047	46025	1,12	0
mir-21	101618	116255	1,14	0
mir-15a	4445	5096	1,15	<0,01**
mir-199a-1/2	13	15	1,15	0,92
mir-1278	13	15	1,15	0,92
mir-3613	3708	4324	1,17	0,25
mir-107	1545	1833	1,19	0,81
mir-15b	3097	3679	1,19	0,77
mir-196b	15868	18894	1,19	0,65
mir-5094	189	226	1,20	1,00
mir-3938	128	154	1,20	0,96
mir-450a-1/2	3134	3804	1,21	0,55
mir-125a	30443	36957	1,21	0,06
mir-548l	22	27	1,23	0,93
mir-548ag-1/2	79	97	1,23	0,86
mir-10b	1644920	2065460	1,26	0
mir-1-1/2	205	261	1,27	0,51
mir-4517	54	70	1,30	0,66
mir-548k	995	1293	1,30	0,05
mir-548t	13	17	1,31	0,81
mir-106a	1183	1572	1,33	<0,01**
mir-660	926	1236	1,33	<0,01**
mir-30c-1/2	24713	33382	1,35	0
mir-561	225	304	1,35	0,17
mir-421	1791	2438	1,36	<0,01**
mir-548e	566	787	1,39	<0,01**
mir-10a	3814906	5321388	1,39	0
mir-4652	15	21	1,40	0,64
mir-548h-1/2/3/4/5	144	204	1,42	0,12
mir-221	8370	12046	1,44	0
mir-212	358	526	1,47	<0,01**
mir-148b	146	215	1,47	0,05
mir-548n	61	90	1,48	0,21
mir-183	62636	92828	1,48	0
mir-2964a	16	24	1,50	0,48
mir-340	6854	10352	1,51	0
mir-548d-1/2	488	744	1,52	<0,01**
mir-331	118	182	1,54	<0,01**
mir-99a	155658	241891	1,55	0

Table S2. continued

Name	miApoB (rpm)	shApoB (rpm)	Fold change	p value
mir-1276	25	39	1,56	0,30
mir-450b	1194	1865	1,56	<0,01**
mir-2467	116	182	1,57	<0,01**
mir-548z	15	24	1,60	0,38
mir-100	471	764	1,62	<0,01**
mir-5683	35	57	1,63	0,15
mir-301a	149	249	1,67	<0,01**
mir-548w	100	173	1,73	<0,01**
mir-548o	76	133	1,75	<0,01**
mir-101-1	13	23	1,77	0,26
mir-582	495	885	1,79	<0,01**
mir-548aq	20	36	1,80	0,14
mir-941-1/2/3/4	3125	5688	1,82	<0,01**
mir-378g	221	416	1,88	<0,01**
mir-24-1	14	28	2,00	0,11
mir-199b	183	376	2,05	<0,01**
mir-548y	957	2069	2,16	0
mir-20a	62666	139055	2,22	<0,01**
mir-95	219	500	2,28	<0,01**
mir-548b	151	365	2,42	<0,01**
mir-1271	5483	13299	2,43	0
mir-579	22	54	2,45	0,00
mir-301b	271	703	2,59	<0,01**
mir-361	2307	5985	2,59	<0,01**
mir-1284	15	42	2,80	0,00
mir-96	27894	91513	3,28	<0,01**
mir-374b	448	1537	3,43	0,00
mir-126	115	399	3,47	<0,01**
mir-577	1403	5197	3,70	0
mir-624	59	234	3,97	0
mir-374a	486	1934	3,98	<0,01**
mir-548c/2/am	61	243	3,98	0
mir-32	139	626	4,50	0
mir-549	11	76	6,91	<0,01**
mir-548i-1/2/3/4	65	542	8,34	<0,01**
mir-18b	40	0	NA	<0,01**
mir-29a	39	0	NA	<0,01**
mir-124-1/2/3	53	0	NA	<0,01**
mir-135b	0	10	NA	<0,01**
mir-147b	11	0	NA	<0,01**
mir-153-1/2	0	16	NA	<0,01**
mir-184	12	0	NA	<0,01**

Table S2. continued

Name	miApoB (rpm)	shApoB (rpm)	Fold change	p value
mir-203	13	0	NA	<0,01**
mir-216a	0	11	NA	<0,01**
mir-216b	10	0	NA	<0,01**
mir-342	51	0	NA	<0,01**
mir-378b	43	0	NA	<0,01**
mir-449b	0	6	NA	<0,01**
mir-500b	55	0	NA	<0,01**
mir-548a-1/2	0	16	NA	<0,01**
mir-548a-3	10	0	NA	<0,01**
mir-548ad	0	5	NA	<0,01**
mir-548al	0	6	NA	<0,01**
mir-548au	0	16	NA	<0,01**
mir-548g/x/2	10	0	NA	<0,01**
mir-548u	0	10	NA	<0,01**
mir-550a-3	12	0	NA	<0,01**
mir-592	27	0	NA	<0,01**
mir-597	17	0	NA	<0,01**
mir-615	10	0	NA	<0,01**
mir-643	10	0	NA	<0,01**
mir-653	83	0	NA	<0,01**
mir-664	48	0	NA	<0,01**
mir-766	0	11	NA	<0,01**
mir-887	15	0	NA	<0,01**
mir-888	0	11	NA	<0,01**
mir-934	13	0	NA	<0,01**
mir-937	17	0	NA	<0,01**
mir-1255b-1/2	16	0	NA	<0,01**
mir-1272	10	0	NA	<0,01**
mir-1273c	38	0	NA	<0,01**
mir-1273d	10	0	NA	<0,01**
mir-1275	128	0	NA	0
mir-1285-1	12	0	NA	<0,01**
mir-1288	35	0	NA	<0,01**
mir-1294	0	12	NA	<0,01**
mir-1295a	34	0	NA	<0,01**
mir-1304	194	0	NA	0
mir-3131	20	0	NA	<0,01**
mir-3158-1/2	14	0	NA	<0,01**
mir-3178	88	0	NA	0
mir-3184	12	0	NA	<0,01**
mir-3196	16	0	NA	<0,01**
mir-3200	13	0	NA	<0,01**

Table S2. continued

Name	miApoB (rpm)	shApoB (rpm)	Fold change	p value
mir-3605	0	10	NA	<0,01**
mir-3661	14	0	NA	<0,01**
mir-3676	32	0	NA	<0,01**
mir-3691	11	0	NA	<0,01**
mir-3912	0	13	NA	<0,01**
mir-4461	39	0	NA	<0,01**
mir-4497	36	0	NA	<0,01**
mir-4523	25	0	NA	<0,01**
mir-4645	12	0	NA	<0,01**
mir-4664	13	0	NA	<0,01**
mir-4665	11	0	NA	<0,01**
mir-4742	11	0	NA	<0,01**
mir-4804	11	0	NA	<0,01**
mir-5100	88	0	NA	0
mir-5187	10	0	NA	<0,01**
mir-5579	0	22	NA	<0,01**
mir-5698	11	0	NA	<0,01**
mir-5701-1/2	61	0	NA	<0,01**

Table S3. Functional categorization of changes in shApoB injected animal. RPKM gene expression values were compared to shScr using Kal's test (Z-test) with Bonferroni correction. All genes that changed significantly in AAV-shApoB-injected animal ($p<0,05$) and were expressed higher than 0,1 (RPKM>0,1) were included in the analysis. Functional analysis of the significantly changing genes was done with the functional annotation tool DAVID (Database for Annotation, Visualization and Integrated Discovery v6.7; National Institute of Allergy and Infectious Diseases, NIH) that allows finding combination of co-ocurrent genes under study with respect to a reference list [49,50]. The annotations were done simultaneously with the reference to Gene Ontology databases (GOTERM_BP_FAT and GOTERM_MF_FAT, www.geneontology.org)) and to KEGG pathway database (KEGG_PATHWAY; www.genome.ad.jp/kegg/pathway.html). The redundancy in the gene list was manually analyzed and significant annotations were grouped in 8 categories and the percentage of genes in each category was calculated with reference to all genes that were annotated in DAVID analysis.

Genes found	Significant genes	Function annotations to GO, KEGG
	shApoB analysis	
	downregulated	
		Response to stimuli
11	KNG1, SERPINA3K, OAZ1, SERPINA1B, SERPINA6, SERPINA1A, SERPINF2, SERPINA1D, SERPINA1C, SERPINC1, SERPINA1E	BP:0034097~response to cytokine stimulus BP:0043434~response to peptide hormone stimulus MF:0004867~serine-type endopeptidase inhibitor activity BP:0009725~response to hormone stimulus KEGG: 04610:Complement and coagulation cascades
16	CYP2D9, CYP2C37, CYP2F2, CYP2C44, CYP2C67, CYP2C29, CYP4F14, CYP2E1, CYP1A2, CYB5, FTH1, TDO2, PGRMC1, CYP2A5, CAT, HPD	GO:0020037~heme binding GO:0046906~tetrapyrrole binding GO:0005506~iron ion binding GO:0009055~electron carrier activity
8	SERPINA3K, SERPINA1B, SERPINA1A, ALB, APOE, SERPINA1D, SERPINA1C, SERPINA1E	BP:0009719~response to endogenous stimulus BP:0010033~response to organic substance
8	SERPINA3K, SERPINA1B, SERPINA1A, SERPINA1D, SERPINA1C, ALDOB, SERPINA1E, AGXT	MF:0004866~endopeptidase inhibitor activity MF:0030414~peptidase inhibitor activity MF:0004857~enzyme inhibitor activity
		Lipid metabolism and transport
8	APOA2, APOB, APOE, APOC4, APOC3, APOC1, APOC2	MF:0006869~lipid transport MF:0010876~lipid localization MF:0042157~lipoprotein metabolic process

upregulated		
		Lipid metabolism and transport
2	RDH9, LPL, APOA4	MF:0042157~lipoprotein metabolic process BP:0008610~lipid biosynthetic process GO:0008202~steroid metabolic process
		Drug metabolism
12	CYP2C70, GSTM1, GSTA1, GSTA2, GSTM2, UGT1A9, GSTM3, GSTM4, CYP3A11, UGT2B1, UGT2B5, EPHX1	KEGG: 00982:Drug metabolism
8	CYP2C70, CYP2A12, UGT1A9, CYP4A12A, CYP3A11, UGT2B1, UGT2B5, CYP2A4	mmu00982:Drug metabolism mmu00830:Retinol metabolism GO:0070330~aromatase activity mmu00983:Drug metabolism
		Inflammation
9	C8A, SERPINA3N, SAA2, SERPINA1B, HC, C3, SERPINA1A, SAA1, AHSG	BP:0002526~acute inflammatory response BP:0006954~inflammatory response BP:0006953~acute-phase response
7	SERPINA3N, PZP, SERPINA7, HC, C3, ITIH4, AHSG	MF:0004866~endopeptidase inhibitor activity MF:0030414~peptidase inhibitor activity MF:0004857~enzyme inhibitor activity MF:0004867~serine-type endopeptidase inhibitor activity
		Cell growth and death
7	C8A, GPX1, LYZ2, KRT18, HC, KRT8, CLU	BP:0019835~cytolysis BP:0008219~cell death BP:0016265~death
		Response to stimuli
8	EGR1, FOS, APOA2, GCK, HPX, GPX4, JUN, NR4A1	BP:0010033~response to organic substance BP:0010604~positive regulation of macromolecule metabolic process BP:0051789~response to protein stimulus BP:0051173~positive regulation of nitrogen compound metabolic process BP:0010033~response to organic substance
		MAPK singalling pathway
5	FOS, DUSP1, JUN, NR4A1, DUSP6	KEGG:04010 MAPK signaling pathway

Table S4. Functional categorization of changes in miApoB injected animals. RPKM gene expression values were compared to miScr using Kal's test (Z-test) with Bonferroni correction. All genes that changed significantly in AAV-miApoB-injected animal ($p<0,05$) and were expressed higher than 0,1 (RPKM>0,1) were included in the analysis. Functional analysis of the significantly changing genes was done with the functional annotation tool DAVID (Database for Annotation, Visualization and Integrated Discovery v6.7; National Institute of Allergy and Infectious Diseases, NIH) that allows finding combination of co-ocurrent genes under study with respect to a reference list [49,50]. The annotations were done simultaneously with the reference to Gene Ontology databases (GOTERM_BP_FAT and GOTERM_MF_FAT, www.geneontology.org)) and to KEGG pathway database (KEGG_PATHWAY; www.genome.ad.jp/kegg/pathway.html). The redundancy in the gene list was manually analyzed and significant annotations were grouped in 8 categories and the percentage of genes in each category was calculated with reference to all genes that were annotated in DAVID analysis.

Genes found	Significant genes	Function annotations to GO, KEGG
		miApoB analysis
		downregulated
		Drug metabolism
22	GSTA1, GSTA2, GSTA4, CYP2C54, CYP2C44, CYP2C67, UGT2B1, CYP1A2, GSTM1, CYP2A12, GSTM2, GSTM3, UGT1A9, GSTM4, UGT2B34, FMO1, ADH4, CYP2A5, UGT2B5, CYP2D26, MGST1, CYP2A4	KEGG:00982:Drug metabolism KEGG:00980:Metabolism of xenobiotics by cytochrome P450 KEGG: 00480:Glutathione metabolism
10	GSTM1, GSTA1, GSTA2, GSTM2, GSTM3, GSTM4, GSTA4, GM3776, MGST1	MF:0004364~glutathione transferase activity MF:0016765~transferase activity, transferring alkyl or aryl (other than methyl) groups
36	SC5D, CYP2C44, CYP2F2, HSD3B7, CYP2C67, HSD3B5, UGDH, FTH1, AKR1C14, RDH9, CYP2A12, TDO2, CYP4A12A, FMO1, ADH4, HMOX1, BC089597, HSD17B6, IDH1, DMGDH, CAT, HPD, SCD1, CYP2C54, FADS1, FADS2, CYP1A2, CYP7B1, CYP27A1, H6PD, HSD11B1, CYP2A5, AOX3, CYP2D26, HPGD, CYP2A4	BP:0055114~oxidation reduction BP:0008202~steroid metabolic process MF:0016229~steroid dehydrogenase activity
7	G6PC, UGT1A9, UGT2B34, UGT2B1, UGT2B5, UGDH, UGP2	KEGG:00500:Starch and sucrose metabolism KEGG:00140:Steroid hormone biosynthesis KEGG:00053:Ascorbate and aldarate metabolism KEGG:00983:Drug metabolism KEGG:00150:Androgen and estrogen metabolism KEGG:00232:Caffeine metabolism

		Lipid metabolism and transport
6	APOB, APOA4, LDLR, PCSK9, APOM, APOBEC2	MF:0006869~lipid transport MF:0010876~lipid localization
11	ABCG8, NPC1, G6PC, APOB, FECH, LDLR, MLXIPL, PCSK9, SCARB1, NR5A2, MTP	GO:0055092~sterol homeostasis GO:0055088~lipid homeostasis
12	RDH9, GC, CYP7B1, G6PC, SC5D, SERPINA6, HSD3B7, HSD3B5, INSIG1, HSD11B1, HSD17B6, CAT	BP:0008610~lipid biosynthetic process GO:0008202~steroid metabolic process
10	G6PC, APOB, INSIG2, ANG, SERINC1, INSIG1, PCSK9, CAT, FABP5, MTP	GO:0046486~glycerolipid metabolic process GO:0006641~triglyceride metabolic process
7	SC5D, ELOVL3, FADS1, ELOVL2, FASN, FADS2, SC4MOL	GO:0006633~fatty acid biosynthetic process
		Ion binding and transport
26	SC5D, FTL1, CYP2F2, CYP2C44, CYP2C67, TRF, FTH1, CYP2A12, TDO2, CYP4A12A, HMOX1, PGRMC1, CAT, HPD, SCD1, CYP2C54, FADS1, FADS2, CYP1A2, CYP7B1, CYP27A1, CYP2A5, AOX3, CYP2D26, SLC40A1, CYP2A4	MF:0005506~iron ion binding MF:0020037~heme binding MF:0046906~tetrapyrrole binding MF:0016712~oxidoreductase activity MF:0070330~aromatase activity MF:0009055~electron carrier activity
		Response to sitmuli
18	KNG1, PZP, MUG1, C3, SERPING1, SERPINA3K, PZP, SERPINA3N, SERPINA3M, SERPINA1B, SERPINA6, SERPINA1D, SERPINA1C, ITIH4, SERPINC1, ITIH2, SERPIND1, ITIH3	BP:0009611~response to wounding BP:0034097~response to cytokine stimulus BP:0050817~coagulation BP:0007596~blood coagulation BP:0007599~hemostasis BP:0042060~wound healing BP:0009725~response to hormone stimulus BP:0050878~regulation of body fluid levels BP:0009719~response to endogenous stimulus
8	SCD1, CYP4A12A, ACSL1, CYP27A1, FADS2, FABP5, CPT1A, PCK1	mmu03320:PPAR signaling pathway

STable S4. continued

Genes found	Significant genes	Function annotations to GO, KEGG
		miApoB analysis
		upregulated
		Oxidoreductase activity and processes
33	ATP5D, ATP5E, NDUFB6, NDUFB7, NDUFB9, COX7C, COX5A, COX5B, UQCRQ, ATP5G3, NDUFB2, NDUFS5, UQCR10, UQCR11, COX6B1, ATP5L, ATP5O, ATP5H, NDUFS2, ATP5K, ATP5J, NDUFA4, NDUFA5, NDUFA2, ATP5J2, NDUFA3, NDUFB10, COX4I1, NDUFC1, COX6C, UQCRH, COX6A1, UQCRB	KEGG:00190:Oxidative phosphorylation BP:0006091~generation of precursor metabolites and energy BP:0022900~electron transport chain BP:0055114~oxidation reduction
		Lipid metabolism and transport
7	CYP4A10, ACAA2, ADH1, CYP4A14, ACAA1A, ACAA1B, ALDH3A2	KEGG:00071:Fatty acid metabolism KEGG:03320:PPAR signaling pathway MF:0003988~acetyl-CoA C-acyltransferase activity GO:0006641~triglyceride metabolic process GO:0046486~glycerolipid metabolic process
11	APOA2, APOE, APOC4, APOC3, APOC1, LPL GPX1, PIGYL, PEMIT, SLC27A5	MF:0006869~lipid transport MF:0010876~lipid localization MF:0042157~lipoprotein metabolic process
18	CYB5R3, HSD17B11, EBP, PCTP, AMACR, APOC1, FDPS, AKR1C20, APOA2, APOA1, AKR1C6, APOE, APOF, SULT1A1, APOC3, PON1, LIPC, SLC27A5	GO:0008202~steroid metabolic process GO:0008203~cholesterol metabolic process
		Nucleobase, nucleoside and nucleotide biosynthetic processes
20	ATP5D, ATP5E, COX7C, COX4I1, COX5A, COX5B, UQCRQ, ATP5G3, COX6C, UQCR10, UQCR11, UQCRH, COX6B1, COX6A1, ATP5L, ATP5O, ATP5H, ATP5K, ATP5J, UQCRB	BP:0006754~ATP biosynthetic process BP:0046034~ATP metabolic process BP:0034654~nucleobase, nucleoside, nucleotide and nucleic acid biosynthetic process

Table S5. Comparison of lipid-related gene expression profiles in AAV-shApoB, AAV-miApoB and siApoB injected animals based on our NGS data and siApoB Taqman data from Tep *et al.* (48). For each entry the fold change between sample and respective negative control were calculated. If expression of a given gene in the sample was lower than expression in the negative control the fold change had a negative value.

Gene	AAV-shApoB	AAV-miApoB	siApoB
Aacs	-1,11	-1,29	-2,60
Acaca	-2,50	-1,55	-2,08
Acacb	-2,51	1,07	-4,81
Acat2	1,04	1,49	-2,14
Acly	-2,34	1,06	-1,75
Acsf2	-1,40	1,13	2,00
Acsl1	-1,62	-1,29	-1,26
Acsl3	-1,25	1,35	-1,85
Acsl4	-2,63	1,96	-2,02
Acsl5	-1,64	-1,13	-2,24
Acss2	-1,49	-1,18	-3,49
ActB	1,49	1,69	1,00
Adi1	1,24	1,20	-1,78
Agpat1	1,52	1,20	-1,27
Agpat2	-1,12	1,11	-1,67
Agpat3	-1,36	1,30	-1,67
Agpat4	1,04	1,26	10,00
Agpat5	2,12	1,63	-1,05
Agpat6	1,42	1,17	-1,25
Agpat9	1,90	1,67	-1,11
Angptl4	1,94	-1,22	-4,76
ApoA1	1,16	-1,13	-1,93
ApoB	-11,83	-3,12	-8,27
ApoC3	1,26	-1,63	-1,00
ApoE	1,50	-1,23	-1,08
Baat	-1,21	1,30	-1,39
Cds1	-1,93	1,08	-1,86
Chpt1	1,18	-1,13	-1,45
Cyb5r3	1,31	-1,49	-1,91
Cyp27a1	-1,54	-1,06	-1,77
Cyp39a1	-1,79	1,79	-3,00
Cyp46a1	1,46	-1,17	-1,27
Cyp7a1	1,27	1,76	1,19
Cyp7b1	-2,20	1,17	-2,47
Cyp8b1	1,06	-1,36	-1,57
Dgat1	1,34	1,17	-5,55
Dgat2	-1,12	1,07	-1,90
Dhcr24	-1,34	1,29	-1,80
Dhcr7	-1,39	1,46	-1,25
Elovl1	1,74	-1,06	-3,55

Table S5. continued

Gene	AAV-shApoB	AAV-miApoB	siApoB
Elovl2	1,14	1,77	-3,80
Elovl3	-2,03	1,51	1,79
Elovl4	-1,79	1,14	-5,22
Elovl5	-1,52	1,24	-3,19
Elovl6	-1,42	1,31	-3,49
Fads1	-1,83	1,12	-3,72
Fads2	-2,08	2,07	-2,00
Fads3	1,09	1,32	-2,45
Fasn	-2,63	1,32	-1,62
Fdft1	1,21	1,20	-2,87
Fdps	1,54	1,08	-1,09
Gpat	1,88	1,24	-1,92
Gpr65	1,01	3,02	-1,11
Haao	1,07	-1,41	-1,47
Hmgcr	-1,28	1,82	-2,06
Hmgcs1	-1,44	1,59	-9,09
Hsd17b6	-5,37	-1,30	-1,96
Hsd3b7	-1,38	1,14	-2,52
Idi1	-1,56	1,19	-1,19
Ldlr	-1,75	1,23	-1,42
Lpcat4 (Agpat7)	1,38	1,44	-4,54
Lrp8	ND	ND	4,17
Lycat (Agpat8)	ND	ND	-1,72
Mogat1	ND	ND	1,96
Mogat2	ND	ND	1,19
Mtp	-1,85	1,21	-1,59
Mvd	1,20	1,66	-1,81
Mvk	-1,59	1,09	1,96
Pcsk9	-2,69	1,02	-1,59
Pcyt2	1,10	-1,30	-1,63
Pmvk	1,13	1,34	-3,21
Ppap2a	-1,47	1,31	-50,53
Ppap2b	-1,03	1,38	-1,07
Ppap2c	-1,49	1,03	-1,13
Ppara	-1,32	1,06	-1,37
Ppard	-1,58	2,19	-2,16
Pparg	2,16	1,47	-2,00
Ppia	1,01	-1,21	-1,09
Scap	-1,01	-1,04	-1,04
Scarb1	-1,79	1,42	-1,14
Scd1	-3,14	-1,63	-4,92
Scd2	-1,25	2,24	2,08

Supplementary Table 5. continued

Gene	AAV-shApoB	AAV-miApoB	siApoB
Sgpl1	-1,99	1,10	-1,09
Sgpp1	1,09	1,46	-1,02
Slc27a5	1,03	1,20	-1,75
Soat1	1,49	3,80	-1,96
Soat2	-1,47	-1,46	-1,81
Splc1	ND	ND	-1,35
Srebf2	-1,59	1,35	-1,41
Stard3	1,39	1,19	-1,20
Tm7sf2	1,62	-1,04	-2,55
Vldlr	ND	ND	-1,04
Xpnep3	-2,19	1,83	1,35

Table S6. Antibodies used in the study

Antibody	Host	Code	Dilution	Incubation time/temp
CK-18[1]	Rabbit	1924-1	1:200	60 min, RT
Ki67 (Clone SP6)[2]	Rabbit	RM-9106-S0	1:2000	60 min, RT
CD31[3]	Rabbit	LS-B4737-250	1:50	Overnight, 4°C
Cleaved Caspase-3[4]	Rabbit	9661L	1:200	60 min, RT
AP Polymer anti-Rabbit[5]	-	MON-APP201	undiluted	30 min, RT
HRP Plymer anti-Rabbit[5]	-	MON-APP202	undiluted	30 min ,RT

RT- room temperature
[1] Epitomics,Inc, Burlingame, CA
[2] Thermo Fisher Scientific/Labvision, Fremont, CA
[3] LifeSpan Biosciences Inc., Seattle, WA
[4] Cell Signaling Technology Inc., Danvers, MA
[5] MONOSAN, Uden, The Netherlands

Reference list

1. Fire, A, Xu, S, Montgomery, MK, Kostas, SA, Driver, SE and Mello, CC (1998). Potent and specific genetic interference by double-stranded RNA in Caenorhabditis elegans. *Nature*; **391:** 806-811.
2. Paddison, PJ, Caudy, AA, Bernstein, E, Hannon, GJ and Conklin, DS (2002). Short hairpin RNAs (shRNAs) induce sequence-specific silencing in mammalian cells. *Genes Dev*; **16:** 948-958.
3. Soutschek, J, Akinc, A, Bramlage, B, Charisse, K, Constien, R, Donoghue, M, et al. (2004). Therapeutic silencing of an endogenous gene by systemic administration of modified siRNAs. *Nature*; **432:** 173-178.
4. Boudreau, RL, Martins, I and Davidson, BL (2009). Artificial microRNAs as siRNA shuttles: improved safety as compared to shRNAs in vitro and in vivo. *Mol Ther*; **17:** 169-175.
5. Grimm, D (2009). Small silencing RNAs: State-of-the-art. *Adv Drug Deliv Rev*; **61:** 672-703.
6. Zamore, PD, Tuschl, T, Sharp, PA and Bartel, DP (2000). RNAi: double-stranded RNA directs the ATP-dependent cleavage of mRNA at 21 to 23 nucleotide intervals. *Cell*; **101:** 25-33.
7. Ahn, M, Witting, SR, Ruiz, R, Saxena, R and Morral, N (2011). Constitutive expression of shRNA in vivo triggers build up of mature hairpin molecules. *Hum Gene Ther*; **22:** 1483-1497.
8. Borel, F, van Logtenstein R., Koornneef, A, Maczuga, P, Ritsema, T, Petry, H, et al. (2011). In vivo knock-down of multidrug resistance transporters ABCC1 and ABCC2 by AAV-delivered shRNAs and by artificial miRNAs. *J RNAi Gene Silencing*; **7:** 434-442.
9. Bridge, AJ, Pebernard, S, Ducraux, A, Nicoulaz, AL and Iggo, R (2003). Induction of an interferon response by RNAi vectors in mammalian cells. *Nat Genet*; **34:** 263-264.
10. Grimm, D, Streetz, KL, Jopling, CL, Storm, TA, Pandey, K, Davis, CR, et al. (2006). Fatality in mice due to oversaturation of cellular microRNA/short hairpin RNA pathways. *Nature*; **441:** 537-541.
11. Sledz, CA, Holko, M, de Veer, MJ, Silverman, RH and Williams, BR (2003). Activation of the interferon system by short-interfering RNAs. *Nat Cell Biol*; **5:** 834-839.
12. Jackson, AL, Bartz, SR, Schelter, J, Kobayashi, SV, Burchard, J, Mao, M, et al. (2003). Expression profiling reveals off-target gene regulation by RNAi. *Nat Biotechnol*; **21:** 635-637.
13. McBride, JL, Boudreau, RL, Harper, SQ, Staber, PD, Monteys, AM, Martins, I, et al. (2008). Artificial miRNAs mitigate shRNA-mediated toxicity in the brain: Implications for the therapeutic development of RNAi. *Proc Natl Acad Sci U S A*; **105:** 5868-5873.
14. Giering, JC, Grimm, D, Storm, TA and Kay, MA (2008). Expression of shRNA from a tissue-specific pol II promoter is an effective and safe RNAi therapeutic. *Mol Ther*; **16:** 1630-1636.
15. Maczuga, P, Koornneef, A, Borel, F, Petry, H, van Deventer, S, Ritsema, T, et al. (2012). Optimization and comparison of knockdown efficacy between polymerase II expressed shRNA and artificial miRNA targeting luciferase and Apolipoprotein B100. *BMC Biotechnol*; **12:** 42.
16. Judge, AD, Sood, V, Shaw, JR, Fang, D, McClintock, K and MacLachlan, I (2005). Sequence-dependent stimulation of the mammalian innate immune response by synthetic siRNA. *Nat Biotech*; **23:** 457-462.
17. Kariko, K, Bhuyan, P, Capodici, J, Ni, H, Lubinski, J, Friedman, H, et al. (2004). Exogenous siRNA mediates sequence-independent gene suppression by signaling through toll-like receptor 3. *Cells Tissues Organs*; **177:** 132-138.
18. Kleinman, ME, Yamada, K, Takeda, A, Chandrasekaran, V, Nozaki, M, Baffi, JZ, et al. (2008). Sequence- and target-independent angiogenesis suppression by siRNA via TLR3. *Nature*; **452:** 591-597.
19. Witting, SR, Brown, M, Saxena, R, Nabinger, S and Morral, N (2008). Helper-dependent adenovirus-mediated short hairpin RNA expression in the liver activates the interferon response. *J Biol Chem*; **283:** 2120-2128.
20. Kenworthy, R, Lambert, D, Yang, F, Wang, N, Chen, Z, Zhu, H, et al. (2009). Short-hairpin RNAs delivered by lentiviral vector transduction trigger RIG-I-mediated IFN activation. *Nucleic Acids Res*; **37:** 6587-6599.
21. Jackson, AL and Linsley, PS (2010). Recognizing and avoiding siRNA off-target effects for target identification and therapeutic application. *Nat Rev Drug Discov*; **9:** 57-67.
22. Boudreau, RL, Spengler, RM and Davidson, BL (2011). Rational design of therapeutic siRNAs: minimizing off-targeting potential to improve the safety of RNAi therapy for Huntington's disease. *Mol Ther*; **19:** 2169-2177.

23. Caffrey, DR, Zhao, J, Song, Z, Schaffer, ME, Haney, SA, Subramanian, RR, et al. (2011). siRNA off-target effects can be reduced at concentrations that match their individual potency. *PLoS ONE*; **6:** e21503.
24. Maczuga, P, Lubelski, J, van Logtenstein, R, Borel, F, Blits, B, Fakkert, E, et al. (2013). Embedding siRNA sequences targeting Apolipoprotein B100 in shRNA and miRNA scaffolds results in differential processing and in vivo efficacy. *Mol Ther*; **21:** 217-227.
25. Young, SG (1990). Recent progress in understanding apolipoprotein B. *Circulation*; **82:** 1574-1594.
26. Rozema, DB, Lewis, DL, Wakefield, DH, Wong, SC, Klein, JJ, Roesch, PL, et al. (2007). Dynamic PolyConjugates for targeted in vivo delivery of siRNA to hepatocytes. *Proc Natl Acad Sci U S A*; **104:** 12982-12987.
27. Tarugi, P, Averna, M, Di, LE, Cefalu, AB, Noto, D, Magnolo, L, et al. (2007). Molecular diagnosis of hypobetalipoproteinemia: an ENID review. *Atherosclerosis*; **195:** e19-e27.
28. Visser, ME, Akdim, F, Tribble, DL, Nederveen, AJ, Kwoh, TJ, Kastelein, JJ, et al. (2010). Effect of apolipoprotein-B synthesis inhibition on liver triglyceride content in patients with familial hypercholesterolemia. *J Lipid Res*; **51:** 1057-1062.
29. Rawlings, ND, Tolle, DP and Barrett, AJ (2004). Evolutionary families of peptidase inhibitors. *Biochem J*; **378:** 705-716.
30. Silverman, GA, Bird, PI, Carrell, RW, Church, FC, Coughlin, PB, Gettins, PG, et al. (2001). The serpins are an expanding superfamily of structurally similar but functionally diverse proteins. Evolution, mechanism of inhibition, novel functions, and a revised nomenclature. *J Biol Chem*; **276:** 33293-33296.
31. Irving, JA, Pike, RN, Lesk, AM and Whisstock, JC (2000). Phylogeny of the serpin superfamily: implications of patterns of amino acid conservation for structure and function. *Genome Res*; **10:** 1845-1864.
32. Martin, LJ and Tremblay, JJ (2009). The nuclear receptors NUR77 and SF1 play additive roles with c-JUN through distinct elements on the mouse Star promoter. *J Mol Endocrinol*; **42:** 119-129.
33. Shao, Q, Shen, LH, Hu, LH, Pu, J, Qi, MY, Li, WQ, et al. (2010). Nuclear receptor Nur77 suppresses inflammatory response dependent on COX-2 in macrophages induced by oxLDL. *J Mol Cell Cardiol*; **49:** 304-311.
34. Bermudez, O, Pagès, G and Gimond, C (2010). The dual-specificity MAP kinase phosphatases: critical roles in development and cancer. *Am J Physiol Cell Physiol*; **299:** C189-C202.
35. Suhy, DA, Kao, SC, Mao, T, Whiteley, L, Denise, H, Souberbielle, B, et al. (2012). Safe, long-term hepatic expression of anti-HCV shRNA in a nonhuman primate model. *Mol Ther*; **20:** 1737-1749.
36. Tadin-Strapps, M, Peterson, LB, Cumiskey, AM, Rosa, RL, Mendoza, VH, Castro-Perez, J, et al. (2011). siRNA induced liver ApoB knockdown lowers serum LDL-cholesterol in a mouse model with human-like serum lipids. *J Lipid Res*; **52:** 1084-1097
37. Zimmermann, TS, Lee, AC, Akinc, A, Bramlage, B, Bumcrot, D, Fedoruk, MN, et al. (2006). RNAi-mediated gene silencing in non-human primates. *Nature*; **441:** 111-114.
38. Crooke, RM, Graham, MJ, Lemonidis, KM, Whipple, CP, Koo, S and Perera, RJ (2005). An apolipoprotein B antisense oligonucleotide lowers LDL cholesterol in hyperlipidemic mice without causing hepatic steatosis. *J Lipid Res*; **46**: 872-884.
39. Visser, ME, Akdim, F, Tribble, DL, Nederveen, AJ, Kwoh, TJ, Kastelein, JJ, et al. (2010). Effect of apolipoprotein-B synthesis inhibition on liver triglyceride content in patients with familial hypercholesterolemia. *J Lipid Res*; **51:** 1057-1062.
40. Savary, S, Trompier, D, Andreoletti, P, Le, BF, Demarquoy, J and Lizard, G (2012). Fatty acids-induced lipotoxicity and inflammation. *Curr Drug Metab*; **13**:1358-1370
41. Penaud-Budloo, M, Le Guiner, C, Nowrouzi, A, Toromanoff, A, Ch+¬rel, Y, Chenuaud, P, et al. (2008). Adeno-Associated Virus Vector Genomes Persist as Episomal Chromatin in Primate Muscle. *J Virol*; **82:** 7875-7885.
42. Castanotto, D, Sakurai, K, Lingeman, R, Li, H, Shively, L, Aagaard, L, et al. (2007). Combinatorial delivery of small interfering RNAs reduces RNAi efficacy by selective incorporation into RISC. *Nucleic Acids Res*; **35:** 5154-5164.
43. Keck, K, Volper, EM, Spengler, RM, Long, DD, Chan, CY, Ding, Y, et al. (2009). Rational design leads to more potent RNA interference against hepatitis B virus: factors effecting silencing efficiency. *Mol Ther*; **17:** 538-547.
44. Flood, C, Gustafsson, M, Pitas, RE, Arnaboldi, L, Walzem, RL and Boren, J (2004). Molecular mechanism for changes in proteoglycan binding on compositional changes of the core and the surface of low-density lipoprotein-containing human apolipoprotein B100. *Arterioscler Thromb Vasc Biol*; **24:** 564-570.

45. Olivecrona, G and Olivecrona, T (2010). Triglyceride lipases and atherosclerosis. *Curr Opin Lipidol*; **21:** 409-415.
46. Okuyama, S, Marusawa, H, Matsumoto, T, Ueda, Y, Matsumoto, Y, Endo, Y, et al. (2012). Excessive activity of apolipoprotein B mRNA editing enzyme catalytic polypeptide 2 (APOBEC2) contributes to liver and lung tumorigenesis. *Int J Cancer*; **130:** 1294-1301.
47. Mikl, MC, Watt, IN, Lu, M, Reik, W, Davies, SL, Neuberger, MS, et al. (2005). Mice deficient in APOBEC2 and APOBEC3. *Mol Cell Biol*; **25:** 7270-7277.
48. Tep, S, Mihaila, R, Freeman, A, Pickering, V, Huyhn, F, Tadin-Strapps, M, et al. (2012). Rescue of Mtp siRNA-induced hepatic steatosis by DGAT2 siRNA silencing. *J Lipid Res*; **53:** 859-867.
49. Koornneef, A, Maczuga, P, van Logtenstein, R, Borel, F, Blits, B, Ritsema, T, et al. (2011). Apolipoprotein B knockdown by AAV-delivered shRNA lowers plasma cholesterol in mice. *Mol Ther*; **19:** 731-740.
50. van der Loos, CM (2008). Multiple immunoenzyme staining: methods and visualizations for the observation with spectral imaging. *J Histochem Cytochem*; **56:** 313-328.
51. Chen, C, Ridzon, DA, Broomer, AJ, Zhou, Z, Lee, DH, Nguyen, JT, et al. (2005). Real-time quantification of microRNAs by stem-loop RT-PCR. *Nucleic Acids Res*; **33:** e179.
52. Livak, KJ and Schmittgen, TD (2001). Analysis of relative gene expression data using real-time quantitative PCR and the 2-[delta][delta] CT method. *Methods*; **25:** 402-408.
53. Mortazavi, A, Williams, BA, McCue, K, Schaeffer, L and Wold, B (2008). Mapping and quantifying mammalian transcriptomes by RNA-Seq. *Nat Methods*; **5:** 621-628.
54. Edgar, R, Domrachev, M and Lash, AE (2002). Gene Expression Omnibus: NCBI gene expression and hybridization array data repository. *Nucleic Acids Res*; **30:** 207-210.
55. Szklarczyk, D, Franceschini, A, Kuhn, M, Simonovic, M, Roth, A, Minguez, P, et al. (2011). The STRING database in 2011: functional interaction networks of proteins, globally integrated and scored. *Nucleic Acids Res*; **39:** D561-D568.
56. Huang, dW, Sherman, BT and Lempicki, RA (2009). Systematic and integrative analysis of large gene lists using DAVID bioinformatics resources. *Nat Protoc*; **4:** 44-57.
57. Huang, dW, Sherman, BT and Lempicki, RA (2009). Bioinformatics enrichment tools: paths toward the comprehensive functional analysis of large gene lists. *Nucleic Acids Res*; **37:** 1-13.

CHAPTER 6

Regulated knockdown of Apolipoprotein B100 and Huntingtin by the GeneSwitch mifiprestone-inducible system

Piotr Maczuga[1,2], Angelina Huseinovic[1], Annemart Koornneef[1], Sander van Deventer[2], Harald Petry[1] and Pavlina Konstantinova[1]

[1]Department of Research & Development, uniQure, Amsterdam, the Netherlands;
[2]Department of Gastroenterology and Hepatology, Leiden University Medical Center, Leiden, the Netherlands;

Abstract

RNA interference (RNAi) emerges as a potent approach for inhibition of disease-related genes. However overexpression of RNAi inducers may cause cytotoxicity because of saturation of the endogenous microRNA (miRNA) processing pathway. Expression of short hairpin RNA (shRNA) or artificial miRNA from constitutive or tissue specific polymerase II (pol II) promoters has been shown to reduce RNAi toxicity *in vivo* and *in vitro* and controlling and limiting expression by using inducible pol II promoters would allow time- and dose-dependent expression of therapeutic shRNA or miRNA when the inducer is administered. In this study we evaluated the GeneSwitch (GS) system for inducible expression of artificial miRNA targeting Apolipoprotein B100 (miApoB). Highly effective luciferase reporter inhibition by GS-miApoB was observed after induction with mifiprestone (MFP) and the effect was dependent on the amount of the GeneSwitch transactivator (TA). Deletion analysis of the core elements of the GS pol II promoter, the TATA box (TATA) and initiator sequence (INR) revealed that both are important for the functioning of the promoter in response to the inducer and any deletions result in loss of function. When TA and GS-miApoB encoding cassettes were placed in 4 different orientations in a single backbone, variant #3, where the transcription occurs in the opposite directions, showed the best luciferase reporter knockdown when MFP induced and least basal activity when non-induced. Quantification of small interfering RNA (siRNA) processed from the different GS variants revealed that the variant #3 expressed the highest amount of molecules. Finally, we showed that 4 miRNAs targeting the Huntingtin gene (Htt) cloned into the GS variant #3 demonstrated increased GFP and siRNA expression when induced with MFP. Our results demonstrate that the GeneSwitch system is capable of driving expression of artificial miRNA in a controlled manner *in vitro* when placed on a single backbone without compromising its properties. Controlled expression of therapeutic miRNA with the GeneSwitch system may constitute additional safety measure to limit toxicity of RNAi based gene therapy.

Introduction

One of the goals of the RNAi gene therapy is the delivery of inhibitory molecules to the targeted tissue to achieve stable and therapeutic inhibition of disease related genes. However the ability to express high levels of shRNA/miRNA for extended periods of time creates the need for drug-regulated gene expression systems. shRNA have been shown to induce acute toxicity when over-expressed *in vivo*, which leads to fatality in mice [1,2], particularly when potent polymerase III (pol III) promoters are used to drive expression of shRNA, resulting in saturation of the endogenous RNAi machinery leading to the global deregulation of gene expression. The toxicity may be circumvented by expressing shRNA from the weaker pol II promoters which can be tissue specific or inducible [3-7], but the exact rules for successful expression of shRNA from pol II promoters are far from understood. As an alternative to shRNA, artificial miRNA scaffolds can be used as miRNA are naturally expressed from pol II promoters [8]. Inducible expression of artificial miRNA can provide an additional safety level where expression can be quantitatively and temporally controlled.

Several inducible gene expression systems have been developed including tetracycline, rapamycine, IPTG, ecdysone, and MFP dependent technologies. [9-12]. Generally they consist of two elements: the first is a chimeric protein capable of modulating gene expression in a drug-dependent manner and the second is an inducible promoter which is often a minimal pol II promoter linked to sequences recognized by the chimeric protein. Additionally, two mechanisms of gene regulation can be distinguished, called On- and Off-switch. In the first mechanism, the chimeric transactivator protein binds specifically to its DNA recognition sequence within the inducible promoter in the presence of the inducer, which in consequence activates gene expression. In the second mechanism the chimeric protein-repressor is constantly bound to its recognition sequences and upon induction dissociates allowing transcription. Any inducible gene expression system should fulfill several requirements for safe and long term gene therapy application including a low basal expression in the absence of inducer and a high induction ratio. Another important safety requirement is that the chimeric proteins used in inducible systems, in active or inactive form, do not interfere with endogenous gene expression, because chimeric proteins are formed from potent transcription factors that can lead to unspecific activation of endogenous promoters and thus interfere with cellular processes [13]. The safety aspects should also be determined for all inducible system components within the context of immune system activation.

The GeneSwitch regulated expression is one of the best characterized systems for inducible gene expression [11,12,14-16]. It exploits a hybrid transactivator (TA) containing a DNA binding domain from the yeast Gal4 protein (Gal4 BD), a truncated ligand binding domain from human progesterone receptor (PR) and a

p65 transcriptional activation domain of the human NF-kappa B transcription factor (hp65). The second component is the GeneSwitch inducible promoter, which consists of minimal pol II promoter with upstream activation sequences (Gal4) that can be recognized by Gal4 BD domains of the TA protein. The system is induced by MFP, which is an anti progestin that binds to the PR domain of the TA protein. Upon induction the TA changes its confirmation and as a dimer specifically binds to the Gal4 sites to activate gene transcription. The major advantage of the system is that it lacks virally- or bacterially-derived components thus limiting a potential immune reaction to TA expression. Another advantage of the system is its inducer, which is a marketed drug with well characterized pharmacokinetics whereas the induction occurs at sub-therapeutic concentrations [17]. On the other hand, MFP has been shown to interfere with biological pathways which increase toxicity risk for applications where prolonged exposure to the inducer may be necessary [18]. Additionally some of the interactions of TA domains have been already described. Expression of TA for one month resulted in transcriptional changes in the liver [13]. However they were not associated with any biochemical or morphological changes, this aspect needs more attention.

Unlike the doxycycline and tetracycline (Tet) inducible systems, GeneSwitch has not been validated for RNAi induction. [19-24]. The former systems are derived from the bacterial tetracycline inducible system where tetracycline repressor protein (TetR) controls expression of the TetA protein that pumps tetracycline antibiotic out of the cell by binding to tetracycline responsive elements (TRE) upstream of the TetA promoter. Addition of tetracycline (or doxycyline) leads to a change in the TetR confirmation which dissociates from the promoter region and allows expression of TetA. Tetracycline-inducible systems such as TetOn, TetOff or Trex have been shown to be able to control shRNA or artificial miRNA expression *in vitro* and *in vivo* [19-24]. Regulated TetOff expression of shRNA targeting Polo-kinase 1 (Plk1) resulted in 97% mRNA knockdown *in vitro* [22]. Subsequently the Plk1 protein was inhibited up to 86% which correlated with a significant inhibition of tumor cell growth [22]. Additionally, a conditionally replicating Human immunodeficiency virus (HIV)-based vector that stably expresses an inducible antiviral shRNA against HIV-1 was proposed as vaccine for HIV infections [23]. Upon doxycyline induction, virus was shown to spread efficiently to all HIV-susceptible cells. Subsequent doxycycline withdrawal the constitutive shRNA expression cassette was active resulting in viral inhibition [23]. Proof-of-concept has also been established in transgenic mice enabling inducible and reversible expression of shRNA against Replication protein A, subunit 3 (Rpa3) which resulted in a block of cell proliferation and rapid atrophy of the intestinal epithelium which led to weight loss and lethality within 8–11 day after shRNA induction [24]. However, the use of TetOn and TetOff systems in preclinical and clinical studies is limited because they are dependent on bacterially derived –potentially immunogenic

proteins [25-27]. Other systems validated for shRNA or artificial miRNA expressions are the IPTG and ecdysone inducible systems [28,29]. The first one was shown to tightly regulate and induce shRNA targeting luciferase and tumor suppressor protein p53 in both transiently transfected cells and established stable clones [29]. Knockdown of the p53 protein *in vitro* was also demonstrated with the ecdysone-inducible system [30], where dose- and time-dependent inhibition of p53 was associated with changes in cell morphology and concomitant reduction of p21, downstream target of p53. Withdrawal of the inducer completely reversed the phenotype.

In the current study we evaluated the GeneSwitch system for inducible expression of an artificial miRNA that efficiently targets ApoB. In order to facilitate usage of the GeneSwitch system *in vivo*, its structural elements were incorporated in a single backbone in 4 different variants, which were later evaluated for knockdown efficiency, basal expression and inducibility. Variant #3, where the two elements are transcribed in an antisense orientation, was identified as the best configuration as it demonstrated lowest basal expression when non-induced and highest activation rate in the induced state. Finally to check the system robustness, inducible expression of four additional miRNAs targeting the Htt gene was shown for variant #3. Our data demonstrate the feasibility of the GeneSwitch inducible miRNA expression system that should be considered for future therapeutic RNAi applications.

Results

Knockdown efficacy of GS-miApoB depends on TA concentration and duration of the induction

We have previously identified and tested *in vivo* a highly active artificial miRNA targeting Apolipoprotein B100 (miApoB) [31]. However, the knockdown effect decreased over time and some signs of mild toxicity have been observed. Therefore, as a next step we developed a regulated miApoB expression based on the MFP-inducible GeneSwitch system. The two components of the GeneSwitch system were a chimeric TA that activates transcription exclusively in presence of MFP and the miApoB expressed from the GeneSwitch promoter (GS-miApoB) in response to TA binding (Fig. 1a). As a negative control, a scrambled miRNA not targeting any gene in the mammalian genome was placed under the control of the GeneSwitch (GS-miScr) or CMV promoters (CMV-miScr). Constitutive expressed miApoB (CMV-miApoB) was used as positive control. All constructs expressed green fluorescent protein version emerald (EmGFP), which allowed monitoring of the transfection efficacy and MFP induction (Fig. 1a). The inhibitory effect of GS-miApoB was evaluated by co-transfecting human embryonic kidney 293T (HEK293T) cells with a reporter expressing renilla luciferase that contained the ApoB target sequence in its 3'UTR (Luc-ApoB) and increasing amounts of the TA-encoding plasmid (Fig. 1b). By adding

10 nM MFP 24 h post transfection, transcription from GS-miApoB was induced and luciferase luminescence was measured 48 h later. As a negative control CMV-miScr or GS-miScr were used where the renilla/firefly luciferase ratio was set at 100% and the relative inhibition of the Luc-ApoB reporter was calculated.

In the absence of TA, basal expression resulted in ~60% knockdown of Luc-ApoB both in MFP induced and non-induced state (Fig 1b). When increasing amounts of the TA plasmid were added, relative luciferase inhibition in non-induced cells was between 60% and 85% and upon MFP induction even stronger knockdown was measured (Fig. 1b). Addition of 10 ng TA to GS-miApoB resulted in lowest basal expression and highest induction rate therefore it was chosen for other experiments.

Because GeneSwitch inducible expression peaks between 24 and 72 h after MFP induction, the maximal inhibitory effect was determined over time. HEK293T cells were co-transfected with 50 ng GS-miApoB, 10 ng Luc-ApoB and 10 ng TA plasmids (Fig. 1c). Twenty four hours after transfection cells were induced with MFP and after another 24, 48, and 72 h samples were harvested and luciferase inhibition was measured. Maximal Luc-ApoB knockdown was observed 48 h after MFP induction and it was ~80% in induced cell compared to ~50% in non-induced cells. After 72 h the Luc-ApoB knockdown was weaker and was 51% and 22% in MFP induced and non-induced cells, respectively (Fig. 1c).

GeneSwitch promoter analysis reveals that TATA box and INR are essential components and play important role in MFP induction

Initially we confirmed that the GeneSwitch system is capable of driving miApoB expression and established the optimal TA concentration and MFP induction time. Next, the inducible promoter was optimized to reduce the miApoB basal expression levels since without MFP induction, a ~50% knockdown of Luc-ApoB was already observed. Based on manual sequence identification, two core components of the GeneSwitch promoter, a TATA box and an initiator element (INR) were identified. In order to evaluate their function for basal expression and/or maximal induction of GS-miApoB, mutants lacking TATA (ΔTATA-miApoB), INR (ΔINR-miApoB) or both TATA and INR (ΔTATAΔINR-miApoB) were designed (Fig. 2a). HEK293T cells were co-transfected with 50 ng GS-miApoB, ΔTATA-miApoB, ΔINR-miApoB or ΔTATAΔINR-miApoB together with 10 ng of Luc-ApoB reporter and 10 ng TA plasmid. By adding 10 nM MFP transcription of miApoB was induced and Luc-ApoB knockdown was measured 48 h post induction with reference to CMV-miScr and GS-miScr controls. Upon induction luciferase knockdown by GS-miApoB was 64% while it was 31%, 34% and 36% for ΔTATA-miApoB, ΔINR-miApoB and ΔTATAΔINR-miApoB mutants (Fig. 2b). Moreover, none of the deletion constructs was MFP induced above basal levels indicating that the TATA and INR elements are essential for transcriptional activity of the GeneSwitch promoter. Additionally no GFP expression from the deletion mutants was observed (data not shown).

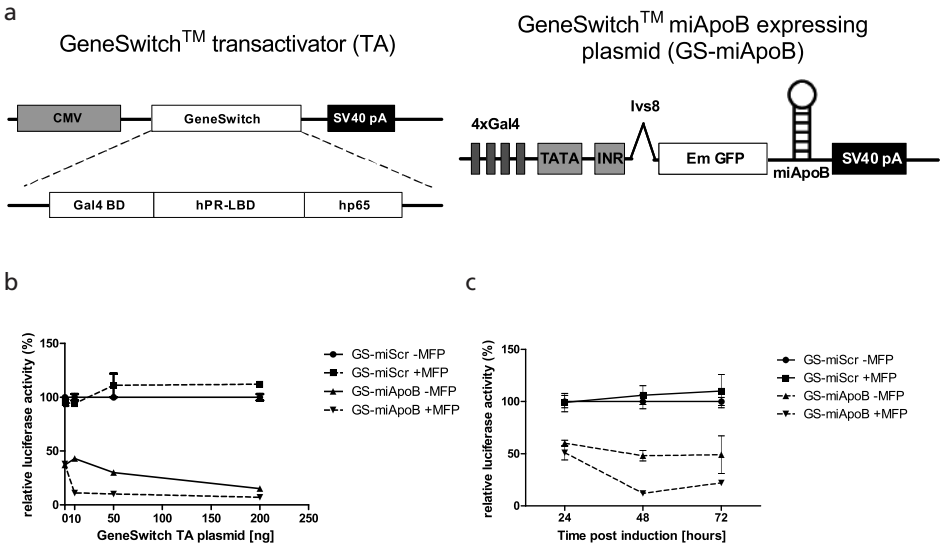

Figure 1. Structure and knockdown efficacy of miRNA targeting ApoB (miApoB) expressed from the GeneSwitch system. (a) Schematic representation of the GeneSwitch system for inducible expression of artificial miRNA. The system consists of two structural components: the transactivator protein (TA) expressed from the CMV promoter and miRNA expressing construct (GS-miApoB). Gal4 BD - Yeast Gal4 DNA binding domain, hPR-LBD - Human progesterone receptor ligand binding domain, p65 - Human NF-kB activation domain subunit, Gal4- Gal4 BD binding site, TATA- TATA box, INR- initiator sequence, EmGFP- Emerald Green Fluorescent Protein (b) Knockdown of Luc-ApoB reporter by GS-miApoB. Cells were transfected with 10 ng Luc-ApoB reporter, 50 ng GS-miApoB expressing plasmid and 10, 50, 100 or 250 ng of GeneSwitch TA expressing plasmid. Twenty four hours after transfection medium was changed and samples were induced with 10 nM MFP (+MFP) or were not induced (-MFP). Renilla and firefly luciferase were measured 48 h post-MFP induction. Renilla luciferase expression was normalized to firefly luciferase expression. CMV-miApoB was used as a positive control, CMV-miScr and GS-miScr served as negative controls and were set at 100%. Data are represented as mean values ±SD from a representative experiment from three independent experiments. (c) Knockdown of the Luc-ApoB reporter, by GS-miApoB at 24, 48 and 72 h post-MFP induction. Cells were transfected with 10 ng Luc-ApoB reporter, 50 ng GS-miApoB expressing plasmid and 50 ng of GeneSwitch TA expressing plasmid. Experimental conditions are as described in Fig. 1b.

Incorporation of GS-miApoB and TA elements in a single backbone results in high MFP inducibility and high basal expression levels

Inducible systems where all components can be integrated in a single backbone are desirable for therapeutic RNAi applications. Therefore the TA and GS-miApoB elements were placed adjacent to each other in a single vector backbone (Fig. 3a). The TA expression cassette was cloned upstream to GS-miApoB resulting in sense orientation of the two elements (Fig. 3a). HEK293T cells were co-transfected with 50 ng of the GS-miApoB single backbone variant with 10 ng of Luc-ApoB. Twenty four hours post transfection cells were induced and after another 48 h GFP induction was monitored. High GFP expression was observed for both GS-miScr and GS-miApoB only upon MFP

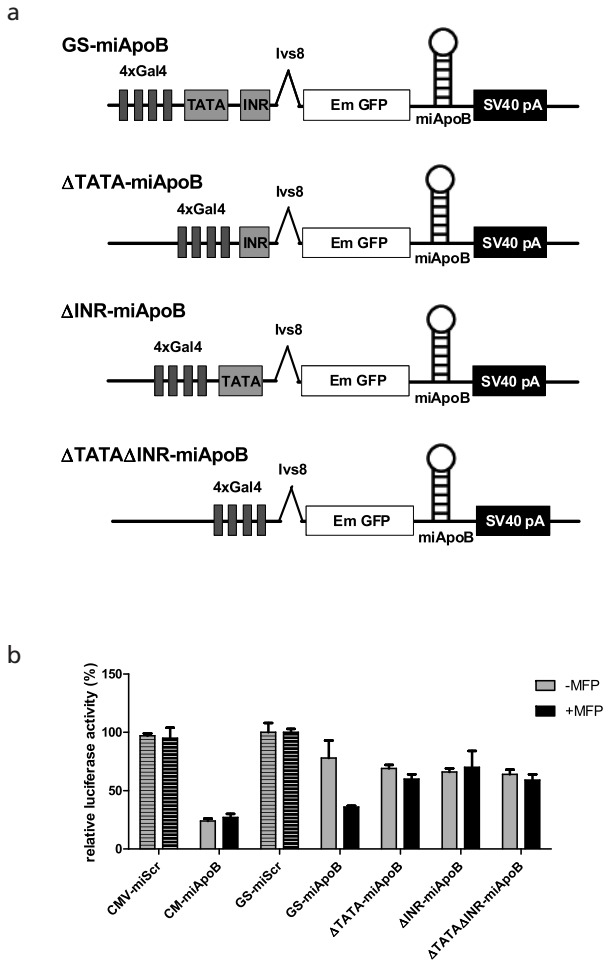

Figure 2. Structure and knockdown efficacy of miApoB expressed from a single backbone GS-miApoB. (a) Schematic representation of GS-miApoB for inducible expression of artificial miApoB, where all structural components were placed in a single backbone. The names of the structural components are indicted in Fig. 1. Arrows represent the direction of transcription (b) Representative image of GFP fluorescence 48 h without (-MFP) or after induction with 10 nM MFP (+MFP). Cells were transfected with 10 ng Luc-ApoB reporter and 50 ng GS-miApoB expressing plasmid. Pictures were taken using the same exposure and magnification settings. (c) Changes in the number of GFP positive cells after MFP induction. Experimental setup was as described in (b) 1000 events were counted with flow cytometry and fold change of GFP expression was calculated for each construct by dividing the amount of cells GFP positive after MFP induction by the number of GFP positive cells without MFP induction. (d) Knockdown of Luc-ApoB reporter, by the single backbone GS-miApoB system. Cells were transfected with 10 ng Luc-ApoB reporter and 50 ng GS-miApoB expressing plasmid. Twenty four hours after transfection medium was changed and samples were either induced with 10 nM MFP (+MFP) or were not induced (-MFP). Renilla and firefly luciferase were measured 48 h post-induction. Renilla luciferase expression was normalized to firefly luciferase expression. CMV-miApoB was used as a positive control, CMV-miScr and GS-miScr served as negative controls and were set at 100%. Bars with stripes represent negative controls. Data are represented as mean values ±SD from a representative experiment from three independent experiments.

induction (Fig. 3b). Quantification of GFP positive cells with flow cytometry revealed that there were ~4 fold more GFP positive cells for GS-miScr and GS-miApoB when induced with MFP compared to non-induced cells (Fig. 3c). To determine whether the induction observed on GFP correlates with Luc-ApoB knockdown by the GS-miApoB single backbone variant, luciferase assay was performed. Surprisingly for the single backbone GS-miApoB variant MFP induction did not further decrease Luc-ApoB expression (Fig. 3d). In both non-induced and induced cells Luc-ApoB was inhibited

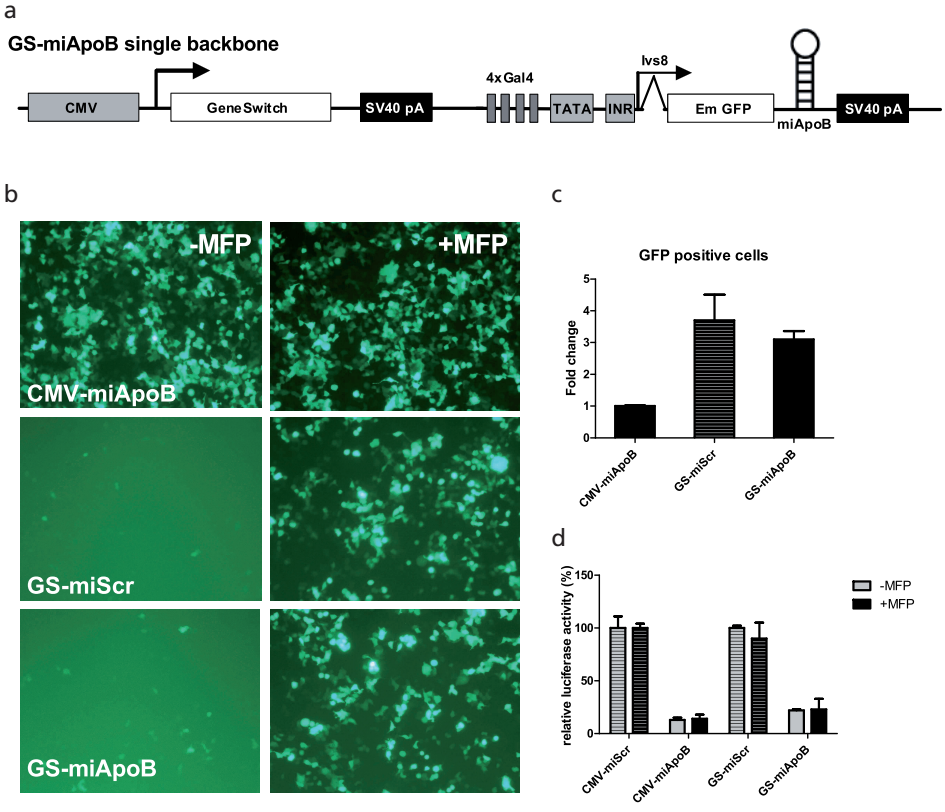

Figure 3. Structure and knockdown efficacy of GS-miApoB expressed from the GeneSwitch system with consecutive deletions in the inducible promoter. (a) Schematic representation of GS-miApoB for inducible expression of artificial miRNA, where several structural parts were deleted. Three different GeneSwitch deletion variants were designed where the TATA box (ΔTATA-miApoB), the INR sequence (ΔINR-miApoB) or both components were deleted (ΔTATAΔINR –miApoB) (b) Knockdown of Luc-ApoB reporter, by GS-miApoB after induction with the different GeneSwitch deletion variants: ΔTATA-miApoB, ΔINR-miApoB or ΔTATAΔINR–miApoB. Cells were transfected with 10 ng Luc-ApoB reporter, 50 ng GS-miApoB, ΔTATA-miApoB, ΔINR-miApoB or ΔTATAΔINR–miApoB and 10 ng of the TA plasmid. Reaction conditions were as described in Fig. 1b. Bars with stripes represent negative controls. Data are represented as mean values ±SD from a representative experiment from three independent experiments.

up to 80% indicating that the basal expression with the single backbone GS-miApoB was greater than with the two plasmids system. Reduction of the GS-miApoB and MFP concentrations did not show an improvement in basal expression which still resulted in ~80% Luc-ApoB knockdown (data no shown).

Inducibility and basal expression depends on the positioning and orientation of GS-miApoB and TA elements within a single backbone

It has been shown that the expression and activity of the inducible systems depends on the orientation of expression cassettes in a single backbone [32-34]. To achieve optimal induction and minimal basal expression, the TA and GS-miApoB elements were cloned in different orientations resulting in 4 distinct variants (Fig. 4a). In all variants GS-miApoB was cloned upstream of TA expression cassette. In variant #1 both cassettes were in sense orientation. In variant #2 GS-miApoB and TA cassettes were in a head-to-head orientation. In variant #3 and #4 GS-miApoB and TA cassettes were opposite and antisense to each other, respectively (Fig. 4a). HEK293T cells were co-transfected with 50 ng of variants #1-#4, induced with MFP 24h later and 48 h post induction, Luc-ApoB knockdown was measured (Fig. 4b). As anticipated, the different orientations varied in terms of basal expression and induction. Variants #1 and #2 exhibited mild induction and low basal activity. For variant #1 the Luc-ApoB knockdown was 32% and 38% for non-induced and MFP induced cells, respectively. For variant #2 knockdown was 28% for non-induced and 42% for MFP induced cells respectively. Variants #3 and #4 exhibited lowest basal activity and highest induction rate. For variant #3 basal expression resulted in 25% knockdown of Luc-ApoB, which was stronger upon induction and reached 59%. Similarly variant #4 resulted in 22% and 51% knockdown when non-induced and MFP induced, respectively.

Next, the correlation was determined between the inhibitory effect, induction rate, and the number of processed siApoB molecules from the GS-miApoB variants #1-#4

Figure 4. Structure and knockdown efficacy of GS-miApoB expressed from a single backbone with four different orientations of the GeneSwitch and TA elements. (a) Schematic representation of variants #1 - #4 of the single backbone GS-miApoB, with different orientations of the GeneSwitch and TA elements In variant #1 both cassettes were in sense orientation. In variant #2 GS-miApoB and TA cassettes were in head-to-head orientations. In variant #3 and #4 GS-miApoB and TA cassettes were opposite and antisense to each other, respectively. The names of the structural components are indicted in Fig. 1a. Arrows represent direction of transcription. (b) Knockdown of the Luc-ApoB reporter, by the single backbone GS-miApoB system variants #1 to #4. Cells were transfected with 10 ng Luc-ApoB reporter and 50 ng GS-miApoB variants #1-#4. Reaction conditions are as described in Fig. 1b. Bars with stripes represent negative controls. Data are represented as mean values ±SD from three experiments analyzed with the factor correction method. (c) siApoB expression in HEK293T cells from the single backbone GS-miApoB variants #1-#4. RNA was isolated 48 hours post-MFP induction and siApoB-specific small RNA TaqMan was performed. siRNA copy number per cell was calculated based on the amplification plot of a dilution series of synthetic siApoB RNA standard (IDT, Coralville, IA). The trend line value of the standard line was used to calculate the siApoB copy number cell, assuming 15 pg RNA per cell [39]. ►

a

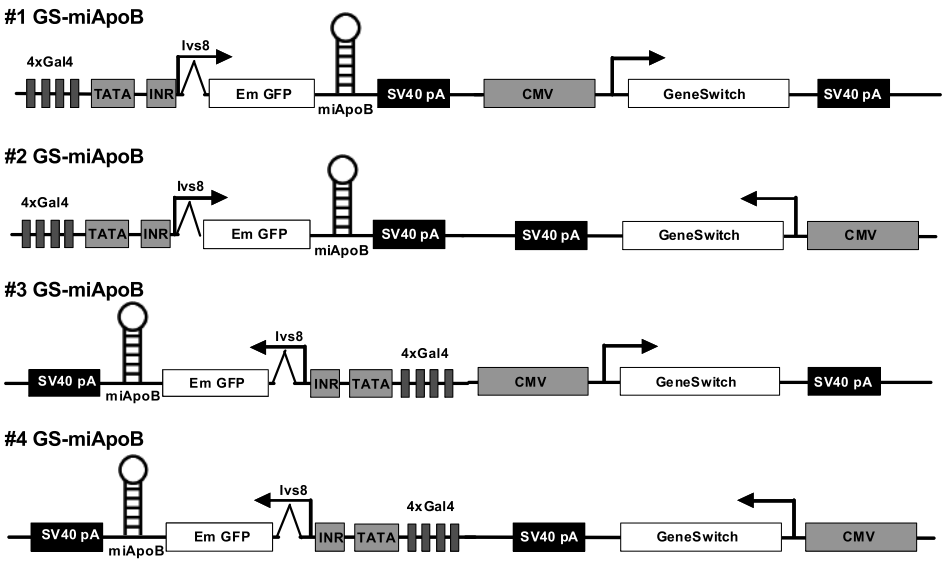
#1 GS-miApoB
4xGal4
TATA
INR
Ivs8
Em GFP
miApoB
SV40 pA
CMV
GeneSwitch
SV40 pA
#2 GS-miApoB
4xGal4
TATA
INR
Ivs8
Em GFP
miApoB
SV40 pA
SV40 pA
GeneSwitch
CMV
#3 GS-miApoB
SV40 pA
miApoB
Em GFP
Ivs8
4xGal4
INR
TATA
CMV
GeneSwitch
SV40 pA
#4 GS-miApoB
SV40 pA
miApoB
Em GFP
Ivs8
4xGal4
INR
TATA
SV40 pA
GeneSwitch
CMV

b

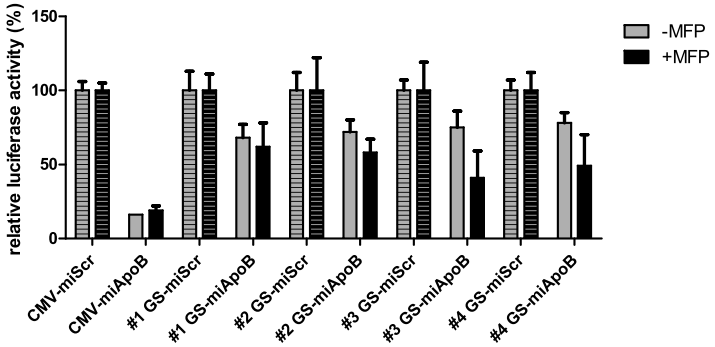
relative luciferase activity (%)
150
100
50
0
-MFP
+MFP
CMV-miScr
CMV-miApoB
#1 GS-miScr
#1 GS-miApoB
#2 GS-miScr
#2 GS-miApoB
#3 GS-miScr
#3 GS-miApoB
#4 GS-miScr
#4 GS-miApoB

c

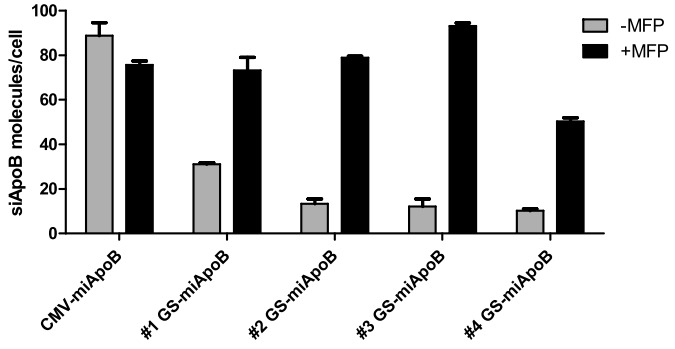
siApoB molecules/cell
100
80
60
40
20
0
-MFP
+MFP
CMV-miApoB
#1 GS-miApoB
#2 GS-miApoB
#3 GS-miApoB
#4 GS-miApoB

(Fig. 4c). Small RNA specific Taqman assay was designed for detecting the guide strand of miApoB and the amount of molecules per cell was calculated based on synthetic standard line. All variants showed a clear increase of the amount of siApoB molecules per cell after MFP induction. Variant #1 expressed the highest amount of siApoB molecules compared to other variants. Variants #3 and #4 exhibited lowest basal expression and highest induction rate which is in line with Luc-ApoB knockdown data.

Variant #3 where the GS-miApoB and TA elements were positioned opposite to each other showed the best configuration for inducible expression of artificial miRNA targeting ApoB. To check if this is a general rule, we tested the inducibility of four additional efficient miRNAs targeting the Htt gene cloned in GS variant #3. miH10, miH12, miS7 and miS15 are targeting different regions of Htt and have been already validated as potent huntingtin inhibitors (data not shown). HEK293T cells were co-transfected with 50 ng of GS-miH10, GS-mH12, GS-miS7 or GS-miS15 variants #3 and 48 h post MFP induction total RNA was isolated (Fig. 4b). The induction was measured by quantifying the siRNA molecules expressed with and without MFP induction using specific small RNA Taqman assay. The results show between 4 and 7 times siRNA induction proving the robustness of GS variant #3 for inducible miRNA expression (Fig. 5a).

Discussion

Recent developments towards clinical applications of RNAi made it apparent that regulable and temporal expression may be necessary to circumvent toxicity resulting from aspecific off-targeting effects or oversaturation of the endogenous miRNA pathway. Inducible systems have been widely used for control of gene expression. These systems are composed of a chimeric transcription factor, inducer and a promoter that reacts upon transcription factor binding. The GeneSwitch inducible system is one of the promising candidates for RNAi gene therapy since it lacks bacterially derived components and the MFP inducer is an already approved drug with known pharmacokinetics. Although the GeneSwitch system can effectively regulate gene expression *in vivo* and *in vitro* using plasmid or viral delivery, to date there are no reports of its application for RNAi induction. We addressed this question by optimizing miApoB expression from the GeneSwitch system initially using a two-plasmid system and later by combining the GeneSwitch elements in four different orientations in a single backbone.

The transactivator and promoter elements are essential parts of each inducible system that characterize its parameters: basal expression, fold induction, and maximum expression levels. Therefore, we investigated the optimal conditions for minimal basal activity without induction with MFP and the maximal inducibility after addition of inducer. By increasing the amount of TA plasmid the basal expression of the inducible promoter also increased suggesting that even in non-active state TA is

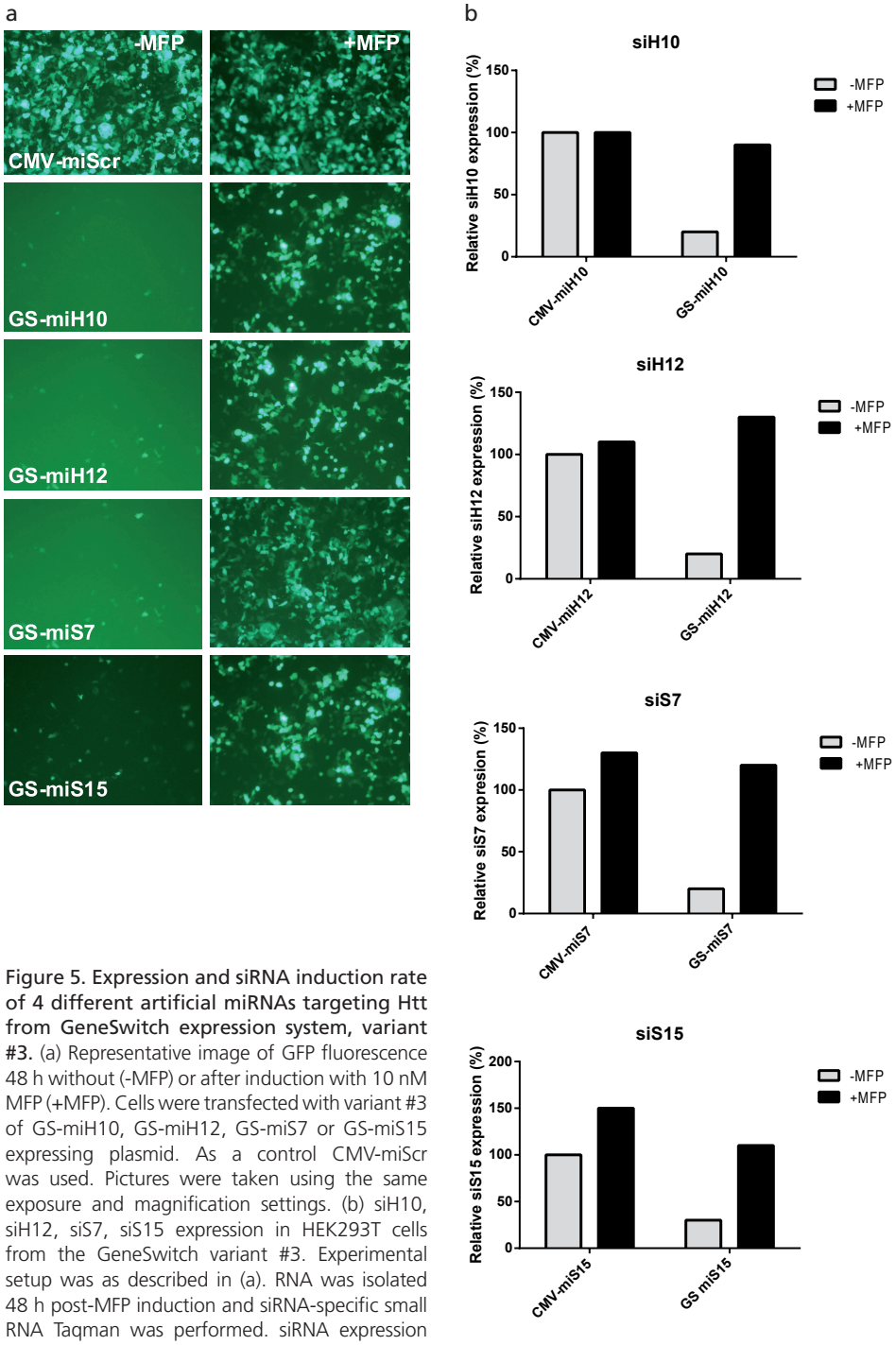

Figure 5. Expression and siRNA induction rate of 4 different artificial miRNAs targeting Htt from GeneSwitch expression system, variant #3. (a) Representative image of GFP fluorescence 48 h without (-MFP) or after induction with 10 nM MFP (+MFP). Cells were transfected with variant #3 of GS-miH10, GS-miH12, GS-miS7 or GS-miS15 expressing plasmid. As a control CMV-miScr was used. Pictures were taken using the same exposure and magnification settings. (b) siH10, siH12, siS7, siS15 expression in HEK293T cells from the GeneSwitch variant #3. Experimental setup was as described in (a). RNA was isolated 48 h post-MFP induction and siRNA-specific small RNA Taqman was performed. siRNA expression levels were normalized to beta-actin as an internal control, and the relative gene expression $2^{-\Delta\Delta Ct}$ method of Livak and Schmittgen was used for analysis of PCR data [40].

capable of binding to Gal4 elements in the GeneSwitch promoter. Another important aspect of the inducible systems is their temporal control of gene expression. The effect of the induction is dose dependent and increases until it reaches maximal expression. Generally after 24 h the expression using GeneSwitch system reaches maximum level *in vitro* [11,35], however in our case 24 hours time was not sufficient to observe increase in luciferase inhibition. The maximal knockdown of luciferase was observed after 48 hours and after 72 hours the inhibition of luciferase was weaker.

In this study, we also carried out deletion analysis of the GeneSwitch promoter to identify regions that control the responsiveness and the spatiotemporal gene expression. Manual analysis of the GeneSwitch promoter identified common elements of pol II promoters: a TATA box and an INR sequence [36,37]. Deletion analysis showed that both TATA box and INR are essential components of the GeneSwitch promoter and any perturbations resulted in a functional loss probably due to inefficient transcription. An interesting alternative to the promoter modification is to incorporate more Gal4 sequences upstream to the promoter, which can improve promoter inducibility. This was already shown for mIFNb expression with the GeneSwitch inducible system [14]. Although we did not optimize the TA expression cassette itself an interesting option is to use tissue specific promoters for expression of the TA protein. This would lower the extent of unregulated expression associated with the constitutive TA expression from the CMV promoter. Alternatively TA can be expressed from the promoter that, like the transgene, is responsive to MFP. In this auto-inducible system, the TA can induce both the transgene and its own expression.

A vector based regulated expression for GeneSwitch system has already been validated *in vitro* and *in vivo* using mouse interferon beta (mIFNb) [14]. Similarly to our studies four variants of a single backbone expression system with different orientations were tested and all 4 variants resulted in mIFNb *in vitro* induction raging from 360 – 1480 fold. In two variants (pGT23 and pGT24) the mIFNb cassette was cloned upstream of TA expression cassette in sense and opposite orientations respectively. In two other (pGT25 and pGT25) the TA expression cassette was upstream of mIFNb and was cloned in sense and head-to-head orientations respectively. This means that pGT23 is equivalent to our variant #1, pGT24 is variant #3 and pGT25 is GS-miApoB. pGT26 does not have equivalent in our study. The variant which exhibited the greatest induction was pGT23 followed by pGT26, pGT24 and pGT25. Interestingly, all single backbone variants outperformed the two-plasmid system in the inducible rate and the level of mIFNb expression but all construct, when induced, expressed less mIFNb than the constitutive CMV promoter. Surprisingly, *in vivo* measurement of IP-10, which is a validated biomarker for mIFNb showed a different trend and the variant that resulted in the best IP-10 induction was pGT26 followed by variants pGT25, pGT24 and pGT23. *In vivo* all variants were as active as the two-plasmid system in

IP-10 induction and they were also outperforming CMV expressed mIFNb. Despite the similar approach to optimize the GeneSwitch system, a direct comparison to our results is not feasible because the luciferase knockdown is caused by an increase of the siRNA amount which in consequence inhibits the protein expression. Additionally the exact mechanism of the GeneSwitch system induction has not been investigated thus a high protein expression may be a combination of an increased transcription and increased translation or both. By contrast to reported induction of mIFNb, our results show much lower induction of expressed siRNA: 4-6 fold increase in MFP induced cells compared to the non-induced cells.

Inducible expression is an interesting approach to avoid potential problems that can be associated with therapeutic RNAi applications. It has been reported that shRNA can lead to severe toxicity when high doses are used [1,2] and that by lowering siRNA expression -either using pol II promoters or by incorporation of a siRNA sequence in an artificial miRNA scaffold [9]- toxic side effects can be abolished. In our previous study, we have demonstrated a more sustained ApoB target knockdown by miApoB over the shApoB in long-term *in vivo* experiments [31]. Nonetheless, the inhibitory effect of miApoB expressed with a liver-specific promoter and shApoB was lost after 27 weeks. Additionally it has been shown that processing of shRNA and miRNA may lead to unanticipated silencing of other genes (off-targeting) which also can cause toxicity. Because of the complexity of RNAi processing *in vivo*, these interactions are difficult to predict and evaluate. Still RNAi toxicity has been shown to be dose dependent therefore limiting the expression of siRNA molecules with inducible systems may reduce potential risk. Although the present study provides a proof of concept for controlling siRNA expression *in vitro*, the reduction of the toxicity of GeneSwitch expressed miRNA *in vitro* and *in vivo* needs to be further investigated.

An important aspect is the robustness of the GeneSwitch system, which should be capable of expressing any miRNA. We have shown that variant #3 was also capable of driving expression of 4 miRNAs targeting Htt. Unequivocal induction of both GFP and miRNA expression was observed. Additionally gene knockdown *in vivo,* using the GeneSwitch system, needs to be investigated. The plasmids described in this study could be used in the context of viral vectors such as AAV for a long-term expression *in vivo*. Beside Htt knockdown for Huntington disease and ApoB for FH, other potential applications that can be treated with GeneSwitch inducible RNAi include cancer and viral infections (HIV, Hepatitis B virus and Hepatitis C virus).

In conclusion, we have tested the GeneSwitch system and constructed a single backbone to express the artificial miRNA targeting ApoB and Htt. This vector enabled regulation of the miRNA expression and proved efficient in Luc-ApoB knockdown *in vitro*. Combination of the AAV delivery and the inducible expression of an artificial miRNA would allow a long-term therapeutics effect simultaneously limiting possible

side effects. This will provide an additional safety level for future clinical applications compared to the ubiquitously expressed shRNA/miRNA.

Materials and methods

DNA constructs

GeneSwtich miApoB (GS-miApoB) construct was made by amplification of a 1384 bp fragment of pCDNA6.2 construct containing EmGFP and miApoB using pr967 and pr968 primers and ligating into the NcoI and KpnI sites of the pIF1683 (Inovio, San Diego, CA). The pIF1683 contains minimal pol II promoter with 4 upstream activation elements (Gal4). The construction of pCDNA6.2 containing miRNA targeting ApoB has been described previously [36]. Similarly negative scrambled control miRNA (GS-miScr) was made by PCR amplification o pcDNA6.2-GW/EmGFP-miR-neg (Invitrogen, Carlsbad, CA) using the same primer set. The GeneSwitch TA plasmid was constructed by amplification of 2200 bp fragment of pGS1984 (Inovio, San Diego, CA) using primers pr965 and pr966 and ligating into the XbaI and RsrII sites of the pTRCGW vector (Inovio, San Diego, CA). pGS1984 contains TA under the control of the beta-actin promoter. The end construct expressed TA protein form constitutive CMV promoter. All miRNA and primer sequences are listed in Table S1.

The GeneSwitch inducible promoter mutation variants variant were designed as followed. Promoter fragments of 200 bp with desired mutation (ΔTATA, ΔINR, ΔTATAΔINR) were synthesized and cloned into pIDTsmart vector resulting in pIDTsmartΔTATA, pIDTsmartΔINR, pIDTsmartΔTATAΔINR vectors (IDT, Coralville, IA). Then pIDTsmartΔTATA smart was digested with EcoRI and XhoI ligated into pIF1683 plasmid digested with the same restriction sites resulting in ΔTATA-miApoB construct. ΔTATAΔINR-miApoB was constructed analogously to ΔTATA-miApoB construct. ΔINR-miApoB was made by with EcoRI and BglI digestion of pIDTsmartΔINR and ligation into the same restriction sites of pIF1683.

The GeneSwitch single backbone variant was designed as followed. The GS fragment (1223 bp) was cut from pIF1683 plasmid by SbfI and Acc65I digestion and ligated into the *PstI* and *Acc65I* digested pKS+ (Stratagene, La Jolla, CA) resulting in pKS-GS plasmid. Next the TA expressing plasmid was digested with SspI and FspI and blunt ligated into BamHI sites of pKS-GS resulting in pKS-GS-TA plasmid. To replace beta-actin for CMV promoter in the TA expression cassette, the GS-TA fragment (2539 bp) was obtained by NheI digestion of pKS-GS-TA and ligated into SpeI digested pTRCGW. The construct was named as pTRC-GS-TA. Finally, the 1384 bp fragment of pCDNA6.2 construct containing EmGFP and miApoB was PCR amplified using primers miRfw and miRrv and ligated into the SacII and NotI sites of the pTRC-GS-TA resulting in a single backbone GS-miApoB construct. GeneSwitch orientations #1-#4 were designed as followed. The TA expression cassette was digested with KpnI and ligated into GS-miApoB construct,

which was digested with the same enzyme. The insert was ligated in sense or antisense orientations resulting in variant #1 and variant #3. To create variants #2 and #4 the GS-miApoB expression cassette in variants #1 and #3 was inverted by SbfI digestion and relegation. The presence of miApoB was verified by sequencing.

To create vectors expressing miRNA targeting Htt, 278 bp fragments of pCDNA6.2 constructs containing miH10, miH12, miS7 and S15 were PCR amplified with primers prGS3fw and prGS3rv and the inserts were blunt ligated into DraV and EcorV digested variant #3 construct. Construction of the Luc-ApoB reporter vector has been described before [38] Generation of this reporter vector has been described previously. All the sequences of the oligonucleotides used in this study are listed in Table S1.

Cell culture and transfections

The human embryonic kidney (HEK293T) cell line were maintained in Dulbecco's modified Eagle's medium (DMEM; Life Technologies, Grand Island, NY) containing 10% fetal calf serum, 100 U/ml penicillin and 100 U/ml streptomycin, at 37°C and 5% CO_2. For luciferase assay or siRNA expression analysis, cells were seeded in 96- or 24-well plates at a density of 3×10^4 or 1.2×10^5 cells per well, respectively, in DMEM one day prior transfection. Transfections were performed with Lipofectamine 2000 reagent (Life Technologies, Grand Island, NY) according to the manufacturer's instructions. Cells were induced with 10 nM mifiprestone (Sigma) which was prepared the day of the induction from the 1mM stock.

Luciferase assay

HEK293T cells were transfected with 10 ng Luc-ApoB reporter, 50 ng GS-miApoB expressing plasmid and 10, 50, 100 or 250 ng of TA expressing plasmid or with 10 ng Luc-ApoB reporter or 50 ng of GeneSwitch variants #1- #4. Twenty four hours after transfection medium was changed and samples were induced with 10 nM Mifiprestone (+MFP) or were not induced (-MFP). Renilla and firefly luciferase were measured at indicated time points post-MFP induction. Renilla luciferase expression was normalized to firefly luciferase expression. CMV-miApoB was used as a positive control, CMV-miScr and GS-miScr served as negative controls and were set at 100%. Transfected cells were assayed at 48 h post-transfection in 20 µl 1x passive lysis buffer (Promega, Madison, WI) using the Dual-Luciferase Reporter Assay System (Promega, Madison, WI).

Flow cytometry

Cells were transfected with 10 ng Luc-ApoB reporter and 50 ng of GS-miApoB single backbone variant. Twenty four hours after transfection medium was changed and samples were induced with 10 nM Mifiprestone (+MFP) or were not induced (-MFP). Cells were fixed and analyzed on FACSCalibur flow cytometer instrument (BD Biosciences, San Jose, CA). 1000 events were counted and fold change of GFP

expression was calculated for each construct by dividing the amount of cells GFP positive after MFP induction by the number of GFP positive cells without MFP induction.

siRNA and miRNA detection by small RNA Taqman assay

RT reactions for siApoB, siH10, siH12, siS7 and siS15 expression were performed with the TaqMan MicroRNA Reverse Transcription Kit (Applied Biosystems, Foster City, CA) using 10 ng RNA and 3 µl custom-made specific RT-stem-loop primers (Applied Biosystems, Foster City, CA) according to the manufacturer's instructions. The TaqMan assay was done in 20 µl using 1,33 µl cDNA, 1 µl custom-made siRNA-specific primer with FAM-labeled fluorogenic probe (Applied Biosystems) and 10 µl TaqMan 2× Universal PCR Master Mix (Applied Biosystems). Amplification of the beta actin gene was used as a RNA quality and loading control. For siApoB copy number per cell was calculated based on the amplification plot of a dilution series of synthetic siRNA standards (IDT, Coralville, IA). Tenfold dilutions (100 pg – 1 fg) of the guide strand of the synthetic siRNA oligo were used to create a standard line. The copy number of each dilution was calculated according to the formula 1 mol = 6.02×10^{23} molecules. The trend line value of the standard line was used to calculate the siRNA copy number per cell, assuming 15 pg RNA per cell. siH10, siH12, siS7 and siS15 expression levels were normalized to beta actin as an internal control, and the relative expression $2^{-\Delta\Delta Ct}$ method of Livak and Schmittgen was used for analysis of the induction [40].

Supplementary material

Table S1. Oligonucleotides used in this study

Name	Sequence (5'-3')
pr965	CGTCTAGAGCATTGGAACGCGGATTCCC
pr966	TTCGGTCCGTCGAGCCCTACAGGTTGTC
pr967	TTCCATGGGCAGGCTTTAAAACCATGGTGAGCAAGGGCGAGGAGCTGTC
pr968	TTGGTACCATGCATCCTGCAGGCTAGAGCCCCAGCTGCGCAGATCCATCAGAGATTTTGAGAC
miRfw	ACTCCGCGGGCAGGCTTTAAAACCATGGTGAG
miRrv	ACTGCGGCCGCGTACAAGAAGCTGGGTCTAGAT
prGS3fw	GGCATGGACGAGCTGTACAA
prGS3rv	CTCTAGATCAACCACTTTGT

Reference list

1. Borel, F, van Logtenstein, R, Koornneef, A, Maczuga, P, Ritsema, T, Petry, H, et al. (2011). In vivo knock-down of multidrug resistance transporters ABCC1 and ABCC2 by AAV-delivered shRNAs and by artificial miRNAs. *J RNAi Gene Silencing*; **7:** 434-442.
2. Grimm, D, Streetz, KL, Jopling, CL, Storm, TA, Pandey, K, Davis, CR, et al. (2006). Fatality in mice due to oversaturation of cellular microRNA/short hairpin RNA pathways. *Nature*; **441:** 537-541.
3. Giering, JC, Grimm, D, Storm, TA and Kay, MA (2008). Expression of shRNA from a tissue-specific pol II promoter is an effective and safe RNAi therapeutic. *Mol Ther*; **16:** 1630-1636.
4. Song, J, Pang, S, Lu, Y, Yokoyama, KK, Zheng, JY and Chiu, R (2004). Gene silencing in androgen-responsive prostate cancer cells from the tissue-specific Prostate-specific antigen promoter. *Cancer Res*; **64:** 7661-7663.
5. Song, J, Pang, S, Lu, Y and Chiu, R (2004). Poly(U) and polyadenylation termination signals are interchangeable for terminating the expression of shRNA from a pol II promoter. *Biochem Biophys Res Commun*; **323:** 573-578.
6. Xia, H, Mao, Q, Paulson, HL and Davidson, BL (2002). siRNA-mediated gene silencing in vitro and in vivo. *Nat Biotech*; **20:** 1006-1010.
7. Xia, XG, Zhou, HX, Samper, E, Melov, S. Xu, ZS. (2006). Pol II-expressed shRNA knocks down Sod2 gene expression and causes phenotypes of the gene knockout in mice *PLoS Genet*;**2**: 73-80.
8. Boudreau, RL, Martins, I and Davidson, BL (2009). Artificial microRNAs as siRNA shuttles: improved safety as compared to shRNAs in vitro and in vivo. *Mol Ther*; **17**: 169-175.
9. Henriksen, JR, Løkke, C, Hammerø, M, Geerts, D, Versteeg, R, Flřgstad, T, et al. (2007). Comparison of RNAi efficiency mediated by tetracycline-responsive H1 and U6 promoter variants in mammalian cell lines. *Nucleic Acids Res*; **35:** e67.
10. Matthess, Y (2005). Conditional inhibition of cancer cell proliferation by tetracycline-responsive, H1 promoter-driven silencing of PLK1. *Oncogene*; **24:** 2973-2980.
11. Nordstrom, JL (2003). The antiprogestin-dependent GeneSwitch system for regulated gene therapy. *Steroids*; **68:** 1085-1094.
12. Xu, ZL, Mizuguchi, H, Mayumi, T and Hayakawa, T (2003). Regulated gene expression from adenovirus vectors: a systematic comparison of various inducible systems. *Gene*; **309:** 145-151.
13. Reboredo, M, Kramer, MG, Smerdou, C, Prieto, J and De Las, RJ (2008). Transcriptomic effects of Tet-on and mifepristone-inducible systems in mouse liver. *Hum Gene Ther*; **19:** 1233-1247.
14. Harkins, RN, Szymanski, P, Petry, H, Brooks, A, Qian, HS, Schaefer, C, et al. (2007). Regulated expression of the interferon-[beta] gene in mice. *Gene Ther*; **15:** 1-11.
15. Bhat, RA, Stauffer, B, Komm, BS and Bodine, PVN (2004). Regulated expression of sFRP-1 protein by the GeneSwitch system. *Protein Expr Purif*; **37:** 327-335.
16. Taylor, J, Rohatgi, P, Spencer, HT, Doyle, D and Azizi, B (2010). Characterization of a molecular switch system that regulates gene expression in mammalian cells through a small molecule. *BMC Biotechnol*; **10:** 15.
17. Burcin, MM, Schiedner, G, Kochanek, S, Tsai, SY and O'Malley, BW (1999). Adenovirus-mediated regulable target gene expression in vivo. *Proc Natl Acad Sci U S A*; **96:** 355-360.
18. Cadepond, F, Ulmann, A and Baulieu, EE (1997). RU486 (mifepristone): mechanisms of action and clinical uses. *Annu Rev Med*; **48:** 129-156.
19. Seibler, J, Kleinridders, A, Kuter-Luks, B, Niehaves, S, Bruning, JC and Schwenk, F (2007). Reversible gene knockdown in mice using a tight, inducible shRNA expression system. *Nucleic Acids Res*; **35:** e54.
20. Aagaard, L, Amarzguioui, M, Sun, G, Santos, LC, Ehsani, A, Prydz, H, et al. (2007). A facile lentiviral vector system for expression of doxycycline-inducible shRNAs: knockdown of the pre-miRNA processing enzyme drosha. *Mol Ther*; **15:** 938-945.
21. Premsrirut, P, Dow, L, Kim, S, Camiolo, M, Malone, C, Miething, C, et al. (2011). A rapid and scalable system for studying gene function in mice using conditional RNA interference. *Cell*; **145:** 145-158.
22. Kappel, S, Matthess, Y, Zimmer, B, Kaufmann, M and Strebhardt, K (2006). Tumor inhibition by genomically integrated inducible RNAi-cassettes. *Nucleic Acids Res*; **34:** 4527-4536.
23. Westerhout, EM, Vink, M, Haasnoot, PC, Das, AT and Berkhout, B (2006). A conditionally replicating HIV-based vector that stably expresses an antiviral shRNA against HIV-1 replication. *Mol Ther*; **14:** 268-275.
24. McJunkin, K, Mazurek, A, Premsrirut, PK, Zuber, J, Dow, LE, Simon, J, et al. (2011).

Reversible suppression of an essential gene in adult mice using transgenic RNA interference. *Proc Natl Acad Sci U S A*; **108:** 7113-7118.

25. Wiznerowicz, M and Trono, D (2003). Conditional suppression of cellular genes: lentivirus vector-mediated drug-inducible RNA interference. *J Virol*; **77:** 8957-8961.
26. Coumoul, X, Li, W, Wang, RH and Deng, C (2004). Inducible suppression of Fgfr2 and Survivin in ES cells using a combination of the RNA interference (RNAi) and the Cre-LoxP system. *Nucleic Acids Res*; **32:** e85.
27. Konstantinova, P, de Vries, W, Haasnoot, J, ter Brake, O, de Haan, P and Berkhout, B (2006). Inhibition of human immunodeficiency virus type 1 by RNA interference using long-hairpin RNA. *Gene Ther*; **13:** 1403-1413.
28. Gupta, S, Schoer, RA, Egan, JE, Hannon, GJ and Mittal, V (2004). Inducible, reversible, and stable RNA interference in mammalian cells. *Proc Natl Acad Sci U S A*; **101:** 1927-1932.
29. Wu, RH (2007). A tightly regulated and reversibly inducible siRNA expression system for conditional RNAi-mediated gene silencing in mammalian cells. *J Gene Med*; **9:** 620-634.
30. Gupta, S, Schoer, RA, Egan, JE, Hannon, GJ and Mittal, V (2004). Inducible, reversible, and stable RNA interference in mammalian cells. *Proc Natl Acad Sci U S A*; **101:** 1927-1932.
31. Maczuga, P, Lubelski, J, van Logtenstein, R, Borel, F, Blits, B, Fakkert, E, et al. (2013). Embedding siRNA sequences targeting Apolipoprotein B100 in shRNA and miRNA scaffolds results in differential processing and in vivo efficacy. *Mol Ther*; 21: 217-227.
32. Chtarto, A, Bender, HU, Hanemann, CO, Kemp, T, Lehtonen, E, Levivier, M, et al. (2003). Tetracycline-inducible transgene expression mediated by a single AAV vector. *Gene Ther*; **10:** 84-94.
33. Chtarto, A, Yang, X, Bockstael, O, Melas, C, Blum, D, Lehtonen, E, et al. (2007). Controlled delivery of glial cell line-derived neurotrophic factor by a single tetracycline-inducible AAV vector. *Exp Neurol*; **204:** 387-399.
34. Vanrell, L, Di, SM, Blanco, L, Otano, I, Gil-Farina, I, Baldim, V, et al. (2011). Development of a liver-specific Tet-on inducible system for AAV vectors and its application in the treatment of liver cancer. *Mol Ther*; **19:** 1245-1253.
35. Nicholson, L, Singh, GK, Osterwalder, T, Roman, GW, Davis, RL and Keshishian, H (2008). Spatial and temporal control of gene expression in drosophila using the inducible geneSwitch GAL4 system. I. Screen for larval nervous system drivers. *Genetics*; **178:** 215-234.
36. Juven-Gershon, T, Hsu, JY, Theisen, JW and Kadonaga, JT (2008). The RNA polymerase II core promoter - the gateway to transcription. *Curr Opin Cell Biol*; **20:** 253-259.
37. Baumann, M, Pontiller, J and Ernst, W (2010). Structure and basal transcription complex of RNA polymerase II core promoters in the mammalian genome: an overview. *Mol Biotechnol*; **45:** 241-247.
38. Koornneef, A, Maczuga, P, van Lontenstein, R, Borel, F, Blits, B, Ritsema, T, et al. (2011). Apolipoprotein B knockdown by AAV-delivered shRNA lowers plasma cholesterol in mice. *Mol Ther*; **19:** 731-740.
39. Chen, C, Ridzon, DA, Broomer, AJ, Zhou, Z, Lee, DH, Nguyen, JT, et al. (2005). Real-time quantification of microRNAs by stem-loop RT-PCR. *Nucl Acids Res*; **33:** e179.
40. Livak, KJ and Schmittgen, TD (2001). Analysis of relative gene expression data using real-time quantitative PCR and the 2-[delta][delta] CT method. Methods; 25: 402-408.

CHAPTER 7

Discussion

Many diseases, including hereditary diseases, viral infections, hepatitis, cirrhosis, fatty liver disease, and cancer can affect the liver. Most of these are characterized by altered expression of disease-related genes and in some cases progression of the disease may be stopped or even reversed when the disease-related gene is inhibited. Therefore, when inhibition of a "faulty gene" expression is therapeutically beneficial, RNAi is a suitable approach for treatment of liver diseases. The research presented in this thesis covered the design, optimization and comparison of RNAi inducers for treatment of FH by targeting ApoB. However, the results presented in this thesis can be applied for developing RNAi-based therapeutics for other diseases as well.

Development of RNAi-based gene therapy of FH by targeting ApoB

The ApoB protein constitutes a structural part of VLDL-C and LDL-C two classes of lipoproteins that are considered atherogenic. Increased circulating levels of LDL-C and VLDL-C are often associated with development of cardiovascular diseases [1]. In this thesis we focused on ApoB knockdown for treatment of FH using shRNA (shApoB) and artificial miRNA (miApoB). This approach, in combination with an effective AAV delivery method, can provide potent long-term inhibition of ApoB and in consequence lowering of plasma cholesterol. In chapter 2, we reported that shApoB specifically reduce LDL-C in diet-induced dyslipidemic mice, whereas HDL-C remained unaffected [2]. We also reported increased lipid accumulation, which is now recognized to be a commonly observed side effect of ApoB inhibition. In chapter 3, the knockdown efficacy of pol II-expressed shRNA and artificial miRNA was compared. Our results demonstrated that pol II-expressed artificial miRNA have a superior efficacy profile when compared to shRNA. Therefore, in chapter 4 we compared the long-term efficacy of shApoB and miApoB *in vivo.* Although miApoB performed significantly better in silencing ApoB than shApoB, the inhibitory effect mediated by both molecules was lost over the 27 week experiment. We also discovered that shApoB and miApoB are differentially processed *in* vitro. In chapter 5, we further investigated the consequences of these differences by analyzing the effects of shApoB and miApoB expression on liver morphology, transcriptome and endogenous miRNA profile. Finally, in chapter 6 we developed the GeneSwitch regulated expression system for miApoB allowing gene expression to be turned "on and off".

FH is a recessive genetic disorder characterized by very high levels of LDL-C and early cardiovascular disease which are often caused by mutations in Ldl-r or ApoB [3,4]. There are two types of FH: the heterozygous form in which the patient has one normal allele and one mutated, and the homozygous form in which the patient has two mutated alleles. To date there is no cure for this disease and the primary goal of clinical management is to control hypercholesterolemia by lifestyle modification

and/or symptomatic drug treatment in order to decrease the risk of atherosclerosis [5]. Currently inhibitors of HMG-CoA (statins) are the most effective and best tolerated lipid-lowering agents. However these drugs are not always effective in all patients [4] and the response may depends on the mutation underlying the disease. Statins also have rare but serious adverse effects, including muscle damage, which may lead to acute kidney failure. Additionally high dose of statins may cause liver toxicity and as a consequence statins are not an appropriate treatment for patients with active liver diseases. For patients who do not respond to the maximal dose or have contraindications, other cholesterol inhibiting drugs including bile acid resin, niacin, fibrate or cholesterol absorption inhibitors may be used as a alternative treatment or combined with lower dose of statins. However even combined treatment for some patients especially with homozygous form of FH does not lead to a satisfactory reduction of LDL-C. For the most severe cases orthotropic liver transplantation maybe considered, but clearly this is not an option for the majority of FH patients.

Because some patients cannot be effectively treated with conventional lipid lowering therapies, several novel approaches have been developed either as alternative therapy or to be used combined with standard therapies. These approaches target genes or miRNA involved in lipid metabolism, in order to lower LDL-C levels. Examples include antisense oligonucleotides to Pcsk9, ApoB, mir-122, inhibitors of Mtp and siRNA against Pcsk9, Mtp or ApoB [6-12]. With the exception of the Mtp inhibitor, which is a small molecule, these new drugs are oligonucleotides inducing mRNA cleavage, translational repression or inhibiting miRNA functions.

The antisense oligonucleotide to ApoB (mipomersen, commercial name Kynamro) developed by ISIS Pharmaceuticals is the most extensively studied as an alternative FH therapy. An antisense oligonucleotide is a nucleic acid that binds to the target RNA sequence and in consequence inactivates the gene of interest by triggering RNAse H-dependent or independent cleavage mechanisms [13,14]. In phase 3 clinical studies on patients with homozygous and heterozygous FH, Kynamro showed an average 36% LDL-C reduction. The most notable side effect was liver fat accumulation accompanied by increase in liver enzymes suggesting liver toxicity, and potentially limiting its clinical applicability. Recently Kynamro also revealed its efficacy in a small phase 2 study in patients with the heterozygous form of FH, that were intolerant to statins. The average reduction of ApoB was 46% which subsequently resulted in 47% reduction of LDL-C [15]. One of the disadvantages of this approach is the fact that the drug has to be delivered weekly via subcutaneous injections for stable therapeutic effect. By contrast, our results showed that AAV delivered shApoB can provide a long-term phenotypic correction with a single intravenous administration. It is argued that the therapeutic goal in FH should be a reduction of cholesterol of at least 30%. Indeed, our data showed that a 32% can be achieved with as low dose as 10^9 gc/animal. The ApoB reduction by AAV-shApoB was dose dependent

and the highest dose 10^{12} gc/animal resulted in 95% reduction of ApoB mRNA and undetectable level of ApoB protein in plasma.

Lomitapide, a small molecule inhibiting Mtp may provide a clinical benefit that is comparable to Kynamro [16]. The Mtp protein is responsible for binding and shuttling individual lipid molecules between membranes and a normal function of Mtp is necessary for synthesis of the ApoB containing lipoproteins VLDL-C and LDL-C. Lomitapide has been evaluated in more than 900 FH patients in clinical trials, and an average LDL-C decrease of 40% was measured [17]. Since Mtp works at a level of lipoprotein synthesis that is comparable to ApoB, its inhibition was also associated with increased fat accumulation in the liver and increase in liver enzymes. Other side reported effects were gastrointestinal problems associated with an increase in dosage.

In contrast to the above mentioned drugs, miravirsen- a LNA oligonucleotide inhibiting mir-122 was not developed specifically for FH but for treatment of HCV viral infections [18]. LNA is chemical modification of oligonucleotides, which improve its affinity to RNA target concominant with higher specificity and stability compared to non-modified oligonucleotides. Mir-122 constitutes about 70% of all liver miRNAs, and it has been shown to play an important role in HCV viral replication [19]. Clinical trials using Miravirsen showed more than 100-fold reduction of viral plasma RNA levels compared to baseline. Interestingly, a reduction of the cholesterol levels in all patients was also reported indicating that targeting mir-122 can also potentially be used in treatment of FH. On the safety aspects, elevated ALP levels were measured, which is considered as a marker of liver injury equivalent to ALT and AST. Similarly to siRNA and antisense drugs, LNA therapeutics for FH would require re-administration for stable correction of cholesterol. One of the larger disadvantages of mir-122 inhibition is that this is not a direct approach targeting proteins involved in lipid metabolism. In fact, inhibition of endogenous miRNA may result in deregulation of multiple liver functions. For example, mir-122 knockout mice displayed hepatic inflammation, fibrosis, and a high incidence of hepatocellular carcinoma, suggesting that mir-122 has a tumor suppressor role in hepatocytes [20].

Another alternative strategy to treat FH is to induce RNA interference by delivering siRNA targeting ApoB or Pcsk9. siRNA administration has been reported to decrease ApoB levels and plasma cholesterol in mice and recently also in non-human primates [11,21]. Tekmira has reported a roughly 20% inhibition of ApoB and LDL-C following siRNA administration in a phase I clinical trial [22]. However the initial efficacy trial has been terminated as one of the patients treated at the highest dose experienced an adverse event comprised of flu-like symptoms, cytokine release and transient hypotension consistent with stimulation of the immune system. This confirms the notion that siRNA can be potent activators of immune response in humans, corroborating previous studies in rodents. In all studies discussed thus far increased lipid accumulation in liver was reported, and this seems to be inherent to inhibition

of ApoB. Another approach is to use siRNA targeting Pcsk9 which plays important role in Ldl-r turnover and degradation. The efficacy of siRNA targeting Pcsk9 has already been shown *in vivo* in mice and primates [12]. In NHP, a single dose of siRNA targeting Pcsk9 resulted in a rapid, durable, and reversible lowering of plasma Pcsk9 which resulted in ~70% inhibition of ApoB and ~60% reduction of LDL-C [12]. No increase in liver enzymes has been reported. Unfortunately, the authors did not include evaluations of lipid accumulation in liver. siRNAs targeting ApoB or Pcsk9 suffer a similar limitation to antisense oligonucleotides, being the that regular siRNA injections would be required for a long-term phenotypic effect.

In contrast to the previously described studies, our data show the feasibility of long-term correction of LDL-C in plasma after a single intravenous injection of AAV encoding shRNA targeting ApoB (chapter 2). AAV have unique properties such as low immunogenicity, the lack of integration into the host genome and the natural occurrence of different serotypes with unique transductional proprieties. In our studies serotype 8 was used which has been shown to efficiently transduce liver in mice and in NHP [23,24]. The AAV delivered DNA was engineered into a self-complementary form that has been shown to provide more rapid and potent transduction compared to single stranded AAV. However our approach was found to have some disadvantages. First, we observed a dose-dependent increase in liver lipid accumulation. As discussed previously, this seems to be a common side effect of all ApoB targeting therapies. It remains to be seen whether this will preclude further development of ApoB targeting therapies, and in the Kynamro clinical trials it was reported that liver fat may stabilize or decline in patients who continue treatment beyond a year [25]. Steatosis may be associated with inflammation and may progress to cirrhosis, thus liver lipid accumulation side effect should be minimized for safe and long term therapy. An attractive approach would be to block the accumulation of hepatic triglycerides by the simultaneous inhibition of another target involved in lipid metabolism. Indeed Merck has recently reported that simultaneous inhibition of Mtp and Dgat2 genes with siRNA resulted in decrease in plasma cholesterol and attenuation of hepatic fat accumulation induced by Mtp silencing [26]. Surprisingly double knockdown of ApoB and Dgat2 or ApoB and Fatbp5 did not result in reduction of lipid accumulation [10].

A significant problem in evaluating treatment efficacy for FH is the species-specific difference in plasma lipid profile in model animals. Wild-type mice have very high levels of anti-atherogenic HDL-C and low pro-atherogenic LDL-C levels. Hence, high fat diets or genetic manipulations are necessary in order to generate models for familiar hypercholesterolemia and coronary atherosclerosis [2,11,27]. Nonetheless, mice with a human-like lipid profile are now available and can be used in preclinical studies [11]. NHPs demonstrate the closest overall match to dyslipidemic humans are sometimes considered the optimal animal model for target validation and drug discovery. However in several aspects NHPs differ from human- for example atherosclerosis plaques are not

observed [28]. For future development of RNAi gene therapy of FH a careful selection of the animal model needs to be done to estimate properly all possible side effects.

The long-term expression provided by AAV vectors can also be seen as a major disadvantage, especially when side effects are being observed during the treatment as it would be impossible to discontinue the therapy. Therefore, in subsequent chapters 3-6 we focused on minimizing possible side effect resulting from AAV-RNAi gene therapy for FH.

Expression of shRNA with different promoters

In our initial experiment (chapter 2), we did observe a loss of the ApoB inhibition over time which was associated with strong shRNA expression. Therefore, in chapter 3 pol II promoters were used as these provide moderate levels of expression. It has been reported that pol II promoters, like the CMV promoter and the liver-specific hAAT promoter, are capable of driving shRNA expression *in vitro* and *in vivo*, which resulted in lower shRNA toxicity [29,30]. An alternative strategy to direct expression of shRNA is to embed the siRNA sequence in artificial miRNA. Artificial miRNAs are sometimes called 2nd generation RNAi, but this phrase is misleading because miRNA and shRNA may behave very differently [31-33]. When driven by pol II promoters, both miRNA and shRNA are less toxic compared to pol III [31,32]. Therefore to optimize pol II shRNA expression, we designed a number of constructs targeting luciferase with different termination signals hairpin stem lengths expressed from the CMV promoter [34]. Surprisingly none of the shRNA configurations tested resulted in strong luciferase knockdown. We believe that this was due to inefficient processing of shRNA by RNAi machinery as pol II transcription start and termination can be shifted on both 5' and 3' ends of the hairpin. In contrast, 2 out of 3 designed CMV expressed miRNAs resulted in 80% inhibition of their targets which was similar to pol III-expressed shRNA [34].

To date only a few examples of direct expression of shRNA from pol II promoters have been reported [29,35,36]. Son *et al.* showed successful silencing of JNK with shRNA expressed with prostate specific antigen promoter in androgen-responsive prostate cancer cells [36]. Giering *et al.* reported successful long-term inhibition of the envelope surface antigen of HBV *in vivo* with shRNA expressed from a liver-specific promoter [29]. They also reported that CMV promoter expressing 25 bp length hairpin with pA resulted in ~40% inhibition of luciferase, but in our experiments this approach resulted in only ~20% inhibition of luciferase. This discrepancy may be explained by different sequences of the hairpin used in both studies. Yuan *et al.* reported effective inhibition of Lamin B2 by shRNA fused to GFP gene and followed by standard polyadenylation signal [37]. This finding is in contrast to previous reports where 5' and 3' overhangs of shRNA were shown to inhibit Dicer processing [38]. We hypothesize that these GFP-fused shRNA resemble artificial miRNA rather than shRNA and that processing by Drosha and Dicer explains their activity. Although our results do

confirm the feasibility of shRNA expression from pol II promoters, we demonstrated that using artificial miRNA is less laborious and provides more efficient gene silencing. A number of tissue specific and inducible promoters has been described [39,40], allowing restriction of the expression of therapeutic siRNA to the target tissue or enabling the expression to be turned "on" and "off".

Long-term efficacy and processing of shRNA and miRNA targeting ApoB *in vivo*

In a subsequent work (chapter 4), we focused on the efficacy of shRNA and miRNA targeting ApoB *in vitro* and *in vivo*. To minimize possible side effects we used the liver specific LP1 promoter to express miRNA targeting ApoB. The efficacy of such an approach may be questioned because a tissue specific promoter was anticipated not to provide sufficient expression levels to induce phenotypic effect [41]. Since the dose which we used was comparable to the one used in the Grimm *et al.* study ($2x10^{11}$ gc/mice) we anticipated that the shRNA would cause toxicity and therefore the silencing effect can be lost over the time and the miRNA would provide stable ApoB inhibition. Surprisingly the inhibitory effect diminished for both molecules over the 27 weeks experiment despite that miApoB expressed less molecules and expression was limited to the liver. Artificial miRNAs have been shown to be non toxic in brain while expression of shRNA resulted in cellular damage [31,33]. Hence, one of the reasons of the discrepancies might be the targeted organ. The central nervous system (CNS) is considered immune privileged due to its isolation behind the blood-brain barrier and lack of conventional lymphatic drainage [42,43]. Although it is possible that immune response against shRNA and miRNA play important role in RNAi toxicity, in our studies no liver inflammation was observed in any experimental group. Additionally our own results did not show interferon response in AAV-shApoB-injected animals [2]. Rather, the loss of efficacy was associated with viral DNA loss over time of the experiment which suggested liver toxicity. However at week 27, no obvious signs of hepatocellular toxicity in AAV-shApoB and AAV-miApoB groups were detected, suggesting that adverse effects may have taken place earlier in time.

There are several reports on long-term RNAi efficacy in mice, rats and NHP. Most commonly siRNAs were used which required repeated administration for a stable effect. Only a limited number of reports on long term efficacy of AAV-shRNA or AAV-miRNA *in vivo* have been pulished; Chen *et al.* reported significant inhibition of HBV for 120 days after single injection of $1x10^{12}$ gc AAV-shRNA [44]. Similarly to our results AAV-shRNA reached peak in inhibition around 23 wk p.i. and then the inhibition effect gradually decreased with time. It should be noted that in their experiment the AAV vectors were infused through intrasplenic injection, which is not a commonly used (or practical) procedure for AAV delivery. Giering *et al.* reported that liver-specific shRNA

expression targeting sAg was detected for more than one year in murine liver [29]. However the doses used in their studies were $3x10^{11}$ and $1x10^{12}$ gc/mice which are 3 fold and 10 fold higher than we used (chapter 4). The authors showed sAg inhibition data for 100 days; however they mention that shRNA expression could be detected for more than one year. Interestingly while the effect of the higher dose was stable, the inhibition provided by the lower dose became weaker over the time.

Initially, we assumed that shApoB and miApoB processing would result in identical siApoB targeting sequences that would mediate the phenotypic effect of LDL-C lowering. To our surprise, and despite the predictions, NGS sequencing revealed that embedding identical siRNA sequences into shRNA or miRNA scaffolds results in processing of a diverse pool of siApoB sequences with different 5' and 3' ends. The length of the processed products varied with shApoB products between 19 and 23 nt long, 21 being the most abundant, and miApoB products between 23 and 25 nt and 24 being the most abundant. miRNAs are endogenously processed by Drosha which cleaves off flanking sequences and subsequently Dicer cleaves the loop and mature miRNA duplex is formed [45]. shRNAs are generally processed by Dicer which cleaves off the loop, however hairpins with a stem shorter than 19 bp may be processed independently from Dicer [46]. Recently, it has been reported that such non-canonical processing uses Ago2 cleavage and yield only a single ~33 nt strand that can effectively induce RNAi (Y.P.Liu, personal communication, 2012). In our experiments, an important observation was that shRNA processing resulted in a wider range of siRNA variants than miRNA processing. Small number of NGS reads represented shRNA that was cut once as the passenger or guide strand and were still linked to the loop. Small number of reads representing the loop of shApoB and miApoB were also detected. The relevance of these findings still needs to be investigated but these cleavage products may result in non specific interactions as single stranded siRNA (ss-siRNA) were shown to enter the RISC complex, activate RNAi and effectively inhibit gene expression [47,48]. Because ss-siRNA are less stable than dsRNA and are rapidly degraded by nucleases, their application in RNAi so far was limited. However recent reports show that chemical modification can stabilize ss-siRNA and provide potent inhibition of gene expression via RNAi [47,48].

Another important observation was that the abundance of guide and passenger strands varied between shApoB and miApoB. The siApoB passenger strand was detected in a very high percentage of the reads from miApoB. Similarly to our results, Gu *et al*. recently reported that mainly the guide siRNA strand of a shRNA was pulled down with Ago2 while both guide and passenger strands were detected from a miRNA scaffold associated with Ago1/2/3/4 [49]. Additionally, the passenger strand from the miRNA was not cleaved and eliminated as efficiently as from the shRNA. However, reporter assays revealed that the passenger siRNA strand was mainly loaded

into non-activated Ago complexes rendering those sequences ineffective at inducing knockdown. Our findings indicate that differential processing and Ago loading of siRNAs originating from different scaffolds may have important consequences as all siRNA variants can be loaded into RISC and this will increase the occurrence of possible aspecific interactions. These distinct differences in processing and loading have critical implications for future design of RNAi-based therapeutics.

RNAi toxicity due to oversaturation of the cellular miRNA processing

RNAi toxicity due to oversaturation of the cellular miRNA processing seems to be one of the major obstacles for therapeutic RNAi applications. It has been shown that pol II-expressed shRNA and artificial miRNA reduce the risk of endogenous RNAi pathway saturation. Our results confirmed the feasibility of tissue specific expression of artificial miRNA which resulted in phenotypic changes *in vivo*. Nonetheless, the knockdown induced by both shApoB and miApoB diminished over time in a dose-dependent manner. Loss of the effect was previously attributed to saturation of endogenous RNAi pathway, in particular Exportin 5 which leads to global deregulation of miRNA expression and has been associated with induced liver toxicity [50]. However in chapter 4 and 5 we did not observe saturation of the endogenous miRNA pathway but rather, the loss of the effect was associated with loss of virally delivered DNA [2] . By *lowering* the dose stable inhibition of ApoB was achieved indicating the critical role of dose in relation to RNAi toxicity. McBride and Grimm have reported similar results indicating that RNAi associated toxicity is dose dependent and that by lowering the dose the toxicity can be abolished [31,50]. It is possible that competition with endogenous RNAi pathway occurs at multiple levels and saturation of Exportin 5 and deregulation of endogenous miRNA levels may not be the only cause for RNAi toxicity. In fact, it has been recently reported that overexpression of shRNA *in vivo* not only saturates Exportin 5, but also all 4 human Ago proteins [51]. Because artificial miRNA enter the RNAi pathway "earlier" than shRNA, it was speculated that this may slow their loading onto RISC and thereby reduce their competition with other small RNAs or RNAi factors. This, together with the differential loading onto Ago proteins support the fact that miRNA has better intrinsic properties for therapeutic RNAi. Nonetheless, the efficacy of AAV delivered shRNA targeting HCV virus in non-human primates has been demonstrated [24]. The authors reported that high-expression levels of shRNA from pol III promoter resulted in dose dependent hepatocellular toxicity, but this problem was overcome by promoter modification which resulted in lower siRNA expression. These results suggest that RNAi toxicity may well be conserved in humans and further optimization of RNAi mediators as well as delivery methods is necessary for the development of safe and effective RNAi therapeutics.

RNAi off-targeting

Perhaps the biggest challenge of RNAi therapy is to eliminate unintended inhibition of transcripts, known as "off-targeting". The side-effect is reminiscent of transcript regulation by endogenous miRNAs, where the seed region plays a key role in target recognition. Because seed-target interactions are often difficult to predict in the design stage RNAi therapeutics can potentially affect a large number of genes. Snøve *et al.* reported that roughly 75% out of 359 siRNA sequences that were previously published had a risk of elucidating non specific effects although their sequences were believed to be highly specific to the target gene [52]. Despite the complexity of the prediction, the authors argue that many target-specific siRNA can be designed by using more stringent prediction methods. In chapter 5 we showed that expression of shRNA and miRNA exerted distinct changes on liver gene and miRNA expression, which resulted in distinct phenotypic changes. Based on the shApoB/miApoB processing data we performed detailed off-target prediction analysis using the Smith-Waterman algorithm and these results were verified with NGS transcriptome analysis *in vivo*. Notably, none of the genes predicted in the analysis were found to be significantly affected for both miRNA and shRNA, but expression levels of several non-predicted genes were affected. Although our off-target prediction covered only the most abundant variants of siApoB guide and passengers strands and some off-targets may have been missed this was still surprising. An important observation is that the majority of these genes were upregulated in shApoB and in miApoB, whereas in case of off-targeting gene downregulation is expected. This may suggest that the observed changes may be a result of various different mechanisms. Of these, AAV infection, RNAi expression and ApoB knockdown may be among the most relevant. Additionally miRNAs may regulate their targets by translational repression; therefore we might speculate that the off-target effects may be stronger at protein level.

Recently Ahn *et al.* reported global changes in gene expression in the liver after delivering adenoviral vector expressing shRNA [53]. We have shown that expression of *identical* siRNA sequences from shRNA or miRNA expression in liver results in differential gene expression in liver, and multiple genes and functions were found to be affected. Interestingly Biglycan (Bgn) and Lipoprotein lipase (Lpl) were upregulated for both AAV-shApoB and AAV-miApoB. Additionally apolipoprotein B mRNA editing enzyme, catalytic polypeptide-like 2 (Apobec2) was downregulated in both groups. These common changes may be specific results of the strong ApoB knockdown in the liver. Despite the same phenotypic effect (i.e. lowering of circulating cholesterol concentrations), genes involved in lipid metabolism were differentially affected in AAV-shApoB compared to AAV-miApoB animals. In AAV-shApoB injected mice, NGS analysis revealed upregulation of genes involved in MAPK pathway, which confirmed liver histology data. Surprisingly transcriptome analysis on the animal injected with AAV-shApoB revealed upregulation

of inflammatory genes but we did not observe hepatic inflammation histologically. A possible explanation would be that the AAV-shApoB induced inflammation at earlier time points and the increased proliferation is consequence of liver injury. However we did not observe an increase in liver transaminases enzymes in AAV-shApoB-injected animals. Both AAV-miScr (control) and AAV-miApoB-injected animals did exhibit mild upregulation of ALT and AST around 4 and 6 wk p.i. but no increase of hepatocyte proliferation was detected. Our results are similar to those of Ahn *et al.* who reported increased liver and apoptosis proliferation in liver as a consequence of shRNA expression without signs of inflammation [53]. In fact it is known that even low shRNA doses may induce mild hepatic damage, followed by compensatory hepatocyte proliferation in mice, without a clinical phenotype [54]. Moreover, mild hepatic injury with active Myc oncogene can accelerate tumorogenesis and cause mortality. This suggests caution regarding potential induction of cancerogenesis by stable shRNA expression in liver. Still similar studies on miRNA expression and cancerogenesis have to be initiated.

Some endogenous miRNA were found to be affected by expression of both shApoB and miApoB and surprisingly a large number of miRNAs were upregulated. It is still unclear whether the observed transcriptome and cellular miRNA changes were a specific effect of shApoB/miApoB expression or ApoB inhibition or a combination of both. In recent years, it has become apparent that beside miRNA also other non-coding RNAs tRNAs, rRNAs, snRNA and snoRNAs are implicated in development and progression of many diseases [55,56]. In our NGS analysis we focused exclusively at the expression of endogenous miRNA and we believe that an analysis of the complete small RNA transcriptome needs to be included in future studies.

Regulated RNAi expression

The RNAi field is a newcomer in the therapeutic armamentarium and one of the big challenges is to improve its safety. Our data indicate that constitutive expression of shRNA and miRNA does have a significant impact on cellular small RNA and gene expression *in vivo*. This finding led us to develop inducible expression of artificial miRNAs, as described in chapter 6. Previous efforts to develop regulable RNAi have resulted in the identification of a number of inducible systems (Table 1). These systems typically utilize a small molecule to activate a chimeric transcription factor, which by binding to its recognition sequences which allow spatio-temporal and quantitive control of shRNA or miRNA expression. This minimizes risk of toxicity resulting from uncontrolled and sustained siRNA or gene overexpression. However, chimeric transcription factors may introduce another source of toxicity as they may be immunogenic or modulate expression of endogenous genes. With some of the systems high basal expression in the absence of the inducer may be a problem. Several groups have reported successful inhibition of target genes with induced expressed shRNA as well as artificial miRNA

Table 1. Comparison of inducible systems

Small molecule-inducible systems	Advantages	Disadvantages
All	- Spatial, temporal and quantitative control of expression - Especially useful for expression of cytokines, chemokines and toxic gene products - Minimum safety risk due to stringent control - Doxycycline, mifepristone and rapamycin are clinically approved drugs	- leakiness might be an issue for some systems - Artificial transactivators might be immunogenic - Effectiveness in humans needs to be validated
TetOn	- can be used with cell-type specific promoters - non-toxic to mammalian cells - no pleiotropic consequences for other cellular metabolic pathways - inducer is well characterized, antibiotic - doxycyline does not interfere with native proteins, reducing the side effects potentials - rapidly metabolized	- immunogenic except may be in brain and eye - doxycycline could be present in meat and other food sources
GeneSwitch	- not a potent immuno activator - inducer can cross the blood brain barrier - auto inducible system available	- Inducer may modulate endogenous gene expression - physiological changes of natural ligand expression may change target gene expression - activation of native steroide receptors possible - slower metabolizing of lipid steroide hormones
Ecdysone	- potent gene induction with short half life - non-toxic and nonteratogenic in mammals - do not affect mammal physiology - validated for regulated expression of shRNA and miRNA	- Ecdysone is asteroid hormone from *D. melanogaster*
Rapamycine	- entirely human origin proteins, so immune response could be lower - low baseline expression and high induction ratio - inducer reconstitutes active transcription factors by inducing dimerization.	- Inducer is a immunosupresive drug

in vitro and *in vivo* [57-65]. However the effectiveness and safety of any of those inducible systems has not been investigated in humans.

The tetracycline inducible system (Tet On) is one of the best characterized. It has been shown to express artificial miRNA targeting luciferase which upon induction resulted in specific inhibition in luciferase expressing transgenic mice [62]. This suppression was reversible and 12 days after doxycyline removal luciferase activity returned to basal levels. Moreover, expression of the artificial miRNA resulted in few or no changes in the expression of endogenous miRNAs in induced state compared to non-induced showing that reversible silencing of gene expression does not disrupt endogenous miRNA processing. On the other hand, because components of the Tet On system are derived from bacterial proteins, the system is highly immunogenic. Additionally the tetracycline-inducible system has a relatively high background of expression in the un-induced state [63]. A main drawback is that doxycycline is commonly used as an antibiotic in agriculture thus it can be found in meat and other food sources, which can result in unintended induction.

The Ecdysone inducible system is more tightly regulated and the components of the system do not affect mammalian physiology due to short half life [57,64]. The system has been shown to regulate expression of shRNA against the tumor suppressor p53 gene, which resulted in phenotypic changes *in vitro*. Remarkably, withdrawal of the inducer resulted in complete reversal of the cellular phenotype. The ecdysone inducible system has been shown to drive expression endogenous mir-122 *in vitro* [64] and embedding of siRNA in the mir-122 scaffold resulted in a potent inhibition of luciferase. The main disadvantage of the system is the inducer, which is a steroid hormone derived from *D.melanogaster*, which can possibly interfere gene expression in animals.

Another system which has been shown to express shRNA is the rapamycine regulated system [65]. It employs a different mechanism of transactivator activation. In contrast to doxycycline and ecdysone, it does induce transactivator dimerization rather than allosteric changes. The system is composed entirely from human derived proteins thus the risk for immunogenicity is minimized. This system exhibits superior inducibility in several cell lines compared to other inducible systems [66]. The main drawback in its application is the fact that rapamycine is immunosuppressive drug which limits its clinical application. Yet, a rapamycine analog, which is biologically non active, has been shown to efficiently act as inducer without compromising system properties [65].

The GeneSwitch system is composed of two components: the first one is the GeneSwitch regulatory protein, which upon induction dimerizes and binds to the regulatory sequence of the second component- the inducible promoter. Although it is not known to drive expression of shRNA or miRNA, it has some potential advantages over the other inducible system. Most importantly the transactivator protein lacks bacterial derived sequences which minimize the risk of immune reaction. Additionally the mifiprestone is a registered drug with extensively characterized activity and pharmacokinetics [67,68]. In chapter 6 we focused on adopting the GeneSwitch system

for expression of artificial miRNA targeting ApoB. Our results indicated that system is able to express miApoB in regulated and dose-dependent manner *in vitro*. Moreover, we have shown that the system is versatile and potentially expresses miRNA targeting Htt. We have cloned the two core components: the GeneSwitch transactivator and the inducible promoter driven miRNA in a single expression cassette, which facilitates production of rAAV. Combination of AAV delivery with inducible expression of miRNA targeting disease-related genes holds a great promise to induce specific gene knockdown concurrent with lack of toxic side effects. However validation of the efficacy, inducibility and safety of the GeneSwitch system *in vivo* still needs to be performed.

Concurrent with the ongoing efforts to employ inducible systems to inhibit disease related genes, a novel method to regulate gene expression by endogenous RNAi has been developed [69,70]. Many miRNAs are expressed in a tissue specific manner and have an important role in maintaining tissue specific functions and differentiation. For example mir-142-3p is specifically expressed in a hematopoietic cell lineage and it is able to regulate target transcripts by binding to specific target sequences. Fusion of mir-142-3p sequence to foreign transgene has been shown to inhibit gene expression in hematopoietic lineage cells, including APCs in both *in vitro* and *in vivo* setup which in consequence leads to attenuation of the immune response against foreign transgenes [71-73]. This approach can be applied for treatment of homozygous diseases where patients often do not express certain proteins and protein substitution therapy often fails due to immune response. Our initial concept studies have confirmed this finding as ovalbumin (OVA) expression was maintained in murine muscle when mir-142-3p binding site were placed in 3'UTR. By contrast expression of OVA lacking mir-142-3p binding sites was lost over the time, which was associated with appearance of anti-OVA specific antibodies. The safety aspects of such an approach need to be investigated. For example, the levels of endogenous miRNA expression including mir-142-3p need to be determined because a highly expressed transgene containing miRNA binding sites may lead to depletion of mir-142-3p or other miRNAs and result in global deregulation of gene expression in hematopoietic cells.

Altered miRNA expression is likely to contribute to many human diseases including cancer where it is implicated in regulating the malignant progression of cancer. This could be employed for the development of disease therapeutics based on cellular miRNA expression or inhibition. For example mir-9 has been found to be important in breast cancer as it overexpression is associated in increased cell motility and invasiveness [74]. Inhibiting mir-9 by using a 'miRNA sponge' in highly malignant cells inhibits metastasis formation. 'miRNA sponge' contains multiple (6-8) bulged tandem binding sites for a miRNA linked to a transgene of interest but it contains more binding sites (6-8), which often are not perfectly complementary. Additionally many miRNAs are downregulated in disease states. In breast cancer- expression of mir-31 in patients correlates inversely with metastasis [75,76]. A possible strategy to overcome

metastasis is to restore endogenous levels by delivering vectors expressing mir-31 in tissue-specific or cancer-specific manner. It has been shown that expression of ABC transporter genes in HCC can be mediated by cellular miRNA [75]. A total number of 79 miRNAs were found to be downregulated and 12 ABC transporters were upregulated in HCC patients [77]. *In vitro* verification revealed that mir-101 and mir-135 regulate the expression level of cholesterol transporter ABCA1 and mir-199a/b and mir-296 of multidrug resistance transported ABCC1. These findings may lead to novel treatment strategies, where endogenous levels of downregulated miRNAs may be artificially increased. By contrast, 'miRNA sponges' can be used to inhibit expression levels of endogenous miRNA to achieve therapeutic effect. For example, this approach have been used to decrease endogenous mir-122 levels, which in consequence resulted in 30% reduction of plasma cholesterol in mice [78]. Both approaches, inhibition of endogenous miRNA and restoration of physiological expression are attractive targets for future therapeutics. Therefore concomitant with screening for novel miRNA targets, attention should be directed to the safety of such approaches.

Challenges and future perspectives of RNAi

Despite the initial hope and excitement about RNAi, along with new developments several issues are being discovered. One of the major challenges is to achieve long term efficacy of RNAi therapeutics without side effects. So far, there are no sufficient data on long-term RNAi treatment and its side-effects. Additionally, the number of safety studies in NHP is very limited. Several RNAi clinical trials have been initiated during past few years but only synthetic siRNA, LNA and antisense oligonucleotides have been used. AAV-delivered RNAi therapeutics have not been brought to clinical trials due to intrinsic limitations of the approach. A major advantage would be the single dosage that should be sufficient to result in a long-lasting therapeutic effect. For the future gene therapy applications, it is desirable to employ inducible expression of shRNA or miRNA that would allow expression of the molecules within a therapeutic window and avoid toxicity.

A comprehensive analysis of side effects is necessary to improve the safety profile of RNAi. Simply employing a more rational design of shRNA targeting Htt resulted in lowering off-target effects. Promising approaches to improve the properties of miRNA are optimization the flanking sequences and the use of different miRNA scaffolds. This may lead to better processing and improved strand selection for RISC incorporation.

A second important challenge is the efficient delivery of RNAi to the target organ. AAV-delivered shRNA or miRNA is a powerful approach for long-term RNAi therapeutics in the liver. By using different AAV serotypes with specific cellular tropism, narrowed targeting can be achieved. Additionally, new serotypes may exhibit better transduction efficacy, which in consequence would result in lowering the dose necessary for inducing therapeutic effect.

Reference list

1. Young, SG (1990). Recent progress in understanding apolipoprotein B. *Circulation*; **82:** 1574-1594.
2. Koornneef, A, Maczuga, P, van Logtenstein, R, Borel, F, Blits, B, Ritsema, T, et al. (2011). Apolipoprotein B knockdown by AAV-delivered shRNA lowers plasma cholesterol in mice. *Mol Ther*; **19:** 731-740.
3. Myant, NB (1993). Familial defective apolipoprotein B-100: a review, including some comparisons with familial hypercholesterolaemia. *Atherosclerosis*; **104:** 1-18.
4. Sjouke, B, Kusters, D, Kastelein, J and Hovingh, G (2011). Familial hypercholesterolemia: present and future management. *Curr Cardiol Rep*; **13:** 527-536.
5. Schonfeld, G, Lin, X and Yue, P (2005). Familial hypobetalipoproteinemia: genetics and metabolism. *Cell Mol Life Sci*; **62:** 1372-1378.
6. Gupta, N, Fisker, N, Asselin, MC, Lindholm, M, Rosenbohm, C, Orum, H, et al. (2010). A locked nucleic acid antisense oligonucleotide (LNA) silences PCSK9 and enhances LDLR expression in vitro and in vivo. *PLoS ONE*; **5:** e10682.
7. Straarup, EM, Fisker, N, Hedtjarn, M, Lindholm, MW, Rosenbohm, C, Aarup, V, et al. (2010). Short locked nucleic acid antisense oligonucleotides potently reduce apolipoprotein B mRNA and serum cholesterol in mice and non-human primates. *Nucleic Acids Res*; **38:** 7100-7111.
8. Elmen, J, Lindow, M, Silahtaroglu, A, Bak, M, Christensen, M, Lind-Thomsen, A, et al. (2008). Antagonism of microRNA-122 in mice by systemically administered LNA-antimiR leads to up-regulation of a large set of predicted target mRNAs in the liver. *Nucleic Acids Res*; **36:** 1153-1162.
9. Robinson, RP, Bartlett, JA, Bertinato, P, Bessire, AJ, Cosgrove, J, Foley, PM, et al. (2011). Discovery of microsomal triglyceride transfer protein (MTP) inhibitors with potential for decreased active metabolite load compared to dirlotapide. *Bioorg Med Chem Lett*; **21:** 4150-4154.
10. Tep, S, Mihaila, R, Freeman, A, Pickering, V, Huyhn, F, Tadin-Strapps, M, et al. (2012). Rescue of Mtp siRNA-induced hepatic steatosis by DGAT2 siRNA silencing. *J Lipid Res*; **53:** 859-867.
11. Tadin-Strapps, M, Peterson, LB, Cumiskey, AM, Rosa, RL, Mendoza, VH, Castro-Perez, J, et al. (2011). siRNA-induced liver ApoB knockdown lowers serum LDL-cholesterol in a mouse model with human-like serum lipids. *J Lipid Res*; **52:** 1084-1097.
12. Frank-Kamenetsky, M, Grefhorst, A, Anderson, NN, Racie, TS, Bramlage, B, Akinc, A, et al. (2008). Therapeutic RNAi targeting PCSK9 acutely lowers plasma cholesterol in rodents and LDL cholesterol in nonhuman primates. *Proc Natl Acad Sci U S A*; **105:** 11915-11920.
13. Boiziau, C, Kurfurst, R, Cazenave, C, Roig, V, Thuong, NT and Toulme, JJ (1991). Inhibition of translation initiation by antisense oligonucleotides via an RNase-H independent mechanism. *Nucleic Acids Res*; **19:** 1113-1119.
14. Veal, GJ, Agrawal, S and Byrn, RA (1998). Sequence-specific RNase H cleavage of gag mRNA from HIV-1 infected cells by an antisense oligonucleotide in vitro. *Nucleic Acids Res*; **26:** 5670-5675.
15. Visser, ME, Wagener, G, Baker, BF, Geary, RS, Donovan, JM, Beuers, UH, et al. (2012). Mipomersen, an apolipoprotein B synthesis inhibitor, lowers low-density lipoprotein cholesterol in high-risk statin-intolerant patients: a randomized, double-blind, placebo-controlled trial. *Eur Heart J*; **33:** 1142-1149.
16. Rizzo, M (2010). Lomitapide, a microsomal triglyceride transfer protein inhibitor for the treatment of hypercholesterolemia. *IDrugs*; **13:** 103-111.
17. Cuchel, M, Bloedon, LT, Szapary, PO, Kolansky, DM, Wolfe, ML, Sarkis, A, et al. (2007). Inhibition of microsomal triglyceride transfer protein in familial hypercholesterolemia. *N Engl J Med*; **356:** 148-156.
18. Santaris Pharma A/S to report new clinical data from miravirsen Phase 2a study to treat Hepatitis C in late-breaking oral presentation at the AASLD 2011 annual meeting (2012). http://www.santaris.com/news/2011/10/03/santaris-pharma-report-new-clinical-data-miravirsen-phase-2a-study-treat-hepatitis-c.
19. Hu, J, Xu, Y, Hao, J, Wang, S, Li, C and Meng, S (2012). MiR-122 in hepatic function and liver diseases. *Protein Cell*; **3:** 364-371.
20. Hsu, SH, Wang, B, Kota, J, Yu, J, Costinean, S, Kutay, H, et al. (2012). Essential metabolic, anti-inflammatory, and anti-tumorigenic functions of miR-122 in liver. *J Clin Invest*; **122:** 2871-2883.
21. Zimmermann, TS, Lee, AC, Akinc, A, Bramlage, B, Bumcrot, D, Fedoruk, MN, et al.

(2006). RNAi-mediated gene silencing in non-human primates. *Nature*; **441:** 111-114.

22. Tekmira Pharmaceuticals completes ApoB SNALP phase I clinical trial.Tekmira Pharmaceuticals. (2010). http://www.tekmirapharm.com/News_and_Events/News_Releases/Tekmira01071001.aspx.
23. Wang, L, Wang, H, Bell, P, McCarter, RJ, He, J, Calcedo, R, et al. (2010). Systematic evaluation of AAV vectors for liver directed gene transfer in murine models. *Mol Ther*; **18:** 118-125.
24. Suhy, DA, Kao, SC, Mao, T, Whiteley, L, Denise, H, Souberbielle, B, et al. (2012). Safe, long-term hepatic expression of anti-HCV shRNA in a nonhuman primate model. *Mol Ther*; **20:** 1737-1749.
25. KYNAMRO™ (mipomersen sodium) data presented at XVI International Symposium on Atherosclerosis (2012). http://ir.isispharm.com/phoenix.zhtml?c=222170&p=irol-newsArticle_Print&ID=1678148&highlight=.
26. Sass, DA, Chang, P and Chopra, KB (2005). Nonalcoholic fatty liver disease: a clinical review. *Dig Dis Sci*; **50:** 171-180.
27. Havel, RJ, Yamada, N and Shames, DM (1989). Watanabe heritable hyperlipidemic rabbit. Animal model for familial hypercholesterolemia. *Arteriosclerosis*; **9:** I33-I38.
28. Singh, V, Tiwari, RL, Dikshit, M and Barthwal, MK (2009). Models to study atherosclerosis: a mechanistic insight. *Curr Vasc Pharmacol*; **7:** 75-109.
29. Giering, JC, Grimm, D, Storm, TA and Kay, MA (2008). Expression of shRNA from a tissue-specific pol II promoter is an effective and safe RNAi therapeutic. *Mol Ther*; **16:** 1630-1636.
30. Xia, H, Mao, Q, Paulson, HL and Davidson, BL (2002). siRNA-mediated gene silencing in vitro and in vivo. *Nat Biotechnol*; **20:** 1006-1010.
31. McBride, JL, Boudreau, RL, Harper, SQ, Staber, PD, Monteys, AM, Martins, I, et al. (2008). Artificial miRNAs mitigate shRNA-mediated toxicity in the brain: Implications for the therapeutic development of RNAi. *Proc Natl Acad Sci U S A*; **105:** 5868-5873.
32. Boudreau, RL, Monteys, AM and Davidson, BL (2008). Minimizing variables among hairpin-based RNAi vectors reveals the potency of shRNAs. *RNA*; **14:** 1834-1844.
33. Boudreau, RL, Martins, I and Davidson, BL (2009). Artificial microRNAs as siRNA shuttles: improved safety as compared to shRNAs in vitro and in vivo. *Mol Ther*; **17:** 169-175.
34. Maczuga, P, Koornneef, A, Borel, F, Petry, H, van, DS, Ritsema, T, et al. (2012). Optimization and comparison of knockdown efficacy between polymerase II expressed shRNA and artificial miRNA targeting luciferase and Apolipoprotein B100. *BMC Biotechnol*; **12:** 42.
35. Song, J, Pang, S, Lu, Y and Chiu, R (2004). Poly(U) and polyadenylation termination signals are interchangeable for terminating the expression of shRNA from a pol II promoter. *Biochem Biophys Res Commun*; **323:** 573-578.
36. Song, J, Pang, S, Lu, Y, Yokoyama, KK, Zheng, JY and Chiu, R (2004). Gene silencing in androgen-responsive prostate cancer cells from the tissue-specific Prostate-specific antigen promoter. *Cancer Res*; **64:** 7661-7663.
37. Yuan, J, Wang, X, Zhang, Y, Hu, X, Deng, X, Fei, J, et al. (2006). shRNA transcribed by RNA Pol II promoter induce RNA interference in mammalian cell. *Mol Biol Rep*; **33:** 43-49.
38. Park, JE, Heo, I, Tian, Y, Simanshu, DK, Chang, H, Jee, D, et al. (2011). Dicer recognizes the 5[prime] end of RNA for efficient and accurate processing. *Nature*; **475:** 201-205.
39. Zheng, C and Baum, BJ (2008). Evaluation of promoters for use in tissue-specific gene delivery. *Methods Mol Biol*; **434:** 205-219.
40. Yamamoto, A, Hen, R and Dauer, WT (2001). The ons and offs of inducible transgenic technology: a review. *Neurobiol Dis*; **8:** 923-932.
41. Grimm, D (2009). Small silencing RNAs: State-of-the-art. *Adv Drug Deliv Rev*; **61:** 672-703.
42. Prins, RM and Liau, LM (2004). Cellular immunity and immunotherapy of brain tumors. *Front Biosci*; **9:** 3124-3136.
43. Gendelman, HE (2002). Neural immunity: Friend or foe? *J Neurovirol*; **8:** 474-479.
44. Chen, CC, Ko, TM, Ma, HI, Wu, HL, Xiao, X, Li, J, et al. (2007). Long-term inhibition of hepatitis B virus in transgenic mice by double-stranded adeno-associated virus 8-delivered short hairpin RNA. *Gene Ther*; **14:** 11-19.
45. Zeng, Y, Yi, R and Cullen, BR (2005). Recognition and cleavage of primary microRNA precursors by the nuclear processing enzyme Drosha. *EMBO J*; **24:** 138-148.
46. Ge, Q, Ilves, H, Dallas, A, Kumar, P, Shorenstein, J, Kazakov, SA, et al. (2010). Minimal-length short hairpin RNAs: the relationship of structure and RNAi activity. *RNA*; **16:** 106-117.
47. Lima, WF, Prakash, TP, Murray, HM, Kinberger, GA, Li, W, Chappell, AE, et al. (2012). Single-stranded siRNAs activate RNAi in animals. *Cell*; **150:** 883-894.
48. Yu, D, Pendergraff, H, Liu, J, Kordasiewicz, HB, Cleveland, DW, Swayze, EE, et al.

(2012). Single-stranded RNAs use RNAi to potently and allele-selectively inhibit mutant huntingtin expression. *Cell*; **150:** 895-908.

49. Gu, S, Jin, L, Zhang, F, Huang, Y, Grimm, D, Rossi, JJ, et al. (2011). Thermodynamic stability of small hairpin RNAs highly influences the loading process of different mammalian Argonautes. *Proc Natl Acad Sci U S A*; **108:** 9208-9213.
50. Grimm, D, Streetz, KL, Jopling, CL, Storm, TA, Pandey, K, Davis, CR, et al. (2006). Fatality in mice due to oversaturation of cellular microRNA/short hairpin RNA pathways. *Nature*; **441:** 537-541.
51. Grimm, D, Wang, L, Lee, JS, Schurmann, N, Gu, S, Borner, K, et al. (2010). Argonaute proteins are key determinants of RNAi efficacy, toxicity, and persistence in the adult mouse liver. *J Clin Invest*; **120:** 3106-3119
52. Snøve, O and Holen, T (2004). Many commonly used siRNAs risk off-target activity. *Biochem Biophys Res Commun*; **319:** 256-263.
53. Ahn, M, Witting, SR, Ruiz, R, Saxena, R and Morral, N (2011). Constitutive expression of shRNA in vivo triggers build up of mature hairpin molecules. *Hum Gene Ther*; **22:** 1483-1497.
54. Beer, S, Bellovin, DI, Lee, JS, Komatsubara, K, Wang, LS, Koh, H, et al. (2010). Low-level shRNA cytotoxicity can contribute to MYC-induced hepatocellular carcinoma in adult mice. *Mol Ther*; **18:** 161-170.
55. Brameier, M, Herwig, A, Reinhardt, R, Walter, L and Gruber, J (2011). Human box C/D snoRNAs with miRNA like functions: expanding the range of regulatory RNAs. *Nucleic Acids Res*; **39:** 675-686.
56. Martens-Uzunova, ES, Jalava, SE, Dits, NF, van Leenders, GJ, Moller, S, Trapman, J, et al. (2012). Diagnostic and prognostic signatures from the small non-coding RNA transcriptome in prostate cancer. *Oncogene*; **31:** 978-991.
57. Gupta, S, Schoer, RA, Egan, JE, Hannon, GJ and Mittal, V (2004). Inducible, reversible, and stable RNA interference in mammalian cells. *Proc Natl Acad Sci USA*; **101:** 1927-1932.
58. Laurenti, E, Barde, I, Verp, S, Offner, S, Wilson, A, Quenneville, S, et al. (2010). Inducible gene and shRNA expression in resident hematopoietic stem cells in vivo. *Stem Cells*; **28:** 1390-1398.
59. Amendola, M, Passerini, L, Pucci, F, Gentner, B, Bacchetta, R and Naldini, L (2009). Regulated and multiple miRNA and siRNA delivery into primary cells by a lentiviral platform. *Mol Ther*; **17:** 1039-1052.
60. Aagaard, L, Amarzguioui, M, Sun, G, Santos, LC, Ehsani, A, Prydz, H, et al. (2007). A facile lentiviral vector system for expression of doxycycline-inducible shRNAs: knockdown of the pre-miRNA processing enzyme drosha. *Mol Ther*; **15:** 938-945.
61. McJunkin, K, Mazurek, A, Premsrirut, PK, Zuber, J, Dow, LE, Simon, J, et al. (2011). Reversible suppression of an essential gene in adult mice using transgenic RNA interference. *Proc Natl Acad Sci U S A*; **108:** 7113-7118.
62. Premsrirut, P, Dow, L, Kim, S, Camiolo, M, Malone, C, Miething, C, et al. (2011). A rapid and scalable system for studying gene function in mice using conditional RNA interference. *Cell*; **145:** 145-158.
63. Seibler, J, Kleinridders, A, Kuter-Luks, B, Niehaves, S, Bruning, JC and Schwenk, F (2007). Reversible gene knockdown in mice using a tight, inducible shRNA expression system. *Nucleic Acids Res*; **35:** e54.
64. Shea, CM and Tzertzinis, G (2010). Controlled expression of functional miR-122 with a ligand inducible expression system. *BMC Biotechnol*; **10:** 76.
65. Rivera, VM, Berk, L and Clackson, T (2012). Dimerizer-mediated regulation of gene expression in vitro. *Cold Spring Harb Protoc*; **2012:** 815-820.
66. Xu, ZL, Mizuguchi, H, Mayumi, T and Hayakawa, T (2003). Regulated gene expression from adenovirus vectors: a systematic comparison of various inducible systems. *Gene*; **309:** 145-151.
67. Im, A and Appleman, LJ (2010). Mifepristone: pharmacology and clinical impact in reproductive medicine, endocrinology and oncology. *Expert Opin Pharmacother*; **11:** 481-488.
68. Bamberger, CM and Chrousos, GP (1995). The glucocorticoid receptor and RU 486 in man. *Ann N Y Acad Sci*; **761:** 296-310.
69. Brown, BD, Venneri, MA, Zingale, A, Sergi, SL and Naldini, L (2006). Endogenous microRNA regulation suppresses transgene expression in hematopoietic lineages and enables stable gene transfer. *Nat Med*; **12:** 585-591.
70. Brown, BD, Cantore, A, Annoni, A, Sergi, LS, Lombardo, A, Della, VP, et al. (2007). A microRNA-regulated lentiviral vector mediates stable correction of hemophilia B mice. *Blood*; **110:** 4144-4152.
71. Annoni, A, Brown, BD, Cantore, A, Sergi, LS, Naldini, L and Roncarolo, MG (2009). In vivo delivery of a microRNA-regulated transgene induces antigen-specific regulatory T cells

and promotes immunologic tolerance. *Blood*; **114:** 5152-5161.

72. Mingozzi, F, Liu, YL, Dobrzynski, E, Kaufhold, A, Liu, JH, Wang, Y, et al. (2003). Induction of immune tolerance to coagulation factor IX antigen by in vivo hepatic gene transfer. *J Clin Invest*; **111:** 1347-1356.
73. Majowicz, A, Maczuga, P, Kwikkers, KL, van der Marel, S, van Logtenstein, R, Petry, H, et al. (2012). Mir-142-3p target sequences reduce transgene directed immunogenicity following intramuscular AAV vector mediated gene delivery. *PLoS ONE submitted*;
74. Selcuklu, SD, Donoghue, MT, Rehmet, K, de Souza, GM, Fort, A, Kovvuru, P, et al. (2012). MicroRNA-9 inhibition of cell proliferation and identification of novel miR-9 targets by transcriptome profiling in breast cancer cells. *J Biol Chem*; **287:** 29516-29528.
75. Borel, F, Han, R, Visser, A, Petry, H, van Deventer, SJ, Jansen, PL, et al. (2012). Adenosine triphosphate-binding cassette transporter genes up-regulation in untreated hepatocellular carcinoma is mediated by cellular microRNAs. *Hepatology*; **55:** 821-832.
76. Borel, F, Konstantinova, P and Jansen, PL (2012). Diagnostic and therapeutic potential of miRNA signatures in patients with hepatocellular carcinoma. *J Hepatol*; **56:** 1371-1383.
77. Boudreau, RL, Spengler, RM and Davidson, BL (2011). Rational design of therapeutic siRNAs: minimizing off-targeting potential to improve the safety of RNAi therapy for Huntington's disease. *Mol Ther*; **19:** 2169-2177.
78. Xie, J, Ameres, SL, Friedline, R, Hung, JH, Zhang, Y, Xie, Q, et al. (2012). Long-term, efficient inhibition of microRNA function in mice using rAAV vectors. *Nat Methods*; **9:** 403-409.

ADDENDUM

Summary in English

The liver plays a major role in the metabolism and has a number of functions in the body, including glycogen storage, decomposition of red blood cells, plasma protein synthesis, hormone production, and detoxification. Familial hypercholesterolemia (FH) is a genetic disorder characterized by high levels of low density lipoprotein cholesterol (LDL-C) and increasing the risk of cardio vascular diseases. FH and many other liver diseases can possibly be treated with RNA interference (RNAi). RNAi is a natural process of regulation of gene expression by binding of small RNA molecules to complementary sequences in the mRNA of a gene and hence inducing its degradation or translational repression. In this thesis, we aimed at developing a safe and robust RNAi-based therapy for FH by inhibiting Apolipoprotein B100 (ApoB). ApoB is a primary component of the low density lipoprotein (LDL), a lipoprotein that transports "bad" cholesterol LDL-C.

In **chapter 2** we tested the inhibitory potential of adeno-associated virus (AAV) delivered shRNA targeting ApoB (shApoB). AAV-shApoB induced a strong knockdown of ApoB mRNA and protein levels which correlated with a reduction in total cholesterol levels and elevated lipid accumulation in the liver. In this study, shApoB was transcribed by the polymerase III (pol III) promoter, which provides high expression levels. This probably resulted in (mild) hepatotoxity, when high doses of AAV-shRNA were used.

Therefore, in **chapter 3**, we explored the possibility of using the weaker pol II promoters to express shRNA. Pol II promoters can also be tissue specific or regulated, which would provide additional safety level for gene therapy applications. However pol II expression of shRNA was not optimal, therefore we developed artificial miRNA as an alternative to shRNA expression. Artificial miRNA demonstrated target knockdown efficiency similar to that of shRNA, while expressing less siRNA molecules.

In **chapter 4,** the long-term efficacy of AAV delivered shRNA and artificial miRNA targeting ApoB (shApoB and miApoB, respectively) *in vivo* was investigated. As additional safety measure miApoB was expressed from the liver specific LP1 promoter. AAV-shApoB and AAV-miApoB provided potent gene knockdown, which resulted in a clear phenotypic effect of cholesterol reduction. Interestingly, the strong ApoB knockdown effect was quickly lost over the time for AAV-shApoB while AAV-miApoB had a more sustained effect. Analysis of shApoB and miApoB revealed differential processing that may have implications for their off-targeting and toxic effects *in vivo*.

The consequences of the differential functioning and processing of shApoB and miApoB were further investigated in **chapter 5** by histological, transcriptome and pathway prediction analysis. Interestingly, AAV-shApoB but not AAV-miApoB increased hepatocytes proliferation and affected genes involved in cell proliferation and death as well as immune response. Additionally, endogenous miRNA profile was differentially affected by both molecules *in vitro* and *in vivo*. In **chapter 6**, inducible

RNAi has been designed and tested as a further step towards safer and robust RNAi gene therapy. The mifepristone-inducible GeneSwitch system was used to express several artificial miRNAs. We optimized the system components in order to minimize basal expression and maximize gene induction rate. *In vitro*, GeneSwitch expressed miRNA demonstrated sequence specific and dose dependent target knockdown indicating that the system can be applied in the future for regulated RNAi expression.

In conclusion, we have shown that RNAi therapy using AAV-delivered artificial miRNA is a promising approach for treatment of FH and possibly other liver diseases. Our mechanistic studies revealed differences in shRNA and miRNA processing and functioning *in vivo*. Finally, our findings have significant impact on understanding and overcoming toxicity and off-targeting related problems of RNAi based gene therapy in the liver using AAV vectors.

Nederlandse samenvatting

De lever heeft een aantal belangrijke metabolisme functies in het lichaam, waaronder glycogeen opslag, afbraak van rode bloedcellen, plasma-eiwit synthese, hormoon productie en ontgifting. Familiaire hypercholesterolemie (FH) is een genetische ziekte gekenmerkt door hoge plasma concentraties van low density lipoproteïne cholesterol (LDL-C) die het risico van hart en vaatziekten verhogen. FH en vele andere leverziekten kunnen mogelijkerwijs worden behandeld met RNA interferentie (RNAi). RNAi is een natuurlijk proces waarbij genexpressie gereguleerd wordt doordat kleine RNA moleculen zich binden aan complementaire sequenties van het messenger RNA (mRNA) van een gen. Hierdoor wordt het mRNA afgebroken waardoor de translatie naar eiwit niet kan plaatsvinden, zogenaamde translationele repressie.

In dit proefschrift hebben we ons gericht op het ontwikkelen van een veilige en robuuste op RNAi-gebaseerde therapie voor FH door het remmen van het afschrijven van mRNA dat codeert voor het eiwit Apolipoprotein B100 (ApoB). ApoB is een hoofdcomponent van low density lipoprotein (LDL), een lipoproteine dat het "slechte" cholesterol LDL-C vervoert. In **hoofdstuk 2** hebben we de remming van ApoB getest door met behulp van adeno-associated virus (AAV) shRNA (shApoB) in de levercellen te introduceren. Inderdaad veroorzaakte AAV-shApoB een sterke vermindering van ApoB mRNA en eiwit. Dit correleerde met een verlaging van totaal cholesterol in het bloedplasma en een opstapeling van vet in de lever. In dit onderzoek werd shApoB afgeschreven door de polymerase III (pol III) promoter, hetgeen leidt tot hoge expressieniveaus. Bijwerkingen, zoals (milde) toxiciteit in de lever, ontstonden waarschijnlijk door de hoge doseringen van AAV-shRNA.

In **hoofdstuk 3**, hebben we daarom de mogelijkheid van het gebruik van de zwakkere pol II promoters onderzocht om shRNA tot expressie te brengen. Pol II promoters kunnen bovendien ook weefselspecifiek of gereguleerd zijn, hetgeen een extra niveau van veiligheid voor gentherapie toepassingen mogelijk maakt. Omdat de pol II expressie van shRNA niet optimaal was, hebben we artificieel miRNA ontwikkeld als alternatief voor shRNA expressie. Artificiële miRNA hebben aangetoond efficiënt knockdown te geven van het target gen, vergelijkbaar met die van shRNA, terwijl ook bekend is dat miRNA minder siRNA moleculen genereren. In **hoofdstuk 4** is de langdurige werking van ApoB knockdown door shRNA of artificiële miRNA (respectievelijk shApoB en miApoB) *in vivo* geïntroduceerd door AAV vergeleken. Als veiligheidsmaatregel is miApoB expressie gestuurd door de lever-specifieke LP1-promoter. AAV-shApoB en AAV-miApoB gaven sterke knockdown, die resulteerde in een duidelijk fenotypisch effect van cholesterol verlaging. Een belangrijke bevinding was dat het sterke knockdown-effect van AAV-shApoB snel was verdwenen, terwijl het AAV-miApoB effect aanhield. Analyse van shApoB en miApoB liet zien dat het verschil in de manier van verwerking gevolgen heeft voor hun specificiteit en toxische effecten *in vivo*.

Het verschil in functioneren en de manier van verwerken van shApoB en miApoB zijn verder onderzocht in **hoofdstuk 5** met behulp van histologie en transcriptome en pathway voorspelling analyse. AAV-shApoB maar niet AAV-miApoB zorgde voor een versnelde hepatocyte proliferatie door een effect op genen die betrokken zijn bij de celproliferatie en celdood. Ook genen die betrokken zijn bij de immuunreactie waren aangedaan. Daarnaast was het miRNA profiel zowel *in vitro* als *in vivo* verschillend aangedaan door beide moleculen.

Hoofdstuk 6 beschrijft het ontwerp en het onderzoek dat gedaan is met een induceerbaar RNAi voor een veiliger en robuuste manier van RNAi gentherapie. Hiervoor is het Mifepristone-induceerbaar GeneSwitch systeem gebruikt om verschillende artificiële miRNAs te expresseren. We hebben de componenten van het systeem geoptimaliseerd op de basale expressie te minimaliseren en de gen introductiegraad te verhogen. GeneSwitch geëxpresseerde miRNA lieten *in vitro* een sequentie-specifieke en dosis-afhankelijke knockdown zien, wat een toekomst biedt voor dit systeem in de gereguleerde RNAi expressie.

Samenvattend hebben we aangetoond dat door AAV afgeleverde artificiële miRNAs de deur openen voor veelbelovende nieuwe therapieën van FH en mogelijkerwijs andere leverziekten. Deze basale studies naar de werking hebben uitgewezen dat shRNA en miRNA *in vivo* verschillen in de manier van verwerken en functioneren. Ten slotte hebben onze bevindingen een belangrijke invloed op het inzicht in het tegengaan van toxiciteit en specificiteits problemen bij gentherapie in de lever gebaseerd op RNAi geïntroduceerd met AAV vectoren.

Streszczenie

Wątroba odgrywa bardzo ważną rolę w metabolizmie oraz pełni wiele istotnych dla organizmu funkcji włączając magazynowanie glikogenu, rozkład czerwonych krwinek, syntezę białek osocza. produkcję hormonów oraz detoksykację. Rodzinna hipercholesterolemia (FH) jest chorobą genetyczną, którą charakteryzuje wysoki poziom LDL (lipoprotein o niskiej gęstości) cholesterolu zwiększających ryzyko chorób układu krążenia. FH, a także wiele innych chorób wątroby może być potencjalnie leczone przy pomocy mechanizmu interferencji RNA (RNAi). RNAi jest naturalnym procesem regulacji ekspresji genów w którym małe cząsteczki RNA wiążąc się do sekwencji w mRNA genu, wywołują zjawisko wyciszania lub wyłączania danego genu. Celem tej pracy było opracowanie skutecznej, a przede wszystkim bezpiecznej terapii FH w oparciu o mechanizm interferencji RNA i wyciszanie genu Apolipoproteiny B100 (ApoB). Białko ApoB jest jednym z głównych składników lipoprotein o niskiej gęstości (LDL), które odpowiedzialne są za transport "złego" cholesterolu LDL-C..

W **rozdziale 2** testowaliśmy shRNA przeciwko ApoB (shApoB), który był dostarczany za pomocą wirusa zależnego od adenowirusów (AAV). AAV-shApoB spowodował silne wyciszenie genu oraz białka ApoB, co w konsekwencji spowodowało spadek poziomu cholesterolu we krwi i jednoczesne zwiększenie zawartości lipidów w wątrobie. W tym badaniu shRNA było produkowane przez promotor polimerazy RNA klasy III, który wykazuje wysoki poziom ekspresji. Prawdopodobnie dlatego wysokie dawki AAV-shRNA spowodowały (łagodne) uszkodzenie wątroby.

Dlatego też, w **rozdziale 3**, zbadaliśmy możliwość zastosowania słabszych promotorów polimerazy RNA II do ekspresji shRNA. Promotory polimerazy RNA II mogą zwiększyć bezpieczeństwo terapii genowej ponieważ, w przeciwieństwie do promotorów pol III, mogą one być regulowane, a także tkankowo-specyficzne- czyli aktywne tylko w danym typie tkanki. Ponieważ uzyskana prez nas ekspresja shRNA przy wykorzystaniu promotorów pol II nie była optymalna, jako alternatywę użyliśmy sztuczne cząsteczki mikro RNA (miRNA), które wykazały skuteczność porównywalną do shRNA produkowane przez pol III.

W **rozdziale 4**, zbadaliśmy długoterminową skuteczność shRNA oraz sztucznego miRNA przeciwko genowi ApoB (odpowiednio shApoB i miApoB) w warunkach *in vivo*. Jako dodatkowy zabezpieczenie miApoB było produkowane przez promotor polimerazy RNA klasy II, specyficzny dla komórek wątroby (LP1 promotor). Zarówno AAV-shApoB oraz AAV-miApoB spowodowały silne wyciszenie genu ApoB, co zaowocowało wyraźnym fenotypem w postaci obniżonego poziomu cholesterolu we krwi. Co ciekawe, silny efekt wyciszenia genu ApoB przez AAV-shApoB szybko ustał, podczas gdy efekt wywołany przez AAV-miApoB był bardziej długotrwały. Analiza shApoB i miApoB ujawniła, że obydwie cząsteczki ulegają różnej obróbce w komórkach, co może wpływać na ich selektywność w wyciszaniu genów oraz efekty uboczne.

&

Skutki różnicowej obróbki oraz działania shApoB oraz miApoB były kolejno badane przez nas w **rozdziale 5** poprzez analizę histologiczną, transkryptomu (profilu ekspresji genów) oraz komórkowych szlaków metabolicznych. Co ciekawe, wyłącznie AAV-shApoB spowodował wzrost ilości dzielących się komórek wątroby (hepatocytów) oraz wzrost ekspresji genów biorących udział w procesach rozmnażania i śmierci komórek oraz odpowiedzi immunologicznej. Ponadto, wpływ shApoB oraz miApoB na profile ekspresji komórkowego miRNA był także różny

W **rozdziale 6**, w celu dalszego zwiększenia bezpieczeństwa i skuteczności terapii genowej, zaprojektowaliśmy i przetestowaliśmy system do regulowanej ekspresji sztucznych cząsteczek miRNA. W tym celu użyliśmy system GeneSwitch który może być regulowany związkiem chemicznym- Mifepristonem. W celach ulepszenia właściwości systemu tzn. zmniejszenia podstawowej ekspresji oraz zwiększenia maksymalnej aktywacji systemu, poszczególne komponenty systemu zostały szczegółowo zbadane. W badaniach *in vitro* wykazaliśmy, że system GeneSwitch umożliwia specyficzne oraz regulowane, w zależności od dawki, wyciszenie docelowego genu. Nasze badania wskazują, że system może być stosowany w przyszłości w celach terapii genowej opartej na RNAi.

Podsumowując, wykazaliśmy, że terapia genowa za pomocą wirusów AAV oraz sztucznych cząsteczek miRNA jest obiecującą metodą leczenia FH oraz innych chorób wątroby. Badania mechanistyczne wykazały różnice w obróbce i funkcjonowaniu shRNA i miRNA w warunkach *in vivo*. Nasze wyniki mają istotny wpływ na zrozumienie oraz rozwiązanie problemów związanych z bezpieczeństwem i skutkami ubocznymi terapii genowej opartej na zastosowaniu wirusów AAV i interferencji RNA.

Curriculum Vitae

Piotr Maczuga was born on August 9, 1983 in Leżajsk, Poland. After completing the secondary school in 2002 (Zespół Szkół im B. Chrobrego in Leżajsk), in October 2002 he started studying Biology at the Jagiellonian University in Krakow, Poland. During his studies, he participated in the Socrates/Erasmus program and spent one semester working in the Department of Pediatrics, Radboud University Medical Center Nijmegen, The Netherlands. After obtaining MSc in Biology in June 2007 at the Jagiellonian University, in November 2007 he started European Union's Leonardo da Vinci internship at Amsterdam Molecular Therapeutics (now uniQure Biopharma). In February 2008, he started working as a PhD student of the Leiden University Medical Center at Amsterdam Molecular Therapeutics, where the work presented in this thesis was performed. Following the end of the PhD, he started working as a Junior Researcher Emerging Technologies at uniQure where he continued to work on RNAi-based gene therapy.

Publications

1. **Maczuga P**, Lubelski J, van Logtenstein R, Borel F, Blits B, Fakkert E, Costessi A, Butler D, van Deventer S, Petry H, Koornneef A, Konstantinova P (2013). Embedding siRNA sequences targeting Apolipoprotein B100 in shRNA and miRNA scaffolds results in differential processing and in vivo efficacy. *Mol Ther*; **21**: 217-227.
2. Dieteren CE, Koopman WJ, Swarts HG, Peters JG, **Maczuga P**, van Gemst JJ, Masereeuw R, Smeitink JA, Nijtmans LG, Willems PH (2012). Subunit-specific incorporation efficiency and kinetics in mitochondrial complex I homeostasis. *J Biol Chem*; **287**: 41851-41860.
3. **Maczuga P**, Koornneef A, Borel F, Petry H, van Deventer S, Ritsema T, Konstantinova P (2012). Optimization and comparison of knockdown efficacy between polymerase II expressed shRNA and artificial miRNA targeting luciferase and Apolipoprotein B100. *BMC Biotechnol*; **12**: 42.
4. Borel F, van Logtenstein R, Koornneef A, **Maczuga P**, Ritsema T, Petry H, van Deventer SJ, Jansen PL, Konstantinova P (2011). In vivo knock-down of multidrug resistance transporters ABCC1 and ABCC2 by AAV-delivered shRNAs and by artificial miRNAs. *J RNAi Gene Silencing*; **7**: 434-442.
5. Koornneef A, **Maczuga P**, van Logtenstein R, Borel F, Blits B, Ritsema T, van Deventer S, Petry H, Konstantinova P (2011). Apolipoprotein B knockdown by AAV-delivered shRNA lowers plasma cholesterol in mice. *Mol Ther*; **19**: 731-740.

ACKNOWLEDGEMENTS

The completion of this thesis would not have been possible without the help of many people, to which I would like to express my sincere gratitude.

First of all, I want to acknowledge my promotor, **Prof. Sander van Deventer** for his advice, scientific input and for the vigorous scientific discussions we have had: Sander, thank you for your help and support, especially during the final phase. I would like to thank **Dr. Pavlina Konstantinova** for being my co-promotor and supervisor at uniQure. Pavlina, I really appreciate the way you have guided me through these years, giving me the freedom to grow as an independent researcher, whilst at the same time keeping me grounded with encouraging nudges in the right direction.

I also would like to thank my former supervisor **Dr. Tita Ritsema** who initiated the RNAi group in AMT and to **Dr. Harald Petry** for his support and for reviewing my manuscript.

When I started in Amsterdam Molecular Therapeutics in 2007, I joined the Vector Development group and I would like to thank **Dr. Andrew Bakker** and to the present and former group members. **Saskia** - thank you for supervising me during my internship but also for organization of the volleyball tournament. **Bas** - I could always count on you. Thank you for accepting to be my paranymph. **Betty** and **Larbi** - for everyday help and for nice conversations. I also would like to thank **Jacek** who is current Head of the Vector Development group for his help with all sorts of problems - not only scientific. After Vector Development, I joined the RNAi/Emerging Technologies group and I would like to express my gratitude to all members. My favourite postdoc in AMT was **Annemart** - I really enjoyed working with you in the lab and our scientific discussions. I have to say that I learned a lot from you. **Florie** - Thank you for your help during whole PhD process - for you smile and for your enthusiasm. **Jolanda** and **Linaida** - Thank you for your help. I would like to say to a big thank you to **Richard** and **Bas** from the Brain/In vivo group - thank you for help on various in vivo experiments! I would like to thank the Immunology group: **Valerie, Anna, Karin** and **Sander**. It was nice to work with you on the immune-tolerance project. Thank you **Anna** for being my friend since university and I really keep my fingers crossed for your PhD. **Karin** - Thank you for your expertise in immunohistochemistry and for helping me with the Dutch translations. **Sander** - Thank you for your medical and non-medical advices. **Stuart** - it was a lot of fun working with you - Thank you for the corrections. My former officemate – **Nicollo** I wish you good luck with your PhD. I hope we will stay in touch! **Astrid**- Every time you visited us you brought Spanish temper to the company! Finally I would like to thank members of the PD and MF groups especially Jeroen for helping me with virus purifications and Mustafa- for help with cell cultures.

&

Sincere thanks to all my colleagues and former colleagues from Amsterdam Molecular Therapeutics/uniQure: **Dylan, Vincent, Ildo, Arie, Yvet, Jaap, Bart, Florence, Wim, Corina, Albertine, Eelke, Chantal, Bob, Frans** and **Eric**. It was pleasure for me to work with you. I am happy that we managed to get Glybera approved and I really hope that in the future we will also manage to register a RNAi based gene therapy. I just regret that not all people could stay in AMT/uniQure- we were like big family working together.

I would like to thank the people I collaborated with, especially from the Tytgat Institute: **Dr. Piter Bosma, Lysbeth** and **Dagmar**. Additionally, **Dr. Joanne Verheij**, **Dr. Chris van der Loos** and **Gerrit** from the Department of Pathology of the Academic Medical Center for their help on liver histology staining.

I would like to especially thank the special person in my life- my girlfriend **Iwona**. You have supported me all this time, since we met to the current day. Thank you for being there for me, for all the laughs, happiness and love. And, thank you for tolerating my late working hours and occasional bad mood.

Na samym końcu, chciałem podziękować całej mojej rodzinie, a w szczególności rodzicom. **Mamo** i **Tato** - dziękuję Wam za wszystko, za Wasze wychowanie i za Wasze wsparcie na każdym etapie życia. To dzięki Wam znalazłem się w tym miejscu. Z całego serca Wam dziękuję I mam nadzieję, że jesteście ze mnie dumni! Chciałem też Wam podziękować moim kochanym siostrom: **Alicji** i **Sabinie**. Jesteście też częścią mojego życia i zawsze mogłem na Was liczyć. Dziękuje Wam za wspólnie spędzony czas, za nasze rozmowy oraz za pomoc we wszelakich sprawach. Zawsze też możecie na mnie liczyć. Chciałem też podziękować swojej chrzestnej matce - **cioci Hani**. Ciociu- Tobie także dziękuję za Twoją pomoc na każdym etapie życia, w szczególności za wszystkie szczere rozmowy i rady. Na końcu podziękowania dla dziadka **Mariana** i babci **Aleksandry**. Całej rodzinie dziękuję za cierpliwość i wyrozumiałość. Mam nadzieję, że w przyszłości także będziecie mnie wspierać. Przepraszam Was, że czasami nie mogłem Was wszystkich odwiedzić będąc w Polsce.

&